

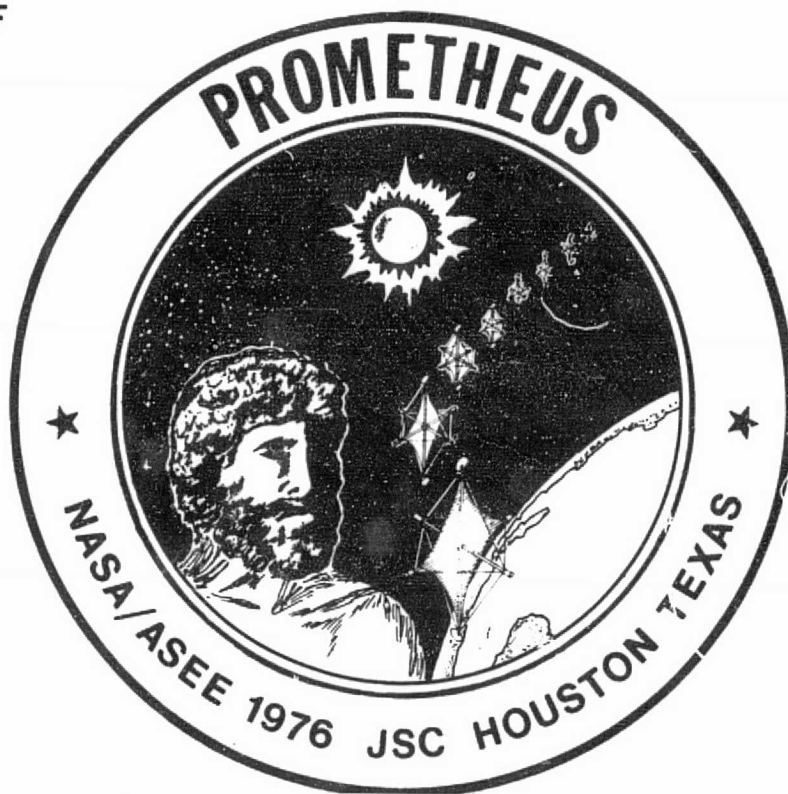
## **General Disclaimer**

### **One or more of the Following Statements may affect this Document**

- This document has been reproduced from the best copy furnished by the organizational source. It is being released in the interest of making available as much information as possible.
- This document may contain data, which exceeds the sheet parameters. It was furnished in this condition by the organizational source and is the best copy available.
- This document may contain tone-on-tone or color graphs, charts and/or pictures, which have been reproduced in black and white.
- This document is paginated as submitted by the original source.
- Portions of this document are not fully legible due to the historical nature of some of the material. However, it is the best reproduction available from the original submission.

LYNDON B. JOHNSON  
SPACE CENTER  
AND THE  
UNIVERSITY OF  
HOUSTON

1976 NASA/ASEE  
SYSTEMS DESIGN  
INSTITUTE



(NASA-TM-X-7468C) SOLAR POWER SATELLITE:  
ANALYSIS OF ALTERNATIVES FOR TRANSPORTING  
MATERIAL TO GEOSYNCHRONOUS ORBIT (NASA)  
265 p HC A12/MF A01

CSCI 22A

N77-21136

Unclas  
24466

G3/12

SOLAR POWER SATELLITE:  
ANALYSIS OF ALTERNATIVES FOR TRANSPORTING  
MATERIAL TO GEOSYNCHRONOUS ORBIT

*W. J. Graff and C. J. Huang*  
*October 15, 1976*  
*Houston, Texas*

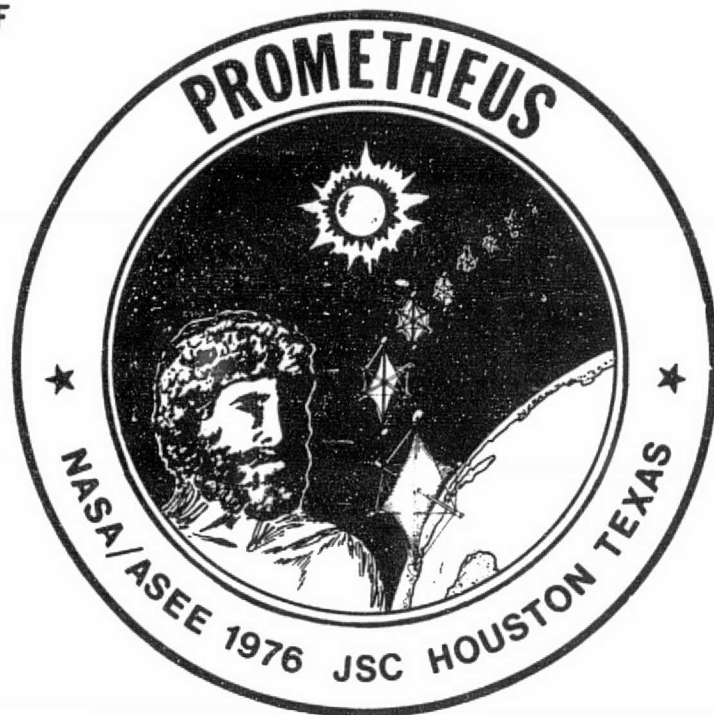


NASA GRANT NGT 44-005-114



LYNDON B. JOHNSON  
SPACE CENTER  
AND THE  
UNIVERSITY OF  
HOUSTON

1976 NASA/ASEE  
SYSTEMS DESIGN  
INSTITUTE



SOLAR POWER SATELLITE:  
ANALYSIS OF ALTERNATIVES FOR TRANSPORTING  
MATERIAL TO GEOSYNCHRONOUS ORBIT

*W. J. Graff and C. J. Huang*  
*October 15, 1976*  
*Houston, Texas*

NASA GRANT NGT 44-005-114

IN GREEK MYTHOLOGY PROMETHEUS  
WAS A TITAN, THE LEGENDARY GIVER  
OF FIRE AND ALL ITS BENEFITS TO  
MANKIND.

GREEK NAME MEANS: "FORETHOUGHT."

PROMETHEUS IS CHAMPION OF THE  
DOWNTRODDEN HUMAN RACE,  
HAVING NOT ONLY GIVEN FIRE, BUT  
NUMBERS, METALLURGY, SHIPS, READING,  
AND DIVINATION.

## AUTHORS

Harm Buning (Team Captain) .....	University of Michigan
Reinaldo Cintron .....	University of Puerto Rico
Dale Cloninger (Team Captain) .....	University of Houston, Clear Lake
Thomas L. De Fazio .....	Florida Institute of Technology
Kenneth W. French .....	John Brown University
Salvador R. Garcia .....	Moody College of Marine Sciences
Thomas J. Gerson .....	Queensborough Community College
Euel W. Kennedy .....	California Polytechnic State University
Fred D. Lewallen .....	Oklahoma State University
Chung K. Liu .....	University of Guam
Bernard McIntyre .....	North Texas State University
Michael Mezzino .....	University of Houston, Clear Lake
Knud B. Pedersen .....	University of Puerto Rico
S. R. N. Rao .....	Prairie View A & M University
Norman M. Schnurr .....	Vanderbilt University
Charles H. Story .....	East Tennessee State University
John W. Weatherly, III .....	Louisiana State University
Norman L. Weed .....	University of Houston, Clear Lake
Min-Yen Wu .....	University of Colorado

## EDITORS

Thomas De Fazio  
 Kenneth W. French  
 Euel W. Kennedy  
 Fred D. Lewallen

Chung K. Liu  
 John W. Weatherly  
 Norman L. Weed  
 Charles H. Story

Charles H. Story  
 Study Manager

William J. Graff  
 NASA—ASEE Systems Design  
 Institute Associate Director



1976 NASA/ASEE ENGINEERING SYSTEMS DESIGN INSTITUTE

Seated: (Left to Right), B. McIntyre, T. De Fazio, C. Liu, S. Garcia, N. Schnurr, D. Cloninger, E. Kennedy, R. Cintron,  
Back Row: B. Graff, N. Weed, S. Rao, K. French, K. Pedersen, H. Buning, C. Story, T. Gerson, F. Lewallen, M. Wu,  
J. Weatherly. (M. Mezzino and C. J. Huang, not pictured)

## ABSTRACT

A systems design study of the alternative methods and relative merits of various approaches to transporting and assembling a solar power satellite in geosynchronous orbit was conducted. State-of-the-art alternatives for chemical and electrical interorbital propulsion were studied and several possible scenarios for construction were proposed.

Construction and assembly of the solar power satellite in geosynchronous orbit would be recommended if a chemical ( $LH_2/LO_2$ ) orbital transfer vehicle is to be used for interorbital transportation. Advantages of chemical propulsion include flexibility and the use of existing technology without requiring significant state-of-the-art advances; the major disadvantage is high propellant usage.

An electrical propulsion option would assume modular construction of the solar power satellite in low Earth orbit. Each module would be provided with electrical thrusters and propelled immediately to geosynchronous orbit for final assembly.

The major advantage of this transportation mode is the efficiency of high impulse engines. Disadvantages include the state of technical development required for the engines, degradation of exposed solar arrays during interorbital transfer and the possibility of collisions with space debris at or near low Earth orbit.

The cost comparison between chemical propulsion and electrical propulsion yielded inconclusive results as to which would provide the lower cost system.

## FOREWORD

This report presents the results of eleven weeks of concentrated effort by the participants in the 1976 summer program sponsored by the National Aeronautics and Space Administration in cooperation with the American Society for Engineering Education. This program, entitled the NASA-ASEE Engineering Systems Design Institute, has been conducted annually at the Johnson Space Center since 1967 and is jointly administered by the University of Houston.

This year the systems design team was composed of 19 faculty members from 16 universities representing 10 states, Guam and Puerto Rico. While primarily made up of professors from the various fields of engineering, the team was also multidisciplinary. Other disciplines represented included physics, mathematics, industrial education, economics and finance.

The purpose of the design project was to study the relative merits of various approaches to transporting large amounts of payload from the ground to low earth orbit and subsequently to geosynchronous orbit. The payload will be whatever materials and modules are needed for construction of very large structures in space, e.g., solar power satellites. State-of-the-art alternatives for orbital transfer using chemical and electrical propulsion were studied and several possible scenarios for construction were evaluated.

## ACKNOWLEDGEMENTS

Appreciation is expressed to the following individuals and groups for their contributions to the project:

To the National Aeronautics and Space Administration for fiscal support and housing, and to the consultants and advisors (Appendix D) for technical assistance;

To Harold Benson and Harmon Roberts of the Johnson Space Center Urban Systems Project Office for technical guidance;

To the program Co-Directors, Barbara Eandi and C. J. Huang, and the Associate Director, W. J. Graff, for administration and coordination of the program;

To the secretaries, Mary Kerber, Donna Lamb, and Linda Mayo for administrative assistance;

To the numerous persons who conducted seminars (Appendix C);

And finally, to the University of Houston for overall support and encouragement throughout the project.

## TABLE OF CONTENTS

	Page
Project Logotype .....	ii
Authors and Credits .....	iii
Group Photograph .....	iv
Abstract .....	v
Foreword .....	v
Acknowledgements .....	vi
Table of Contents .....	vii
List of Figures .....	xiv
List of Tables .....	xix
CHAPTER 1 SUMMARY .....	1
1.1 Primary Objective and Tasks .....	2
1.2 Method of Attack .....	2
1.3 Structure of Study .....	2
1.4 Major Conclusions .....	2
1.5 Recommended Research and Development Areas .....	3
References .....	3
CHAPTER 2 INTRODUCTION .....	4
2.1 Energy Resources and Needs .....	5
2.2 Problem Background .....	5
2.3 Problem Statement .....	6
2.4 Definition of Terms .....	7
References .....	8
CHAPTER 3 STRUCTURES .....	9
3.1 Introduction .....	10
3.1.1 General .....	10
3.1.2 Loads .....	10
3.1.3 Structural Requirements .....	10
3.1.4 Structural Configuration .....	10
3.1.5 Material Requirements .....	10
3.1.6 Optimization .....	10
3.2 Choices Among Structural Possibilities .....	11
3.2.1 Nonmetallic Composite or Metal .....	11
3.2.2 Jointed Elements or Monocoque .....	11
3.2.3 Slat or Tube .....	11

3.2.4	Pinned or Fixed Joint .....	12
3.2.5	Lugs or Crimped or Shaped Ends .....	12
3.2.6	Adhesives or Fusing .....	12
3.3	Structural Materials .....	12
3.3.1	Material Requirements .....	12
3.3.2	Current State-of-the-Art .....	13
3.3.2.1	Adhesives .....	16
3.3.2.2	Coatings .....	16
3.3.3	Projected Development .....	17
3.4	Truss Configuration .....	17
3.4.1	Basis for Selection .....	17
3.4.2	Fabrication Site .....	17
3.4.3	Dimensions .....	17
3.4.4	Truss Pattern .....	18
3.5	A Comparison Between Thin Walled Tube and Slats .....	18
3.5.1	Basis of Comparison .....	18
3.5.2	Self-Healing Condition for Slat .....	21
3.5.3	Gross (Euler) Buckling of Element .....	22
3.5.4	Moment of Inertia of Slat .....	22
3.5.5	Local Buckling of Thin-Walled Tube .....	23
3.5.6	Local Buckling of Slat .....	23
3.5.7	Comparisons .....	24
3.6	Dynamics of SPS Truss Structures .....	25
3.6.1	Basis of Consideration .....	25
3.6.2	Response Times of Structure .....	26
3.6.3	Means of Estimation .....	27
3.7	Thruster Attachments .....	27
3.7.1	Basis of Consideration .....	27
3.7.2	Single Thruster Fixed-Mounting .....	27
3.7.3	Gimballed Manifold Mounting .....	28
3.7.4	Extent of Supplementary Structure .....	28
3.8	Column-Cable Configuration .....	28
3.8.1	The Concept .....	28
3.8.2	Geosynchronous Orbit Assembly .....	28
3.8.3	Low Earth Orbit Subassembly .....	29
3.8.4	Structural Hard Spots .....	29
3.9	Conclusions and Recommendations .....	30

3.9.1	Conclusions	30
3.9.2	Comments on Specific Design	31
3.9.3	Recommendations	31
	References	32
CHAPTER 4 TRANSPORTATION TO LOW EARTH ORBIT		33
4.1	Introduction	34
4.2	Launch Site	34
4.3	Cargo Vehicle	37
4.3.1	Specifications and Requirements	37
4.3.2	Candidates	38
4.3.3	Payload	40
4.3.4	Cost Estimates	43
4.3.5	Operations	47
4.4	Personnel Vehicle	48
4.4.1	Specifications and Requirements	48
4.4.2	Candidates	48
4.4.3	Personnel	49
4.4.4	Cost Estimates	49
4.4.5	Operations	49
4.5	Summary and Conclusions	49
	References	50
CHAPTER 5 ORBITAL TRANSFER BY ELECTRICAL PROPULSION		51
5.1	Introduction	52
5.2	Propulsion	52
5.2.1	Points of Concern and Problems	52
5.2.1.1	Availability	52
5.2.1.2	Environmental Impact	52
5.2.1.3	Cost	52
5.2.1.4	Thruster Mounting	52
5.2.1.5	Control and Power Conditioning	52
5.2.2	Thruster Characteristics and Solutions	52
5.2.2.1	Availability	52
5.2.2.2	Environmental Impact	54
5.2.2.3	Cost	54
5.2.2.4	Thruster Mounting	54
5.2.2.5	Control and Power Conditioning	54

5.3	Orbital Mechanics	54
5.3.1	Introduction	54
5.3.2	Geometry of the Transfer Spiral	55
5.3.3	Ideal, $\Delta V$ , Propellant Requirement	56
5.3.3.1	Coplanar Altitude Change	56
5.3.3.2	Plane Change	56
5.3.3.3	Propellant Required	56
5.3.4	Time History of Transfer	56
5.3.4.1	Coplanar Part of Transfer	56
5.3.4.2	The Plane Change	57
5.3.4.3	Occultation	57
5.3.5	Final Approach GEO	58
5.4	Space Environment Aspects	58
5.4.1	Aerodynamic Effects in Low Earth Orbit	58
5.4.1.1	Aerodynamic Environment	58
5.4.1.2	Orbital Lifetime	59
5.4.1.3	Effect of Differential Drag	60
5.4.2	Objects in Earth Orbit — The Potential Collision Problem	60
5.4.2.1	Introduction	60
5.4.2.2	Collision Probability Modeling Overview	62
5.4.2.3	The Pseudo Collision Model	63
5.4.2.4	The Langley Collision Model	63
5.4.2.5	The Approximate Collision Model	64
5.4.2.6	The Flux Model	66
5.4.2.7	Comparison of the Models	66
5.4.2.8	Conclusions and Recommendations	69
5.4.3	Radiation	70
5.4.3.1	Types of Radiation in Space	70
5.4.3.2	Environmental Effects on Man	74
5.4.3.3	Environmental Effects on Solar Cells	77
5.4.3.4	Conclusions and Recommendations	80
5.4.4	Exhaust Plume Considerations	81
5.4.4.1	Plume Effects	81
5.4.4.2	Thruster Placement	81
5.5	Design Requirements	83
5.5.1	Engine Selection Tradeoffs	83
5.5.1.1	Modeling Assumptions	83
5.5.1.2	Comparative Analysis of Electrical Thruster Performance	85

5.5.2	Transorbital Configurations .....	93
5.5.2.1	Configuration Comparisons .....	93
5.5.2.2	Module Design .....	93
5.6	Summary and Conclusions .....	95
5.6.1	Conclusions .....	95
5.6.2	Recommendations .....	96
	References .....	96
CHAPTER 6 ORBITAL TRANSFER BY CHEMICAL PROPULSION .....		99
6.1	Introduction and Ground Rules .....	100
6.2	Low Earth Orbit Staging Base .....	100
6.3	Cargo Transportation .....	102
6.3.1	Vehicle Types and Scaling .....	102
6.3.1.1	Reduction to Three Independent Variables .....	102
6.3.1.2	Absolute Simplicity in Mass Modeling .....	103
6.3.1.3	Absolute Simplicity in Flight Cost Modeling .....	103
6.3.1.4	Modeling Limits .....	103
6.3.2	Mass Modeling .....	103
6.3.2.1	The Model .....	103
6.3.2.2	Propellant to Payload Ratio .....	104
6.3.2.3	Vehicle to Payload Ratio .....	104
6.3.2.4	Tank to Payload Ratio .....	104
6.3.3	Flight Cost Modeling .....	105
6.3.3.1	The Model .....	105
6.3.3.2	Tankage Cost .....	105
6.3.3.3	Propellant Cost .....	106
6.3.3.4	Turnaround Fractionalized .....	106
6.3.4	Staging Rationale .....	106
6.3.4.1	Cost Aspects .....	106
6.3.4.2	Recoverability Aspects .....	107
6.3.4.3	Operations Aspects .....	107
6.3.5	Mode of Propellant Resupply .....	107
6.3.5.1	Impact on the Orbital Transfer Vehicle .....	109
6.3.5.2	Impact on the Heavy Lift Launch Vehicle Payload .....	110
6.3.5.3	Impact on the Space Trash Problem .....	112
6.3.5.4	Impact on the Staging Base Operation .....	112
6.4	Personnel Transportation .....	113
6.4.1	Personnel Carrier Module .....	113
6.4.1.1	Background and Related Factors .....	113
6.4.1.2	Requirements .....	113
6.4.1.3	Concerns .....	114
6.4.1.4	Physical Characteristics .....	114
6.4.2	Personnel Orbital Transfer Vehicle .....	116
6.4.2.1	Background .....	116
6.4.2.2	Discussion .....	117
6.5	Summary and Conclusion .....	117
6.6	Conclusions .....	118
	References .....	120

CHAPTER 7 CONSTRUCTION OF SOLAR POWER SATELLITE: FABRICATION & ASSEMBLY .....	121
7.1 Introduction .....	122
7.2 Technology Issues .....	122
7.2.1 Solar Blanket and Structures .....	122
7.2.1.1 Structures .....	122
7.2.1.2 Solar Blanket .....	122
7.2.1.3 Radiation Resistance .....	124
7.2.2 Power Distribution System .....	125
7.2.3 Microwave Antenna .....	126
7.2.3.1 Dc-rf Conversion .....	127
7.2.3.2 Transmitting Antenna and Phase Front Control .....	127
7.2.3.3 Pointing Control .....	128
7.3 Fabrication and Assembly .....	129
7.3.1 Solar Blanket and Structure .....	129
7.3.1.1 The Manual Mode .....	130
7.3.1.2 The Automated Mode .....	132
7.3.2 Power Distribution System .....	133
7.3.3 Microwave Antenna .....	134
7.3.3.1 Transmitting Antenna Primary Structure .....	135
7.3.3.2 Slotted Waveguide Subarray Panels .....	135
7.4 Control System .....	135
7.5 Construction Attitude Considerations .....	136
7.6 Construction Impact on the Transportation Cost .....	137
7.7 Summary and Conclusions .....	138
References .....	139
CHAPTER 8 ECONOMIC CONSIDERATIONS .....	140
8.1 Introduction .....	141
8.2 Cost Approach .....	141
8.2.1 Transportation Cost Model .....	141
8.2.2 Cost Estimating Methodology for Electrical Propulsion .....	142
8.3 Applications of the Transportation Cost Model .....	143
8.3.1 Baseline Data and Total Transportation Cost .....	144
8.3.2 Sensitivity Analysis .....	144
8.3.3 The Effect of Various Changes on Transportation Costs .....	144
8.3.3.1 Partial Assembly in LEO .....	147
8.3.3.2 Equatorial Launch .....	147
8.3.3.3 Transfer of Personnel by COTV .....	147
8.3.3.4 Reusability of the HLLV Payload Shroud .....	147
8.3.4 Synthesis .....	148
8.4 Electric Propulsion .....	148
8.5 Economic Comparison of Satellite Delivery Schemes .....	156
8.5.1 The Effect of Delivery Delays on the Time Value of Money .....	156
8.5.2 The Effect of the Time Value of Money on the Cost of Generated Electricity .....	158
8.5.3 Comparison of Capital Charge Requirements on Estimates of Future Electrical Charges .....	160
8.5.3.1 Effects of Interest Rates on Estimates of Future Electrical Charges .....	160
8.5.3.2 Regional Electrical Markets and the Economic Rationalization of the SPS Unit .....	161
8.5.4 Summary .....	161
8.6 Satellite Scheduling .....	161
8.6.1 The Effects of Scheduling on Payoff and Initial Funding .....	161

8.6.2	The Effects of Scheduling on Present Value .....	162
8.6.3	Satellite Scheduling Summarized .....	165
	References .....	166
CHAPTER 9 FINDINGS AND RECOMMENDATIONS .....		167
9.1	Summary of Mission Alternatives .....	168
9.2	Findings .....	168
9.2.1	Transportation .....	168
9.2.1.1	Earth Launch .....	168
9.2.1.2	Chemical Propulsion .....	168
9.2.1.3	Electrical Propulsion .....	169
9.2.1.4	Personnel Transportaiton .....	169
9.2.1.5	Transportation Economics .....	169
9.2.2	Space Environment .....	169
9.2.3	Solar Power Satellite .....	169
9.2.3.1	Structure .....	169
9.2.3.2	Fabrication and Assembly .....	170
9.3	Recommended Areas of Research and Development .....	170
9.3.1	General .....	170
9.3.2	Chemical Propulsion .....	170
9.3.3	Electrical Propulsion .....	170
9.3.4	Economic .....	170
9.3.5	Space Environment .....	170
9.3.6	Solar Power Satellite .....	171
9.3.6.1	Structure .....	171
9.3.6.2	Fabrication and Assembly .....	171
9.3.6.3	Space-Based Manufacturing Site .....	171
APPENDICES .....		172
A.	Statement of Work .....	173
B.	Institute Participants .....	177
C.	List of Project Seminars .....	181
D.	Consultants and Advisors .....	185
E.	Systems Analysis .....	187
F.	Glossary of Acronyms and Nomenclature .....	194
G.	Orbital Mechanics Formulae and Derivations .....	204
H.	Transportation Cost Model .....	215
I.	Development Models .....	221
J.	Gravity-Gradient Torques .....	224
K.	Electric Thruster Mass and Transportation Analysis Program .....	228
L.	Effect of Attitudinal Variations Relative to the Sum .....	239

## LIST OF FIGURES

### CHAPTER 2

2-1	JSC Baseline Configurations .....	6
2-2	Mission Alternatives .....	7

### CHAPTER 3

3-1	Choices Among Structural Possibilities .....	11
3-2	Fabrication of Thin-Wall Tubing From Flat Stock .....	12
3-3	Strength Properties of Conventional Alloys and Fiber Reinforced Composites at Room Temperature .....	15
3-4	Strength Loss of Carbon-Reinforced Plastics Due to Environmental Aging .....	15
3-5	Effect of Isothermal Exposure on Room Temperature Tensile Strength of Al. Matrix Composites ..	16
3-6	Influence of Thermal Cycling on Room Temperature Tensile Strength of Al. Matrix Composites ..	16
3-7	Basic Element of the Structure .....	18
3-8	Primary Truss of the Structure .....	20
3-9	Secondary Truss of the Structure .....	20
3-10	Truss Modules .....	20
3-11	Truss Segment for Transportation .....	20
3-12	Main Truss of the Structure .....	21
3-13	Curved Slat .....	21
3-14	Buckling Modes for Pinned End Column .....	22
3-15	Moment of Inertia of Curved Slat .....	23
3-16	Curved Slat-Local Buckling Region .....	23
3-17	Slat Definitions .....	24
3-18	Structural Response Times and Control Characteristic Times .....	26
3-19	Column-Cable Configuration .....	28
3-20	Folded Column-LEO Subassembly .....	29
3-21	Axial View: COTV with Folded Beam .....	30
3-22	Hard Spot (Structural Node) .....	30

### CHAPTER 4

4-1	Fuel and Total Velocity Required for Chemical Propulsion to GEO Versus Inclination Angle .....	34
4-2	Equatorial Candidates for Launch Sites .....	35
4-3	Christmas Island .....	37
4-4	Modified Single Stage to Orbit Launch Vehicle .....	38
4-5	Two Stage Winged Launch Vehicle .....	38
4-6	Two Stage Ballistic Launch Vehicle .....	39

4-7	Diameter and Area Versus Volume .....	40
4-8	Payload Capacity and Density Versus Shroud Mass .....	41
4-9	Shroud Costs .....	42
4-10	TFU and Average Unit Costs .....	42
4-11	Payload Mass Distribution (Full Shroud) .....	43
4-12	Payload Mass Distribution (Partial Shroud) .....	43
4-13	Uncertainty in Cost Composition of Average HLLV Mission .....	47
4-14	Personnel and Priority Cargo Launch Vehicle (PLV) .....	48

#### CHAPTER 5

5-1	Thruster/Propellant Selection .....	55
5-2	Typical Low Thrust Spiral Transfer Geometry .....	55
5-3	Geometry of Low Thrust Plane Change .....	56
5-4	Time vs. Altitude, Low Thrust Transfer .....	57
5-5	Low Thrust Program for Orbital Plane Change .....	57
5-6	Final Approach Phase to Desired Orbit .....	58
5-7	Lifetime in Circular Orbit .....	60
5-8	Pseudo Collision Model Geometry .....	63
5-9	Approximate Collision Model Geometry .....	64
5-10	Geometry of the Flux Model .....	68
5-11	Comparison of Four Collision Models .....	69
5-12	Region of Constant Radiation Flux .....	70
5-13	Dose Rates in the Earth's Radiation Belt .....	73
5-14	Accumulated Dose in Rads .....	73
5-15	No-shield Dose Accumulated During Orbital Transfer .....	73
5-16	Total Dose Rate as a Function of Shield Thickness .....	74
5-17	Comparison Between Doses Received in LEO and in GEO .....	77
5-18	Maximum Efficiency of Silicon Solar Cells Versus Temperature .....	79
5-19	Solar Cell Trade-offs for Orbital Transfer .....	81
5-20	Module With Engine Clusters .....	83
5-21	Module With Engine Clusters and Attitude Control .....	83
5-22	Corner Mounted Thrusters .....	83
5-23	Solar Cell Degradation .....	84
5-24	Mass Analysis .....	91
5-25	Solar Cell Deployment .....	92
5-26	SECS Growth .....	92
5-27	LEO Start Mass Sensitivity .....	92
5-28	Orbital Transfer Model .....	94

## CHAPTER 6

6-1	Unistage .....	102
6-2	Personnel Carrier Module on Unistage .....	102
6-3	Two and One-half Stage with HLLV Compatible Payload Based on Unistage .....	102
6-4	OTV Characteristics .....	108
6-5	Geosynchronous Ascent/Deboost Profile .....	108
6-6	Influences of Mode of Propellant Resupply .....	109
6-7	Orbital Transfer Vehicle Profiles .....	109
6-8	Potential HLLV Payload Compositions .....	110
6-9	Transportation Scenario I .....	111
6-10	Transportation Scenario II .....	112
6-11	Some Sources of Expendable Items .....	112
6-12	Tank Disposal for Scenario I .....	119
6-13	Mission Events Sequence for Personnel Carrier Module .....	114
6-14	Transfer at LEO of GEO Bound Passenger Module From Orbiter to OTV .....	115
6-15	Personnel Carrier Module .....	115
6-16	Personnel Orbital Transfer Vehicle Characteristics .....	117

## CHAPTER 7

7-1	A Typical P-N Junction Solar Cell .....	123
7-2	Efficiency Versus Gap Energy at Different Temperatures .....	124
7-3	Absorption Constant $\alpha$ Versus Energy .....	124
7-4	Functional Diagram for Power Distribution System .....	125
7-5	MPTS Concept .....	126
7-6	MPTS Functional Program .....	126
7-7	Amplatron Assembly .....	127
7-8	Outline of the 48 KW Solenoid Klystron .....	128
7-9	Microwave Power Beam - Idealized .....	129
7-10	Array-Subarray Organization .....	129
7-11	Command and Adaptive Phase Front Control Concepts .....	129
7-12	Microwave Antenna Mechanical Pointing System .....	129
7-13	Schematic Rotary Joint .....	130
7-14	Snap Joint Method .....	131
7-15	Basic Solar Cell Module Power Distribution .....	131
7-16	Partial Construction of Column/Cable Configuration .....	132
7-17	Construction Base Concept for Truss Configuration .....	132
7-18	Concept for Solar Cell and Concentrator Deployment .....	132

7-19	Computer-controlled Automatic Fabrication and Assembly Concept .....	133
7-20	Computer Graphics of Solar Array Structure .....	133
7-21	Computer Graphics of Microwave Antenna Structure .....	134
7-22	Power Distribution Lateral Power Flow .....	135
7-23	Functional Block Design Diagram of the SPS Flexible Body Altitude Control System .....	136

#### CHAPTER 8

8-1	Effect of Launch Site Latitude on $C_T$ .....	147
8-2	Cost of Transportation .....	149
8-3	Transportation Cost Components .....	154
8-4	Two Comparative Approaches .....	158
8-5	Scheduling Schemes for SPS System .....	163
8-6	Schedule A - Cash Flows .....	165
8-7	Schedule C - Cash Flows .....	165

#### APPENDIX E

E-1	Team Organization .....	188
E-2	Group Organization (Mid-Term Transition) .....	189
E-3	Administrative Organization .....	189
E-4	GANTT Chart .....	189
E-5	PERT Network .....	190
E-6	Systems Analysis Flow Chart - Final Report .....	191

#### APPENDIX G

G-1	Elliptic Transfer Trajectory from LEO to GEO .....	208
G-2	Geometry of Dog-Leg Maneuver Combining Plane Change With Circularization .....	208
G-3	Axis System for Equations of Motion .....	209
G-4	Ideal $\Delta V$ for Low-Thrust Circular Orbit Transfer .....	212
G-5	Stage Mass Fraction .....	212

#### APPENDIX I

I-1	SPS Population .....	223
I-2	Origin Shift .....	223
I-3	Unsymmetrical .....	223

#### APPENDIX J

J-1	Axes in the Orbit Plane .....	225
J-2	Orientations for Baton in Orbit .....	226

APPENDIX K

K-1A	COMBIN Flow Chart .....	230
K-1B	COMGIN Flow Chart .....	230
K-1C	COMBIN Flow Chart .....	231
K-1D	COMBIN Flow Chart .....	231

APPENDIX L

L-1	SECS Configuration .....	240
L-2	Geometry of Solar Concentrator .....	240
L-3	Geometry for $0 \leq \beta \leq 30^\circ$ .....	242
L-4	Geometry for $30 \leq \beta \leq 60^\circ$ .....	242
L-5	Effective Solar Concentration Ratio .....	243

LIST OF TABLES

CHAPTER 3

3-1	Comparison of Two Critical Parameters in Various Materials .....	13
3-2	List of Some Resin Matrix Composites .....	14
3-3	List of Some Metal Matrix Composites .....	14
3-4	Comparative Slenderness Ratios of Alternate Proposals .....	19
3-5	Buckling Criteria for Tubes and Slats .....	24
3-6	Response Times of Structure in Seconds .....	26

CHAPTER 4

4-1	Equatorial Launch Site Information .....	36
4-2	HLLV Candidate Features .....	40
4-3	DDT & E and TFU Costs for Two-stage Vehicles .....	44
4-4	DDT & E and TFU Costs for Payload Shrouds .....	45
4-5	Preliminary Cost Estimates of Factors Related to Reusability of HLLV's .....	46
4-6	Total Number of Personnel Vehicles and Trips .....	50
4-7	Shuttle-Derived Personnel Launch Vehicle Mission Costs .....	50

CHAPTER 5

5-1	Potential OTV Thruster Characteristics .....	53
5-2	Dynamic Pressure Based on Local Atmospheric Density and Circular Speed as a Function of Altitude .....	59
5-3	Altitude Loss per Orbit for Typical Objects in a 500 Km Altitude Circular Orbit .....	61
5-4	Pseudo Collision Model .....	64
5-5	Langley Collision Model .....	65
5-6	Approximate Collision Model .....	67
5-7	Increase in Spatial Density by Number of Objects for a Fixed Volume Element .....	67
5-8	Future Predictions of SPS Impact Rate Using the Flux Model .....	68
5-9	Chemical Composition of Galactic Cosmic Rays .....	71
5-10	Suggested Exposure Limits and Exposure Accumulation Rate Constraints .....	76
5-11	Damage to Solar Cells .....	79
5-12	Potential Degradation of Spacecraft Components from Impinging Propellants .....	82
5-13	Mass Fraction Estimates .....	86
5-14	Electrical Thruster Performance Data .....	87

## CHAPTER 6

6-1	OTV Mass Modeling Table .....	101
6-2	OTV Flight Cost Modeling .....	101
6-3	Number of HLLV Launches Required per SPS for Each Area Indicated .....	106
6-4	Expendable Items - The Alternatives .....	120

## CHAPTER 7

7-1	Dc-rf Converter Parameters .....	128
-----	----------------------------------	-----

## CHAPTER 8

8-1	Baseline Data .....	145
8-2	Baseline Transportation Cost Estimate .....	146
8-3	Sensitivity of Independent Parameters .....	146
8-4	Effect of Partial Assembly in LEO on Total Transportation Cost .....	148
8-5	Transportation Time-Cost Relationship for Variable Orbit Time Resistojet LH <sub>2</sub> .....	150
8-6	Transportation Time-Cost Relationship for Variable Orbit Times Arc-Jet LH <sub>2</sub> .....	151
8-7	Transportation Time-Cost Relationship for Variable Orbit Times Arc-Jet NH <sub>3</sub> .....	152
8-8	Transportation Time-Cost Relationship for Variable Orbit Times MPD Argon .....	153
8-9	Elasticity Measures for Electrical Propulsion .....	155
8-10	Total Transportation Cost-Electrical Propulsion .....	155
8-11	Total Cost - Electrical Propulsion .....	157
8-12	Interest Adjustment Factors for Delivery Delays of SPS Units .....	157
8-13	Baseline Cost Comparisons of Alternative Transportation Modes .....	159
8-14	Interest Factors for Capitol Charges in Annual Payments and Mills per Kilowatt Hour per Billion Dollar Cost of Completed SPS .....	159
8-15	1975 Electric Rates and 2000 Projections for Selected Areas, USA .....	162
8-16	Number of Years Required for SPS System to Cover All Capital Charges and Become Self-supporting at Various Scheduling Schemes and Interest Rates .....	163
8-17	Maximum Number of SPS Units Outstanding (Unpaid) for Various Scheduling Schemes at Various Rates of Interest .....	164
8-18	Present Values of Cash Inflows and Cash Outflows (Net of Operating and Maintenance Expenses) of SPS System for Various Scheduling Schemes and Interest Rates Expressed in Revenue Years .....	164
8-19	Considerations for Accelerated SPS Scheduling .....	166

APPENDIX E

E-1	Study Teams .....	192
E-2	Report Organization .....	193

APPENDIX K

K-1	Listing of Computer Program COMBIN .....	232
K-2	Electric Thruster Mass and Transportation Cost Analysis Program .....	237

**CHAPTER 1**  
**SUMMARY**

# CHAPTER 1

## SUMMARY

### 1.1 PRIMARY OBJECTIVE AND TASKS

The National Aeronautics and Space Agency has recently begun considering the feasibility of placing large Solar Power Satellites in geosynchronous orbit, capable of generating 10 gigawatts of electricity. These satellites are being studied with respect to alleviating projected long-term energy shortages.

The 1976 NASA/ASEE Systems Design Institute was given the task of exploring a portion of the Solar Power Satellite system, with special emphasis on transportation and construction options. The primary objective of the study was to explore the various approaches to transporting satellite components from earth to low earth orbit and subsequently to geosynchronous orbit.

In order to accomplish the study objective, NASA (Johnson Space Center) provided members of the design team with pertinent information from contractors and "in-house" studies (see Ref. 2-8) relating to the total system. Certain constraints were placed on the study in the form of ground rules. For example, the team was provided two baseline configurations of a satellite functioning in geosynchronous orbit. Both configurations included physical as well as various structural characteristics.

### 1.2 METHOD OF ATTACK

Three mission scenarios were identified in the original statement of work; two were selected for final consideration. The two scenarios were: (1) For electrical propulsion, construct square satellite modules in low earth orbit and transport to geosynchronous orbit for final assembly; (2) for chemical propulsion, use low earth orbit only as a depot, transporting materials to geosynchronous orbit for total construction and assembly.

Two teams were formed to analyze the mission scenarios. Each team elected a captain and recorder

to serve until mid-term. During the second half of the summer, the Faculty Fellows were divided into six working parties. The Study Manager and the Systems Design Institute Associate Director worked together in coordinating the activities of the 19 member Systems Design Institute.

### 1.3 STRUCTURE OF STUDY

As mentioned earlier, the main composition of the study evolved around two primary scenarios for electrical and chemical propulsion. These scenarios are discussed in detail in Chapters 5 and 6. The following two sections summarize the findings, conclusions, and recommendations of the eleven week design institute.

### 1.4 MAJOR CONCLUSIONS

As reported in Chapter 9, the preliminary nature and scope of the Solar Power Satellite concept, coupled with the project time constraints prevented the deduction of absolute conclusions. The design team did, however, reveal numerous factors which precipitated the following conclusions. Based on the findings of the team, and considering the basic assumptions as outlined within the chapters, three major conclusions were reached:

**a.** For chemical propulsion, complete assembly at GEO is recommended for the Solar Power Satellite.

**b.** For electrical propulsion, partial assembly of the satellite in square modules at LEO is recommended. The hydrogen electric arcjet appears to be the most likely candidate for solar-electric propulsion to GEO at this time.

**c.** The cost comparison between chemical and electrical propulsion yielded inconclusive results as to which would provide the lowest cost system. This conclusion was reached using the best information available for both systems. The degree of possible error in the data will have to be reduced in order to warrant further consideration.

## **1.5 RECOMMENDED RESEARCH AND DEVELOPMENT AREAS**

The findings and conclusions of the study are given in Chapter 9. The eight major areas for research and development identified in Chapter 9 are:

**a.** Further study is recommended regarding an equatorial launch site, regarding heavy lift launch vehicle risks and costs, and regarding orbital transfer vehicle mission profiles and cost.

**b.** More research is needed regarding cryogenic transfer in space, as well as compatibility of orbital transfer vehicle stages with heavy lift launch vehicle payload configurations.

**c.** Concerning electrical propulsion, a dedicated research program is needed to ascertain usability of thrusters, effect on the environment, and methods for optimizing orbital transfer.

**d.** An indepth study of the potential radiation hazards to personnel and materials in low earth and geosynchronous orbits should be initiated and a review of Space Radiation Standards is recommended.

**e.** An indepth investigation into the risks of collision of the Solar Power Satellite during construction with space debris is recommended. This must include the implications for location and modes of construction for the satellite.

**f.** The economic study revealed a need for further study in resource usage and market analysis.

**g.** Several areas regarding the Solar Power Satellite will require additional Research and Development such as new materials, adhesives, welding, and joining techniques.

**h.** An indepth study of the benefits of creating a space-based manufacturing site in support of any program requiring extensive fabrication in space is recommended.

**CHAPTER 2**  
**INTRODUCTION**

## CHAPTER 2

### INTRODUCTION

#### 2.1 ENERGY RESOURCES AND NEEDS

With uranium and fossil fuels heading towards depletion, solar energy has emerged as a promising alternative for long range energy needs. Sunlight, an indispensable item for sustaining life, is almost taken for granted by the vast majority of the world's peoples. Yet, as a solution to the energy crisis, the sun may be harnessed to produce electricity, synthetic liquid and gaseous fuels, and high temperature thermal energy for industrial processes. (Ref. 2-1).

According to ERDA (Energy Research and Development Administration), solar energy, the "white hat" of energy sources, is clean and boundless. The development has been accelerating in all its many forms. But to make solar energy economically competitive will require good, hard-nosed engineering. In 1976, a record 90 million dollars was allocated for seeking ways to convert sunshine into economical energy. By the end of this century, solar technology could fill about ten percent or more of the United States' energy needs (Ref. 2-2).

This nation is not alone in recognizing the potential of solar energy. Japan has announced its "Sunshine Project," for which multi-billion dollar expenditures are being planned over the next 25 years. Australia is planning an expanded solar energy program, and similar efforts are under way in Europe. The Soviet Union has had and is continuing to pursue a significant solar energy development program (Ref. 2-3).

#### 2.2 PROBLEM BACKGROUND

The idea of a Solar Power Satellite was first proposed in 1968 by Peter Glaser of the Arthur D. Little Company. The concept was presented later before a congressional committee on Energy and Space Technology. Glaser showed how solar energy can be converted directly to electricity by means of solar cells (photovoltaic conversion), from large satellites in geosynchronous earth orbit (Ref. 2-4).

The first successful solar cell was demonstrated in 1953. Nearly every spacecraft that has ever rocketed skyward has depended on these purple-blue panels of solar cells. The first totally solar-powered orbiting laboratory--NASA's Skylab Space Station--also was operated by solar cells. Though crippled after losing one wing of cells at launch, Skylab sustained nine astronauts for 171 days in orbit. The output of the remaining 840 square foot solar cell array kept the mission going.

Other satellite power concepts have been proposed such as POWERSAT by the Boeing Company. This idea uses a thermodynamic method of energy conversion, with large Rankin engines operating from solar reflector arrays (Ref. 2-5).

In contrast to thermodynamic conversion, photovoltaic conversion involves no moving parts, no circulating fluid, and no consumption of material. Furthermore, a solar cell can operate for long periods without maintenance (Ref. 2-6). However, serious degradation can occur if silicon cells are subjected to prolonged radiation exposure. New materials and innovative manufacturing methods are needed in order to produce solar cells at more reasonable prices.

One of the challenges of orbiting a satellite power station is to develop transportation delivery systems. Such programs as the Space Shuttle and Heavy Lift Launch Vehicle (HLLV) will be necessary to deliver satellite payloads to low earth orbit. By developing these and other space transportation capabilities, power stations could be constructed in orbit thus ridding our planet of much of the thermal pollution associated with power generation. Useful energy would be radiated to the earth's surface in the form of microwave beams, and finally, be converted back to electricity at high efficiency.

Ehrlicke claims the vacuum of space is a much more benign environment to machines than is the earth's surface with its humidity, fog, and corrosive salt air. A machine in space, unless it is vacuum sensitive, can operate indefinitely. Space (earth orbits for now, and

later, translunar regions) can provide a favorable sink for many industrial activities (Ref. 2-6).

According to Fletcher, space systems may not be the total answer to our energy needs, but they certainly represent one of the directions in which we should be looking. What is important is that we begin to consider other alternatives. If we had placed the same emphasis years ago on ways to utilize solar energy as we have put into the development of a nuclear generating capacity, we might already be well along the road to solving the energy shortage (Ref. 2-7).

### 2.3 PROBLEM STATEMENT

Numerous studies have been undertaken recently by NASA concerning Solar Power Satellite systems. In keeping with this theme, the 1976 Systems Design Institute was assigned the task of studying a special phase of the SPS system. Specifically, the objective of the study was to investigate and determine the relative merits of various approaches to transporting large quantities of material from low earth orbit and subsequently to geosynchronous orbit. (See Statement of Work, Appendix A). Pertaining to the SPS system, eight subsystems were identified in the work statement:

- a. Propulsion Systems (electrical and chemical)
- b. Orbital Mechanics
- c. Structures
- d. Power Systems
- e. Environmental (radiation) Effects
- f. Operational Suitability
- g. Manufacturing
- h. Economics

Ground rules were established to form a "working base" for the study. These rules were based on the statement of work and served as guidelines for limiting the scope of the total project. They were as follow:

- a. Use NASA (Johnson Space Center) baseline configurations for the Satellite Power Station, (Figure 2-1). These two configurations utilize photovoltaic solar arrays of 144 square kilometers each.
- b. The study team was provided Solar Power Satellite Data from Johnson Space Center studies (Ref. 2-8). Additional information was obtained from various NASA contractors.
- c. The study design was to be compatible with future space transportation systems such as the Space Shuttle, Heavy Lift Launch Vehicle, and others.

Among the most significant areas of investigation was how to transport personnel and materials from earth to low orbit and subsequently to geosynchronous orbit. In addition, two types of propulsion, electrical and chemical, were considered for orbital transfer. (Two teams, operating in parallel, were organized around the two propulsion alternatives, Appendix E.) The third major factor in the systems study was where to construct and assemble the satellite components, at LEO or GEO?

Three mission scenarios were identified in the original work statement; the design team identified a fourth for consideration. The four mission alternatives were as follow:

#### Chemical Propulsion (Orbital Transfer)

- a. Partial Assembly in LEO, Module transfer to GEO
- b. Complete Assembly in GEO, Depot services only in LEO

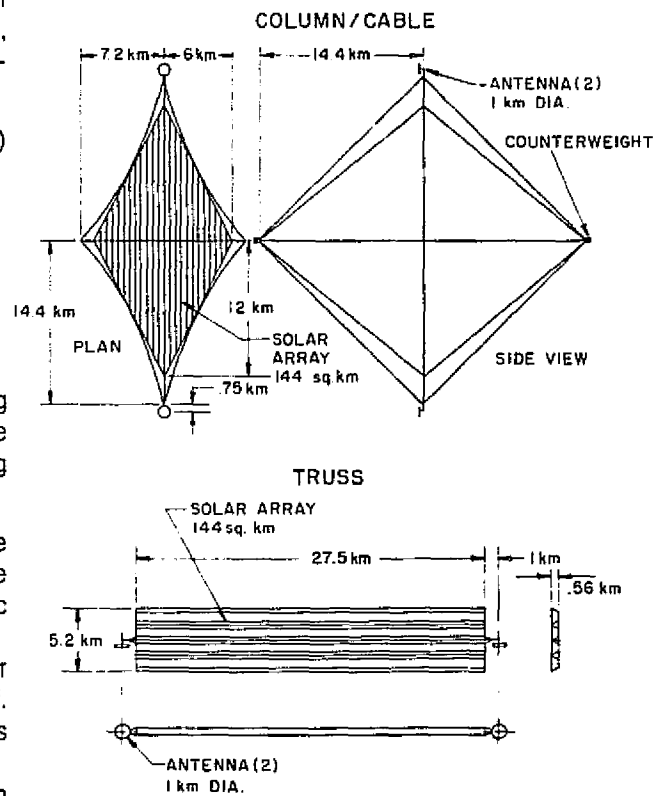


FIGURE 2-1 NASA (JSC) BASELINE CONFIGURATIONS

**Electric Propulsion (Orbital Transfer)**

**c.** Partial Assembly in LEO, Module transfer to GEO

**d.** Full Assembly in LEO, transfer of entire SPS to GEO

Due to technical and economic reasons, options a and d were not considered in any depth. Options b and c were chosen (Fig. 2-2) and received primary consideration, one option per team.

**2.4 DEFINITION OF TERMS**

Among the Terms used most frequently in this report are the following:

**SPS**--Solar Power Satellite, one of two baseline configurations with a 144 square kilometer photovoltaic solar array, as specified by the NASA Johnson Space Center Study (Ref. 2-8).

**LEO**--Low Earth Orbit, 270 mile altitude.

**GEO**--Geosynchronous Orbit, 22,300 mile altitude.

**Gigawatts**-- $10^9$  watts.

**HLLV**--Heavy Lift Launch Vehicle, under study for transporting large quantities of material from earth to low earth orbit.

**OTV**--Orbital Transfer Vehicle, for transferring payloads from LEO to GEO.

**POTV**--Personnel Orbital Transfer Vehicle.

**SECS**--Solar Energy Collection System.

A comprehensive listing of terms, acronyms, and nomenclature is in Appendix F.

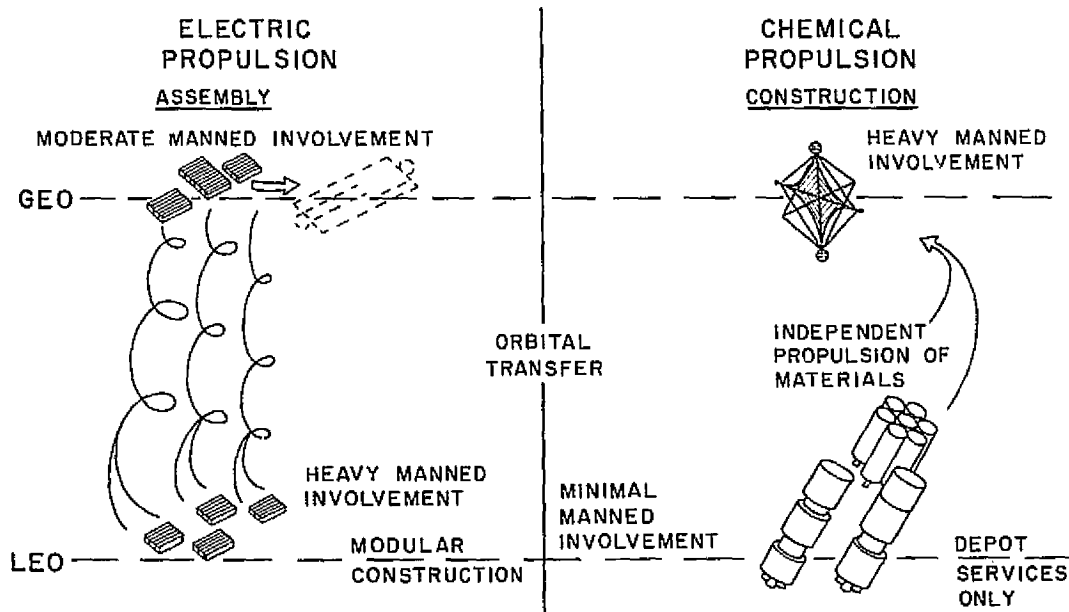


FIGURE 2-2 CONSTRUCTION AND PLACEMENT OPTIONS

## REFERENCES

**2-1** Harnessing the Sun's Energy for Heating and Cooling, National Aeronautics and Space Administration, George C. Marshall Space Flight Center, Huntsville, Alabama.

**2-2** Wilhelm, John L., "Solar Energy, the Ultimate Powerhouse," National Geographic, March 1976, pp. 381-397.

**2-3** Glaser, Peter E., "The Solar Energy Options--Approaches to Develop New Energy Resources," A paper presented National Engineers Week, Boston, MA, February 1975.

**2-4** Glaser, Peter E., "The Satellite Solar Power Station--A Focus for Future Space Activities," presentation to the Subcommittee on Science and Technology, U.S. House of Representatives, July 22, 1975.

**2-5** Taylor, Richard W., "POWERSAT, A Viable Solar Power Option," Supplement to Senate Subcommittee on Aerospace Technology and National Needs, January 19, 1975.

**2-6** Ehrlicke, Krafft, "Space Shuttle--Social Relevance," Skyline, Vol. 30, No. 2, North American Rockwell, 1972, pp. 50-55.

**2-7** Fletcher, James C., Administrator, National Aeronautics and Space Administration, from an address delivered at the National Academy of Engineering in Washington, D.C., November 1975.

**2-8** Initial Technical, Environmental, and Economic Evaluation of Space Solar Power Concepts, Volumes I and II, NASA Lyndon B. Johnson Space Center, July 15, 1976.

**CHAPTER 3**  
**STRUCTURES**

## CHAPTER 3

### STRUCTURES

#### 3.1 INTRODUCTION

The SPS unit consists of a solar-array 144 Km<sup>2</sup> in area, two antennas of 1 Km diameter each and joints to make the whole unit knit together with all the needed mobility for relative motion. The structure needed to support such a system should be able to maintain its integrity under the dynamic and static forces that may be imposed on it during its construction, fabrication, transportation, and during the lifetime of the structure.

##### 3.1.1 General

The largest items of mass are the solar cell blankets. According to the preliminary estimate by NASA, they constitute about fifty percent of the total weight of the SPS.

The design of the structure depends upon: (1) the loads that the structure has to withstand, (2) the structural requirements such as stiffness and stability, (3) the materials of which it is built, and (4) the optimization processes that properly combine all these variables.

##### 3.1.2 Loads

The primary natural load in geosynchronous orbit is the gravity gradient torque. At low altitude, aerodynamic drag and gravity gradient are important considerations. Other loads on the structure are thruster loads, current loop interaction with the magnetic field of the earth, microwave recoil from the antenna, loads due to thermal gradient arising from eclipses, and solar pressure. The emphasis in design, therefore, is on dynamic characteristics of the structure. The structure should be able to maintain its shape and dimensions under the loads to maintain the solar cell blanket in required alignment always.

##### 3.1.3. Structural Requirements

The structure should not only support the solar arrays, the conductors, the antennae, etc., without yielding under the thermal stresses in space, but also should be strong enough to permit rotation about its own axis so

as to ensure that the solar cells are always facing the sun during its orbit around the earth. To achieve this objective, the structure should be quite stiff, essentially rigid.

In case of electric propulsion, for which the truss structure is most suitable, and for easy transportation from LEO to GEO, the structure will have to be fabricated in parts. Each such segment should not only possess sufficient stiffness for itself, but should also be rigid enough to be easy to assemble with other segments in GEO. The structural segments should have nodes or "hard spots" for proper attachment of thrusters, antennae, etc.

##### 3.1.4 Structural Configuration

The several types of structures proposed in the many preliminary studies by NASA and other agencies can be grouped into two categories. In this report the "Column-Cable" concept and the "Truss" concept are discussed as examples under each one of these two categories.

##### 3.1.5. Material Requirements

The material used for building the structure should have a high elastic modulus to density ratio and should have been chosen in accordance with the principle of least weight for required strength. It should have a low coefficient of thermal expansion, be highly resistant to radiation, and be readily amenable to space fabrication. In addition, the material should have low volatility so there will be essentially no out-gassing in space.

The material has to be such as to have minimum or no degradation in the space environment. The material should be easy to manipulate both with remote control and with EVA in space.

##### 3.1.6. Optimization

The design of any large engineering system involves many aspects of loads, deflections, and other requirements so that optimization is inevitable. Some of the factors that have to be considered are: (1) least weight

for the required strength versus overall stability, (2) minimum production difficulties versus component complexity and automation, (3) minimum service troubles versus capital cost, (4) maximum reliability versus miniaturization and multiplicity. The best design must compromise the variables and meet the requirements and functions of the structure as nearly as possible.

### 3.2 CHOICES AMONG STRUCTURAL POSSIBILITIES

#### 3.2.1 Nonmetallic Composite or Metal

The flow chart (Fig. 3-1) indicates some of the choices faced by the structural designer. Some of these choices have been carefully considered, some briefly considered. A lack of necessary test information or knowledge causes some choices to remain unaddressed.

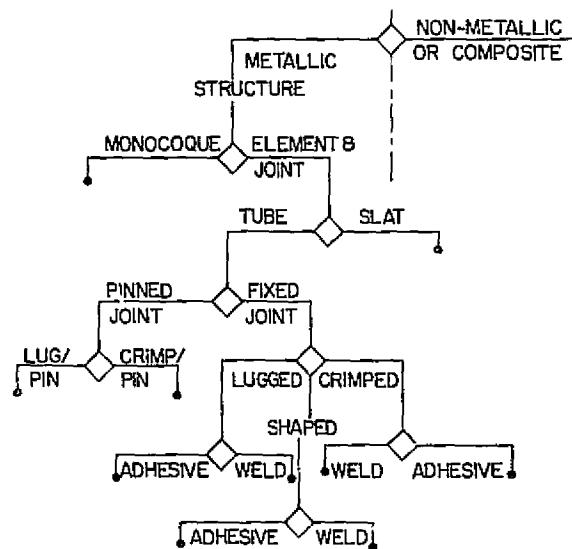


FIGURE 3-1 CHOICES AMONG STRUCTURAL POSSIBILITIES

Figure 3-1 is to be considered to be bilaterally symmetric about the centerline, through the choice of the nature of the material, whether metallic or a non-metallic or composite, and this choice is one that remains unaddressed. Advantages and disadvantages of both metals and composites for this application are known, but the behavior of nonmetallics and com-

posite matrices in the environmental extremes of space is not known sufficiently well and many such materials may even be unqualified for service in space. Any structural material is subject to degradation when exposed to a flux of energetic particles such as would be encountered in the Van Allen radiation belt, and composite matrices may be more sensitive than metals. Many plastics, including acrylics, styrenes, and polyesters are known to be sensitive to, and to degrade, in the presence of ultraviolet radiation, and it is typical that noncrystalline materials, polymers included, change their mechanical properties drastically with changes in temperature. If there are volatile components such as plasticizers in a composite matrix, they will evaporate into the vacuum of space.

Palliatives exist for many of the problems, for example, coatings may serve to protect polymers from ultraviolet radiation. In addition, the relatively low coefficient of linear thermal expansion of composites ( $.4$  to  $1.4 \times 10^{-5} \text{C}^{-1}$ ) as compared with aluminums ( $2$  to  $2.5 \times 10^{-5} \text{C}^{-1}$ ) (Ref. 3-1) is very attractive and may indeed be a necessity for control of the alignment of the transmitting antennas.

#### 3.2.2 Jointed Elements or Monocoque

A monocoque or stressed-skin structure is usually considered for large, extensive structures, especially if loading is diffuse rather than concentrated. It occurs that jointed substructures, or trusses made of elements, can be designed to accept the loads and still contribute a small percentage of the overall mass of the satellite. If a monocoque baffled box of the same extent and mass were to be built, its skin thickness would be impractically small, on the order of  $10^{-3}$  mm.

#### 3.2.3 Slat or Tube

Structural elements consisting of curved slats have been considered but passed over in favor of a more conventional tube structure. In spite of many advantages of such a structure of slats, it is felt that the tube structure offers more, especially in terms of strength adequate to carry the loads of orbit transfer. This subject is examined in greater detail within the chapter.

### 3.2.4 Pinned or Fixed Joint

Under usual circumstances, the choice of a pinned joint or a fixed joint offers a unique set of advantages and disadvantages. The fixed joint structure ideally is stronger and better able to resist buckling loads due to the increased fixity at the joints but in actuality may put elements closer to buckling due to eccentricities resulting from assembly or loading deformations. The ideal pinned joint, on the other hand, is very difficult to achieve, especially so in space where only dry lubricants have any effect. It is felt that fixed joints offer more advantages, both in terms of buckling strength and in terms of predictability, than pinned joints.

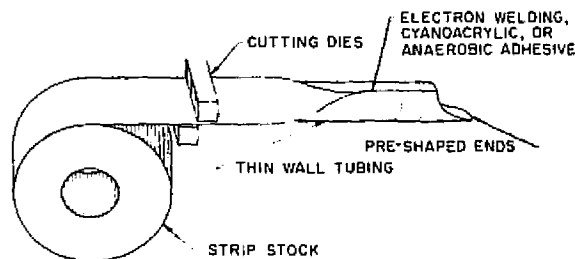


FIGURE 3-2 FABRICATION OF THIN WALL-TUBING FROM FLAT STOCK  
Note: Ends are pre-shaped by die cutting to allow mating fit to adjacent tubes in structure

### 3.2.5 Lugs or Crimped or Shaped Ends

Fixing the ends of the structural elements provides many choices--attachment can be via formed lugs, by crimped ends, or by the ends being cut to shape and mated. Lugs add substantially to the weight of the structure and prospects for manufacture of lugs to sufficiently fine tolerance to accept tubes of the order of 0.01 cm wall thickness snugly are poor. Crimped ends combine disadvantages of pinned-joint and fixed-joint construction, and ends die-cut to shape seem to offer the best prospects.

### 3.2.6 Adhesives or Fusing

Note that a number of different die-cut end shapes will be required, and these may be manufactured in space from strip stock by use of the proper dies as suggested in the drawing, Fig. 3-2. Mating of adjacent tubes would, of necessity, be either by adhesive bonding or by welding or brazing. Any are possible, and no attempt has been made to distinguish amongst them as a decision will depend strongly on choice of materials and there are many unknown factors. The response of structural adhesives to the space environment, techniques for welding and brazing thin-wall members with acceptable distortion, and many other matters will require further study.

## 3.3 STRUCTURAL MATERIALS

The study of materials that could be used for the construction of the SPS (Solar Power Satellite) involves a wide range of macrostructures. In this section, we will

focus attention on the materials that could be used for the construction of the basic support frame of the SPS. Later chapters will deal with materials used for power distribution, solar blankets, solar concentrators, as well as antenna sub-arrays and microwave transmission systems

As with other sections of this report, this section is not intended to be a definitive study of the SPS; it is, however, the intention of this section to illuminate some areas of study that deal with materials, especially as they pertain to the structure of the SPS. Along with this intent, is the desire to support the goal of this report which is to be an "Analysis of Alternatives for Transporting Material to Geosynchronous Orbit" (Ref. 3-2).

### 3.3.1 Material Requirements

The materials selected for the construction of the structure would meet certain requirements as demanded by the space environment and by the nature and size of the satellite. These requirements are:

- High modulus/density ratio
- Low coefficient of thermal expansion
- Able to withstand UV radiation
- Able to withstand nuclear radiation
- Have low volatility
- Have a low dissipation factor in the microwave frequency range
- Good interlaminar bonding strength (composites)
- Ease of fabrication (manufacture in space).

### 3.3.2 Current State-of-the-Art

At this early stage in the design process, engineers at NASA-JSC and MSFC have estimated the mass of the SPS structure (excluding the rotary joints and antennas) to be less than 10% of the total mass of the SPS. This means that the structure has a low density which will require adequate stiffness characteristics. The stiffness will be a major parameter in the design of the SPS due to the fact that the large area of the satellite makes the structure flexible.

In the various studies that have already been made by NASA and by contractors, there appears to be a common recommendation on the possible candidates for structural materials. This recommendation involves composites. NASA-JSC, for example, suggests: aluminum/boron, epoxy/graphite, and Kevlar 40 fiber, as well as aluminum alloys, and even stainless steel. In comparing the characteristics of metals vs. composites we notice there are various differences, two of which are critical in the design of the SPS; and these are (1) density and (2) coefficient of thermal expansion. See Table 3-1.

This comparison of two critical parameters may help in narrowing down the field of candidate materials which are being studied. First of all, if a heavy material can be replaced with a lighter one (without penalizing stiff-

ness), then a tremendous savings in launching costs can be realized. Not only would the costs to launch from earth to LEO be lower, but also the costs of orbit transfer between LEO and GEO. Another advantage of a lighter material is that it helps to minimize the moment of inertia of the satellite. Secondly, in choosing a material with a low coefficient of thermal expansion it is possible to reduce distortions and induced oscillations caused by thermal stresses. This also helps to maintain proper alignment of the satellite and its antennas.

Another advantage in using a material like graphite/epoxy or graphite/polyimide for the construction of the antenna would be that it would allow up to 8,100 W/m<sup>2</sup> maximum waste heat power density. Aluminum would only allow up to 3,800 W/m<sup>2</sup>. Furthermore, the use of a composite (such as graphite/polyimide) would allow a desirable 5.1 db taper for the microwave converter Gaussian distribution (Ref. 3-3). This characteristic is in keeping with the requirement that the material have a low dissipation factor in the microwave range. The subject of construction of the antenna reflectors will be addressed in more detail in Chapter 7. Suffice it to say that "graphite/epoxy materials and manufacturing techniques have been developed which are suitable for fabrication of lightweight low distortion antenna reflectors" (Ref. 3-4).

Table 3-1 COMPARISON OF TWO CRITICAL PARAMETERS IN VARIOUS MATERIALS

MATERIAL	DENSITY (g/cm <sup>3</sup> )	COEFFICIENT OF THERMAL EXP.
Aluminum	2.62 - 2.82	13.7 x 10 <sup>-6</sup> in/in/°F
Titanium	4.43 - 4.73	7.1 x 10 <sup>-6</sup> in/in/°F
Steel	7.75 - 8.14	8.3 x 10 <sup>-6</sup> in/in/°F
Graphite/Epoxy	1.12 - 2.40	0.5 x 10 <sup>-6</sup> in 0° dir 0.9 x 10 <sup>-6</sup> in 90° dir
Boron/Aluminum	1.12 - 2.40	3.3 x 10 <sup>-6</sup> in 0° dir 10.7 x 10 <sup>-6</sup> in 90° dir

Table 3-2 LIST OF SOME RESIN MATRIX COMPOSITES

MATRIX CONSTITUENTS	REINFORCING MATERIAL	
1. Epoxies	1. Glass Fibers	
2. Polyesters	2. S Glass	
3. Silicones	3. E Glass	
4. Polyimides	4. A Glass	12. Aluminum Oxide
5. Polybenzothiazoles	5. C Glass	13. MAR Steel
6. Polyquinoxalines	6. D Glass	14. Iron Whiskers
7. Pyrroles	7. Boron Fiber	15. Tungsten
8. Polybenzimidazoles	8. Graphite	
9. Polysulfones	9. PRD-49 Fiber	
10. Polyethersulfones	10. Silicon Carbide	
11. Polyarylsulfones	11. Quartz	

Table 3-3 LIST OF SOME METAL MATRIX COMPOSITES

METAL MATRIX COMPOSITES		
MATRIX CONSTITUENTS	REINFORCING MATERIAL	
Aluminum	Boron	SiO <sub>2</sub>
Titanium	Steel	Borsic (Boron Silicon Carbide)
Super Alloys	Beryllium	SiC (Silicon Carbide)
Nickel	S Glass	Graphite

Composite materials may be broken down into two main categories: (1) Resin matrix composites, Table 3-2 and (2) Metal matrix composites, Table 3-3.

108 Figure 3-3 shows strength properties of conventional alloys and advanced fiber reinforced composites at room temperature. Experiments as well as some actual practical applications have shown that temperature can have an adverse affect on the specific strength of various materials. Metals can withstand higher temperatures than can composites, as a general rule. But both types of materials suffer damage and weaken considerably at very high temperatures. Some composites even suffer at room temperature (daily fluctuations) due to "environmental aging." One example is given in Fig. 3-4 where two particular types of carbon-reinforced plastics lost considerable strength over a period of 200 days. If composites are going to be used for any construction in space, especially if they are going to be used for the construction of the structure, they must be able to withstand temperature variations and cycling between  $-160^{\circ}$  to  $+93^{\circ}\text{C}$  ( $-256^{\circ}$  to  $+200^{\circ}\text{F}$ ). This requirement can be met by several composite materials now on the market. A perfect example of a composite material being used for a structure on a geosynchronous satellite is a graphite epoxy reflector support truss for the Applications Technology Satellite (ATS).

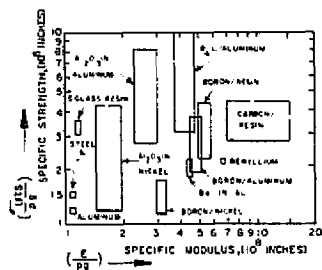


FIGURE 3-3 STRENGTH PROPERTIES OF CONVENTIONAL ALLOYS AND FIBER REINFORCED COMPOSITES AT ROOM TEMPERATURE REF 3-5

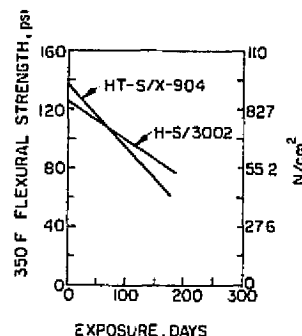


FIGURE 3-4 STRENGTH LOSS OF CARBON - REINFORCED PLASTICS DUE TO ENVIRONMENTAL AGING (EXPOSED AT ROOM TEMPERATURE, AMBIENT RELATIVE HUMIDITY) REF 3-6

Metal Matrix composites have some advantages over resin matrix composites; for instance, they can be processed using conventional metallurgical operations, and:

- they are able to conduct electricity
- they can conduct heat
- they have the matrix shear strength
- they have abrasion resistance
- they can be joined
- they have ductility
- they can be coated easily.

According to a recent NASA Tech Brief (Ref. 3-7) Marshall Space Flight Center conducted some tests on aluminum/boron and aluminum/graphite composites by subjecting them to metal working methods such as drawing and rolling. It was found that FI/B composite fabrication was not as fast as that of fabricating homogeneous metals, however, it was fast enough to reduce fabrication costs. It was also found that graphite composites were not readily adaptable to these metal working techniques. One possible solution may be to use electron beam heating which is an expensive method.

Another interesting study conducted at TRW Inc. (Ref. 3-8), see Figs. 3-5 and 3-6, shows where five types of aluminum matrix composites were subjected to high temperatures. In one case isothermal exposure and in another thermal cycling exposure--both to see what effect they would have on Room Temperature Tensile Strength. Note that the highest temperature is beyond the temperature encountered at GEO.

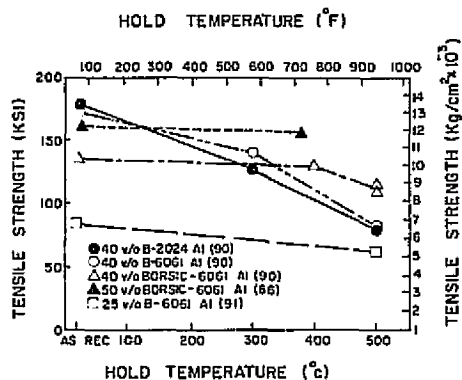


FIGURE 3-5 EFFECT OF ISOTHERMAL EXPOSURES ON ROOM TEMPERATURE TENSILE STRENGTH OF AL MATRIX COMPOSITES(REF 3-8)

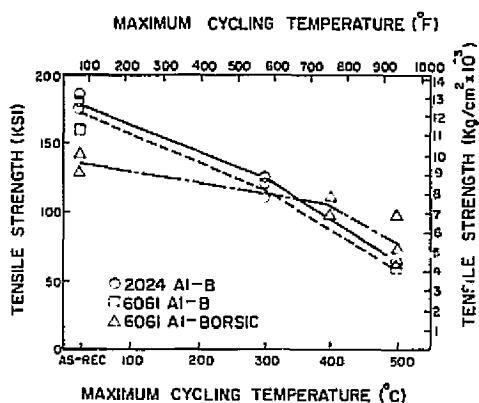


FIGURE 3-6 INFLUENCE OF THERMAL CYCLING (2000 CYCLES) ON ROOM TEMPERATURE TENSILE STRENGTH OF AL MATRIX COMPOSITES (REF. 3-8)

### 3.3.2.1 ADHESIVES

Adhesives have an advantage over conventional fasteners in aerospace vehicles and structures due to their low density as well as to their characteristic resistance to fatigue and corrosion. Adhesives can also join a large number of dissimilar materials (structural as well as non-structural). In order for adhesives to perform well in a space environment they must also exhibit:

- good lap shear strength
- good peel strength
- long term aging

These qualities have been improved for adhesives for such characteristics as:

over the past 25 years, however, more research and development needs to be done especially to improve long term aging.

One of the problems that has always plagued adhesives (such as polyimide adhesives) is the problem of degradation due to volatiles produced by out-gassing. This problem has been reduced, however, by beginning with a low VCM (Volatile Condensable Material) adhesive and baking the components that have been adhered in a thermal vacuum.

Currently several manned spacecraft such as mariner and pioneer (whose missions are projected to last from several months to several years) are using epoxy based adhesives in their structures. Other adhesive systems that have been used in the space program include nitrile-phenolic adhesives as well as epoxy-nylon adhesives.

Adhesives that are currently being considered for space applications and are being tested in laboratories include:

- PMDA (pyromellitic dianhydride)
- NMP or LARC-3 (N-methylpyrrolidone)
- BTDA (3, 3', 4, 4'-benzophenone tetracarboxylic acid dianhydride)

These polyimide adhesives have shown excellent lap shear strength for short periods of time at temperatures of 500°F and moderate lap shear strength for longer durations. Some of these adhesives have been shown to bind metals with non-metals; LARC-3, for example, shows promise in binding Titanium and a polyimide/graphite composite or a polyimide/glass composite.

Further studies on adhesives are needed. Other systems that may be worth exploring include the cyanoacrylates and the anaerobic adhesives.

### 3.3.2.2 COATINGS

The protection of structural materials such as composites and adhesives can be enhanced by the use of coatings. These can be either an inorganic paint system or a reflective metal applied by vapor deposition.

The selection of a coating system to be used in a space environment must include careful consideration

for such characteristics as:

- Resistance to outgassing (low volatile material)
- Resistance to UV radiation
- Resistance to high energy particulate radiation
- Little or no weight loss upon heating
- Good overall thermal control (-256°F to +200°F)

### Inorganic Paint System

These coatings consist of refractory or ceramic type pigment, dispersed in an inorganic vehicle. An example of one of these type coatings is Z-93. Z-93 is a zinc oxide in potassium silicate. It has been used on the Apollo Command Service Module where it was exposed to 650°C (1200°F) temperatures created by the RCS plume impingement.

### 3.3.3 Projected Development

"Carbon fibers are becoming of greater interest, and looking further ahead, silicon carbide and perhaps single crystal alumina (sapphire) may find application in aluminum matrix composites of the future," (p. 141, Ref. 3-8).

"In the more distant future it is likely that boron will be replaced by continuous graphite filament as a reinforcement for aluminum. It is predicted that advanced graphite reinforced aluminum produced from inherently low cost raw materials by the continuous casting process will be developed to achieve a price of well under \$50/lb." (p. 201, Ref. 3-8.)

## 3.4 TRUSS CONFIGURATION

### 3.4.1 Basis for Selection

The major portion of SPS (Solar Power Satellite) is the structure to support the solar array. This has to be rigid enough to maintain its shape under the dynamic effects of attitude control, transportation, etc. For construction in space, it is advantageous to have modular construction. As much of automation as possible in fabrication is desirable. Repetitive process makes automation more feasible. The transportation from LEO to GEO will be simpler if the huge structure can be divided into symmetrical parts of smaller sizes.

The space truss configuration seems to be the structural configuration which can satisfy the above requirements more readily than others. However, the other

type of configuration considered, namely "Column-Cable," Configuration has an advantage of having considerably less mass than the truss configuration.

### 3.4.2 Fabrication Site

Earlier investigations by NASA-JSC and others, have indicated that it is desirable to have most of the fabrication, if possible, in LEO and then transport the fabricated parts of the structure to GEO, with minimum of assembly done in GEO to place the satellite in operation. Further considerations (see section on Orbital Mechanics) describe some very serious difficulties of LEO fabrication. The transportation from LEO to GEO will be simpler if the dimensions of the object to be transported are equal, as a square block. The truss configuration is easily capable of being divided into small symmetrical units for transportation purposes, and at the same time maintaining that the bulk of the fabrication is to be done in LEO. This has a definite advantage when electrical propulsion is used for transportation. The small part of the truss will have part of its solar array to supply the needed power for transportation.

### 3.4.3 Dimensions

The base line for truss configuration considered in this report is the same as proposed by NASA-JSC in their report--"Initial Technical, Environmental, and Economic Evaluation of Space Solar Power Concepts" of July 15, 1976 (Ref. 3-9).

The most significant dynamic loading frequency is the 12-hour gravity gradient cycle. NASA-JSC has selected a minimum natural frequency of  $2.3 \times 10^{-4}$  Hz. to keep the dynamic response to a minimum and arrived at the conclusion that the depth of the truss should be of the order of 600 m. The depth of 560 m and a width of 5200 m in the NASA-JSC report (Ref. 3-9) has been used for computations of this report. The 5200 m width allows for placing eight solar cell blankets, 650 m wide with reflecting surfaces side-by-side providing a concentration factor of two. The solar cells are placed at half-depth. The reduction in truss depth along the direction of width of the truss is compensated by the shorter dimension of width to maintain the rigidity along that direction.

The length of the truss, however, has been slightly modified. Modification is based on the assumed size of

the segments of truss for transportation from LEO to GEO. As the inertia forces and thruster sizes depend on the dimension of the segment to be transported, it is found to be advantageous to have the truss divided into smaller segments for transportation purposes. Asymmetrical segments will have minimum problems for transportation, truss segments 2.6 Km by 2.6 Km were selected as basic units for transportation. Twenty-two of such segments will give an area of 28.6 Km by 5.2 Km for the entire truss as against 27.5 Km by 5.2 Km proposed in the report (Ref. 3-9).

### 3.4.4 Truss Pattern

The selection of the truss pattern has to satisfy the criteria of simplicity, ease with which it can be assembled in space, ease with which it can be automated with remote control, and structural stiffness. It is evident that innumerable solutions are feasible, all satisfying these criteria.

The pattern that is selected for discussion in this report is, with slight modification, one that is proposed in the NASA report. The modifications are based on the following assumed guidelines.

- a. It is simpler to carry one type of material into space, such as rolls of slat-strips, than two types, such as slat-strips and cables.
- b. The entire truss configuration is triangulated. This completely avoids using cables.
- c. The Longest member in the proposed configuration is smaller than used in the original NASA study.
- d. The slenderness ratios ( $L/p$ ) of the members in this proposal are close to the design assumptions of 200, but on the conservative side.
- e. When the truss is assembled in 22 parts in LEO, for easy transportation to GEO each unit is rigid and square in shape.
- f. The basic element of the truss, namely tube, is made from a slat of greater width than assumed in the report (Ref. 3-9).
- g. The longest lengths of the tube (with which the primary truss is assembled), the dimension of the primary truss (with which the secondary truss is fabricated) and the dimensions of the secondary truss (with which the main truss is constructed) are different from the NASA proposal. The modifications make the structure more rigid.

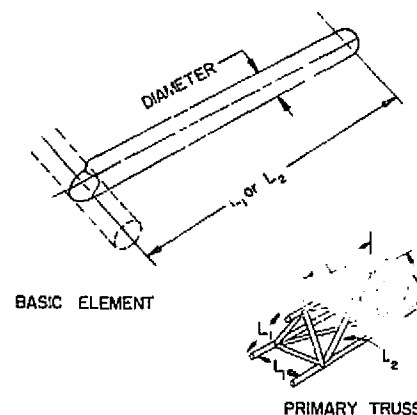
h. The proposed prism truss modules are much simpler to fabricate (and for automation and modular construction) than the pyramid configuration suggested in the NASA proposal.

i. The increase in the weight of the structure due to this modification is negligible. Even otherwise this will be minor as the weight of the structures forms a very minor fraction of the total weight of the SPS. Table 3-4 and Figures 3-7 and 3-12 illustrate the comparative properties of the NASA-JSC proposal and other proposals presented in this report.

## 3.5 A COMPARISON BETWEEN THIN-WALLED TUBES AND SLATS

### 3.5.1 Basis of Comparison

The use of curved slats of configuration similar to Venetian blind slats has been proposed as the basic structural element in certain orbiting solar power stations. See, for example, SPS Survey Report (Ref. 3-10). Such an unconventional structural element presents several advantages, such as compact storage by nesting, ease of fabrication, and the possibility of



ALTERNATES		I	II	III	IV	V
THICKNESS	cm	0.0127	0.0127	0.00635	0.00635	0.00635
DIAMETER	cm	16	16	16	16	2.35
$L_1$	cm	250	400	450	450	450
$L_2$	cm	350	570	640	640	640
$L_2/p$		61	100	113	113	77

FIGURE 3-7 BASIC ELEMENT (TUBE) OF THE STRUCTURE

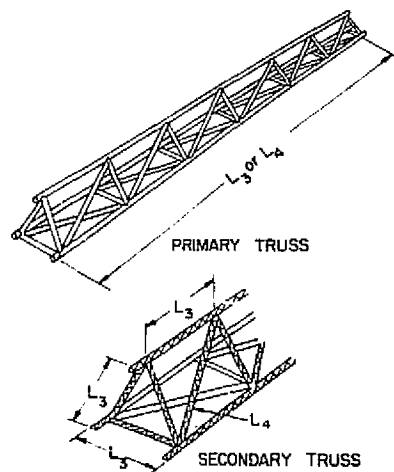
Table 3-4 COMPARATIVE SLENDERNESS RATIOS OF ALTERNATE PROPOSALS

		NASA	Alternate Configurations*				
			I	II	III	IV	V
<b>Basic Element</b>							
Width or Circumference	cm	Slat 5	Tube 5	Tube 5	Tube 5	Tube 5	Tube 5
Radius of Curvature	cm	0.58	0.8	0.8	0.8	0.8	7.38
Thickness (t)	cm	0.0127	0.0127	0.00635	0.00635	0.00635	0.00635
Moment of Inertia (I)	cm <sup>4</sup>	0.0007	0.0204	0.0102	0.0102	0.0102	0.032345
Cross Section Area	cm <sup>2</sup>	0.0635	0.0635	0.03175	0.03175	0.03175	0.047
Radius of gyration (ρ)	cm	0.11	0.57	0.57	0.57	0.57	0.047
Longest Member (L)	cm	35.0	35.0	56.6	63.6	63.6	63.6
Slenderness Ratio <sup>2</sup> (L <sub>2</sub> /ρ)		321	61	100	113	113	77
<b>Primary Truss</b>							
Width of truss (L <sub>1</sub> )	cm	25	25	40	45	45	45
Cross Sectional Area	cm <sup>2</sup>	0.381	0.381	0.1905	0.1905	0.1905	0.282
Moment of Inertia (I)	cm <sup>4</sup>	24.8	24.9	31.8	40.24	40.24	59.68
Radius of gyration (ρ)	cm	8.06	8.08	12.92	14.53	14.53	14.55
Longest Member (L <sub>4</sub> )	cm	2,300	2,300	2,545	2,545	2,121	2,121
Slenderness Ratio (L <sub>4</sub> /ρ)		285	284	197	175	146	146
<b>Secondary Truss</b>							
Width of Truss (L <sub>3</sub> )	cm	1,600	1,600	1,200	1,200	1,500	1,500
Cross Sectional Area	cm <sup>2</sup>	2.286	2.286	1.143	1.143	1.143	1.692
Moment of Inertia (I)	cm <sup>4</sup>	609,749	609,750	385,953	386,004	267,891	396,920
Radius of gyration (ρ)	cm	516.46	516.46	581.12	581.13	464.12	484.32
Longest Member (L <sub>6</sub> )	cm	91,900	91,900	91,900	91,900	72,700	72,700
Slenderness Ratio (L <sub>6</sub> /ρ)		178	178	158	158	150	150
<b>Modular Unit</b>							
Segment Size		Pyramid	Pyramid	Pyramid	Pyramid	Prism	Prism
Number of Segments		---	---	---	---	---	2.6Km x 2.6Km
Truss Length	Km	27.5	27.5	27.5	27.5	27.5	28.5
Truss Width	Km	5.2	5.2	5.2	5.2	5.2	5.2
Truss Depth	Km	0.56	0.56	0.56	0.56	0.56	0.56

\*NASA-Slate is used.

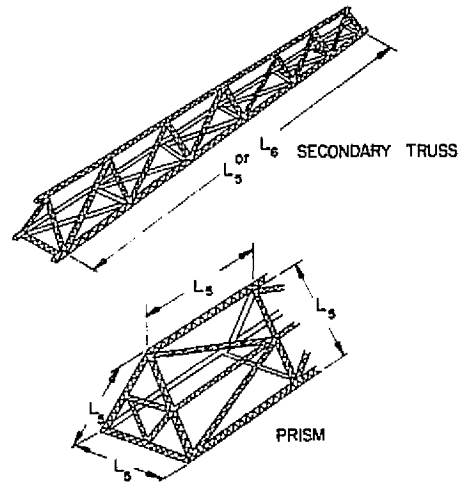
- #1 0-Same as NASA but slat is molded into tube.
- #2 - Same as #1 but thickness of tube is reduced and truss dimensions are changed.
- #3 - Same as #2 but dimensions of the primary truss are different.
- #4 - Same as #3 but ratio of width to length of trusses are maintained at 1/50 approximately.
- #5 - Same as #4 but diameter of the tube is changed to see that it has same strength both in buckling and crippling.

unassisted recovery from buckling. On the other hand, the element is unconventional and bears examination and comparison with more conventional structural elements, such as the tube or the box-section, for its ability to bear loads below the levels of elastic (buckling) instability. This section makes such a comparison with a thin-walled tube element.



ALTERNATES		I	II	III	IV	V
$L_3$	cm	1600	1800	1800	1500	1500
$L_4$	cm	2300	2545	2545	2121	2121
$L_4/\rho$		284	197	175	146	146

FIGURE 3-8 PRIMARY TRUSS OF THE STRUCTURE



ALTERNATES		I	II	III	IV	V
$L_6$	cm	65000	65000	65000	65000	65000
$L_6$	cm	91900	91900	91900	72700	72700
$L_6/\rho$		178	158	158	150	150

FIGURE 3-9 SECONDARY TRUSS OF THE STRUCTURE

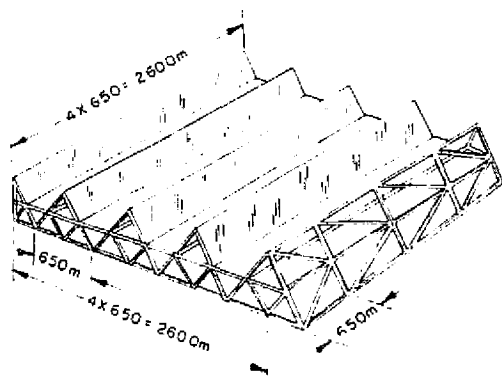
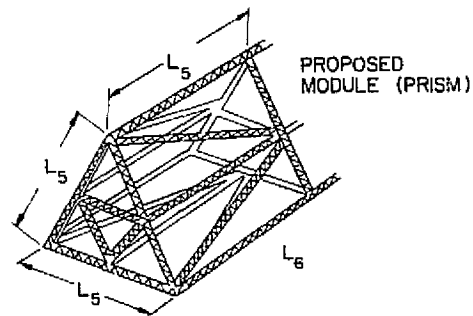


FIGURE 3-11 TRUSS SEGMENT FOR TRANSPORTATION  
NOTE ONE 22 SEGMENTS (2.6km X 2.6km)

$L_6 = 727 \text{ M}$   
 $L_5 = 650 \text{ M}$



$L_5 = 650 \text{ M}$   
 $L_6 = 919 \text{ M}$

MODULE PROPOSED BY JSC STUDY (PYRAMID)

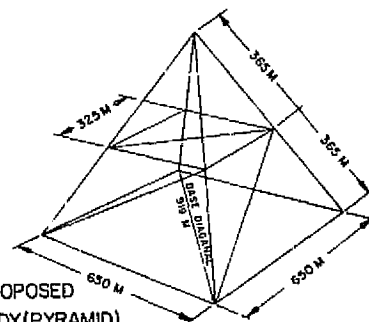


FIGURE 3-10 TRUSS MODULE

ORIGINAL PAGE IS  
OF POOR QUALITY

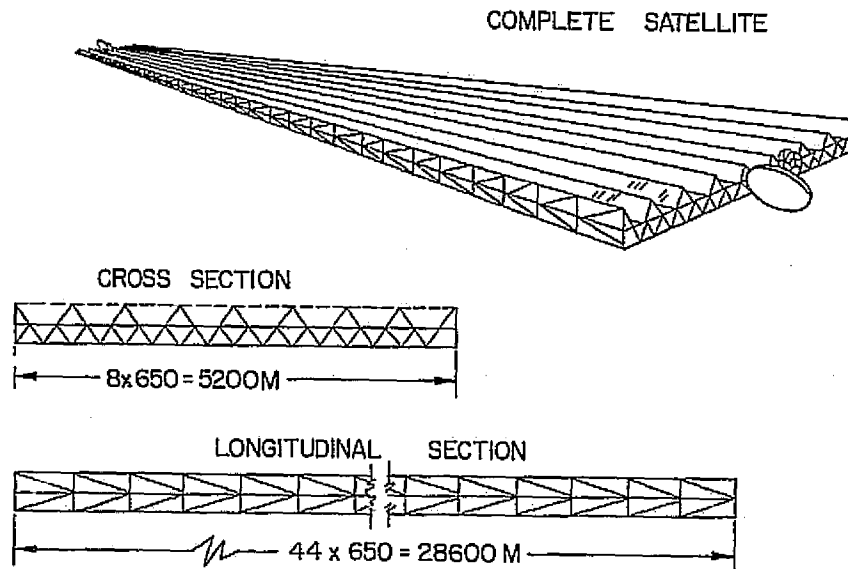


FIGURE 3-12 MAIN TRUSS OF THE STRUCTURE

### 3.5.2 Self-Healing Condition for Slat

Since a major advantage of the slat element is the matter of unassisted recovery from a buckled condition, the limit on this action is considered first. The requirements for such recovery are simple; the normal configuration must be at a lower elastic energy state than the buckled configuration (which is satisfied by the curved slat), and there must be no plastic deformation anywhere in the transition from normal to buckled configuration. This latter requirement can be interpreted quantitatively as providing a limit of the section thickness of a curved slat. A simplified analysis of this problem follows.

It is considered that a curved slat has buckled when the slat is flattened (i.e., curvature 0), that the curved slat is made of an elastic-plastic material with a distinct yield stress and yield strain ( $\sigma_{YS}$  and  $E_{YS}$ ). Anticlastic curvature (the three-dimensional stress state of flattening the slat) is ignored. A slat of constant radius is assumed, see Figure 3-13.

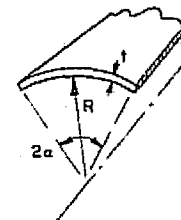


FIGURE 3-13 CURVED SLAT

$$E \propto \text{Curvature.}$$

To flatten a section of slat:

$$E_{MAX} = \left(\frac{t}{2}\right) \left(\frac{1}{R}\right) = \frac{t}{2R}$$

To avoid plastic deformation:

$$E_{MAX} \leq \sigma_{YS}/E$$

Combining gives:

$$\left(\frac{t}{R}\right)_{MAX} < 2\sigma_{YS}/E \quad (3.5.1)$$

The relationship that curvature is equal to the inverse of radius has been used implicitly. In the case of the parabolic slat (as proposed), under proper conditions (shallow parabola) Equation 3.5.1 can be specialized:

$$\text{CURVATURE} \sim \frac{d^2y}{dx^2}$$

$$t/2 \frac{d^2y}{dx^2} \text{MAX} < \frac{\sigma_{YS}}{E}$$

for the parabola  $y = Kx^2$ , this becomes:

$$kt < \sigma_{YS}/E$$

As an example, consider the parabolic section as proposed in the cited report to be made of aluminum for which  $E \cong 6.9 \times 10^{10} \text{ N/M}^2$ ,  $\sigma_{YS} \cong 2.8 \times 10^8 \text{ NM}^2$  ( $E \cong 10^7 \text{ psi}$ ;  $\sigma_{YS} \cong 4 \times 10^4 \text{ psi}$ .)

$$y \cong (.05 \text{ cm}^{-1} (.13 \text{ in}^{-1})) x^2$$

The criterion, Equation 1 gives:

$$(t \cong .08 \text{ cm.}) \text{ or } t \cong .032 \text{ in.}$$

The cited design uses ( $t = .013 \text{ cm.}$ ) or  $t = .007 \text{ in.}$

### 3.5.3 Gross (Euler) Buckling of Element

The critical question about any extensive lightweight structure is its elastic stability under gross or local compressional loads, that is, its buckling stability. If the structure incorporates a large degree of static indeterminacy, the entire structure must be considered. On the other hand, a statically determinate structure allows the compressional consideration of the individual elements. For purposes of estimation, a statically determinate structure is assumed and the individual element is considered.

Buckling can be by gross deformation as in a slender column or by local deformation as in a short piece of thin-walled tube under compression. Physical examples of these modes are, say, the buckling of a yardstick under compression (gross buckling), or the wrinkling of the wall and subsequent collapse of a deep-draw aluminum beer can under end compression (local buckling). If compressional failure of a thin-walled element is by local buckling, a thicker wall is indicated, while if consistently by gross buckling, a thicker wall is a poor use of materials for suppression of buckling. To compare different structural shapes,

one need compare both local and gross buckling of thin-walled tube. If the local and gross buckling criteria are combined eliminating the critical force, a relation involving wall thickness is obtained. For various geometries, local and gross buckling critical forces are available in tabulations, and these are used where available. Where necessary information has not been available, suitable approximations have been made to develop buckling criteria. Since a statically determinate structure is assumed, a pinned-pinned element is assumed for gross buckling calculations.

Critical forces for the gross buckling of a pinned end slender column (see Figure 3-14) are given by:

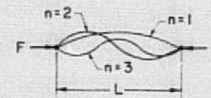


FIGURE 3-14 BUCKLING MODES FOR PINNED-END COLUMN

We are interested only in the first buckling mode ( $m = 1$ ), thus the critical force is given by:

$$F = \left(\frac{\pi}{L}\right)^2 EI$$

### 3.5.4 Moment of Inertia of Slat

Young's modulus is denoted by  $E$ , and  $I$  is the minimum area moment of inertia of the column cross-section. For a thin-walled circular tube, the moment of inertia is given by:

$$I = \pi R^3 t$$

where  $R$  is tube radius and  $t$  is wall thickness. Combining this with the critical force gives:

$$F = \left(\frac{\pi R}{L}\right)^3 Et \quad (3.5.2)$$

The moment of inertia for a curved slat is much more complicated, and an approximation is used here. The slat proposed in the cited reference is a very shallow (50 mm wide, 3 mm deep) parabola. For many of the calculations, a circular arc of the same dimensions is

considered. In this configuration, moment of inertia is given by Roark (Ref. 3-11) as:

$$I = R^3 t \left( \alpha + \sin \alpha \cos \alpha - \frac{2 \sin^2 \alpha}{\alpha} \right)$$

This is tabulated and plotted as function of  $\alpha$ , following:

$\alpha$ , RADIANS	$\alpha$ , DEGREES	$K(\alpha) = I/tR^3$
$\pi/12$	15	.0000544
$\pi/6$	30	.00168
$\pi/4$	45	.0122
$\pi/3$	60	.0478
$\pi/2$	90	.298
$2\pi/3$	120	1.81
$\pi$	180	3.14

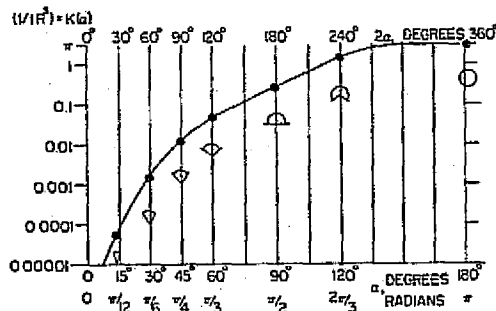


FIGURE 3-15 MOMENT OF INERTIA OF CURVED SLAT, NOTE LOGARITHMIC SCALE

Following Figure 3-15, the critical buckling force for a slender curved-slat column may be approximated by:

$$F = K(\alpha) \frac{\pi^2 R^3}{L^2} Et \quad (3.5.3)$$

### 3.5.5 Local Buckling of Thin-Walled Tube

Equations 2 and 3 represent the critical force for the gross buckling of thin-walled tube and curved-slat slender columns respectively. Roark indicates that the critical force for local buckling of a thin-walled tube

(assumed to be loaded symmetrically) is:

$$F = 2t^2 E \quad (3.5.4)$$

For example, a deep-draw single-draw aluminum beer can ( $t \cong 5 \times 10^{-3}$  in.,  $t \cong 1.3 \times 10^{-2}$  cm.,  $E \cong 6.9 \times 10^{10}$  N/M<sup>2</sup>, ( $E \cong 10^7$  lbs./in.<sup>2</sup>)), the critical force is about 2224 N. (500 lbs.) (Ref. 3-12). It is easily verified that an empty beer can of this description can support a person, but often buckles if the person aboard bounces.

### 3.5.6 Local Buckling of Slat

The critical force for the local buckling of a curved slat is apparently not commonly tabulated. It was necessary to find an approximation to this quantity. The basis of the approximation is that local buckling may occur when stored compressional elastic energy ( $E_C$ ) is greater than or equal to the energy ( $E_F$ ) necessary to flatten an area ( $2b^2$ ) of the slat, see Figure 3-16.

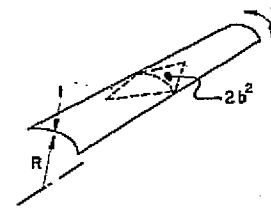


FIGURE 3-16 CURVED SLAT LOCAL BUCKLING REGION

The stated criterion may be written: buckling occurs when

$$E_C \geq E_F$$

But

$$E_C = \frac{\sigma^2 V}{2E} \quad (V \text{ is volume}) = \left( \frac{F}{bt} \right)^2 \frac{btL}{2E};$$

$$E_C = \frac{F^2 L}{2Ebt}$$

and

$$E_F = \int \sigma \epsilon dV = 2b^2 \int_{-t/2}^{t/2} \sigma \epsilon dy$$

deformed volume

$$E_F = 2b^2 E \int_{-t/2}^{t/2} \epsilon^2 dy, \text{ but } \epsilon = y/R$$

$$E_F = 2E \left( \frac{b}{R} \right)^2 \int_{-t/2}^{t/2} y^2 dy = \frac{E}{6} \left( \frac{b}{R} \right)^2 t^3$$

Substituting the expressions for  $E_C$  and  $E_F$  into the buckling criterion gives:

$$\frac{F^2 L}{2EBt} > \frac{E}{6} \left(\frac{b}{R}\right)^2 t^3,$$

or, local buckling occurs when:

$$F_1 > \frac{Ebt^2}{R} \left(\frac{b}{3L}\right)^{1/2} \quad (3.5.5)$$

### 3.5.7 Comparisons

Note that Equations 3.5.2 and 3.5.4 and Equations 3.5.3 and 3.5.5 respectively may be combined to give a criterion for a wall thickness appropriate to other dimensions. All the foregoing results are summarized in the following table, Table 3-5, with criteria pertaining to the thin-walled tube in the lefthand column and criteria pertaining to the curved slat in the righthand column.

It only remains now to compare various element cross-sections for load-bearing ability and use of materials. For purposes of comparison, Young's Modulus  $E \sim 6.9 \times 10^{10} \text{ N/M}^2$  ( $E \sim 10^7 \text{ lbs./in.}^2$ ) is assumed. Considering the thin-walled tube proposed for construction of the column-cable configuration in the SPS Survey Report (Ref. 3-10):

$$R \sim 3.3\text{cm} \quad (R \sim 1.3\text{in.}) \quad D/t \sim 400$$

$$t \sim .18\text{mm} \quad (t \sim .007\text{in.})$$

$$L \sim 2.5\text{m} \quad (L \sim 100\text{in.}) \quad L/\rho \sim 100$$

The gross buckling force is 2224 m (500 lbs.) and the local buckling force is 4448 m (1000 lbs.). This is a nicely-designed element.

To consider the curved slat proposed in the cited reference for the truss configuration, its cross-section is approximated by a sector of a circle and the parameters  $\alpha$ ,  $R$ , and  $b$  are determined. This is as follows, see Figure 3-17:

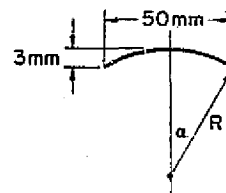


FIGURE 3-17 SLAT DEFINITIONS

Table 3-5 BUCKLING CRITERIA FOR TUBES AND SLATS

<u>TUBE</u>	<u>SLAT</u>
<u>I. GROSS BUCKLING</u>	
$F = \frac{(\pi R)^2}{L^2} Et$	$F = K(\alpha) \frac{\pi^2 R^3}{L^2} Et$
<u>II. LOCAL BUCKLING</u>	
$F = 2t^2 E$	$F = \frac{Ebt^2}{R} \left(\frac{b}{3L}\right)^{1/2}$
<u>III. MINIMUM WALL THICKNESS</u>	
$t = \frac{(\pi R)^3}{2L^2}$	$t = \frac{\pi^2 R^4}{bL^2} \left(\frac{3L}{b}\right)^{1/2} K(\alpha)$
CRITERIA I & II COMBINED	

$$\sin \alpha = 25/R \quad \cos \alpha = R-3/R$$

$$R = 105\text{mm} \sim (4.1 \text{ in.})$$

$$\sin \alpha \sim .236$$

$$\alpha \sim .25 \sim 14.5^\circ$$

$$2\alpha \sim 29^\circ$$

$$t \sim .18\text{mm} (t = .007 \text{ in.}) (\text{per SPS Report})$$

$$K(\alpha) \sim 5 \times 10^{-5}$$

$$b = 2\alpha R \sim 5.33\text{cm} (2.1 \text{ in.})$$

$$I \sim 5 \times 10^{-5} R^3$$

$$(bt)_{\text{slat}} = 2\pi (Rt)_{\text{tube}}$$

$$t = \frac{(\pi R)^3}{L^2} \text{ for tube}$$

The subsequent thin-wall tube dimensions are:

$$t = .064 \text{ mm} (.0025 \text{ in.})$$

$$R = 2.3 \text{ cm} (.92 \text{ in.})$$

Once again, numbers pertaining to the thin-walled tube are in the lefthand column, numbers pertaining to the slat are in the righthand column:

Having determined the necessary parameters of the curved slat, a thin-walled tube of the same wall-thickness and the same cross sectional area (i.e., the same amount of material) is postulated for purposes of direct comparison. The radius of this thin-walled tube is given by:

$$2\pi R_{\text{tw}} = b \quad R_{\text{tw}} \cong .33 \text{ in.}$$

Again, numbers pertaining to the thin-walled tube are in the lefthand column and numbers pertaining to the slat are in the righthand column.

TUBE	SLAT
Gross Buckling	
$F \cong 31 \text{ N. (7 lbs.)}$	$F \cong 3.1 \text{ N. (.7 lbs.)}$
Local Buckling	
$F \cong 4448 \text{ N. (1000 lbs.)}$	$F \cong 8.9 \text{ N. (2 lbs.)}$

The tube appears to be quite superior to the slat in this comparison. The choice of the same wall thickness in this comparison was quite arbitrary, and this is clear from the very high force (4448 N. (1000 lbs.)) necessary to cause local buckling in the tube. A comparison more favorable to the tube can be had applying a slightly modified wall thickness criterion to design of the tube. Again, we shall consider a tube and a slat made of the same quantity of the same material, of the same cross-section area and the same length (2.5 m (1000 in.)), but the radius and wall-thickness of the tube will be chosen to allow local buckling soon after gross buckling. The relevant questions are:

#### TUBE

#### SLAT

##### Gross Buckling

$$F \cong 278 \text{ N. (62.5 lbs.)} \quad F \cong 3.1 \text{ N. (.7 lbs.)}$$

##### Local Buckling

$$F \cong 556 \text{ N. (125 lbs.)} \quad F \cong 8.9 \text{ N. (2 lbs.)}$$

Mass and Cross-Sectional Area Are Common (Equal).

##### Dimensions

2.5m (100 in.) Length 2.5m (100 in.)

2.3cm (.92 in.) Radius 10.6cm (4.1 in.)

.064mm (.0025 in.) Wall Thickness .13mm (.007 in.)

In spite of the "self-healing" potential of the slat structure, slats seem to be a poor use of materials when compared with a more conventional tube structure, and a thin-walled tube structure is recommended.

One matter, which could be of importance, has not even been considered at all, this is the matter of torsional rigidity. Torsional rigidity is the thin-walled tube's strongest suit, and if considered, would show the tube to be even more strongly superior.

### 3.6 DYNAMICS OF TRUSS

#### 3.6.1 BASIS OF CONSIDERATION

The structures under consideration are very light, very extensive, and will be subject to attitude control forces, and reactions from assembly operations. For purposes of the design of control and attitude control systems it is important to have an idea of the dynamic

behavior of the structure. The structure is considered, laden with its solar cell array but lacking the power transmitting antennas and associated articulation hardware, lacking attitude control and orbital-transfer engines, fuel, and fuel tanks. The structure itself is grossly simplified, and the assumption that the structural materials are distributed in a stiff configuration is made. The results can be considered as approximations at best, subject to significant change with changes in lading of the structure.

### 3.6.2 Response Times of Structure

Many sorts of disturbances can propagate along the truss structure--compression and shear waves, flexural waves, and torsional waves. The propagation time for each is approximated and listed below; the methods of approximation are described last

It is well to note that the disturbance modes are not, in general, independent. They may be, and often are, coupled. For example, the fact that the plane of structural symmetry parallel to the plane of the structure (neutral axis) does not pass through the center of mass of the structure implies that longitudinal compressive

waves will be coupled with shear and flexural waves--none can exist without exciting the others. Results are tabulated in Table 3-6 and Figure 3-18.

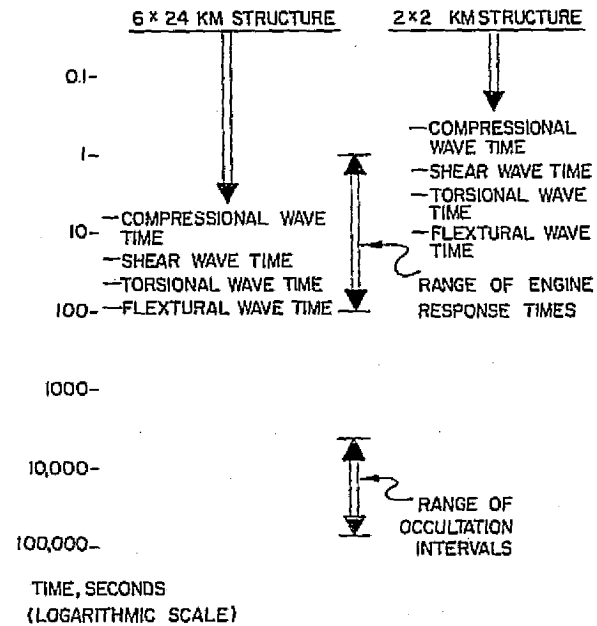


FIGURE 3-18 STRUCTURAL RESPONSE TIMES AND CONTROL CHARACTERISTIC TIMES

Table 3-6 RESPONSE TIMES OF STRUCTURE IN SECONDS

	6 x 24 KM STRUCTURE	2 x 2 KM STRUCTURE
Compressional (Longitudinal) Wave Time	7.5	0.60
Shear (Transverse) Wave Time	12.1	1.0
Torsional Wave Time	16.6	1.3
Flexural Wave Time (Bi-Harmonic Beam)	40.0	1.0
Flexural Wave Time (Plate)	49.0	1.0

### 3.6.3 Means of Estimation

Compressional and shear wave times were inferred from respective wave speeds and the dimensions of the structure. Nonstructural weight is included in calculation of the wave speeds.

Two means were used to estimate flexural mode response times; first, the truss was considered as a slender beam in flexure inferring response time from the group velocity for a half-wave of the length of the truss structure; second, the truss was treated as a free plate. Both estimates involve approximations, the similar results appear in the table. For reference, group velocity of a beam in flexure, determined from the dispersion relationship, is:

$$V_g = \frac{4\pi}{\lambda} \left( \frac{EI}{\zeta A} \right)^{1/2}$$

$\lambda$  is wavelength,  $EI$  is stiffness,  $A$  is mass per length,  $V_g$  is group velocity.

The lowest-mode period of a nonsolid "plate" can be approximated by:

$$T = \frac{4\pi L^2}{\alpha} \sqrt{\frac{\zeta(1-\nu^2)}{Et_e h}}$$

$T$  is period,  $L$  is plate length,  $\zeta$  is average density,  $\nu$  is Poisson's ratio,  $E$  is Young's modulus,  $t_e$  is equivalent box-section skin-thickness,  $h$  is plate depth, and  $\alpha$  is a constant (order of 15) dependent upon aspect ratio of plate plan (Ref. 3-13).

Torsional Response Time is inferred from the lowest-mode torsional frequency found by Rayleigh's method (see, for example, Ref. 3-14). Kinetic energy is conventionally evaluated, angle of twist  $\phi$  assumed to vary linearly along the structure. Shear strain potential energy is based on the following approximation to shear strain:

$$\gamma \sim \frac{2\phi}{L} \sqrt{t^2 + w^2}$$

$\gamma$  is shear strain,  $w$  is width,  $t$  is depth,  $L$  is length. The following approximation for square of the natural frequency results:

$$\omega^2 \sim \frac{72 G \zeta_e}{mL} (t + w) [1 + (t/w)^2]$$

## 3.7 THRUSTER ATTACHMENTS

### 3.7.1 Basis of Consideration

Necessary arrangements for mounting the engines which power the orbital transfer maneuver depend on many matters not yet resolved, such as whether engine thrust will be directed by mounting engines on gimbals or by using redundant engines facing in various directions; whether engines will be individually mounted or whether they will be mounted in clusters; whether clusters, if used, will be gimballed or fixed; what effect engine plumes will have on structure, etc. Two extremes are addressed here in a qualitative way, and in all cases engine-mounting appears to be attainable even if in some cases additional structure must be added. The two extremes considered are the following: direct and fixed mounting of individual engines; and, gimballed mounting of engine cluster.

Note that the resources for detailed structural analysis have not been available and that only crude approximations to true mounting needs have evolved.

Assuming as the basic structural element a circular thin-wall tube of aluminum, with diameter of about 4.7 cm, length about 2.5 m and wall-thickness about .0064 cm, a perfect element symmetrically loaded can bear about a 267 N. (60 lb.) load. Eccentric loading or dimensional imperfections decrease the load-carrying ability; increased end-fixity increases the buckling load-carrying ability. Assuming complete end-fixity of structural elements and the junction of several elements at each node, it is reasonable to conclude that a structural node can handle a force of the order of 44 N. (10 lbs.) in any direction, if appropriately applied, but that forces of the order of 440 N. (100 lbs.) at any node in any direction would cause buckling damage.

### 3.7.2 Single-Thruster Fixed-Mounting

It is considered, then, that an engine or a fixed cluster of engines may be mounted fairly casually across three (or more) structural nodes as long as any forces, thrust or inertial, resulting from mounting the engine or cluster are the order of 44 N. (10 lbs.) or less. The only associated caution is that the mounting hardware be contrived to feed loads to the structure such as to cause no significant deformation. Each of the Electric Propulsion Candidates (Ref. 3-15), except the Resist-

jet qualify for casual mounting; that is, each may be individually mounted in a fixed configuration to any three nodes of the structure. There are independent reasons for striking the Resistojet from active consideration--with a low  $I_{sp}$  it requires too much stored propellant mass. Thus, effectively, every engine considered may be casually mounted if mounted fixed and singly.

### 3.7.3 Gimballed Manifold Mounting

If engines are to be mounted in gimballed clusters capable of forces of the order of 10 lbs. or greater, either thrust or inertial, casual mounting will not be adequate. As an example, a gimballed cluster of engines to yield thrust on the order of 1780 N. (400 lbs.) is being considered. Such a cluster, with all its associated hardware, must be limited in (earth) weight to less than  $1 \times 10^{sv3^2} N$ . ( $4 \times 10^6$  lbs.) to keep inertial forces below 1780 N. (400 lbs.) (accelerations of up to  $.098 \text{ cm sec}^{-2}$  ( $10^{-4}$  G) are assumed).

### 3.7.4 Extent of Supplementary Structure

A supplementary structure must be provided to spread the force throughout a sufficient volume of the structure; in addition, such a structure must be sufficiently contrived and compliant so as to spread its load evenly across the region of the structure so as not to initiate local damage. It is estimated, for example, that such a 1800 N. (400 lbs.) load would need to be spread over perhaps 40 or more structural nodes in a region of typical dimensions about 100 m. Of course, such a supplementary structure with engines would necessarily have to be removed if a modular assembly is done in geosynchronous orbit. The assembly could conceivably be treated as a reusable tug which shuttles between low-earth orbit and geosynchronous orbit, ferrying successive modules into their assembly region.

## 3.8 COLUMN-CABLE CONFIGURATION

### 3.8.1 The Concept

The column-cable concept represents one extreme in the design range. It is intended to provide adequate strength while minimizing structural mass. The configuration is essentially a kite with diamond stays (Fig.

3-19) and a first version has been described in detail (Ref. 3-16). Its salient feature is the low structural mass. The main structure and the adjoining microwave antenna structure together constitute 2.4% of the satellite mass. And of this small percentage the antenna constitutes about 2/3; so the main structure is less than 1% of the entirety.

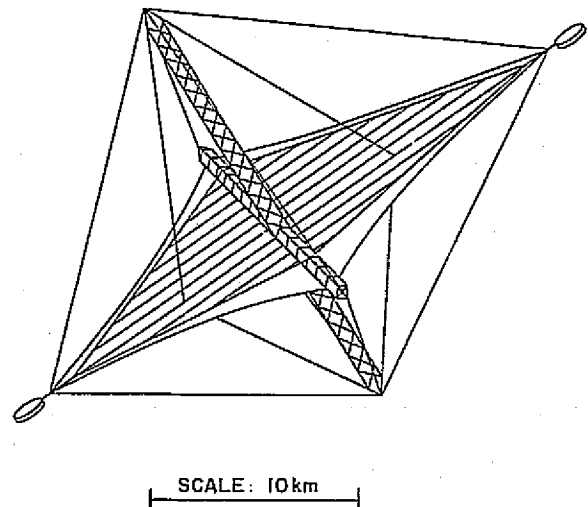


FIGURE 3-19 COLUMN-CABLE CONFIGURATION

### 3.8.2 Geosynchronous Orbit Assembly

In the attempt to bring the column-cable structure toward the minimum mass, there was a considerable dilution in the local strength. This trend increased the difficulty of inter-orbit transport as an integral unit and in fact the unit is generally associated only with GEO assembly. Various portions of the configuration will, of course, be prefabricated on earth or at LEO as described in the section below.

The structure has been designed to carry loads from pretensioning the cables and the blanket array. It also has the ability to withstand the dynamic loading induced by antenna movement and long term orbit adjustments. However, assembly in LEO would introduce

untenable loads from gravity gradient and atmospheric drag. Commencing the assembly in LEO could be done with the acceptance of a penalty in mass and structural simplicity. The structure could then be propelled by the energy from a partially deployed solar array, as long as no high acceleration phase were included. The mass penalty would come in local strengthening, and in addition from the extra cables, to give the structure integrity when only partially assembled. However, the lack of any local stiffness for engine attachments leaves the configuration highly suspect for an electrical propulsion orbit transfer.

### 3.8.3 Low Earth Orbit Subassembly

The LEO subassembly scheme promotes the fastest appearance of the structural skeleton in GEO. Further advantages are that a portion of the construction personnel will not have to be transported beyond LEO, and that the procedure allows the very economical high density HLLV payloads. The two structural drivers involved are compactness in LEO and the coupling between delivery rate to GEO and assembly. Compactness in LEO is necessary to minimize aerodynamic drag and to permit the high acceleration rates sustained with chemical orbit transfer. The coupling between delivery and assembly rates is crucial since the former is considered to limit the latter, this is apparently the main driver for subassembly in LEO (Ref. 3-17).

Assembly of the main structure is only a small fraction of the total satellite assembly, probably less even than the 1% mass fraction. However, structure assembly is very different from (and hence separable from) assembly of any portion of the satellite. Furthermore, structure completion must precede any other assembly progress. The early stages of the GEO construction will take place at the LEO staging base, it will consist of fabrication of structural subassemblies.

Bulk composite material will be listed to a factory in LEO which will then manufacture column sections in 1.2 KM lengths. These elements will be hinged together in groups of three to form a "folded-column," Figs. 3-20 and 3-21. As they are completed the "folded-columns" will be delivered to the GEO construction site and immediately added to the structure. The subassemblies will be propelled from the LEO factory to the GEO assembly site by chemical COTV's.

These single-staged reusable vehicles will have a 4MT payload, sized to fly with one "folded-column." A harness will be used to distribute the acceleration loads over the mass of the "folded-column." Since round trip transportation time at these acceleration levels is only 1 or 2 days, a very small fleet of these COTV's could keep ahead of the factory. Only 20 loads of "folded-columns" are required per satellite and perhaps an additional 10 are required for cable joints and fasteners; 30 trips would be required per satellite skeleton.

### 3.8.4 Structural Hard Spots

The structure employed in the column-cable configuration is particularly dilute. It will be necessary to have "hard spots" for attachment of the acceleration harness and for handling during assembly. These "hard spots" will be aluminum fittings spaced at intervals throughout the structure. They will be movable for special operations and will not be integral with the structure. Fig. 3-22 shows a clamping scheme with a self-locking module for attaching cables or for vehicle docking.

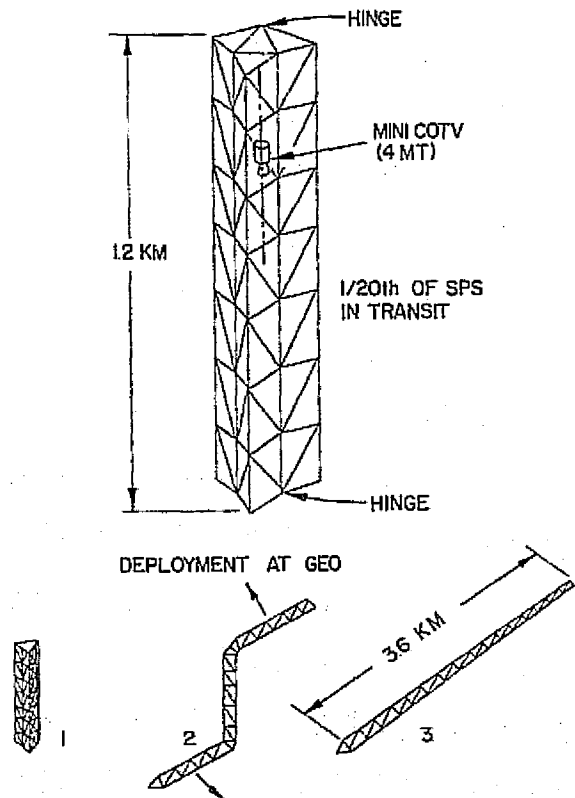


FIGURE 3-20 FOLDED COLUMN-LEO SUB-ASSEMBLY

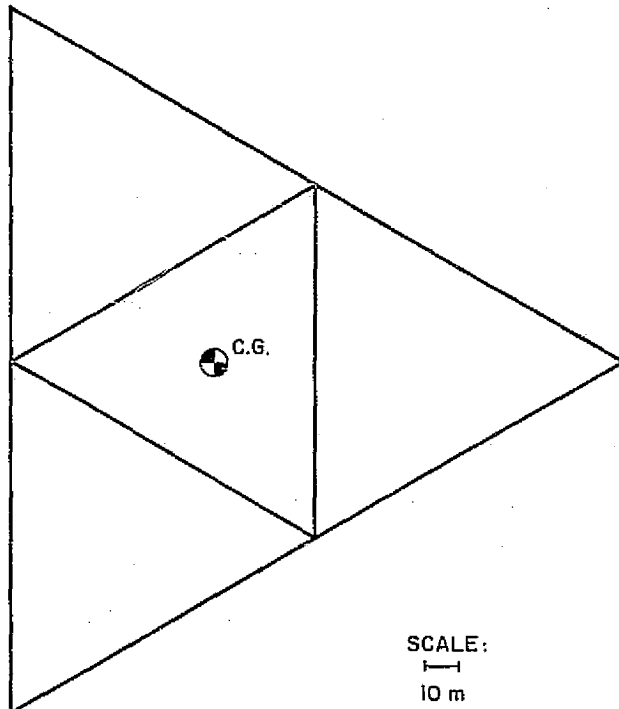


FIGURE 3-21 AXIAL VIEW: COTV WITH FOLDED BEAM

Aluminum shapes for use in the "hard spots" will be obtained from tanks destaged at LEO and GEO by the 250 MT OTV's. The implication is that some of the OTV's would be flown early in the program and that some of the expended tanks would have been specially constructed on earth to provide material in about 5 kg increments after destaging.

### 3.9 CONCLUSIONS AND RECOMMENDATIONS

#### 3.9.1 Conclusions

In the final analysis any structure has to withstand safely all the forces it encounters without jeopardizing the purpose for which it is designed. The design of the structure depends upon the loads imposed on the structure, the structural requirements, the choice of structural materials to be used and the optimization of the design among all the contributing factors. These factors are: weight, strength, production in space, serviceability, and cost.

As most of the required design data are not readily

available at present, the design study has been confined to basic concepts only. On that basis, the following conclusions can be drawn.

a. As in any structure with very broad guidelines, in this case also innumerable solutions are possible.

b. At this stage in time, it appears that the development of the truss configuration requires less new knowledge.

c. A conventional thin wall tube structure with rigid joints is recommended. Table 3-4 and Figures 3--7 to 3-12 show some of the alternate truss configurations studied.

d. In most aviation structures, alternate designs are worked out and a "Structural Index," based on the structural strength and weight of the structure, is used for comparison. As this is not directly applicable for large structures in space, a more suitable "Structural Index" based on dimensions, shape, stability, stiffness, strength, and weight should be devised.

e. Efficient use of material dictates tubing diameter greater than 10 cm and element length greater than 5 m; this implies fewer stages in the hierarchy of structural elements.

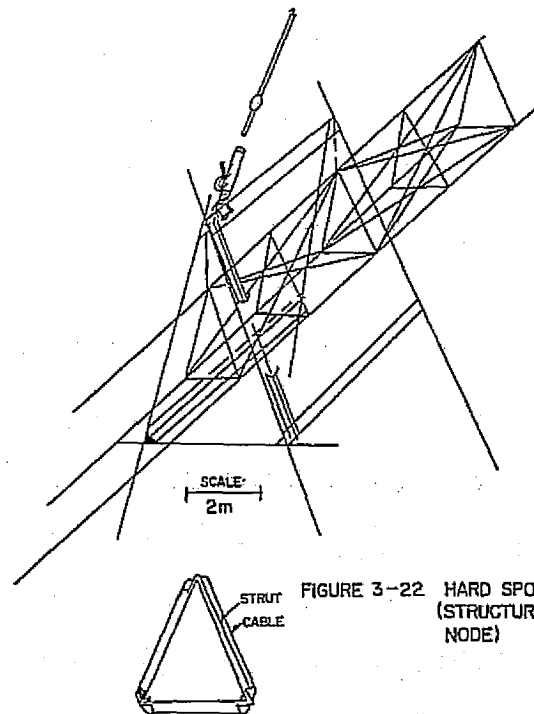


FIGURE 3-22 HARD SPOT (STRUCTURAL NODE)

f. Using a design slenderness ratio ( $L/\rho$ ) greater than 150, the use of high-strength alloys or composites is not recommended.

g. Careful development and testing of any polymeric matrix candidates, and development and testing of protective coatings for such materials, under real or simulated space environmental conditions is recommended strongly.

h. Development of rigid joining methods for tubes which do not involve lugs, as well as development of means of distributing loads into light structure, should be given serious attention.

i. At present no material having all the required properties for building the SPS structure seems to be available.

j. The truss configuration seems to follow more closely established structural design traditions, whereas the column-cable configuration raises many unresolved questions regarding rigidity, etc.

k. Nodes or "hard spots" have to be provided for attachment of thrusters, antenna, etc., where portions of the structure are to be transported from LEO to GEO in segments, as in the case of the truss configuration.

l. Propellant tanks will be strong and stiff in comparison with structure, and may substitute for structure where they are available.

m. Joints must be fused or brazed or bonded rigidly even though pin joints are assumed in the truss analysis. Development of adhesives for bonding joints is recommended.

### 3.9.2 Comments on Specific Design

The satellites under consideration are so extensive and lightly loaded that a monocoque structure efficiently designed to support the load would have an impractically thin wall. A slat structure, while offering some advantages, would be quite heavy for a given loading when compared with a thin wall tube structure. Efficient use of material in a tube structure requires satisfaction of a relationship among tube wall thickness, tube diameter, and tube length. Taking a tubing wall thickness of 0.125 mm (0.005 in.) as a practical minimum and considering the loads on the structure, a tubing diameter of greater than 10 cm (4 in.) and length of greater than 5 m (about 200 in.) are indicated. Implied is a slenderness ratio ( $L/\rho$ ) of about 150. A tube with a length of about 5 m would allow elimination of one step in the hierarchy of trusses made

of elements as compared with earlier structural designs considered by NASA.

With a design slenderness ratio ( $L/\rho$ ) of the order of 150, the structure does not depend on having very strong materials for stability or rigidity. Since material strength is not a problem, high-strength alloys or high-strength composites are not indicated.

Severe effects are associated with the environment of the satellite. With a mean temperature of about 270° C abs., the satellite will be exposed to the radiation temperature of space (about 5° C abs.) and parts of it exposed to temperatures of the order of 320° C abs. due to solar concentrator mirrors. Ultra-violet radiation will be significant. The satellite will be continually exposed to the vacuum of space and continually bombarded by energetic particles of varying mass with energies in the range from 0.02 eV to 10 MeV. Such exposure would be destructive to most polymeric materials, whether thermosetting or thermo-plastic. If polymeric-matrix composite materials are to be considered for structural use, efforts along the lines of development or protection are indicated. If composite materials are necessary in some application, as for example, in fuel tanks, metallic-matrix composites should be considered.

Propellants, whether for chemical propulsion or for electrical propulsion, will generally include one or two fluids (i.e., oxygen, helium, or hydrogen) which are gaseous at moderate pressures of the order of 1-10 atmospheres and at 270° C abs. These propellants will be stored at densities close to liquid densities; thus, propellant tanks are likely to be strong (and stiff) pressure tanks. In general, they will be rather dense as compared with the structure. The tanks can serve as mounting surfaces for structural members and can replace any structure which may otherwise have penetrated the volume of the tanks.

### 3.9.3 Recommendations

One of the outgrowths of this study was the realization of the need for new knowledge in various aspects of space structural design. Further study and research are recommended on the following aspects of design and construction of structures in space:

a. Development of new materials, such as metal-matrix composites, etc.

b. Development of radiation-resistant materials

such as plastics and plastic composites.

**c.** Development of suitable adhesives for proper (long life) bonding in the deep space environment.

**d.** Fusion welding techniques for thin walled members to be used in space.

**e.** Quick joining methods for modular construction in space.

**f.** Automated manufacturing and fabrication methods in space.

**g.** Development of an appropriate "Structural Index" for large space structures.

**h.** Identification of thruster characteristics for orbital transfer of structural segments or subassemblies.

## REFERENCES

**3-1** Materials Selector Guide, 1975. Yearly Periodical of Materials Engineering.

**3-2** Solar Power Satellite: Analysis of Alternatives for Transporting Material to Geosynchronous Orbit. NASA/ASEE Engineering Systems Design Institute Report Outline, 3rd Draft, August 9, 1976.

**3-3** Space-Based Solar Power Conversion and Delivery Systems Study Interim Summary Report, Contract NAS8-31308, ECON Inc., March 31, 1976.

**3-4** Hillesland, Harold L., Development of an Advanced Composite Antenna Reflector, p. 235, in Non-Metallic Materials Selection, Processing, and Environmental Behavior, Vol. 4, 4th National S.A.M.P.E. Technical Conference, Palo Alto, CA, October 19, 1972.

**3-5** Weeton, J.W., and Scala, E., Editors, Composites; State-of-the-Art. Proceedings of Sessions of 1971 Fall Meeting of Metallurgical Society of A.I.M.E., Detroit, MI, A.I.M.E., New York, March 1974.

**3-6** Fleck, J.N., and Hanby, R. R., High-Performance Fiber-Reinforced Polymers, in Weeton and Scala, Ref. 3-5, 1974.

**3-7** Personal Communication with J. M. Stuckey, NASA-JSC, July 22, 1976.

**3-8** Toth, I. J., Brentnall, W. D., and Menke, G. D.; A Survey of Aluminum-Matrix Composites, in Weeton and Scala, Ref. 3-5, 1974.

**3-9** NASA-JSC Report, Initial Technical, Environmental, and Economic Evaluation of Space Solar Power Concepts, Vol. I, July 15, 1976.

**3-10** SPS Survey Report IV.B.(3), Power Station System Collection, Module, Structure, NASA-JSC EZ3-76-27, 6/15/76, EZ3/W. C. Beckham-1976.

**3-11** Roark, Formulas for Stress and Strain, McGraw-Hill, New York.

**3-12** Mechtly, The International System of Units, 2nd Rev., NASA SP-7012, 1973.

**3-13** Timoshenko, S., Vibration Problems in Engineering, 3rd Edition, D. Van Nostrand Co., Princeton, NJ, 1955.

**3-14** Jacobsen, L. S. and Ayre, R. S., Engineering Vibration, McGraw-Hill, NY, 1959.

**3-15** Gerson and Lewallen, Electrical Propulsion Candidates, Table, NASA/ASEE Systems Design Institute, July 1976.

**3-16** NASA-JSC Report, Initial Technical, Environmental, and Economic Evaluation of Space-Solar Power Concepts, Vol. II, July 15, 1976.

**3-17** Personal Communication, R. Ried; June 14, 1976, June 22, 1976; and Fred Stebbins; June 22, 1976, July 7, 1976.

**CHAPTER 4**  
**TRANSPORTATION TO LOW EARTH ORBIT**

## CHAPTER 4

# TRANSPORTATION TO LOW EARTH ORBIT

### 4.1 INTRODUCTION

A dedicated, optimized transportation system consisting of personnel launch vehicles (PLV) and heavy lift launch vehicles (HLLV) is required to transport personnel and cargo to a staging base in low earth orbit (LEO). The system must provide return capability to personnel.

The transportation mode to LEO will not depend on the structural configuration (truss or column/cable), construction site (LEO or GEO), or the interorbital (LEO-GEO) propulsion mode (electrical or chemical).

### 4.2 LAUNCH SITE

There is considerable incentive to move the launch site from Kennedy Space Center (KSC) to an equatorial location. The main reasons are economics due to fuel savings. These savings accrue because of the velocity gain (1500 ft./sec.) at launch due to the equatorial bulge, the due east launch, and because no plane change is required to obtain geosynchronous orbit after the launch. Other factors which favor an equatorial launch are:

- more launch windows,
- return velocity is reduced, and
- reduced wind shear.

Figure 4-1 shows the total velocity change, and the fuel required to change from LEO to GEO assuming a 295 tonnes (650,000 lbs.) COTV. The main savings occur both from the cost of the fuel and the cost of transporting it to LEO. Assuming a cost of \$20/lb. to go from earth to LEO this would amount to a transportation cost of 2.5 million dollars per launch for a COTV weighing 295 tonnes (650,000 lbs.), if initial launch was from KSC.

This savings would be partially offset by the ground transportation costs from the manufacturing center to the launch site. How these costs would compare to the transportation costs to KSC cannot be determined until a launch site and manufacturing sites are selected. It would seem reasonable to suspect that they would be comparable.

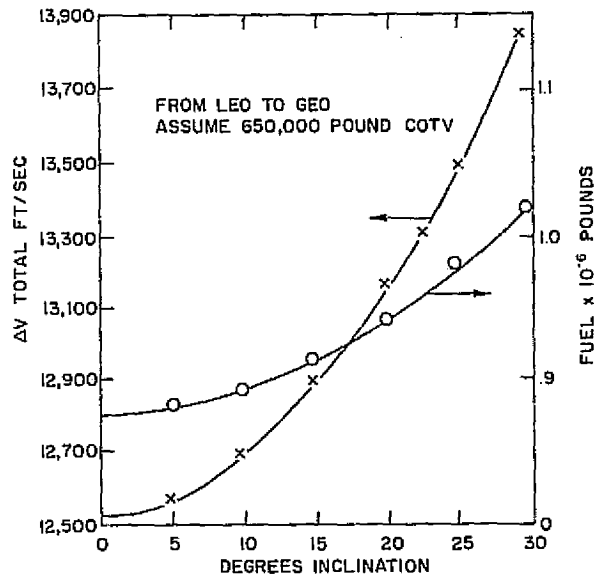


FIGURE 4-1 FUEL AND TOTAL VELOCITY REQUIRED FOR CHEMICAL PROPULSION TO GEO VERSUS INCLINATION ANGLE

We further neglect the cost of constructing a new launch facility, since this would have to be done at KSC. The costs of construction elsewhere would be comparable.

The net cost effect of an equatorial launch site, then, is a considerable savings over a KSC launch at 28.5° Lat.

In considering a launch site other than KSC, i.e., an equatorial site, areas other than economical and technical must necessarily come into play. These include the following:

- Political
- Transportation
- Environmental
- Social
- International

A brief discussion of these follows.

#### Political

An equatorial launch necessarily means that the site will not be in the continental U.S. or any of its territories. A problem that is sure to arise is the advisability of

foregoing the potential dollar savings and keeping the site in the continental U.S. in order to bolster the economy here.

### Transportation

We are considering the movement of huge pieces of equipment. This fact dictates that construction be on the Atlantic or Pacific coast, with subsequent movement by sea-going barges. It should not be forgotten that the Panama Canal is 104 feet wide, and the dimensions of various components could be of that order of magnitude. Transportation through the Canal would not be a routine journey. It is also extremely doubtful that passage through the Straits of Magellan would be practical because of the weather and the seas. The conclusion is that construction and launch would be in the Pacific or the Atlantic areas.

### Environment

The effects will be the same no matter where the launch. Furthermore, there is not sufficient data to surmise the long term effect. About all that can be said is that if a launch is made in the middle of the ocean, the obvious atmospheric effects would probably be dissipated before reaching areas of dense populations.

### Social

If the launch site selected were to be near a populated area the magnitude of such an undertaking could have serious disrupting effects on the local society.

### International

If a site is considered in the Pacific Ocean, it is soon discovered that most of the suitable islands are British Colonies. Hence, the State Department would be required to obtain an agreement allowing use of the island for a launch site.

Several of the advantages to using a Pacific island launch site follow:

- a. No suitable islands exist in the Atlantic Ocean.
- b. Noticeable atmospheric effects will be dissipated before they reach heavily populated areas.
- c. Both stages can be dropped in the ocean.
- d. The population of the islands are small and generally situated in one part of the island so that there would be little disruption of established communities.
- e. Several of the islands have sufficient land areas and the necessary ports to accommodate a launch complex of this magnitude.

f. There is the possibility of making  $LO_2$  and  $LH_2$  from seawater on site, using solar collectors for the energy.

g. In some cases it might be possible to store the  $LO_2$  and  $LH_2$  on different islands.

h. Another possible advantage is that of floating the HLLV components to the launch pad which would be submerged until the HLLV is mounted and then pumped dry. The pad could then be submerged again for fixing.

Figure 4-2 serves to locate the likely candidates for launch sites. Hawaii is roughly in the middle of the Pacific and about 1100 miles north of the equator. Tarawa is in the Gilberts. Of the five most likely sites; Christmas, Fanning, Malden, Nauru, and Tarawa, the most attractive appear to be Christmas and Tarawa. Both have sufficient area; both are quite close to the equator with latitudes  $1^{\circ}51'N$  and  $1^{\circ}25'N$ ; both have ports; both have airstrips; Christmas has almost no population, and Tarawa's population is concentrated mostly in the south. The main advantage of Christmas is that it is closer to the continental U.S.

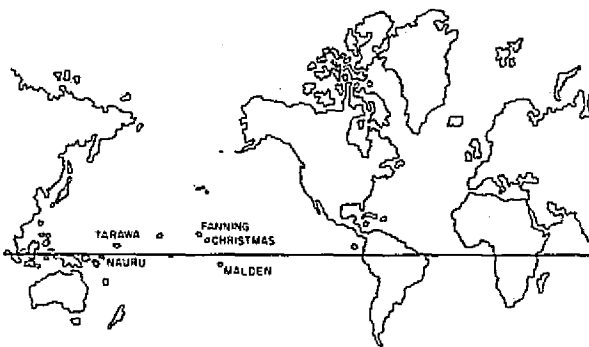


FIGURE 4-2 EQUATORIAL CANDIDATES FOR LAUNCHING SITES

All this information is summed up in Table 4-1. All of these are British Colonies except for Nauru which is independent, and all are atolls except for Nauru which is coral.

Figure 4-3 shows Christmas Island which is the largest atoll in the world and fairly typical of these islands. They are coral reefs surrounding a lagoon. The lagoon is on the Northwest end of Christmas and is not completely enclosed. Small boats can enter the lagoon. There are two airstrips which were developed by U.S. forces during WWII, and are now classified as international. The Bay of Wrecks is on the east and Vaskess

Table 4-1 EQUATORIAL LAUNCH SITE INFORMATION

	LONGITUDE	LATITUDE	AREA (Mi <sup>2</sup> )	POPULATION	BELONGS TO
CHRISTMAS	157°23'W	1°51'N	222.6 94 (Land)	52 360	British Colony Questioned by U.S.
FANNING	159°19'W	3°52'N	12.3	NONE 500	British Colony
MALDEN	154°59'W	4°3'S	15	NONE	British Colony
NAURU	165°56'E	0°31'S	8	5,200	Independent
TARAWA	173°E	1°25'N	14	3,582	British Colony

Bay is on the west. It was not possible to obtain topographical maps of Christmas Island; however, it is safe to say the elevations are only a few feet above sea level.

Tarawa also is an atoll, but somewhat different from Christmas Island. It consists of nine large and many small islets on a 22 mile reef. The lagoon is not enclosed. It has an airstrip and a submarine base, both developed during WWII by U.S. forces. It has a land area of about 14 sq. miles. Elevations are a few feet above sea level.

The remaining islands were excluded from additional consideration due to small size and location.

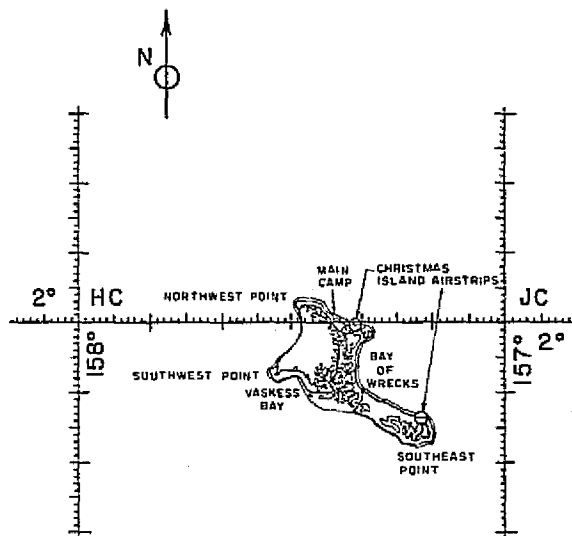


FIGURE 4-3 CHRISTMAS ISLAND

## 4.3 CARGO VEHICLE

### 4.3.1 Specifications and Requirements

Study of the heavy lift launch vehicles (HLLV) was limited to candidates provided in the material available. MSFC is the prime contractor for studies concerning the heavy lift launch vehicle. HLLV's are used for transportation of the components of the solar power satellite (SPS), support equipment, orbital transfer vehicles (OTV), and their propellants to low earth orbit

(LEO). Earth to LEO transportation is independent of the mode of interorbital transfer in the sense that both chemical and electrical modes would use the same HLLV system.

Following are some of the specifications and requirements imposed on the heavy lift system.

#### Some Basic Vehicle Specifications

- a. Maximum acceleration on payload, including shroud is 4 g's.
- b. Maximum temperature allowed in payload bay: 366°K (200°F).
- c. Minimum launch reliability factor: 0.97.
- d. Acoustics and structural dynamics on payload are to be at least equal to those of space transportation system (STS) cargo bay.
- e. No vehicle-payload service interaction shall be provided.
- f. Allowed launch rate capability margin: 50% beyond average annual rate requirement, including operational LEO needs and OTV losses.
- g. Orbital maneuvering system (OMS) payload penalty: 3%.

#### Mission, Performance, and Size Requirements

- a. Mission consists of vertical take off from adequate launch site, eastward orientation, insertion of payload into 80 x 500 Km elliptic orbit, circularization by orbital maneuvering system (OMS) of net payload into 500 Km altitude low earth orbit (LEO), cargo unloading, and horizontal soft landing or vertical water recovery of HLLV stages. Reuse goal is 300-500 trips.
- b. Guidance and navigation accuracy shall be consistent with unloading and recovery operations. OMS package will provide rendezvous capability. OMS engines and avionics will be returned and recovered, if feasible.

c. Transportation capability to place up to seven SPS per year, despite launch window constraints, is assumed.

d. Vehicle safe return shall require either normal mission completion or cargo jettison. Intact abort capability shall be provided only for range safety consideration.

e. Payload capacity range: 150-900 metric tons including shroud; payload density: 40-80 Kg/m<sup>3</sup>; payload bay dimensions compatible to largest and heaviest irreducible SPS component; payload diameter: 12-35 m.

f. Dry weight contingency added: 20%; pro-

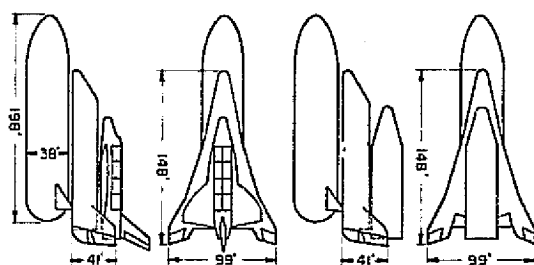
pellant tank increase for water impact-reuse factor: 20%.

### 4.3.2 Candidates

To provide a payload environment (acceleration, shock, vibration, temperature) similar to that of space transportation system (STS), but not vehicle-payload service interaction, and to achieve mission requirements, several candidates are considered.

Vehicles considered are either single stage or two-stage winged or ballistic which use liquid hydrocarbon fuel (propane or kerosene) for the first stage and liquid hydrogen for the second stage. HLLV options are shown in Figures 4-4 through 4-6 (Ref. 4-2).

Modified single-stage-to-orbit (SSTO) features an expendable hydrogen external tank (ET) and may carry 100-175 tonnes of payload in a modified winged orbiter cargo bay, or up to 450 tonnes payload in an aerodynamic, protective, reusable shroud. Either component can be recovered.



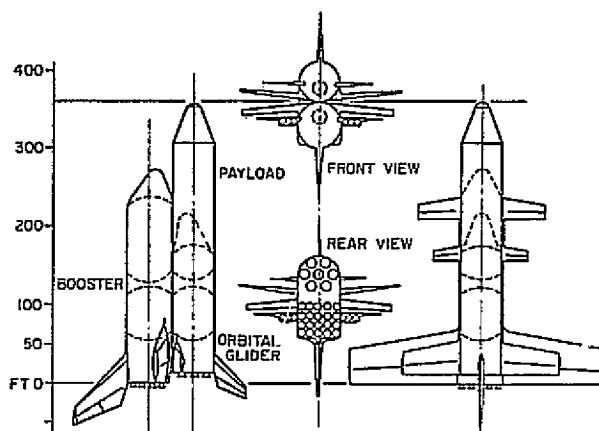
PAYLOAD, TONS, 105 X 105 km, TONS	105
MODIFIED ORBITER INERT, TONS	61
STAGE INERT, TONS	166
STAGE OXIDIZER, TONS	2352
EXTERNAL TANK INERT, TONS	69
EXTERNAL TANK FUEL, TONS	392
GROSS LIFT-OFF WEIGHT, TONS	3143
NUMBER OF ENGINES (UPRATED SSME'S)	15
TANK STAGING ALTITUDE, km	111
TANK STAGING VELOCITY, km/sec	7.82
THRUST/WEIGHT RATIO	1.25

FIGURE 4-4 MODIFIED SINGLE STAGE TO ORBIT LAUNCH VEHICLE (FIG. VI-1, REF 4-1)

The two-stage winged vehicle with a 450 metric tons payload capacity, has operational and cost advantages of horizontal soft landing near the earth launch site.

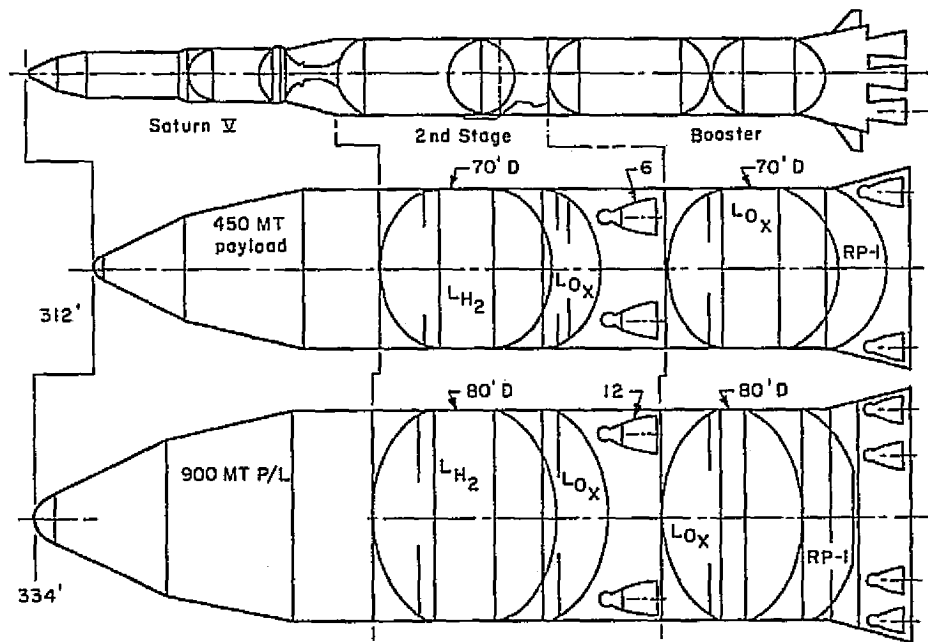
The two-stage ballistic candidate, with a payload range of 450-900 tonnes has an initial cost advantage because of its Saturn V aerodynamics. Vertical water recovery is under study.

A brief summary of candidate features appears in Table 4-2.



	LH <sub>2</sub>	BOOSTER TYPE RP-1	PROPANE
PAYLOAD TONS, 90 X 500 km	477	477	477
STAGE 1 INERT, TONS	1602	1331	1347
STAGE 1 PROPELLANT, TONS	7034	9279	9880
STAGE 2 INERT, TONS	368	432	444
STAGE 2 PROPELLANT, TONS	1570	1838	1891
GROSS LIFT-OFF WEIGHT, TONS	11,051	13,357	13,738
NUMBER OF ENGINES, STAGE 1	12	22	20
NUMBER OF ENGINES, STAGE 2	6	7	7
STAGING ALTITUDE, km	70.83	58.4	57.2
STAGING VELOCITY, % LATIVE	2.93	2.70	2.65

FIGURE 4-5 TWO STAGE LAUNCH VEHICLE (FIG. VI-2, REF. 4-1)



	O <sub>2</sub> /RP-1 BOOSTER		O <sub>2</sub> /PROPANE BOOSTER	
PAYLOAD, TONS, 90x500 km	454	907	454	907
STAGE 1 INERT, TONS	470	889	485	860
STAGE 1 PROPELLANT, TONS	4441	8236	4410	8170
STAGE 2 INERT, TONS	233	400	245	421
STAGE 2 PROPELLANT, TONS	1937	3599	2065	3832
GROSS LIFT-OFF WEIGHT, TONS	7565	14031	7659	14203
NUMBER OF ENGINES, STAGE 1	12	24	12	24
NUMBER OF ENGINES, STAGE	6	12	6	12
STAGING ALTITUDE, km	43.4	43.5	41.3	40.6
STAGING VELOCITY(REL)km/sec	1.84	1.91	1.70	1.78
BOOSTER MAXIMUM DOWN-RANGE	381	396	346	357

FIGURE 4-6 TWO STAGE BALLISTIC LAUNCH VEHICLE  
(FIG. VI-3, REF 4-1)

Table 4-2 HLLV CANDIDATE FEATURES

VEHICLE TYPE	PAYLOAD M.T.	MAIN ADVANTAGE
SINGLE-STAGE WINGED (ORBITER)	100-175	HORIZONTAL SOFT LANDING
SINGLE-STAGE BALLISTIC (SHROUD)	450	REUSABLE PAYLOAD SHROUD
DOUBLE-STAGE WINGED	450	HORIZONTAL SOFT LANDING
DOUBLE-STAGE BALLISTIC	450-900	LITTLE BOOSTER REFURBISHMENT

### 4.3.3 Payload

Payloads of 300-900 tonnes, with a density range from 20 to 100 kg/m<sup>3</sup> are considered. The volume range is 3000-45000 m<sup>3</sup>. Body and shroud are assumed to be made of aluminum honeycomb (area density = 20 Kg/m<sup>2</sup>).

Diameter and area versus volume for various length-to-diameter (L/D) ratios of cylindrical section appear in Figure 4-7. For a given volume, surface area is minimum when length equals diameter (L/D = 1).

Minimum shroud mass for various payload densities and payload capacities appear in Figure 4-8. For a typical payload density of 80 Kg/m<sup>3</sup> (skylab payload density was 85 Kg/m<sup>3</sup>), the shroud mass varies from 26.1 tonnes to 54.3 tonnes for a payload range of 300-900 tonnes. This represents 6-9 percent of the total payload to LEO (by contrast, the skylab shroud penalty on the payload was 13 percent).

Design, development, testing, and evaluation (DDT&E) costs and theoretical first unit (TFU) costs (\$/Kg) for both expendable and reusable shrouds appear in Figure 4-9. Expected TFU and average unit costs are derived and shown in Figure 4-10 using 87% learning curve for expendable and 300-trip reusable shrouds.

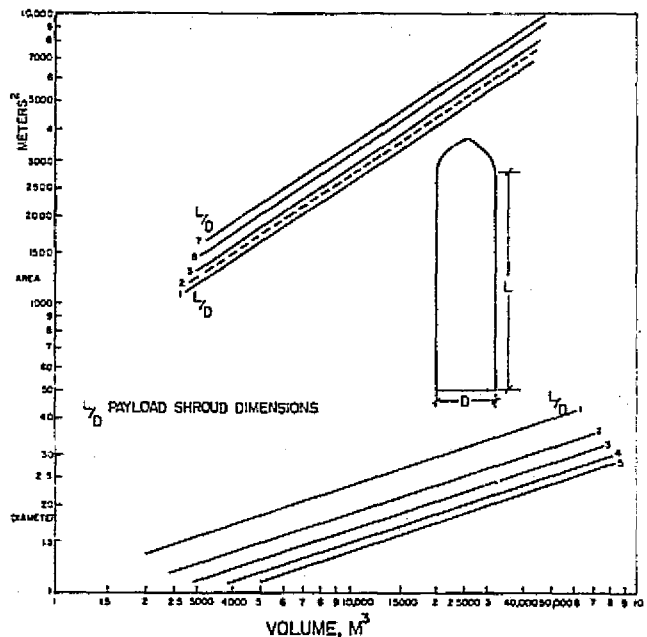


FIGURE 4-7 DIAMETER AND AREA VERSUS VOLUME

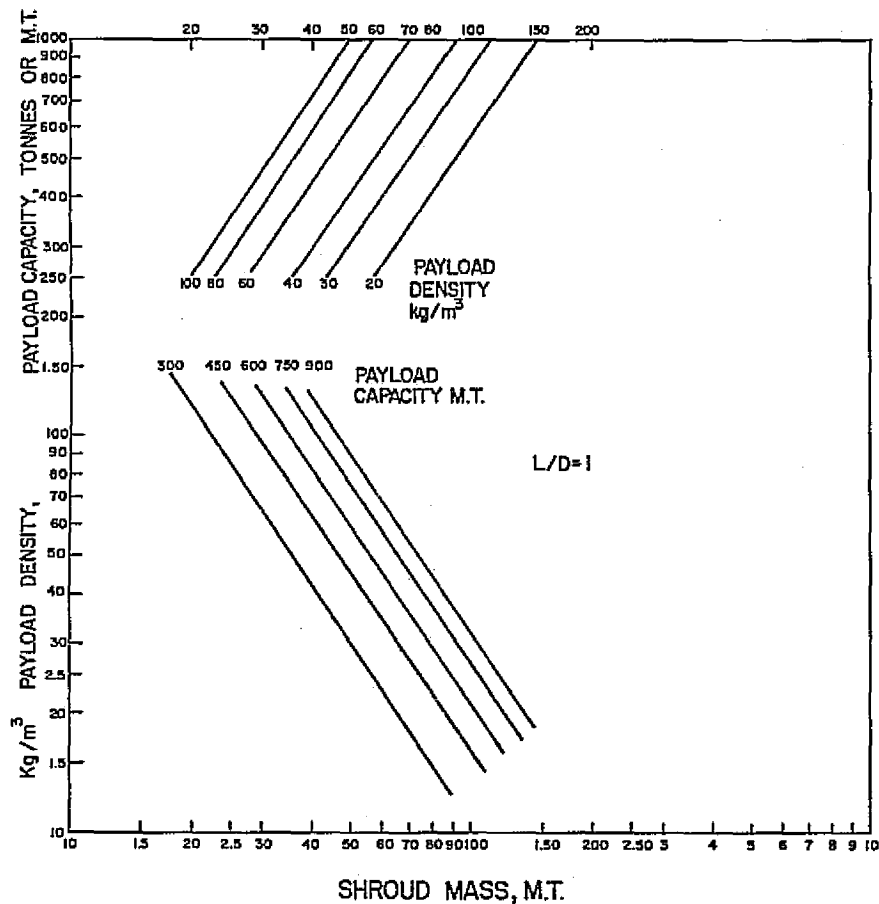


FIGURE 4-8 PAYLOAD CAPACITY AND DENSITY VERSUS SHROUD MASS

A payload of 750 tonnes would require a 48 tonne shroud to cover all the payload. Based on these estimates an expendable shroud costs \$2.5 million, whereas a reusable shroud is \$14.3 million, or \$.05 million per trip, excluding recovery and refurbishment costs.

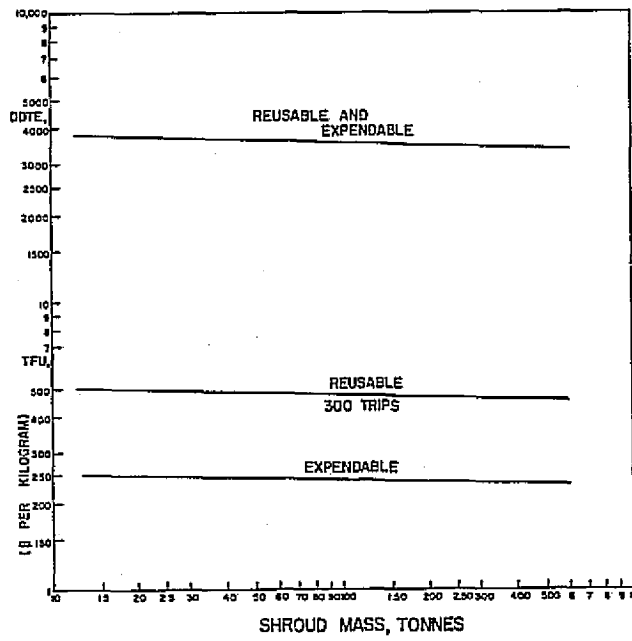


FIGURE 4-9 SHROUD COSTS (\$/kg)

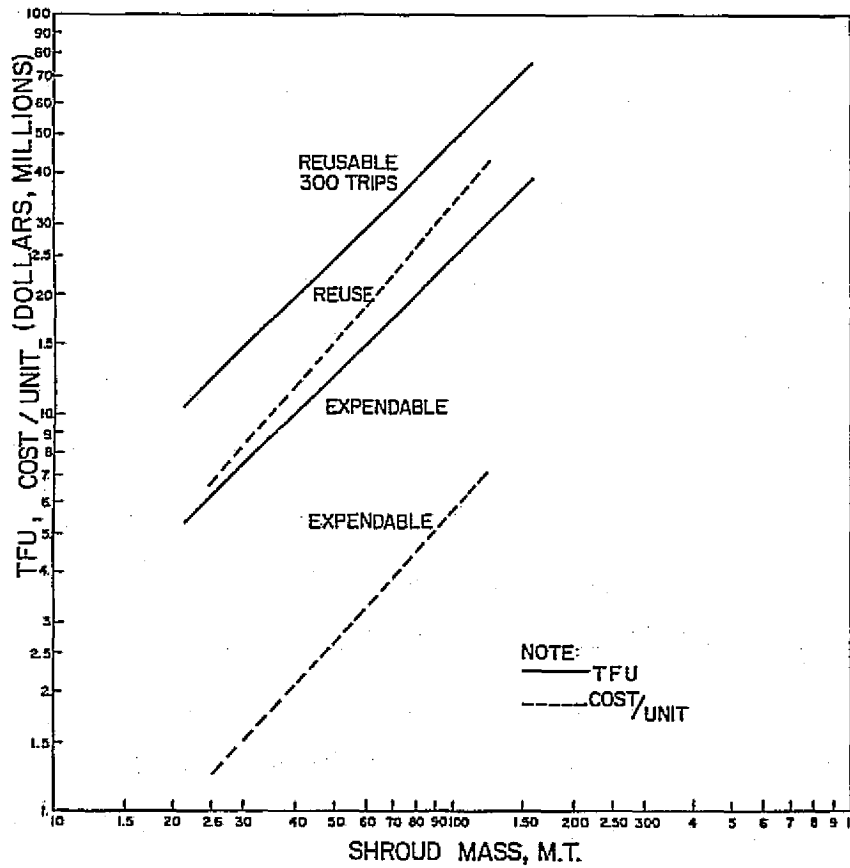
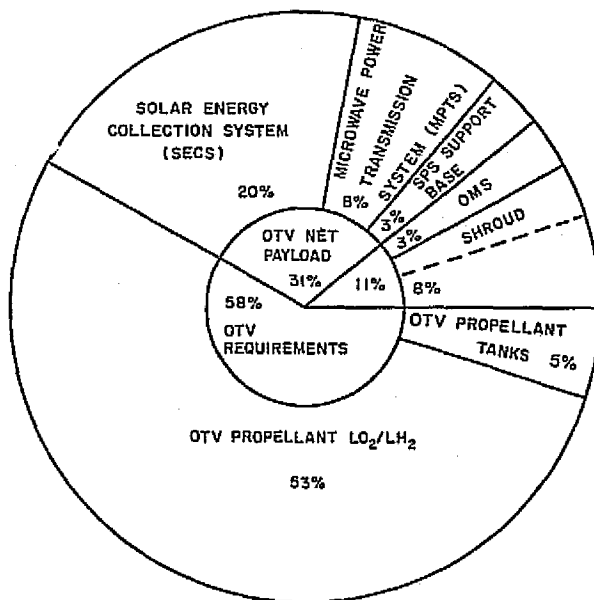


FIGURE 4-10 TFU AND AVERAGE UNIT COSTS

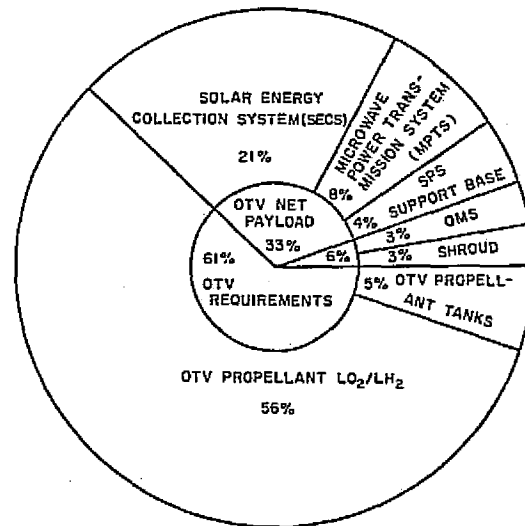
ORIGINAL PAGE IS  
OF POOR QUALITY

Since total payload to LEO includes net payload to GEO, orbital transfer vehicles and propellants both payload penalty and cost decrease by covering only net payloads (since propellant tanks may not require shrouds). Figures 4-11 and 4-12 show payload mass distribution for total and partial shrouds. Net payload to GEO is about one-third of total payload, including shroud and OTV propellant. Unit and trip costs of partial shrouds are reduced accordingly.



ASSUMPTIONS: COLUMN CABLE SPS  
OPTIMAL OTV DESIGN  
NO ORBITAL PLANE CHANGE  
ALL PAYLOAD IS COVERED

FIGURE 4-11 PAYLOAD MASS DISTRIBUTION (FULL SHROUD)



ASSUMPTIONS: COLUMN/CABLE SPS  
OPTIMAL OTV DESIGN  
NO ORBITAL PLANE CHANGE  
ONLY NET PAYLOAD COVERED

FIGURE 4-12 PAYLOAD MASS DISTRIBUTION (PARTIAL SHROUD)

### 4.3.4

#### Cost Estimates

Propellant, refurbishment, recovery, manpower, vehicles, shrouds, and necessary DDT&E are required to estimate launch costs.

DDT&E and TFU costs for vehicle candidates using a 95 percent learning curve are given in Table 4-3. Similar information for payload shrouds appears in Table 4-4. Average cost per flight using data from JSC Economic Division (Debbie Webb) appears in Table 4-5. Expendable full shrouds for ballistic options may cost more than the vehicle itself. They represent 8-16% of flight costs which vary from \$12.2 million for propane-fueled ballistic with a 450 tonne payload capacity to \$22.6 million for hydrogen fueled winged vehicles with 450 tonne payload capability.

Table 4-3 DDT & E AND TFU COSTS  
FOR TWO-STAGE VEHICLES

			OVERALL Cost, \$M	UNIT Cost, \$M	FLIGHT Cost, \$M
WINGED 450 M.T.	LOx/LH <sub>2</sub>	DDT/E	11 510	51,7	0,17
		TFU	1016	828,0	2,76
	LOx/RP1	DDT/E	10 730	48,2	0,16
		TFU	984	802,0	2,67
	LOx/LPR	DDT/E	10 520	47,2	0,16
		TFU	911	742,5	2,47
BALLISTIC 450 M.T.	LOx/RP1	DDT/E	4630	20,8	0,07
		TFU	510	415,6	1,39
	LOx/LPR	DDT/E	4210	18,9	0,06
		TFU	454	370,0	1,23
BALLISTIC 900 M.T.	LOx/RP1	DDT/E	5210	46,8	0,16
		TFU	807	677,9	2,26
	LOx/LPR	DDT/E	4790	43,0	0,14
		TFU	708	594,7	1,98

Table 4-4 DDT & E AND TFU COSTS  
FOR PAYLOAD SHROUDS

			OVERALL Cost, \$M	UNIT Cost, \$M	FLIGHT Cost, \$M
PAYLOAD: 450 M.T. SHROUD: 34,2 M.T.	EXPENDABLE	DDT/E	124,83	,0019	,0019
		TFU	8,4	1,73	1,73
	REUSABLE	DDT/E	124,83	,560	,0019
		TFU	16,5	9,6	,032
PAYLOAD: 750 M.T. SHROUD: 48,0 M.T.	EXPENDABLE	DDT/E	173,76	,0043	,0043
		TFU	11,6	2,50	2,50
	REUSABLE	DDT/E	173,76	1,30	,00433
		TFU	23,2	14,3	,048
PAYLOAD: 900 M.T. SHROUD: 54,3 M.T.	EXPENDABLE	DDT/E	195,48	,0058	,0058
		TFU	13,4	2,86	2,86
	REUSABLE	DDT/E	195,48	1,75	,0058
		TFU	26,0	16,4	,055

Table 4-5 PRELIMINARY COST ESTIMATES OF FACTORS RELATED TO  
REUSABILITY OF HLLV'S (\$M)

	WINGED 450 m.t.			BALLISTIC 450		BALLISTIC 900	
	HYDROGEN	KEROSENE	PROPANE	KEROSENE	PROPANE	KEROSENE	PROPANE
Propellants	9.3	3.0	2.9	2.7	2.7	5.0	5.0
Refurbishment	6.5	6.7	6.0	3.5	2.9	5.8	4.7
Recovery	—	—	—	1.5	1.5	1.7	1.7
Humanpower	2.1	2.1	2.1	2.1	2.1	2.1	2.1
Vehicle	2.8	2.7	2.5	1.4	1.2	2.3	2.0
Expendable full shrouds	1.7	1.7	1.7	1.7	1.7	2.9	2.9
DDT/E	0.17	0.16	0.16	0.07	0.06	0.17	0.15
Total Trip Cost	22.6	16.4	15.4	13.0	12.2	20.0	18.6
Shroud Percent	8.0	10.4	11.0	13.0	13.9	14.5	15.6

NOTE: Recovery includes operations (\$1.1M), retroengines and parachutes  
(\$0.4M for 450 m.t., adn \$0.6M for 900 m.t.).

### 4.3.5 Operations

This section will consider as operational areas all phases of restoring a heavy lift launch vehicle to operational status. Data from references 4-1 and 4-2 are used whenever possible. Cost analysis of a number of areas discussed below is neither detailed nor accurate at the present. Unfortunately, those areas of uncertainty dominate the total HLLV cost picture. Unless otherwise indicated, the material of this section applies to the HLLV candidates of section 4.3.2.

One way to understand the nature and extent of operations required to bring an HLLV unit back on line is to examine a mission events sequence.

#### HLLV Mission Events Sequence

- a. Earth launch--Stage 1 burn.
- b. Retro units/parachutes return Stage 1 to surface. Recovery operations, equipment, and personnel required.
- c. Stage 2 burn places payload in elliptical orbit.
- d. Retro units/parachutes return Stage 2 to surface. Recovery operations, equipment and personnel required.
- e. Shroud jettisoned.
- f. OMS circulatization burn puts payload in LEO (HLLV primary mission objective achieved).
- g. Stages 1 and 2 are returned to maintenance site. Stages receive maintenance/refurbishment and functional verification.
- h. Payload assembled and mated with OMS and shroud.
- i. HLLV assembled. This includes stage and payload mating and interface verification.
- j. Prelaunch. This phase includes propellant loading and preflight testing.

The above list provides an indication of the complexity of the operations required to return an HLLV to operational status.

The extent of uncertainty in HLLV costing will now be considered. The baseline model for this analysis is the 900 tonnes (992 tons) HLLV. Forecast analyses done for the space transportation system section of the "Outlook for Space" study NASA SP-386, January 1976, predicted transportation costs of \$44 per kilogram (\$20/lb.) to low earth orbit. Projections from Ref. 4-1 indicated minimum costs of \$22 per kilogram (\$10/lb.) to LEO for a 900 tonnes HLLV. It will be

assumed that 830 tonnes (915 tons) are delivered to LEO. This accepts an 8% average penalty for the OMS and shroud. Figure 4-13 was developed using the preceding data and the information in Section 4.3.4 on DDT&E, unit costs, propellant and shroud costs. Shroud costs were reduced from those of Table 4-4 since propellant tanks will meet part of the shroud requirements for both chemical and electrical transportation systems (OTV's). An expendable shroud was considered due to uncertain recovery costs for reusable shrouds.

Recovery and refurbishment costs of the stages are expected to figure significantly in the unallocated portions (56% and 76%) of Figure 4-13. Accurate investigation of the economics and risks associated with recovery and refurbishment are required before the optimal candidate among the horizontal ground landing candidates (2 stage winged) or the vertical water landing candidates (2 stage ballistic) can be determined. The Shuttle program will have features in common with both the above candidates. Since the Shuttle has reusability as one of its performance requirements, it should provide significant information for the important areas of recovery and refurbishment.

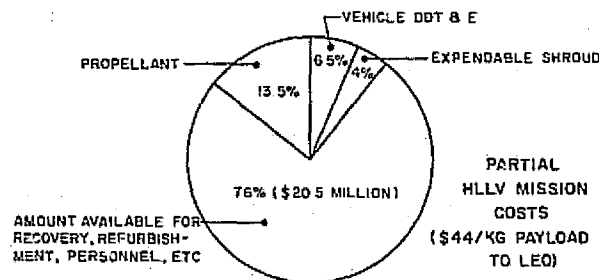
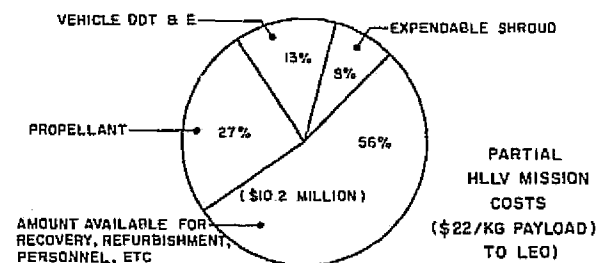


FIGURE 4-13 UNCERTAINTY IN COST COMPOSITION OF AVERAGE HLLV MISSION

A second area of concern is whether the HLLV should have LEO capability or not; that is, whether the second stage or a third stage (for example, stages 1 and 2 ballistic and a 3rd winged stage) should be capable of obtaining LEO, deploying cargo from a payload bay, retrieving cargo (for example, expended propellant tanks) and returning to earth. Analysis of this alternative is dependent upon the mode of interorbital (OTV) transportation. Electrical propulsion will not require the services provided by a LEO capability. However, a chemical propulsion system from LEO to GEO will require substantial quantities of propellants which will be brought to LEO in expendable tanks. A LEO capability of the HLLV would allow reuse of these tanks. This area is considered in Chapter 6.

#### 4.4 PERSONNEL VEHICLE

A personnel and high priority cargo launch vehicle (PLV) will be required to transport all personnel between earth and LEO. If current, proposed crew requirements for the solar power satellites (see section 4.4.3) are not increased significantly, it is reasonable to assume that a modified shuttle or a vehicle derived from the shuttle would be capable of meeting the personnel transportation demands. The orbiter part of the PLV would carry a personnel carrier module (PCM) internally in its payload bay.

The next section states several specifications and requirements for the personnel launch vehicle.

##### 4.4.1 Specifications and Requirements

- a. A separate shuttle-derived personnel and high priority cargo launch vehicle (PLV) is considered for transportation to the staging base in low earth orbit. Reuse goal is 100 trips/vehicle.
- b. The launch site shall be the same for both the PLV and the HLLV.
- c. Cross-range for once around, abort only and full abort capability including pad abort, shall be provided.
- d. Normal passenger stay time shall be six hours, including five hours maximum flight time, which allows for loading and transfer of the PCM for both the ascent and descent mission.
- e. LEO passive docking capability, with 24-hour emergency stay time will be provided.

- f. Passenger capacity range: 40-100 passengers per trip.

##### 4.4.2 Candidates

A separate personnel launch vehicle (PLV) is required to transport all personnel and high-priority delivery to staging LEO.

It would seem preferable to modify the current Shuttle in order to increase the payload capacity to 45 tonnes by adding structural mass, and decreasing propellant requirements and operating costs by replacing solid boosters with liquid rocket boosters (LRB) using hydrocarbon fuel (kerosene or propane) rather than design new vehicles for the PLV. The LRB, featuring water recovery, is 10 m in diameter and uses four F1 engines with series burn operations. This results in smaller gross lift-off mass (GLOW) by using smaller, less expensive external tanks. The PLV configuration is shown in Figure 4-14.

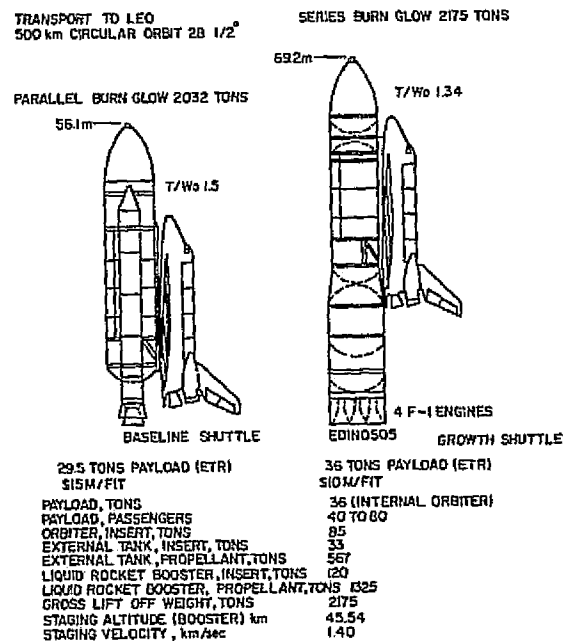


FIGURE 4-14 PERSONNEL AND PRIORITY CARGO LAUNCH VEHICLE (PLV) (FIG. VI-4 REF 4-2)

### 4.4.3 Personnel

A 68 passenger orbiter concept has been proposed, but a range of 40 to 100 passengers per personnel carrier module will be assumed. It is also assumed that a PLV will deploy and retrieve a fully loaded PCM each trip.

Estimated personnel requirements for the column/cable SPS are 474 and 574 for the truss configuration. For simplification, a nominal 525 will be used. It should be noted that duty tours are 6 months, so that transportation will be required for 1050 men per SPS. Table 4-6 gives the number of vehicles and trips needed for 112 satellites if PCM capacities of 40, 70, and 100 passengers are specified. A 15 percent contingency factor was added to the number of vehicles required. The actual number of trips would most likely exceed the figures given due to variations in the personnel loading at the SPS site, and the inability of the PLV to always carry a fully loaded PCM.

### 4.4.4 Cost Estimates

Table 4-7 provides average costs per mission for two hydrocarbon fueled personnel launch vehicles. The passenger capacity is assumed to be in the range of 40 to 100.

### 4.4.5 Operations

The personnel (and high priority cargo) launch vehicle (PLV) will transport a personnel carrier module (PCM) from earth to a low earth orbit staging base. The PCM is carried internally in the payload bay of the PLV. Extended passive docking of the PLV at the LEO staging base may be required if the construction and support personnel for the solar power satellite undergo an orientation period at the LEO base. Both electrical and chemical propulsion options will require the services of a PLV which is assumed to be a Shuttle derived or modified vehicle. The modes of personnel deployment from LEO to GEO will be dependent upon whether the electrical or chemical option is selected. The electrical option will require the services of a new vehicle, the personnel orbital transfer vehicle (POTV), which will dock with the PCM at LEO and provide propulsion for the PCM mission to the GEO construction or assembly site. The chemical option assumes that the (cargo) orbital transfer vehicle will have the capability to provide propulsive power for the PCM to GEO. Details con-

cerning the PCM and POTV are provided in Section 6.4. It is assumed that the PLV will be capable of retrieving a loaded PCM from the LEO staging base, that is, it will provide earth to LEO capability for one personnel complement and LEO to earth transportation for another complement.

## 4.5 SUMMARY AND CONCLUSIONS

Preliminary analysis indicates that regardless of the mode of interorbital transfer (chemical or electrical), an equatorial launch site presents several well defined technical advantages over alternative sites such as Kennedy Space Center. The technical and economic advantages are judged sufficient to recommend an in-depth analysis of alternative sites and their implications for the SPS program.

Investigation of the risks and economics of recovery and refurbishment of heavy lift launch vehicles is considered to be an important area for study. It may well have the largest impact on the heavy lift launch vehicle mission cost picture. Particularly of interest is a comparison between horizontal ground landing candidates (2 stage winged) and vertical water landing candidates (2 stage ballistic). The rationale for this study is that projected space programs of the immediate future (next quarter century) will almost certainly benefit from vehicles with a high reusability factor, and, in fact, support for future programs can be partially based upon the fact that economical earth to LEO transportation is available.

It appears after considering the cost of two expendable tanks for chemical orbital transfer vehicles (see Chapter 6) per mission and at least a partial shroud per HLLV mission, that the possibility exists that an HLLV with a second or third stage capable of retrieving expended tanks from LEO could be cost effective. It is recommended that further study into the cost trade-off problem of expendable tanks and shrouds versus a second or third stage with LEO capability be conducted.

Table 4-6 TOTAL NUMBER OF PERSONNEL VEHICLES AND TRIPS

PASSENGER CAPACITY	NUMBER OF TRIPS (112 SPS's)	TOTAL NUMBER OF VEHICLES REQUIRED
40	3024	35
70	1680	20
100	1232	15

Table 4-7 SHUTTLE-DERIVED PERSONNEL LAUNCH  
VEHICLE MISSION COSTS \$M.

	40 - 80 PASSENGERS	
	4-Engine Kerosene	3-Engine Propane
Propellants	0.8	0.6
Refurbishment	2.8	2.8
Recovery	1.2	1.2
Humanpower	2.1	2.1
External Tanks	2.1	2.1
Vehicle	2.9	2.8
DDT/E	0.006	0.013
Total trip cost	11.9	11.6

NOTE: Recovery includes operations (\$1.1M), retro-engines and parachutes (\$0.1M)

### REFERENCES

- 4-1 Initial Technical, Environmental, and Economic Evaluation of the Space Solar Power Concepts. Volume I Summary, NASA, Houston, July 1976.  
4-2 *ibid.* Volume II

**CHAPTER 5**  
**ORBITAL TRANSFER BY ELECTRICAL PROPULSION**

## CHAPTER 5

# ORBITAL TRANSFER BY ELECTRICAL PROPULSION

### 5.1 INTRODUCTION

One of the largest detractors to sending a large mass into space is the terrific cost of the delivery system. The conventional chemical rockets currently used have only a 20% payload capability. One possible way to increase the percentage of payload is to use engines or thrusters with a higher specific impulse. Of the many possibilities, one which should be strongly considered is the electrical-powered jet. Electrical power is used to effect an acceleration of some stored propellant, thus providing a thrust.

Specific impulses in the order of 20,000 have been deemed possible and thrusters delivering greater than 10,000 lps have been demonstrated (Ref. 5-1). The electrical thruster requires a considerable amount of electrical energy to develop these high specific impulses and a solar power satellite can provide the electrical power necessary to operate certain types of these thrusters.

Solar electric propulsion (SEP) could be brought to readiness for first use as primary spacecraft propulsion by 1980. The technology for each of the essential elements of a total SEP system is presently available. System level integrations and extensive functional, environmental, and duration testing remain to be accomplished (Ref. 5-2).

### 5.2 PROPULSION

#### 5.2.1 Points of Concern and Problems

The electrical thruster study included both descriptive specifications and societal impact. The following questions were considered for each candidate thruster.

##### 5.2.1.1 AVAILABILITY

Is the thruster available today, and if not, it is projected to be available at the required time in the future? Is this projection realistic and based on sound forecasting techniques, or just wishful dreaming?

##### 5.2.1.2 ENVIRONMENTAL IMPACT

Will a thruster require the use of a propellant that will harm man's environment? Will it require depletion of a significant amount of the earth's resources?

##### 5.2.1.3 COST

What will a thruster cost? If in the developmental stage, what will it cost to complete it? How many will be needed?

##### 5.2.1.4 THRUSTER MOUNTING

How will the thrusters be attached to the satellite and how will the satellite be modified to accommodate them?

##### 5.2.1.5 CONTROL AND POWER CONDITIONING

How will the electrical power and propellant be conditioned and supplied to the thruster and how will they be controlled?

### 5.2.2 Thruster Characteristics and Solutions

The thrusters considered most viable as candidates for orbital transfer have high specific impulse, high efficiency, low power requirements, and a high thrust/weight ratio. The characteristics of several candidate thrusters are given in Table 5-1 (Ref. 5-3).

##### 5.2.2.1 AVAILABILITY

Thruster availability is a matter of great concern and must be carefully sized in the very near future since only current technology is involved (Ref. 5-3 and 5-4). Additional development and testing of larger (than currently available) thrusters would be required. The hydrogen and ammonia fueled, electric arc-jet, while requiring more development than the resistojet, also uses only current or near future projected technology (Refs 5-3 and 5-4).

ORIGINAL PAGE IS  
OF POOR QUALITY

Table 5-1 POTENTIAL OTV THRUSTER CHARACTERISTICS

	Resistojet	Electric Arc-Jet	Electric Arc-Jet	MPD	ION	
Propellant	LH <sub>2</sub>	NH <sub>3</sub>	LH <sub>2</sub>	ARGON	ARGON	
Specific Impulse, Sec	1K	1.5K	3K	10K	30cm 5K	100cm 20K
Thrust, N (LB <sub>f</sub> )	444.8 - 4448 (100K)	22.2 - 222 (5-50)	22.2 - 222 (5-50)	22.2 - 222 (5-50)	.09 (.02)	3.76 (.845)
Input Elec. Power, KW	3.4-34 x 10 <sup>3</sup>	.41-4.1 x 10 <sup>3</sup>	.65-6.5 x 10 <sup>3</sup>	1.6-16 x 10 <sup>3</sup>	3.3	459
Voltage, Volts (DC)	100-1K(AC/DC)	100	200	300	600	10K
Thrust/Mass (g <sub>0</sub> x T/W)	1.0	1 x 10 <sup>-2</sup>	2 x 10 <sup>-2</sup>	8 x 10 <sup>-3</sup>	6 x 10 <sup>-4</sup>	2.3 x 10 <sup>-4</sup>
KWe/N(lbf) Thrust	7.9 (35)	18 (80)	29.2 (130)	51.7 (300)	39.3 (175)	122 (543)
Overall Efficiency, Pin/Pjet	65	40	50	70	68	88
Thermal Efficiency, 1-% Waste Heat	98	80	90	90		

Both the MPD and ION (electrostatic) thrusters will require more development time than either the resistojet or the arc-jet. The technology level necessary to produce these thrusters in the proper size and reliability has not yet been attained and extensive research and development will be required to do so. (Ref. 5-5).

#### 5.2.2.2 ENVIRONMENTAL IMPACT

Environmental impact must be considered from several viewpoints, since there is concern for both man's protection, the earth's environment, and the environment of the satellite itself. Choice of the propellant must also be included in this study since some of the proposed propellant appears to present greater hazards (both to man and the satellite) than others.

As far as man's environment is concerned, the effects are two-fold. The exhaust plume of all the thruster candidates consists of high energy particles. Some of the propellants, such as cesium and mercury, are potentially dangerous to man and satellite even in a low energy state and become extremely so when accelerated to high velocities in a thruster (Ref. 5-6). The propellants presenting the lowest environmental problems appear to be argon and hydrogen.

The effects of the exhaust plume on the satellite can be quite pronounced for certain thruster-propellant combinations. Certain propellants create more of a hazard for the solar cells and others seem to be potentially damaging to the structure. Preliminary analysis and investigations indicate a substantial amount of shielding may be necessary to protect critical portions of the satellite from the exhaust plume, regardless which propellant is used (Refs. 5-7 and 5-8). This potential problem will be further addressed in Section 5.4.6

There appears to be an abundance of both argon and hydrogen, since they can be manufactured from the atmosphere (Ar) or from water (H<sub>2</sub>), but manufacturing capacity must be increased (Ref. 5-9).

#### 5.2.2.3 COST

The cost of a prototype thruster is somewhat difficult to ascertain, especially for the types requiring long development time. This matter is discussed at length in Chapter 8 and thruster costs are tabulated there.

#### 5.2.2.4 THRUSTER MOUNTING AND CONTROL

The electrical power supplied to the thruster will have to be conditioned (voltage level, current capability, stability, etc.) from the raw electrical power available from the solar cells. Certain of the thrusters need only one voltage level (Resistojet) and others as many as fourteen voltage levels (Ion).

#### 5.2.2.5 CONTROL AND POWER CONDITIONING

Control of the thrusters is somewhat dependent on their location on the satellite. Clustering the thrusters, tank, and power conditioning equipment may provide some economy over a scattered arrangement. Location of the thrusters must be considered from several viewpoints and once chosen, the propellant and power delivery system should then be optimized. This subject will be addressed in more detail in Sections 5.4.4 and 5.5. Figure 5-1 shows some of the complexities and interrelationships involved in choosing a thruster/propellant type.

### 5.3 ORBITAL MECHANICS

#### 5.3.1 Introduction

The very concept of transporting large structures from low earth orbit to geosynchronous orbit (LEO to GEO) implies that the transfer will involve only very low thrust acceleration. Structures of very large area (many km<sup>2</sup>) rule out accelerations in excess of 10<sup>-3</sup> earth g's.

If we are to use part of the power generating capacity of a solar power satellite to generate thrust in electric propulsion systems, their number would become excessive if acceleration higher than 10<sup>-4</sup> earth g's were considered.

For such a low thrust transfer, different equations and geometrics apply as compared to the familiar impulsive orbit transfer problems.

This section presents some useful analytic tools that can be used in the "quick-look" preliminary design feasibility study, to be followed eventually by more detailed computer analyses.

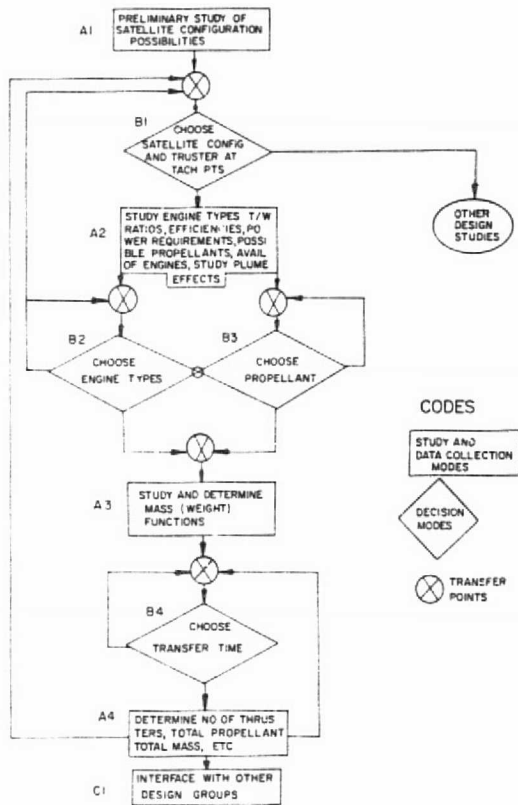


FIGURE 5-1 THRUSTER/PROPELLANT SELECTION

### 5.3.2 Geometry of the Transfer Spiral

The geometry of a typical transfer spiral trajectory is shown in Figure 5-2. It shows that consecutive orbits are initially close together, while, as the altitude increases, they become spaced farther apart. This can be shown by two quantitative relationships applicable to the low thrust transfer.

An expression for the altitude gained in one orbit can be obtained from energy considerations. Equating the work done by the thrust force on the spacecraft during one orbit and the resulting increase in its energy as evidenced by the increase in orbit altitude:

$$T (2\pi r) = \frac{W_0}{g_0} \frac{\mu}{2r^2} \Delta h,$$

or

$$\Delta h = 4\pi R_0 \frac{T}{W_0} \left(\frac{r}{R_0}\right)^3. \quad (5.3-1)$$

Thus the altitude gained per orbit increases with the third power of  $r$ .

This view is consistent with the expression for the flight path angle as a function of altitude,

$$\gamma = 2 \frac{T}{W} \quad (G.4-11)$$

derived in Appendix G, equation G.4-11.  $W$  is the gravitational force in orbit and thus equation G.4-11 may be rewritten as:

$$\gamma = 2 \frac{T}{W_0} \left(\frac{r}{R_0}\right)^2. \quad (5.3-2)$$

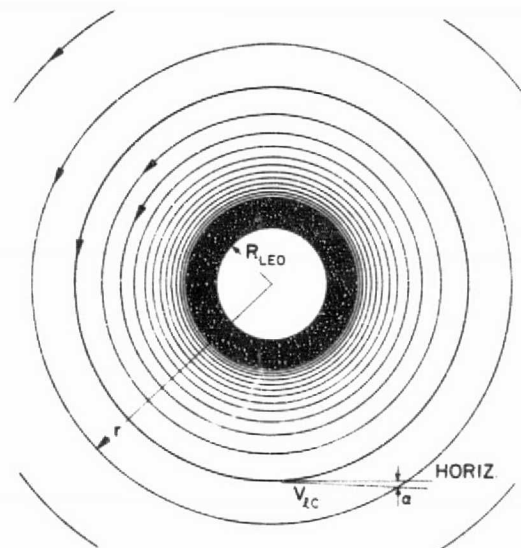


FIGURE 5-2 TYPICAL LOW THRUST SPIRAL TRANSFER GEOMETRY

To appreciate the range of these variables we have, for  $T/W_{LEO} = 10^{-4}$ , at LEO:

$$\frac{\Delta h}{\text{orbit}} = 8.64 \text{ km (4.66 n.m.)},$$

$$\gamma_{LEO} = .0115^\circ,$$

and near GEO:

$$\frac{\Delta h}{\text{orbit}} = 1860 \text{ km (1004 n.m.)};$$

$$\gamma_{GEO} = .433^\circ.$$

### 5.3.3 Ideal $\Delta V$ , Propellant Requirement

#### 5.3.3.1 COPLANAR ALTITUDE CHANGE

Since the thrust force works against gravity and in climbing to higher altitudes the spacecraft in fact loses speed it is not immediately obvious what the ideal speed increment (the speed increment which the spacecraft would achieve in the absence of gravity),  $\Delta V$ , is.

In Section G.4.3 it has been shown, from the basic equations of motion, that the ideal  $\Delta V$  is equal to the difference between the initial and final local circular speeds:

$$\Delta V = V_{icLEO} - V_{icGEO};$$

or numerically, the total  $\Delta V$  for transfer from the initial circular orbit at  $h = 500 \text{ km}$  to an in-plane circular orbit at geosynchronous altitude is:

$$\Delta V = 4543 \text{ m/sec. (14,903 ft./sec.)}$$

#### 5.3.3.2 PLANE CHANGE

In Section G.3.3 it was shown that the impulsive  $\Delta V$  required for simultaneous circularization and a  $28.5^\circ$  plane change was  $1817 \text{ m/sec.}$ , a mere  $371 \text{ m/sec.}$  ( $1218 \text{ ft./sec.}$ ) over that required for an in-plane circularization. This was possible through the efficient

dog-leg maneuver shown in Figure G-2.

In the low thrust transfer we arrive at geosynchronous orbit with near local circular speed and we do not have the capability of impulsively changing the direction of the velocity. Thus the best manner in which to achieve the plane change is by repeated small  $\Delta V$ 's at nodal passage of the orbit and equatorial

$V_{icGEO} i = 1528 \text{ m/sec. (5012 ft./sec.)}$ , where  $i$  is the plane change required (in radians).

The geometry is shown in Figure 5-3.

Thus the theoretical minimum  $\Delta V$  required for the entire

$$\Delta V = 6071 \text{ m/sec. (19,914 ft./sec.)}$$

Additional requirements on the  $\Delta V$  budget are discussed in the section on Design Considerations.

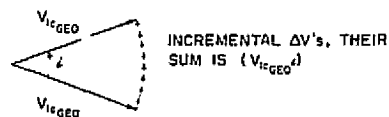


FIGURE 5-3 GEOMETRY OF LOW THRUST PLANE CHANGE

#### 5.3.3.3 PROPELLANT REQUIRED

The  $\Delta V$  requirement discussed above establishes the propellant weight required for the mission by the use of the rocket performance equation:

### 5.3.4 Time History of Transfer

#### 5.3.4.1 COPLANAR PART OF TRANSFER

A relationship between the time since the beginning of thrusting and the altitude, assuming constant thrust acceleration, is derived in Section G.4.4. Equation G.4-10:

$$t = \Delta V / \frac{T}{m} \quad (\text{G.4-10})$$

can be written in terms of altitude:

$$t \text{ (days)} = 90 \left[ 1 - \sqrt{\frac{R_{LEO}}{R_0+h}} \right] \quad (\text{5.3-5})$$

for constant  $T/m = .0001 g_0$ .

This relationship is plotted in Figure 5-4.

The total time to GEO is 53.79 days. Extrapolation to other values of the (constant)  $T/m$  is easily done by realizing that the time is inversely proportional to  $T/m$ . Hence for  $T/m = .001 g_0$ , the total time is 5.38 days; for  $T/m = 10^{-5} g_0$  it is 538 days.

If the thrust remains constant during the transfer, the thrust acceleration,  $T/m$ , will increase due to the propellant consumption. This, of course, depends on the specific impulse of the propulsion system used. By way of illustration, an altitude versus time curve is also shown in Figure 5-4, taking this effect into account for a system with a 1500 Sec specific impulse.

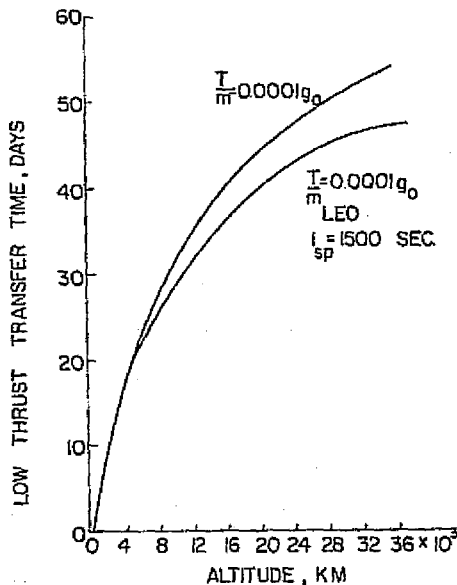


FIGURE 5-4 TIME VS ALTITUDE, LOWTHRUST TRANSFER

### 5.3.4.2 THE PLANE CHANGE

The plane change maneuver is very time consuming since the opportunity to apply the corrections occurs only twice per day at the nodal crossings. It is suggested that the process be speeded up by a thrusting program which begins  $30^\circ$  ahead of the nodal crossing and continues until  $30^\circ$  beyond. The scheme is shown in Figure 5-5.

The penalty associated with this non-impulsive plane change has not been evaluated here, but the minimum time required to change the plane  $28.5^\circ$  at geosynchronous orbit is:

$$t_{\text{plane change}} = 3 \times \frac{V_{\text{TCGEO}} (i)}{(T/m)} = 54.1 \text{ days}$$

for  $\frac{T}{m} = .0001 g_0$ .

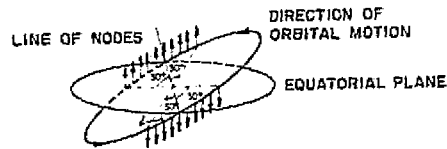


FIGURE 5-5 LOW THRUST PROGRAM FOR ORBITAL PLANE CHANGE

### 5.3.4.3 OCCULTATION

The effect of occultation, the temporary stopping of the thrust when the spacecraft passes through the shadow of the earth, has not been investigated in detail here.

The primary influence on the transfer process is the increase in transfer time by the accumulated time of occultation. The time of occultation during any one orbit is a function of the angle between the earth-sun line and the normal to the orbital plane, as well as of the altitude of the spacecraft. It is thus a function of the time of the year and the orbital inclination.

Analysis has shown that in a worst case, where the sun is continuously in the orbital plane, the accumulated time in darkness is about 18% of the total time. This "worst case" can easily be avoided.

A continuing detailed analysis is currently underway at JSC (Ref. 5-10).

### 5.3.5 Final Approach to GEO

The details of the final approach to a desired circular orbit at GEO altitude is shown in Figure 5-6. Thrust must be terminated at point B prior to arriving at the desired altitude (point C), otherwise overshoot will occur.

At thrust cut-off, the local circular speed at a small flight path angle  $\gamma_B$  will form the initial conditions to a coast phase such that the desired altitude is reached at the apogee of the coast phase ellipse. First approximations to the eccentricity,  $e$ , is that it is equal to  $\sin \gamma_B$  and thus the altitude rise, from B to A, is  $R_B e$  or  $R_B \sin \gamma_B$ .

For the case at hand, this altitude rise is approximately 316 km (170 n.m.), the coast arc near  $90^\circ$ , and the posigrade  $\Delta V$  needed for circularization at apogee is 12 m./sec. (38 ft./sec.).

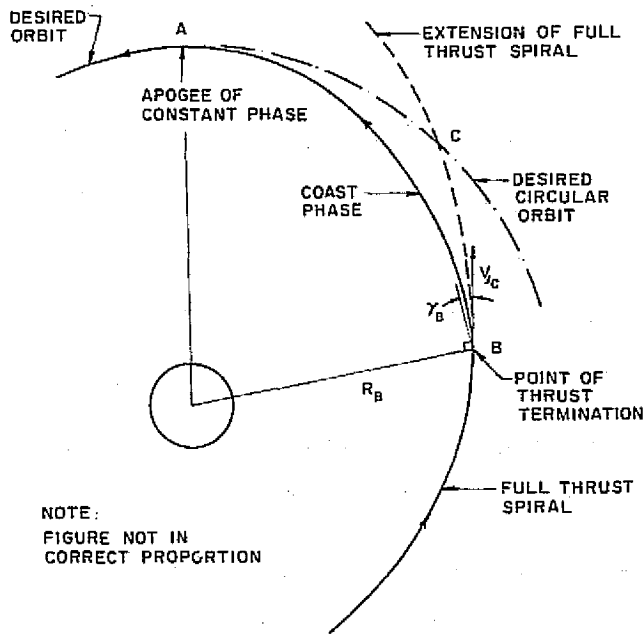


FIGURE 5-6 FINAL APPROACH PHASE TO DESIRED ORBIT

## 5.4. SPACE ENVIRONMENTAL ASPECTS

The environment has a multitude of effects on man and his machines and they, in turn, have many effects

on the environment. The physical constraints imposed by the surroundings will greatly affect the entire SPS project, but it will be particularly affected during transit between LEO and GEO and during construction and operation in GEO where the environment is to a large extent unknown and subject to fluctuations.

The physical surroundings of the satellites or modules will consist of both the natural environment, which is unusual from an earth-bound point of view, and the additions to the environment created by the transfer vehicles themselves. These must be considered in the choices of materials and methods of construction, which must be selected to be compatible with extreme temperature variations superimposed on a vacuum and UV and other types of radiation.

The influence of plasma and radiation-belt environment will also be important in delivery and deployment; some of the effects, such as the effect of radiation pressure on orbital mechanics and obscuration of solar cells due to micrometeorite "dust," will be quite small; others, such as degradation of solar cells and time limits on crew exposure, will yield critical trade-off parameters for system optimization.

The minor effects of the environment on the design will not be considered in this limited study, and the impact of the total SPS on the environment will be considered in a later chapter.

### 5.4.1 Aerodynamic Effects in Low Earth Orbit

#### 5.4.1.1 AERODYNAMIC ENVIRONMENT

Aerodynamic forces, although small in absolute value, may have long range effects on the orbital characteristics of objects in low earth orbits. In particular, the drag, being dissipative in nature, will gradually reduce the total energy and hence the major axis of the orbit. For initially circular orbits, the net effect is a decrease in altitude while the speed remains equal to its local circular value with negligible flight path angle. With speed and atmospheric density increasing with time the trajectory will eventually steepen rapidly, resulting in reentry.

Since aerodynamic effects are proportional to the dynamic pressure,  $q$ :

$q = 1/2 \zeta V^2$ , a measure of the aerodynamic environment at low-orbital altitudes might appropriately be the value of dynamic pressure based on the local air mass density,  $\zeta$ , and the local circular speed,  $V_{IC}$ .

Table 5-2 shows that the dynamic pressure varies by several orders of magnitude in the range of altitudes from 300 to 800 km.

At a given altitude the effect of the drag force on the motion of the spacecraft is dictated by the drag deceleration or the drag force per unit mass of the vehicle. The government spacecraft-dependent parameter is the so-called drag-weight parameter,\*  $D_D A/W_0$ . Here  $C_D$  is the non-dimensional drag coefficient,  $A$  the frontal area, and  $W_0$  the (earth-) weight of the vehicle. The units of the drag-weight parameter are  $m^2/n$  ( $ft.^2/lb.$ ). The larger the value of the drag-weight parameter the more pronounced is the effect of drag.

\*This parameter is the inverse of the Ballistic Number, which is also frequently used in the literature.

#### 5.4.1.2 ORBITAL LIFETIME

Analysis shows that the orbital lifetime,  $T_L$ , of a satellite placed in circular orbit is inversely proportional to the drag-weight parameter. Thus the product  $T_L C_D A/W_0$  is independent of the aerodynamic characteristics of the vehicle. This product, the lifetime parameter, is plotted in Figure 5-7 as a function of altitude (after Ref. 5-11). The analysis assumes constant drag-weight parameter and ignores all other perturbing forces such as solar radiation pressure. At altitudes above 650 km the solar radiation pressure becomes comparable with the aerodynamic pressure (Ref. 5-12).

For an altitude of 500 km (270 n.m.) the lifetime parameter is seen to be .752 days  $m^2/N$  (36 days  $ft.^2/lb.$ ). A completed SPS has a drag-weight parameter of .35  $m^2/N$  (16.3  $ft.^2/lb.$ ) and thus would have a minimum lifetime of 2.2 days, assuming no tumbling motion and a constant attitude (large surface forward) relative to the velocity vector.

Table 5-2 DYNAMIC PRESSURE BASED ON LOCAL ATMOSPHERIC DENSITY AND CIRCULAR SPEED AS A FUNCTION OF ALTITUDE

ALTITUDE $h$ , km (n.m.)	DYNAMIC PRESSURE, $q$ , $N/m^2$ ( $lb/ft^2$ )
278 (150)	$2.20 \times 10^{-3}$ ( $4.59 \times 10^{-5}$ )
370 (200)	$5.31 \times 10^{-4}$ ( $1.11 \times 10^{-5}$ )
463 (250)	$1.70 \times 10^{-4}$ ( $3.55 \times 10^{-6}$ )
556 (300)	$6.85 \times 10^{-5}$ ( $1.43 \times 10^{-6}$ )
648 (350)	$3.21 \times 10^{-5}$ ( $6.71 \times 10^{-7}$ )
741 (400)	$1.54 \times 10^{-5}$ ( $3.21 \times 10^{-7}$ )
833 (450)	$7.95 \times 10^{-6}$ ( $1.66 \times 10^{-7}$ )

\*Standard values of the density as a function of altitude were obtained from Ref. 5-11.

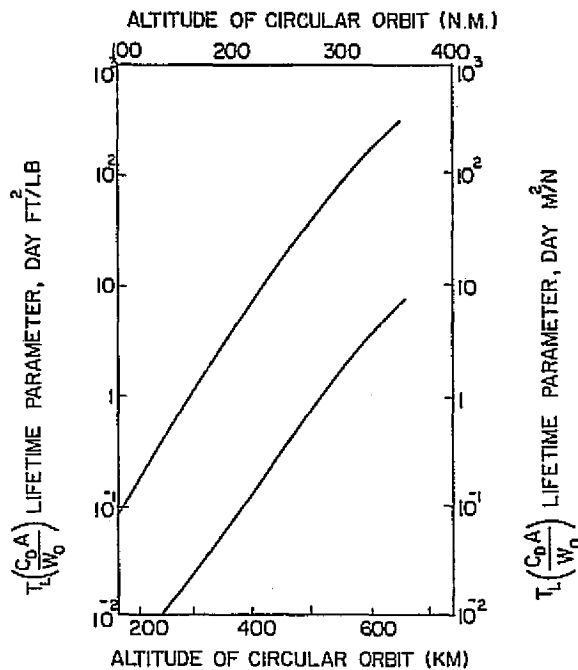


FIGURE 5-7 LIFETIME IN CIRCULAR ORBIT

### 5.4.1.3 EFFECT OF DIFFERENTIAL DRAG

For orbital operations in low-earth orbit in which a number of spacecraft and other objects are involved which are not tethered or otherwise connected with one another, the effect of differential drag is likely to be important. For this application the altitude loss per orbital period is more meaningful than the lifetime.

For low drag forces the altitude loss per orbit is given by:

$$\frac{\Delta h}{\text{orbit}} = - 2\pi \left( \frac{C_D A}{W_0} \right) g_0 \zeta (R_0 + h)^2,$$

where  $g_0$  and  $R_0$  are standard gravitational acceleration on the earth's surface and the radius of the earth respectively. The altitude loss is thus proportional to the drag-weight parameter.

For the reference altitude of 500 km (270 n.m.) the above expression can be written:

$$\frac{\Delta h}{\text{orbit}} = - 812 \left( \frac{C_D A}{W_0} \right) \text{English ft.}$$

$$\frac{\Delta h}{\text{orbit}} = - 11,850 \left( \frac{C_D A}{W_0} \right) \text{metric m}$$

To illustrate the pronounced effect of differential drag, Table 5-3 lists a selection of typical objects that may be involved in the assembly of an SPS with the altitude loss per orbit.

## 5.4.2 Objects in Earth Orbit--The Potential Collision Problem

### 5.4.2.1. INTRODUCTION

Since the beginning of the space age in 1957, the continuing exploration and exploitation of space has resulted in a substantially increasing population of objects in earth orbit. Only a small percentage of these objects are useful additions to the earth's exosphere. Communication, weather, and scientific satellites have increased man's knowledge and wisdom about this part of his environment, and the Skylab experiences have proved that man can live in space for extended periods. In the 1980's, the Space Shuttle will be the main vehicle for placing payloads into orbit and if current planning is realized, man will live in large space colonies during the construction and maintenance of solar power stations (Ref. 5-20). It is imperative, therefore, that this part of the environment is also kept safe for future activities.

In the United States, the task of tracking earth-orbiting objects is performed by the North American Air Defense Command (NORAD). Orbital information regarding each observable object--perigee radius, apogee radius, inclination, etc.--is contained in continuously updated computer files. It is thought that current files are reasonably, but not totally, complete for objects have a radar cross-sectional area greater than or equal to  $.01 \text{ m}^2$  ( $.11 \text{ ft.}^2$ ). In a detailed analysis of the June 1973 NORAD catalog (Ref. 5-13), of the 2565 trackable objects, 55.8% are the result of explosions in orbit, while rocket bodies and debris from payloads add another 27.4%. Only 16.4% of the population can be attributed to payloads, and, of course, most of them are no longer operational.

Table 5-3 ALTITUDE LOSS PER ORBIT FOR TYPICAL OBJECTS IN A 500 KM ALTITUDE CIRCULAR ORBIT

OBJECT	MAXIMUM $C_D A/W_0$		MAXIMUM* ALTITUDE LOSS PER ORBIT	
	m <sup>2</sup> /N	(ft <sup>2</sup> /lb)	m	(ft)
Compact Spacecraft	.0006	(.03)	7.3	(24)
EVA Astronaut	.0016	(.08)	20	(65)
Empty Large Tank	.0048	(.24)	61	(200)
Complete SPSS	.32	(16)	4054	(13,300)
Piece of Solar Blanket	.48	(24)	6100	(20,000)
Piece of Solar Concentrator	4.8	(240)	61000	(200,000)

\*Note here again that the assumption is made that the spacecraft is at a constant attitude relative to the velocity vector resulting in a constant maximum  $C_D A/W_0$ .

The "total" number of objects in earth orbit is assumed to be about 2 1/2 times the trackable population. This figure is assumed to include all objects of radar cross-sectional area greater than or equal to  $10^{-6} \text{m}^2$ . The current estimate for 1976 exceeds 10,000 objects. A typical distribution of orbital debris by semi-major axis (Ref. 5-13, 5-14, and 5-15), however, indicates that the high intensity flux zone occurs in the annular shell between 500 and 1500 km (270-810 n.m.). Over 90% of all earth orbiting objects pass through this region.

In earlier studies (Ref. 5-15 and 5-16) the stationarity and independence of the six classical orbital parameters associated with trackable objects were investigated. The parameters are as follows:

- Semi-major axis (a)
- Right ascension ( $\Omega$ )
- Eccentricity (e)
- Inclination (i)
- Period (P)
- Argument of perigee ( $\omega$ )

From a practical viewpoint, the correlation coefficients between any pair of orbital elements, except for "a" and "P," can be disregarded. The maximum correlation coefficient occurred between "a" and "e" and was .34. This means that only 11.5% of the total variance of "e" could be explained by a linear relationship between "e" and "a." From the scatter diagrams, it is clear that knowledge of one parameter provides very little information in the prediction of another parameter.

The stationarity, with respect to calendar time or increased missile and space activity, of the probability distributions of the classical orbital parameters was investigated to support future collision estimates. If the distributions remain unchanged, then a prediction of future collision probabilities could be obtained by a simple adjustment of the present estimate to account for any changes in the total number of objects. It was concluded that the distributions remain essentially unchanged and that reasonable predictions can be made for several years in the future.

A major concern is the future of the earth orbiting population. Based on historical records, a linear extrapolation of these data determined from the growth rate of the last few years can be obtained (Ref. 5-13). Latest estimates indicate that the trackable population increases at the rate of 280-300 objects per year. If this rate is maintained, approximately 10,000 trackable ob-

jects will be present in 1995, but, if the annual growth rate increases by 10% each year, this figure is reached by 1985. In light of current discussions of space exploration and exploitation, it seems unlikely that space activity will decrease in the foreseeable future.

The following interesting phenomenon, associated with debris growth, has been observed (Ref. 5-14): Although the total number of trackable objects from 1966 to 1970 increased from approximately 1000 to 2000, the number of objects intersecting a 500 km spherical shell (LEO) remained constant at about 230. This suggests that maintaining the current growth rate coupled with secular orbit perturbations caused by gravitational attraction of the moon and sun, atmospheric drag, solar radiation pressure, and higher harmonics of the earth's gravitational potential, will sustain this dynamical equilibrium zone.

#### 5.4.2.2 COLLISION PROBABILITY MODELING OVERVIEW

Any attempt to estimate the probability of a collision between a spacecraft and the objects in earth orbit must model the total orbiting population and hence, must be dependent in some way on the orbital characteristics of the known population. Characteristic of the models which follow, the first three utilize the population spatial data contained within the NORAD catalogs. The fourth model is a simplified approximation which uses the average spatial density and weighted average velocity of the debris to determine the average flux of objects in a spatial zone.

The following assumptions are common to the first three models.

- a.** The target spacecraft orbit is circular.
- b.** Changes in right ascension of the ascending node and argument of perigee are due to the first order secular perturbations caused by the oblateness of the earth.
- c.** Objects which pose a collision hazard are very small compared to target objects.
- d.** The time during which a collision can occur is short compared to the orbital period of either object.
- e.** Orbital decay due to atmosphere drag is neglected.
- f.** Target objects are small compared to the dimensions of their orbits.
- g.** The location of an object in its orbit is random

for any time after the start of a mission. Obviously, all of the models incorporate to some degree the inherent stochastic nature of this environment. In 1966, the NORAD specified tracking uncertainty was 7620 m (25,000 ft.) and currently it is about 1524 m (5000 ft.). For a given instant in time, this distance represents the radius of a sphere, centered along the cataloged orbit, in which the object is actually located.

### 5.4.2.3 THE PSEUDO COLLISION MODEL

The Pseudo Collision Model was developed from the concept of mean time-to-collision (Ref. 5-17), that is, if  $\tau_0$  is the mean time-to-collision and  $\tau^*$  is the mission duration time of the target spacecraft, then the collision probability ( $P_C$ ) is determined by:

$P_C \cong 1 - e^{-\tau^*/\tau_0}$ . In order for a collision to occur between the  $j^{\text{th}}$  satellite and the target spacecraft, it is first necessary for the perigee and apogee radii of the  $j^{\text{th}}$  satellite to bracket the target altitude (see Figure 5-8). At each path coincidence, the amount of time the  $j^{\text{th}}$  satellite spends within a distance  $\Delta L$  of the target altitude is determined from the true anomaly increment  $\Delta V_j$ . Then the total count of passes during the duration of the mission is obtained after correcting for the so-called "beat frequency" between each satellite and the target spacecraft. This adjustment provides an uncorrelated count for the total duration of the mission. Finally, the  $j^{\text{th}}$  satellite collision probability is formed from the product of the uncorrelated count and the probability that the target spacecraft is at the points of orbital intersections. The overall collision probability for the mission is then obtained by summing the individual fluxes (impacts/km<sup>2</sup>-yr) and converting this sum to a probability through the Poisson distribution as follows:

$$P_C = 1 - e^{-\sum_i F_i}$$

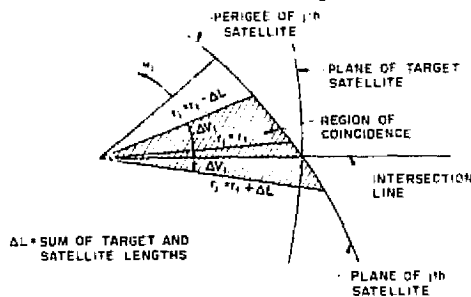


FIGURE 5-8 PSEUDO COLLISION MODEL GEOMETRY

The basic formulation of this model lends itself to a particularly simple (proportional scaling) method for updating collision probabilities due to changes in the number of satellites, mission duration, or cross-sectional area of the target spacecraft.

Table 5-4 represents the impact rate as a function of altitude and inclination for a representative SPS satellite. To interpret this table, choose an altitude and an inclination, say 500 km and 30 degrees, respectively. Then this model says that an SPS at this location would experience about 47 impacts per year on the average. Based on the previous discussion concerning the distribution of orbital debris by size, one could infer that approximately 19 collisions would be caused by objects having a cross-sectional area exceeding 10<sup>-2</sup>m<sup>2</sup> and the remainder would be caused by smaller objects. Although these data represent the impact rates on a randomly oriented surface, this model is generally regarded as a pessimistic approximation of potential collisions.

### 5.4.2.4 THE LANGLEY COLLISION MODEL

The basic geometry of this model is very similar in structure to the geometry of the previous method (Ref. 5-13). There are, however, several additional assumptions which influence the final results. These assumptions are as follow:

- a. Target objects are spheres.
- b. Orbital traces in the vicinity of an intersection are straight lines.
- c. The orbital velocity of an object in the vicinity of an intersection is constant.

Based on a spherical target, as the trace of one orbit moves across the other, the size of the "effective" target available to a piece of debris is not a circle of constant radius but rather a circular target whose radius can vary. This allows one to more sensitively model the changing relative collision zone with time.

The assumption involving linearization in the vicinity of a collision can be very good or very bad. In particular, the final form used for determining the probability of collision can attain a value greater than 1. It was observed, however, that the number of instances for which linearity could not be assumed was small compared with the total number of candidates, and hence, they would probably have a negligible effect on an extended series of probability calculations.

Table 5-4 PSEUDO COLLISION MODEL

ALTITUDE		INCLINATIONS DEG.				
n.m.	Km	10	30	50	70	80
100	185	2	2	2	2	3
200	370	16	20	20	19	30
270	500	39	47	46	52	67
300	556	49	58	57	67	83
400	741	56	69	71	82	94
500	926	60	73	78	81	105
600	1111	33	37	39	42	54

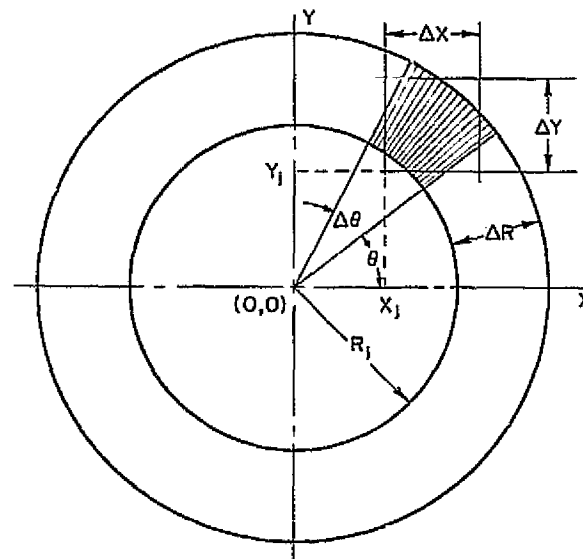
Impact Rate for 1-year with an SPS reference area of 144 Km<sup>2</sup> (56 Mi<sup>2</sup>) based on the 1970 NORAD Catalog.

Table 5-5 reflects the results of the Langley Model. The terms nominal and worst represent inclinations of 30-50 degrees and 110 degrees, respectively. As before, we may use proportional scaling to adjust these predictions for variations in satellite density, target area, or mission duration.

#### 5.4.2.5 THE APPROXIMATE COLLISION MODEL

In reality, in order to use the NORAD catalog to obtain collision probability estimates, it is necessary to make certain assumptions concerning the uncertainties in the data. In this model, the uncertainties associated with the coordinates of the miss distances between the debris and the target spacecraft are Gaussian with the following properties: (a) zero biases, (b) equal variances, and (c) uncorrelated in the three dimensions (Ref. 5-18).

To formulate this model, consider the vector of closest approach between the  $j^{\text{th}}$  satellite and the target spacecraft, say  $R_j$  (see Fig. 5-9). Also, consider the relative velocity vector of the  $j^{\text{th}}$  satellite with respect to the target to be normal to plane containing  $R_j$ .



NOTE: VELOCITY VECTOR OF SATELLITE IS NORMAL TO THE X-Y PLANE

FIGURE 5-9 APPROXIMATE COLLISION MODEL GEOMETRY

Table 5-5 LANGLEY COLLISION MODEL

TIME PERIOD	TRACKABLE OBJECTS	ESTIMATED TOTAL	ALTITUDE							
			500 n.m. nominal		500 n.m. worst		800 n.m. nominal		800 n.m. worst	
			Track	Tot	Track	Tot	Track	Tot	Track	Tot
Estimate, mid-1974	3570	9050	25	63	51	130	65	164	183	464

Impact rate for 1-year with an SPS reference area of 144 Km<sup>2</sup> (56 Mi<sup>2</sup>).

If one had perfect tracking accuracy, then this relative velocity vector would be normal to the plane at (0,0). However, due to tracking errors, the locational uncertainty of the  $j^{\text{th}}$  satellite with respect to the target spacecraft is assumed to be tri-variate spherically normally distributed. The resultant projection of the uncertainty in any arbitrary plane (e.g., the plane which contains  $R_j$ ) is, therefore, bi-variate circularly normally (Rayleigh) distributed.

If we assume that  $\Delta x = \Delta y = \Delta R =$  the approximate length of the target spacecraft plus the other satellite and that  $\sigma_x^2 = \sigma_y^2 = \sigma^2 =$  the NORAD tracking uncertainty in the components of the close approach vector, then the  $j^{\text{th}}$  collision probability is given by:

$$P_{C_j} = \frac{1}{2\pi\sigma^2} \int_{x_j}^{x_j+\Delta x} \exp(-x^2/2\sigma^2) dx \int_{y_j}^{y_j+\Delta y} \exp(-y^2/2\sigma^2) dy$$

$$= \frac{1}{2\pi\sigma^2} \int_{\theta_j}^{\theta_j+\Delta\theta} \int_{R_j}^{R_j+\Delta R} r \exp(-r^2/2\sigma^2) dr, d\theta$$

which integrates immediately to:

$$P_{C_j} = \frac{\Delta\theta}{2\pi} [\exp(-R_j^2/2\sigma^2) - \exp(-(R_j + \Delta R)^2/2\sigma^2)].$$

Table 5-6 shows the sensitivity of this model to variations in uncertainty. As one can see, increased tracking accuracy significantly reduces the expected impact rate and consequently, this model, although it is an attractive combination of the deterministic and stochastic nature of the debris environment, is questionable.

#### 5.4.2.6 THE FLUX MODEL

We mentioned previously that currently (1973) over 90% of all space debris intersects the spherical annulus between 500 and 1500 km. A simple estimate of the impact rate of these particles on a random element, say  $1 \text{ km}^2$ , of the surface area of a sphere can be made (see Fig. 5-10). The flux, measured in impacts per  $\text{km}^2$  - year is given by:

$$F = 1/4 DV$$

where  $D$  is the spatial density of the debris and  $V$  is the weighted average particle velocity (Ref. 5-19). If we assume a linear growth of 250 pieces of debris per year between 500 and 1500 km, then the spatial density would increase by about a factor of 8 by 2035 as shown in Table 5-7.

Table 5-8 represents the average number of impacts an SPS satellite would encounter in this spherical annulus for a period of one year.

Due to the distribution of orbital debris, one expects about one-half the number of impacts at 500 km and about twice this number at 1000 km where all of the models predict the worst collision environment (Ref. 5-20). In order to use the flux model to make accurate collision estimates at a given altitude, say 500 km, one must first determine the flux of objects in near circular orbit at 500 km, second, determine the flux of objects intersection a 500 km shell, and then add the fluxes. For quick estimates, the flux model is attractive and it typically differs only by a factor of two from the more involved simulation modes.

#### 5.4.2.7 COMPARISON OF THE MODELS

A comparison between the four previously discussed models is presented in Figure 5-11. In order for such a comparison to be made, all collision probabilities were adjusted to represent the number of impacts per  $\text{km}^2$  of a randomly oriented surface area for a period of one year. However, for sake of consistency within this report, these values are represented in terms of the maximum exposed cross-sectional area.

Two assumptions were made to determine Figure 5-11. They are:

- a. The flux of particles at 500 km (LEO) will remain in equilibrium until the year 2035.

TABLE 5-6 APPROXIMATE COLLISION MODEL

UNCERTAINTY ( $\sigma$ ) (FEET)	IMPACT RATE (IMPACTS/KM <sup>2</sup> -YR)
5000	1
10000	10
15000	11
20000	18
25000	27
30000	34
50000	40
100000	28

Variation in Impact Rate with Uncertainty for an SPS at 1111 Km (600 n.m.) miles with a 30° inclination for one year.

Table 5-7 INCREASE IN SPATIAL DENSITY BY NUMBER OF OBJECTS FOR A FIXED VOLUME ELEMENT

YEAR	NUMBER OF TRACKABLE OBJECTS	SPATIAL DENSITY (x 10 <sup>-9</sup> /Km <sup>3</sup> )
1973	2100	3.1
1995	7600	11.1
2015	12600	18.4
2035	17600	25.7

Table 5-8 FUTURE PREDICTIONS OF SPS IMPACT RATE USING THE FLUX MODEL

YEAR	IMPACTS BY TRACKABLE DEBRIS	TOTAL NUMBER OF IMPACTS
1973	46	117
1995	165	419
2015	274	695
2035	383	971

Future Predictions of Impact Rate Between 500 and 1500 Km for 1 year with an SPS reference area of 144 Km<sup>2</sup>.

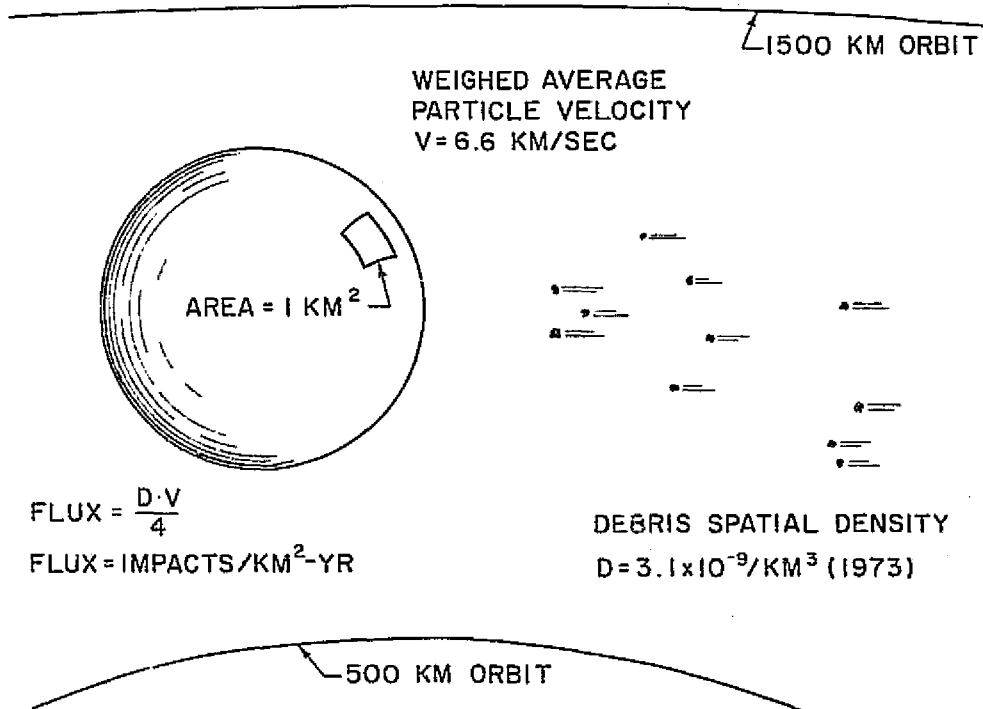


FIGURE 5-10 GEOMETRY OF THE FLUX MODEL

b. The growth in the number of particles between 500 and 1500 km is held constant at 250 per year.

Both assumptions are considered to be very conservative in light of anticipated future space activities associated with SPS construction and maintenance, however, each has its foundation in the historical data.

This comparative analysis reflects the impact rate on the SPS truss configuration during partial construction in LEO and subsequent transportation by electric thrusters to GEO. Each of the five viable engine candidates requires a portion of the total SPS power output for its operation. Therefore, assuming an SPS construction rate of one per year, the impact rate during build-up in LEO can be approximated. Finally, assuming a trip time of 54 days from LEO to GEO, a partially completed SPS will spend about 4 days traveling from 500 to 1500 km where the impact rate is expected to increase by about a factor of 8 by 2035.

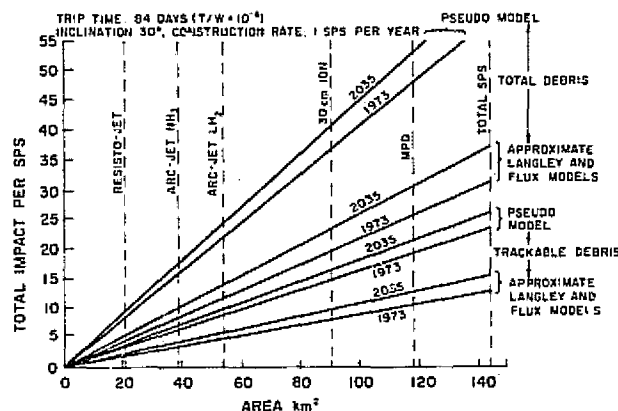


FIGURE 5-11 COMPARISON OF 4 COLLISION MODELS

If, due to economic, engineering, or other constraints,  $LH_2$ , the Arcjet engine is chosen as the thruster, then a conservative estimate of the number of impacts on a single SPS satellite before it reaches GEO is between 12 and 24 by the turn of the century. A further, and possibly more realistic, estimate is obtained if we allow the number of objects intersecting a LEO orbit to increase by ten per year. Then the estimate becomes 25 to 50 impacts by the year 2000. With the projected intense launch activity of HLLV's supporting the SPS program, extreme care must be maintained to prevent a degradation in an environment which already presents serious collision problems.

## 5.4.2.8 CONCLUSIONS AND RECOMMENDATIONS

If unrestrained launch activity continues, it is inevitable that even the life span of small objects will be significantly decreased. If man is to continue to use space to his advantage, this attitude is clearly unacceptable. The gathering of the latest data on orbiting satellites and debris together with improved modeling techniques should continue in order to illuminate the changing nature of this environment with time. In particular, a detailed collision analysis should be performed for long duration GEO orbits to determine the expected impact rate on operational SPS satellites. A deeper understanding of the problem might suggest ways in which practical solutions might be achieved.

Possible general recommendations which could be made have been articulated in a recent manuscript (Ref. 5-20). The following suggestions are listed in order of increasing severity of the problem:

- a. Continue to do nothing.
- b. Perform ground tests to simulate hypervelocity impacts on complex structures.
- c. Design and fly a Shuttle payload to monitor the buildup of objects in earth orbit.
- d. Design a collision avoidance system for spacecraft.
- e. Impose restraints on payloads to minimize the amount of debris in space.
- f. Institute a program to return objects from space which no longer serve a useful function.

A specific recommendation can be made with regard to the SPS truss configuration associated with LEO construction. If, in lieu of one large truss,  $N$  smaller modules are constructed in LEO, independently transported to GEO, and joined together to form a complete solar satellite, the total number of impacts for a complete SPS can be significantly reduced. For a linear construction rate, the area as a function of time is given by:

$$A(t) = \frac{A}{T} \cdot t, \quad 0 \leq t \leq T,$$

where  $A$  represents the randomly oriented surface area,  $T$  is the time to completion, and  $t$  is the elapsed time.

Therefore, if  $F$  represents the flux (impacts per  $\text{Km}^2\text{-yr.}$ ) in LEO, then the number of impacts on the truss ( $I_{\text{Truss}}$ ) in LEO is given by:

$$I_{\text{Truss}} = \frac{F \cdot A}{T} \int_0^T t dt = \frac{FAT}{2} .$$

If  $N$  smaller modules are constructed, each requiring  $T/N$  years to complete, then the number of impacts on the total collection of  $N$  modules ( $I_{\text{Mod}}$ ) is given by:

$$I_{\text{Mod}} = \frac{NFA}{T} \int_0^{T/N} t dt = \frac{I_{\text{Truss}}}{N} .$$

Consequently, a  $1/N$  reduction in expected impacts is gained in LEO if the modular approach is adopted. Of course, the number of collisions during transportation to GEO for either scenario is unchanged if the total area remains constant.

Assuming the same conditions used in the example of Section 5.4.2.7 and assuming 25 modules are constructed, by the turn of the century, the number of impacts for the realistic case becomes 1 to 2 collisions. This is a significant reduction in the total number of collisions, but further research is needed to evaluate the added problems in GEO associated with the necessary aggregation of the modules to complete the satellite.

### 5.4.3 Radiation

Radiation is probably the most pervasive and the least understood part of the environment to be encountered by the SPS itself and by the large construction crew necessary during the transportation and assembly of the SPS. Before such a design can be contemplated it will be necessary to know in detail the flux levels of the many kinds of radiation, their energy spectra and their time variations.

#### 5.4.3.1 TYPES OF RADIATION IN SPACE

One possible method of Classifying radiation in space is by its origin and place of occurrence. For the present purposes, this is the method that will be used.

### Geomagnetically Trapped Radiation

The geomagnetic field consists of lines of force which within the trapping region are closed, well confined, and relatively stable and which are capable of trapping charged particles (Ref. 5-21). The particles trapped in the region are primarily protons ( $\text{H}^1$ ) and electrons ( $e$ ), with less than 1% deuterons ( $\text{H}^2$ ) and tritons ( $\text{H}^3$ ). The region is commonly known as the Van Allen belt.

The coordinate system used for plotting the trapped radiation is based on the invariance of physical properties. For our purposes, and for geosynchronous orbit with a small inclination, it will be sufficient to define the dimension  $L$ ; this is the coordinate of the magnetic shell on which a particle stays as it drifts around the earth in longitude. For a perfect magnetic dipole it has the magnitude of the equatorial distance of the line of force in units of earth radii ( $R_E$ ). In the figure below (Fig. 5-12),  $L$  is used to show the distance to the center of an arbitrary region of constant radiation flux.

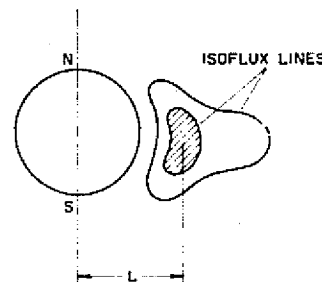


FIGURE 5-12  
REGION OF CONSTANT RADIATION FLUX

Synchronous equatorial orbits will lie on the magnetic shell given by  $L = 6.6 R_E$ . However, the parameter  $L$  is based on measurements made at the earth's surface, and the magnetic field calculations are in error at this altitude due to the effect of the solar wind which interacts with the earth's magnetic field to create the magnetosphere (Ref. 5-22). The coordinate system used in trapped radiation therefore breaks down at geosynchronous altitude.

**Protons.** It is fairly well established that the total radiation as a function of distance from earth has two peaks, the first of these is known classically as the inner radiation zone. Here high energy ( $\sim 40$  MeV)

protons reach a peak flux of  $5 \times 10^4 \text{ H}_1^1/\text{cm}^2 \text{ sec.}$  at a distance of  $L = 1.5 R_E$ . These protons constitute the most penetrating natural component of radiation in the inner zone. Another peak of high energy protons is found in the inner zone at  $L \approx 2.28 R_E$ .

In the outer radiation zone ( $L = 3-5 R_E$ ) there is an important low-energy proton component with energies  $0.1 \leq E \leq 4 \text{ MeV}$  with a peak flux on the order of  $10^8 \text{ H}_1^1/\text{cm}^2 \text{ sec.}$  (Ref. 5-21).

**Electrons.** The other major component of the trapped radiation is the electrons. The electrons exist in relatively high intensity throughout the entire region of durable trapping within the magnetosphere. For the inner radiation zone the flux is greater than  $10^8 \text{ e/cm}^2 \text{ sec.}$  for energies  $>40 \text{ keV}$ . Typical values of electron intensities in the outer radiation zone (at  $L \approx 4 R_E$  near the geomagnetic equator) are:

$$J_0 (E_0 > 40 \text{ keV}) = 3 \times 10^7 \text{ e/cm}^2 \text{ sec.}$$

$$J_0 (E_0 > 230 \text{ keV}) = 3 \times 10^7 \text{ e/cm}^2 \text{ sec.}$$

$$J_1 (E_0 > 1.6 \text{ MeV}) = 3 \times 10^5 \text{ e/cm}^2 \text{ sec.}$$

Whereas the protons in the outer zone are characterized by their stability, the electrons in the outer zone are characterized by their time variability. The fluxes can change by orders of magnitude in hours.

It is interesting that among trapped radiation the electrons constitute the main hazard to humans in the outer zone. The trapped protons at high altitudes do not present much of a radiation hazard because their energies are below 1 MeV (Ref. 5-22). The FLUX subroutine (Ref. 5-24) calculates the proton flux (40 MeV - 110 MeV) and sets the value equal to zero when  $L > 4$ . For the solar cells, however, the damage done by the low energy protons cannot be neglected.

**Galactic Cosmic Radiation.** This radiation source consists of completely ionized atoms (nuclei) (Ref. 5-25). The particles have great energy and it is therefore assumed that they cannot be contained in our solar system but are generated in the galaxy, possibly from a variety of sources (Ref. 5-26). Before they are absorbed near the earth's orbit they have undergone initial acceleration and diffusion through the galaxy, possibly again been accelerated and finally modulated by the solar wind. Because of their diverse nature, but generally high mass and energy, they are usually referred to as HZE particles.

Galactic material ranges from hydrogen through iron with chemical composition as shown in Table 5-9.

Table 5-9 CHEMICAL COMPOSITION OF GALACTIC COSMIC RAYS

Group	Z	Intensity/ $\text{m}^2 \text{ ster. sec}$ $>1.5 \text{ GeV/Nuc.}$	$\frac{\text{Intensity}}{\text{Intensity } Z > 10}$	Average in Universe
H	1	1300	680	3360
He	2	88	46	258
Li, Be, B	3-5	1.9	1.0	$10^{-5}$
C, N, O, F	6-9	5.7	3.0	2.64
$Z > \text{Ne}$	$>10$	1.9	1.0	1.0
$Z > \text{Ca}$	$>20$	0.53	0.28	0.06

The abundance of the elements C, N, O, F, and the presence of Li, Be, and B suggests that the formation of the cosmic rays occurs in a region rich in heavy nuclei and that the lighter nuclei Li, Be, and B are formed by fragmentation of the heavy nuclei upon collision with interstellar hydrogen. The fragmentation parameters for the production of those three elements are known reasonably well (Ref. 5-27) and the amount of matter necessary to be traversed by the cosmic rays in order to produce the yields shown in the table can be calculated. The best current estimate (Ref. 5-28) is  $2.5\text{g/cm}^2$ . It is interesting, but not too surprising, that nuclei of even Z tend to predominate. Even-even nuclei are generally more stable. Recent indications are that approximately 1% of the primary galactic radiation consists of electrons with  $E > 100\text{ MeV}$ .

The effects of high-energy cosmic rays on humans are unknown but are considered by most authorities not to be of serious concern for the relatively short exposures of contemporary spaceflight activity (Ref. 5-25). However, for the long-duration, deep-space missions of the future there may be progressive destruction of nondividing nerve cells. The question of biological effects of HZE particles has been accentuated by the reports of visual light flashes, even with eyes closed, by Apollo crews (Ref. 5-29). In these cases the eye itself has acted as a scintillation detector.

Although the intensities, especially of the electrons in the outer radiation zone, may vary widely, both the geomagnetically trapped radiation and the galactic cosmic rays are referred to as "expected" radiation. Into this classification also falls the emissions from nuclear onboard spacecraft sources (Ref. 5-30).

**Solar Cosmic Radiation.** Solar radiation is classified as "unexpected" radiation presumably due to the fact that it cannot be predicted in advance of solar events. The solar particle radiation consists mainly of high energy protons and their intensities are such that they constitute a considerable hazard to manned flights and have a considerable effect on most types of solar cells. The geomagnetic cutoff energies are not well known in synchronous altitudes, therefore, the differences between free space fluxes and those encountered by synchronous satellites for energies less than 30 MeV are somewhat indeterminate. Above 30 MeV the free space flux should be encountered (Ref. 5-22).

Solar events, in order to be considered, have an integrated intensity of  $10^6\text{ particles/cm}^2$  at energies  $> 30\text{ MeV}$ , observed on earth; this is a threshold (Ref. 5-26). Energy distribution of the particles range from  $10^7\text{ ev}$  and have been observed at  $>10^{20}\text{ ev}$ .

For high altitudes the solar cosmic radiation must be taken into consideration. For example, if the solar event of August 4-9, 1972, had coincided in time with an Apollo mission, the dose within the heavy, well shielded command module would have been 360 rads for the skin and 35 rads for bone and spleen. Inside the thinly shielded Lunar Module or during EVA the dose would have been extremely serious (Ref. 5-25).

Consideration must also be given to secondary radiation, neutrons, and Bremsstrahlung, created by collisions and interactions by cosmic rays or electrons with the material of the spacecraft or within the body subjected to the radiation.

**The Radiation Environmental Dose in LEO and In Orbit Transfer.** Because the radiation environment is so diverse, it is convenient to establish the dose received as the unit of measurement. The dose received at a point is that due to the sum of all of the radiation and is measured in rads, where 1 rad is defined as 100 ergs of energy deposited per gram of whatever material is receiving the dose.

In low-earth orbit (LEO) and in orbital transfer (OT) between LEO and geosynchronous orbit (GEO) material and men are subjected to exposure of radiation in the Van Allen belt. Figure 5-13 shows the daily accumulated dose, in rads, as a function of altitude for a circular orbit with 30 degree inclination (Ref. 5-31). Similar curves are obtained for other orbital inclinations, with the accumulated dose slightly higher for smaller angles. The curves in the figure have shielding thickness as a parameter, varying from  $0.5\text{ g/cm}^2$ , which is representative of spacesuits, to  $4.0\text{ g/cm}^2$  which is representative of a well shielded spacecraft.

The dose received in LEO, as shown in the figure, depends on the altitude chosen for the orbit. Air drag at low altitudes may make it impossible to assemble large, low-density structures due to degradation of orbit; on the other hand, an increase in altitude will mean an increase in radiation dose and will, therefore, require additional shielding for the construction crew. If assembly, or partial assembly is to be done in LEO there will, therefore, be a tradeoff between orbit

degradation and shielding weight.

The dose received in OT will obviously depend on the time spent in going from LEO to GEO, however, the dose will be sufficiently high so that only chemical propulsion should be considered for crew. Figure 5-14 shows the accumulated dose, in rads, as a function of shield thickness, with orbit transfer times of 5.4, 27, and 54 days and with all curves extrapolated back to zero shield thickness, for a 30 degree orbit inclination. The curves were calculated by summing the daily doses, which were determined from the average dose existing at the altitude at which the craft would be on a given day, depending on its thrust to weight ratio (T/W). The calculations were done for  $T/W = 10^{-3}$ ,  $5 \times 10^{-4}$ , and  $10^{-4}$ , and essentially represent a combination of Figure 5-2 and Figure 5-13.

The no-shield doses from Figure 5-14 are plotted as a function of transfer time in Figure 5-15 for two orbit inclinations. The curves should obviously go to zero dose for zero transfer time.

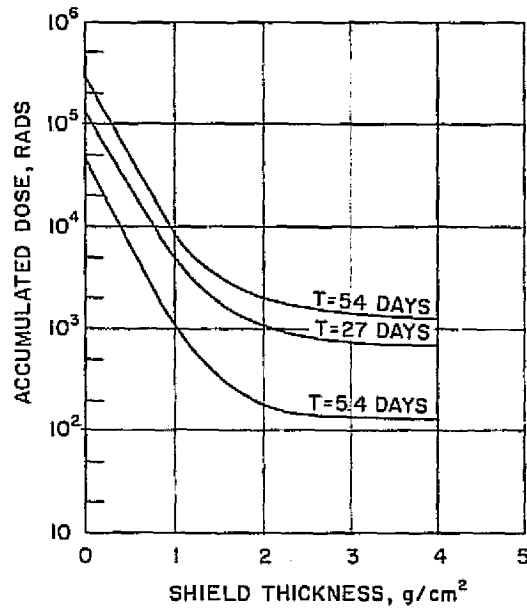


FIGURE 5-14 CALCULATED DOSE ACCUMULATED DURING ORBITAL TRANSFER FROM LEO TO GEO FOR VARIOUS TRANSIT DURATION AS FUNCTION OF SHIELD THICKNESS (30° ORBIT)

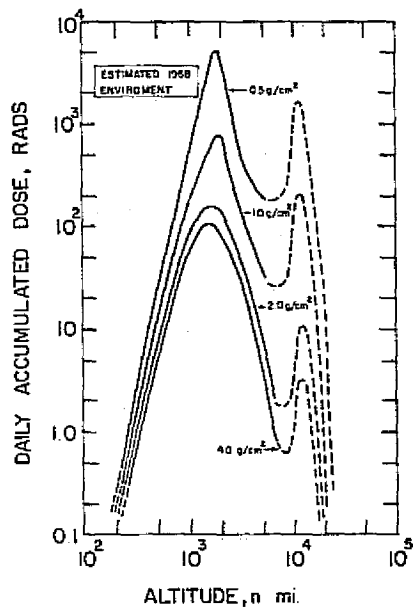


FIGURE 5-13 (REF 5-31) DOSE RATES IN THE EARTH'S RADIATION BELT AS FUNCTIONS OF ALTITUDE FOR VARIOUS SHIELD THICKNESSES (30° ORBIT)

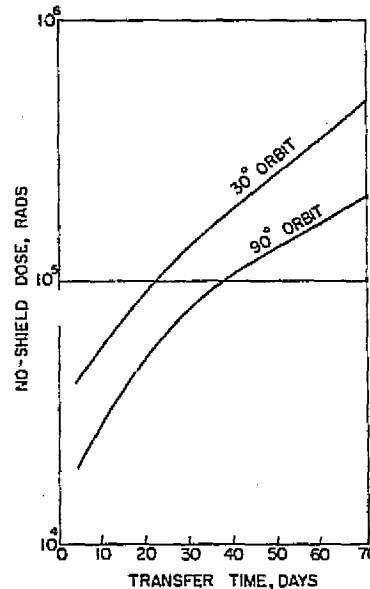


FIGURE 5-15 NO-SHIELD DOSE ACCUMULATED DURING ORBITAL TRANSFER AS FUNCTION OF TRANSIT DURATION.

**The Radiation Environmental Dose in GEO.** In geosynchronous orbit the radiation sources are partly due to the geomagnetically trapped protons and electrons although at an altitude of about 35,000 kilometers the dose due to these is at least three orders of magnitude less than the peak magnitude in the Van Allen belt. The trapped particle flux will vary according to two cycles--the diurnal variation caused by the solar wind, and a long-term variation caused by the solar cycle. The trapped radiation at this altitude consists mainly of electrons with a soft spectrum, trapped proton fluxes are negligible for humans.

The other two components of radiation are due to galactic cosmic rays and solar events. The cosmic ray flux is significantly higher than that in LEO, and the energy spectrum is very hard, causing only small variations in dose rates behind very thick shields (Ref. 5-32).

The solar events are very important when they do occur, and some think that it is necessary to be able to predict, at least several months ahead of time, when these events will occur, before manned stays at geosynchronous altitude should be contemplated (Ref. 5-32); however, the SPS program must be of a continuous nature, and, therefore, solar flare predictions do not suffice to keep human exposure low.

Figure 5-16 shows the dose rates behind various shield thicknesses in geosynchronous altitude with an orbital inclination of 30 degrees, and parked at 110° East. There will be some variations with inclination and longitude but these variations are probably smaller than the uncertainties in the doses shown.

The doses due to solar flare events are not shown in the figure, however, doses averaged over six years are an order of magnitude greater than background (Ref. 5-29). During a solar flare event the dose would be considerably greater.

#### 5.4.3.2 ENVIRONMENTAL EFFECTS ON MAN

Man will be necessary to perform many of the operations connected with the deployment, construction, assembly, and maintenance in the SPS program. It will be necessary to have prolonged residence at both LEO and GEO, and hence radiation protection becomes a significant portion of the safety considerations.

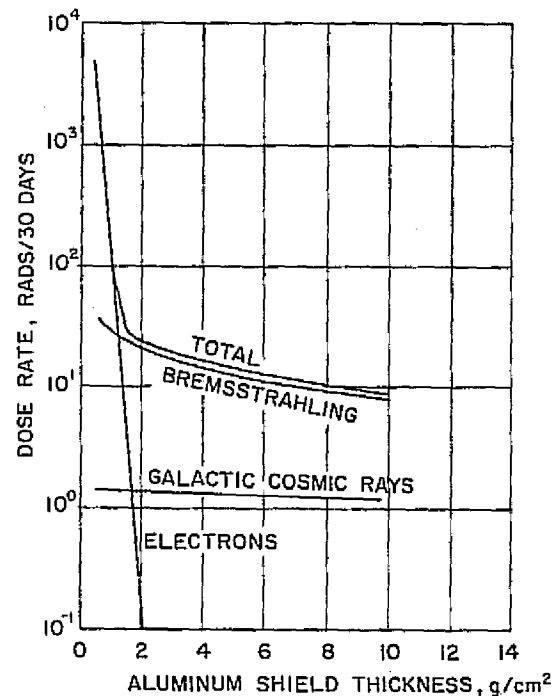


FIGURE 5-16 TOTAL DOSE RATE AS FUNCTION OF SHIELD THICKNESS AT GEOSYNCHRONOUS ALTITUDE, LONGITUDE 110° EAST, 30° INCLINATION (REF. 5-32)

The radiation standards that were determined for the astronauts in the previous short-duration spaceflights will not necessarily be valid for projects such as the SPS, where the nature of both the personnel and of the mission are entirely different. The recommended permissible dose for space has been set much higher than for industrial exposure. This was based partly on the fact that astronauts are volunteers (Ref. 5-29); however, it may be considered that an industrial worker is also willingly accepting a known risk, and is, therefore, also a volunteer.

It is almost certain that new limits will be set in order to protect personnel against the uncertainties of solar events coupled with the length of the proposed missions. It will, likewise, be necessary to provide better shielding and operational procedures and constraints which will minimize both exposure and its effects.

**Radiation Standards.** Whereas exposure limits to industrial workers and to the general public are quite rigidly fixed both by international (Ref. 5-33) and U.S. (Ref. 5-34) agencies, the agencies responsi-

ble for manned flights are permitted to set their own exposure limits, which may exceed the Radiation Protection Guide (RPG). This permission is stated in Ref. 5-35: "There can be no single permissible or acceptable level of exposure without regard to the reasons for permitting the exposure."

Absorbed dose is measured in rads, but if the material in which the radiation is absorbed is biological, then the energy deposit is not a sufficient measure because different kinds of radiation and even different energies of the same kind of radiation will have different effects. The radiation unit used is rem (Roentgen equivalent man) which is the product of the dose in rad and the QF (quality factor). The quality factor is a numerical indication of the given radiation's LET (linear energy transfer). The rem may also be calculated from the dose in rads and the RBE (relative biological effectiveness) where the radiation in question is compared with soft x- or gamma-rays which are given an RBE of 1.

A reference risk has been established (Ref. 5-29), based on the natural probability for the white, male U.S. population between 35 and 55 years of age to suffer death from malignant diseases (neoplasm), and based on the assumption that the risk from radiation for all neoplasms is  $3 \times 10^{-6}$ /rem/year with the total risk of the 20 year period  $6 \times 10^{-5}$ /rem. The natural probability of death from neoplasm is  $2.3 \times 10^{-2}$  and the reference risk becomes  $2.3 \times 10^{-2}/6 \times 10^{-5}$ /rem = 383 rem. This has been rounded off to 400 rem and is the exposure which will give an additional risk, equal to the natural risk, of death and which has been established as the reference risk (career limit). The dose of 400 rem is at a depth of 5 cm which is the average depth of the blood-forming tissue (bone marrow).

It should be pointed out that the assumed risk of  $3 \times 10^{-6}$ /rem/year was based partly on data from victims of radiation accidents and nuclear bomb explosions, neither of which compares with chronic, low-dose exposure. It may be argued that because of healing-effects the chronic exposure allowance becomes conservative when it is based on such one-time exposures.

The effect of rate of exposure is not well understood, for example, the allowed career limit of 400 rem is not much less than the mean lethal dose (MLD) of about 500 rem. In order to be conservative the allowed dose fractions for shorter periods are progressively smaller.

The dose rate and the penetrating ability of the radiation combine to determine whether the effect is one of early incapacitation, progressive incapacitation, or chronic injury. Incapacitation refers to somatic injury whereas chronic injury is genetic and somatic, but based on probabilistic terms.

Table 5-10 shows the value that have been recommended for various exposure times and depths of exposure (Ref. 5-29).

The table shows that the dose to the testes may be limiting, however, the effect of exposure is genetic and not somatic.

**Radiation Protection, Shielding, and Operational Constraints.** Within the constraints imposed by the combination of dose accumulation, dose rates, and radiation environment as discussed, it seems clear that for manned spaceflight in LEO the simplest method of radiation protection is shielding of the spacecraft, and a combination of shielding and exposure-time limits for extravehicular activity (EVA). This is the conclusion of investigators (Ref. 5-36 and 5-37) as well as of measurements actually made (Ref. 5-25 and 5-30).

The amount of shielding necessary in LEO depends, of course, on the length of time to be spent there and on the altitude of the orbit. A thickness of  $2 \text{ gm/cm}^2$  would allow 5 months' operation (Ref. 5-37). This is about the wall thickness of Apollo or Skylab.

If the industrial limits, rather than the limits recommended by the Space Science Board, were in effect, then the 5 months' operation would shrink to 5 days at  $2 \text{ gm/cm}^2$  shield thickness.

In GEO the situation is somewhat different. The flux is much higher but the energy spectra of the electrons and protons are softer, and the dose rate decreases rapidly with increased shield thickness until it is smaller than in LEO (Fig. 5-17). The result is that in GEO the dose behind  $2 \text{ g/cm}^2$  is 1.2 rem/day (Ref. 5-37), (JSC data in the figure shows this to be 0.3 rem/day, essentially equal to the LEO dose) while in an unspecified space suit (probably  $0.2\text{-}0.5 \text{ g/cm}^2$ ) the dose rate is 1920 rem/day (Ref. 5-37), obviously precluding extensive EVA, at least with present-day space suits.

The real difference between LEO and GEO is due to the solar flare events. The occasional presence of

Table 5-10 SUGGESTED EXPOSURE LIMITS AND EXPOSURE ACCUMULATION RATE CONSTRAINTS

Constraint	Primary Ref. Risk (rem at 5 cm)	Bone Marrow (rem at 5 cm)	Skin (rem at 0.1mm)	Ocular Lens (rem at 3mm)	Testes (rem at 3 cm)
1-year average daily rate		0.2	0.6	0.3	0.1
30-day maximum		25	75	37	13
Quarterly maximum <sup>a</sup>		35	105	52	18
Yearly maximum		75	225	112	38
Career limit	400	400	1200	600	200

<sup>a</sup>May be allowed for two consecutive quarters followed by 6 months of restriction from further exposure to maintain yearly limit.

these makes it mandatory to provide a highly shielded part of the spacecraft, where the personnel and certain sensitive instruments and equipment, can stay at least for the duration of a solar flare event, usually on the order of a few days. This "fall-out shelter" could be provided with a shielding thickness, an order of magnitude, or more, greater than the rest of the craft. In addition to this it would be possible to accumulate a "junk yard" around the spacecraft, consisting of spent fuel tanks, burned-out motors, etc.

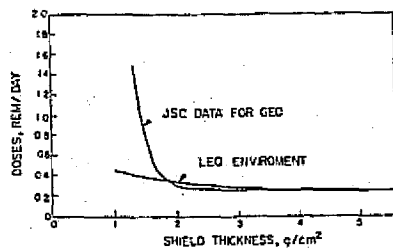


FIGURE 5-17 COMPARISON BETWEEN DOSES RECEIVED IN LEO AND IN GEO AS FUNCTION OF SHIELD THICKNESS (DATA FROM REF 5-37)

The additional shielding of the space station reduces the daily dose and will, therefore, allow a higher dose to be received during EVA, thus allowing a lighter suit. Since the space junk will be there in any case, and, indeed, represents a disposal problem, this disposition could provide substantial savings.

Operational constraints must be used to ascertain that no individual member of a crew will exceed his allowed dose. From experience different crew members on the same mission do not receive identical accumulated doses (Ref. 5-30). For the SPS program there will be continuous crew rotation and it will be necessary to keep running records of an individual's exposure; this must include his dose history as well as periodic adjustments due to the readings of onboard dosimeters. Solar flare events may necessitate early rotation of some crew members and/or placement of crew within the varied radiation field of the craft according to their radiation history.

The dose required to produce temporary loss of fertility and a possibility for later producing mutant offspring is smaller than the dose allowance for bone marrow (see Table 5-10). If the possible psychological impact of this is taken into consideration, then the dose received by the gonads, at least on the male, may be limiting.

An additional operational constraint may, therefore, be that the crew shall consist only of members who have previously elected to be sterilized.

### 5.4.3.3 ENVIRONMENTAL EFFECTS ON SOLAR CELLS

Solar cells are essentially semiconductor materials which convert energy contained in visible light to an electric current. Only those wavelengths of the visible light spectrum whose photons have energy greater than the energy gap of the semiconductor will produce the photoelectric effect. Above this energy gap, the conversion efficiency is a function of energy.

The linear absorption coefficient of the cell will be one of the determining factors in choosing the thickness of the solar cell. The intensity of light in the cell will vary as  $I = I_0 e^{-\mu x}$ , where  $I_0$  is the intensity of the incident beam,  $x$  is the distance traveled through the material, and  $\mu$  is the linear absorption coefficient. For such an exponential relationship, increasing the thickness beyond a few absorption lengths will mean a smaller increase in the fraction of light absorbed, thus the tradeoff between weight, efficiency, and manufacturing capability for producing very thin, large-area semiconductors will dictate the final thickness of the cells.

Single-crystal silicon is the material which is likely to be used for solar arrays because it probably has the best overall combination of desirable properties (Ref. 5-38). For Si the absorption coefficient increases gradually from  $10 \text{ cm}^{-1}$  for  $h\nu \approx 1.2 \text{ eV}$  to  $\approx 3 \times 10^4$  at  $h\nu \approx 3.0 \text{ eV}$ . The energy gap for Si,  $E_G$ , is just over  $1.0 \text{ eV}$ , and between  $\approx 1.2$  and  $3.0 \text{ eV}$  the average  $\nu$  is about  $10^4 \text{ cm}^{-1}$  (Ref. 5-39). Thus, if this linear absorption were used, a cell with a thickness of  $1/\nu = 10^{-4} \text{ cm}$  would absorb  $\sim 2/3$  of the photons with energy between  $1.2$  and  $3.0 \text{ eV}$ . In order to absorb a greater fraction of the lower energy photons the cell would have to be considerably thicker.

Not only does the solar cell absorb visible light, it also absorbs other types of radiation much of which damages the cell and reduces its conversion efficiency. The mechanisms by which radiation damage is caused are very complex and depend both on the type of semiconductor material and the type of radiation as well as on temperature and time, thus, for example, a certain defect which may involve an impurity trapping of a single Si interstitial or vacancy can only be ob-

served at low temperatures since it is annealed at room temperature and does not show after room temperature irradiation. The defect is associated with impurity content (Ref. 5-40).

Irradiation with energetic particles produces many types of defects, displacing atoms from regular lattice sites by collision. The interstitial atoms and lattice vacancies migrate in the crystal and aggregate or associate with impurities in the material. Macroscopic disordered regions in the crystal lattice may also be produced in case a large number of atoms are displaced as the result of a primary collision.

The combination of temperature and irradiation is complicated. Thermal conductivity is reduced by irradiation, with a larger effect at lower temperatures; the effect is due to the defects which scatter the lattice waves responsible for heat conduction. As a result of the induced strain the physical dimension may change (Ref. 5-40). If not allowed to change, there may be structural failure.

The annealing of irradiation effects with temperature often shows complicated behavior. The annealing of one type of defect is accompanied sometimes by the formation of other types of defects (Ref. 5-41).

**Radiation Damage in GEO.** Whereas unannealed degradation due to radiation damage has been estimated to be as little as 5% over a 5 year period (due to an estimated flux of  $10^{15}$  e/cm<sup>2</sup>) and a total degradation of 20% over 30 years (Ref. 5-42), the only long-term exposure of solar cells in GEO has shown a somewhat greater degradation. Silicon cells with a 1-mil quartz cover exposed in GEO over 6-1/2 years showed a 3.5% degradation for the first 3 years and 1.75% per year thereafter (Ref. 5-43). The total degradation for these cells extrapolate to 35% for 30 years.

If it is assumed that the exposure in GEO is 3.5 rad/week at 0° orbit inclination (Fig. 5-13) at 1 g/cm<sup>2</sup> then the degradation after 3 years is 1.75%/year/182 rad/year =  $9.6 \times 10^{-3}$ %/rad.

Different types of cells show different amounts of degradation. For example, ion-implant cells, which showed almost no sign of low-energy proton degradation, exhibited  $P_{max}$  degradation at a greater rate than the standard diffused cells with 6-mil cover shields. However, because of a better contact grid structure

resulting in lower initial series resistance, those cells had almost 10% greater initial maximum power and were considered superior in absolute performance than the diffused cell (Ref. 5-43).

It is not clear what the cover will provide in terms of degradation protection. Comparison between 1-mil covers and 6-mil covers shows an approximately 10% greater decrease in  $P_{max}$  for the 1-mil cover for diffused n/p, 10 ohm-cm Si cell. The 6-mil covers were OCLI and the 1-mil ones were integral, sputtered quartz. Solar flare activity decreased the 6-mil covered cells by 0.85% per  $10^{10}$  protons/cm<sup>2</sup> and the 1-mil covered ones by 1.4% for the same fluence, this is an increase in degradation of 65% relative for the 6-mil cells, however, the covers are an added weight (quartz, which is SiO<sub>2</sub> has a specific gravity of 2.65 thus a 1-mil cover represents a volume of  $2.54 \times 10^{-3} \times 10^{10}$  cm<sup>3</sup>/km<sup>2</sup>, or  $5.7 \times 10^4$  Kg/km<sup>2</sup>), and there is also an initial decrease in the power output of the cell due to cover slide darkening. This effect is 4 to 10% (Ref. 5-43), thus, although it seems that protection is desirable (including edge protection) much more research is needed to find the tradeoff between added weight and percent degradation over the expected lifetime.

Calculations based on 8-mil thick n/p Si with a 6-mil fused silica cover plate show an insignificant degradation in GEO except when large solar flares were encountered (Ref. 5-32); however, a 6-mil thickness of silica would not be practical for large arrays.

#### **Radiation Damage in Orbit Transfer.**

Using the degradation rate of  $9.6 \times 10^{-3}$ %/rad which was derived in the previous section, the degradation experienced by solar cells during orbital transfer from LEO to GEO can be calculated.

If a shield thickness of 1 g/cm<sup>2</sup> is assumed for the solar cell shields (although a 6-mil sheet of SiO is only 0.04 g/cm<sup>2</sup>) then Figure 5-14 shows that the accumulated dose for an orbital transfer time of 5.4 days is  $10^3$  rad, resulting in a degradation of 9.6%. For a 27 day transit the dose with a shield of 1 g/cm<sup>2</sup> would be  $\sim 4.2 \times 10^3$  rads, resulting in a degradation of  $\sim 40\%$ , and for a 54-day transit the degradation would be  $\sim 81\%$ .

Table 5-11 below compares the degradation suffered by Si solar cells in GEO and in transit between LEO and GEO for various transit times.

There is some evidence that radiation damage may saturate (Ref. 5-43), i.e., the defects may diffuse out as

Table 5-11 DAMAGE TO SOLAR CELLS

In GEO	LES-6 Satellite data 3.5% for 3 years + 1.75%/year thereafter 35% degradation (extrapolated) for 30 years for Si with 1 mil cover
In Orbit Transfer	Assuming 1.75%/year, 3.5 rad/week 9.6 x 10 <sup>-3</sup> %/rad, then 5.4 day transit - 9.6% degradation 27 day transit - 40% degradation 54 day transit - 81% degradation
Other Effects	4 - 10% initial degradation due to slide darkening thermal stresses change in efficiency with temperature annealing with temperature, time

fast as they are produced after a certain density of defects has occurred. This diffusion of defects is probably enhanced by temperature, thus annealing should decrease the amount of degradation shown in Table 5-11; however, temperature also decreases the efficiency of the cells, as shown in Figure 5-18, and a tradeoff between annealing effects and efficiency must therefore be made to establish the best operating temperature of the solar cells. The alternative is to let the cells decay to a given efficiency and then occasionally anneal them at an elevated temperature to restore at least part of the efficiency.

**Other Effects on Solar Cells.** In addition to the proton and electron radiation damage to the semiconductor material, other environmental factors influence the total solar array, usually to the detriment of performance.

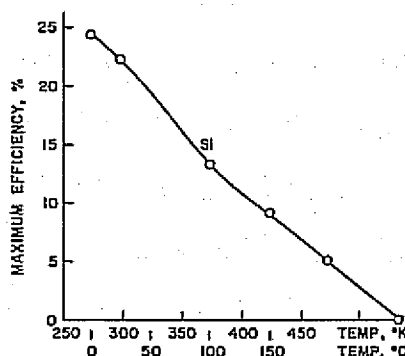


FIGURE 5-18 MAXIMUM EFFICIENCY OF SOLAR CELL VERSUS SILICON TEMPERATURE (DATA FROM REF. 5-38)

A transparent shield must be used primarily for protection against the radiation environment but also against micrometeorites; this shield gives protection against ultraviolet radiation (UV) and provides a degree of cooling by virtue of reflective filters.

Radiation damage in optical material consists of an increase in the absorption in the material in the region of the spectrum which is detrimental to the solar cell due to the reduction of visible light transmitted. The damage is due to the production of electronic states which absorb photons in the visible part of the spectrum.

A principal source of radiation damage in thermal control surfaces is UV radiation. The mechanism of damage must be due to direct electronic, or indirect atomic, displacement, since the UV photons do not have sufficient energy to cause direct atomic displacement damage (Ref. 5-44).

Other mechanisms which limit the life of a solar power system are degradation of mechanical and electronic components, radiation damage to both solar cells and electronic components, and thermal cycle fatigue to array materials and solar cell interconnections (Ref. 5-45).

#### 5.4.3.4 CONCLUSIONS AND RECOMMENDATIONS

The space environment will impose many conditions on the SPS both with respect to its effects on man in space and to its effects on the materials. Although much has been learned in recent years about space, a much better understanding of the radiation environment would be highly desirable as would be the ability to predict the resulting dose and its effects on biological and both inorganic and organic materials.

The following conclusions can be made with respect to the radiation environment:

**a.** The geomagnetically trapped radiation, especially in the inner radiation zone, constitutes a design constraint for manned satellites and a severe restriction on the use of solar cells for propulsion from LEO to GEO.

**b.** In the outer radiation zone there is an increased effectiveness of the shielding due to the softening of the incident, and hence the residual, spectrum. At high altitude less proton shielding would,

therefore, be required for man than at low altitude.

**c.** The shield thickness required in GEO is considerably greater than the thickness of existing space suits.

**d.** Solar flare events constitute a definite threat, possibly involving loss of life, to manned operation in GEO.

**e.** Manned operation in LEO can be performed for a period of up to 4 months with a shield thickness of  $2 \text{ gm/cm}^2$  without exceeding the present radiation dose limits set forth by the Space Science Board so long as the orbit does not include the South Atlantic Anomaly.

**f.** Manned operation can be performed in GEO for a similar length of time with the same shield thickness, but only in the absence of solar flare events.

Some of the Operational Constraints and Procedures which could be used they include:

**a.** Duty rotation of crew according to accumulated doses and dose rates received.

**b.** Preferential treatment of crew members with respect to shielded areas, based on members' dose history.

**c.** Possible parking of space "junk," spent engines and tanks, around craft in order to reduce shielding requirements of the craft proper.

**d.** Prior sterilization of crew, voluntary but a prerequisite for flight status, to remove the dangers of psychological and genetic damage.

These procedures will mainly be of use with respect to the crew; the radiation effects on the solar cells are not easily circumvented with operational procedures, although it is possible that occasional periods at increased temperatures may be used for partial restoration of radiation-damaged cells.

It is probably dangerous to base an SPS design on an expected large increase in solar cell efficiency, since the increase which has been obtained over a period of 10 years has leveled off (Ref. 5-46), however, a system analysis approach to solar cell development should be used to replace the present approach apparently pursued by individual scientists. Figure 5-19 suggests some of the interrelated factors which, if considered as a whole, would yield an optimum solar cell.

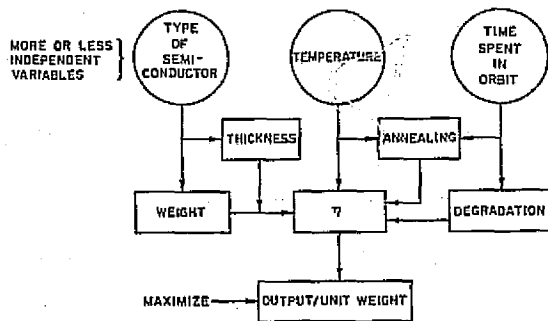


FIGURE 5-19 SOLAR CELL TRADE-OFFS FOR ORBITAL TRANSFER

In addition, the following recommendations are made for investigations which will be needed for solar cell development or for operational aspects of the SPS program.

#### Solar Cells:

a. Research on degradation in a mixed radiation field, possibly in space, using a systematic approach to arrive at optima.

b. The effects of time and temperature on the annealing of defects, the amount of recovery which can be expected, for various materials.

c. Shield effects, the effect of shield thickness, reduction in damage as well as reduction in absorbed light.

d. The phenomenon of saturation damage, its function of rate of dose, synergistic effects.

#### Human and Operational:

a. Cost-benefit analysis of shield weight versus dose in LEO as a function of orbit altitude.

b. The effects of long-term chronic exposure to "low" dose rates, considering that industry standards call for doses which are lower by an order of magnitude.

c. Development of improved space suit for EVA in GEO; these could possibly use a "layer" effect to reduce Br<sub>ms</sub>strahlung and also use strategically-placed extra thickness.

d. Investigation of the legal aspects of the radiation standards set forth by the Space Science Board, considering that future crew members may fall under industrial standards, may be members of unions, etc.

## 5.4.4 Exhaust Plume Considerations

### 5.4.4.1 PLUME EFFECTS

Analyses and experimental data indicated that the exhaust plume of any of the candidate thrusters will expand into at least  $2\pi$  sterad (Ref. 5-47). This is viewed as somewhat of a problem since most thruster locations will allow some of this plume to infringe on some portions of the satellite.

Certain components of the satellite may be degraded by the bombardment of these high energy particles. This degradation could take the form of a material deposition on the component, a chemical reaction, a metallurgical reaction, sputtering erosion, or radiation damage, depending on the propellant type and energy developed, and the component affected (Ref. 5-47).

The potential advantages of thrusters with a higher specific impulse (which causes the high energy exhaust particles) may be partially offset by the necessity of relocating thrusters to less efficient locations or by adding shields to protect certain areas of the satellite. Table 5-12 lists the potential problem areas.

### 5.4.4.2 THRUSTER PLACEMENT

In order to minimize the number of thrusters and the consequent control problem and power and propellant feed problems, gimballed end mounting of the thrusters was originally preferred (Fig. 5-20) (Ref. 5-48). This allows the clustering of propellant tanks and power conditioning equipment. The rotating thruster banks can provide most of the attitude control as well (Fig. 5-21).

Moving the thrusters to opposing corners of the square modules (Fig. 5-22) as proposed by Boeing (Ref. 5-49) will provide the satellite component some protection from the exhaust plume, and exact no control penalty. Should additional protection be needed, it should be minimal for this configuration.

Table 5-12. POTENTIAL DEGRADATION OF SPACECRAFT COMPONENTS FROM IMPINGING PROPELLANTS

DEGRADATION MECHANISM \ SPACECRAFT COMPONENTS AFFECTED	THERMAL CONTROL COATINGS	OPTICAL ELEMENTS AND COATINGS	STRUCTURAL MATERIALS	INSULATORS AND ELECTRODE GAPS	CONDUCTORS	ADHESIVES	MOVING JOINTS	SOLID STATE COMPONENTS
PROPELLANT CONDENSATION AND/OR THRUSTER MATERIAL DEPOSITION	X	X		X				
CHEMICAL REACTION	X	X	X	X		X	X	
METALLURGICAL REACTION	X		X		X		X	
SPUTTERING EROSION	X	X	X	X	X	X	X	X
RADIATION DAMAGE (DEPOSITION OF ENERGY WITHIN SOLIDS, E.G., TONS)	X							X
X POTENTIAL PROBLEM AREA								

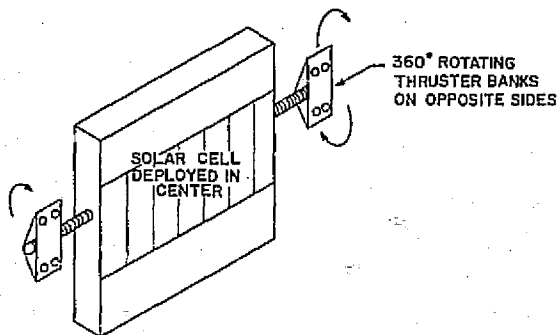
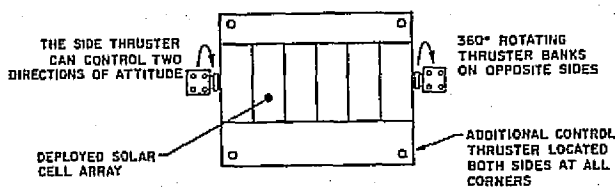


FIGURE 5-20 MODULE WITH ENGINE CLUSTERS  
NOTE: SATELLITE MODULE ABOUT 2km  
SQUARE AND 1/2 km THICK



NOTE: SATELLITE MODULE ABOUT 2KM SQUARE AND  
1/2 KM THICK

FIGURE 5-21 MODULE WITH ENGINE CLUSTERS AND ATTITUDE  
CONTROL

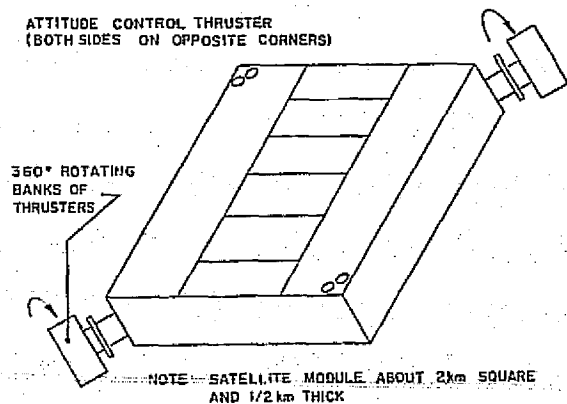


FIGURE 5-22 CORNER MOUNTED THRUSTERS  
(REF. 5-49)

## 5.5 DESIGN REQUIREMENTS

The previous sections of this chapter have identified various issues which must be considered when developing a design for electrically propelling the SPS and/or its constituent components from LEO to GEO. In the present section the design question is addressed directly; first to determine and assess thruster selection tradeoffs and then to propose a suitable configuration for accomplishing the objective.

### 5.5.1 Engine Selection Tradeoffs

Analyses have been performed to ascertain which of the electrical thruster candidates identified in Section 5.1 would be most suitable for accomplishing the transorbital task. This question was approached from two points of view--technical feasibility and overall practicality. A computer program, written to assist in making these comparisons, is listed and explained in Appendix L.

#### 5.5.1.1 MODELING ASSUMPTIONS

The analysis of low thrust orbital transfer using electrical propulsion was approached by treating the transportation question as a whole rather than by looking at the individual requirements of modular sections which might be used to ferry the SPS to geosynchronous orbit. Implicit in this approach is the assumption that the problem is directly scaleable, i.e., that the approximate number of engines, LEO weight, power requirements, etc., for each of the N modular sections could be determined simply by dividing any quantity by N. A more detailed treatment was not considered warranted due to the uncertainty of many of the parameters involved.

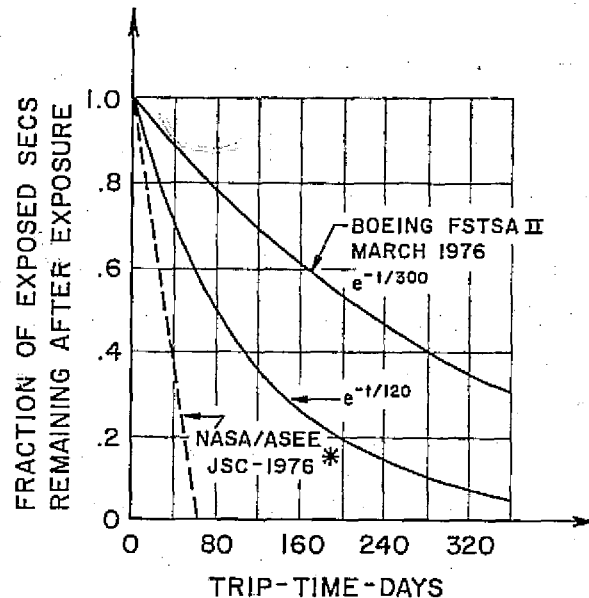
The analysis is based on an SPS whose size and mass are dependent on the particular mission profile under consideration. While the mass of the MPTS was held fixed at 20,427 tonnes (45 million lbm) (Ref. 5-50), the mass of the SECS was permitted to vary from a starting point mass of 65,167 tonnes (144 million lbm) (Ref. 5-51) by an amount which compensates for the radiation degradation experienced in transit. Thus, an SPS brought to GEO using low thrust propulsion would be sized to provide 10 GW on the ground as would its chemically propelled counterpart. Accounting for transmission and conversion efficiencies (Ref. 5-52), this is equivalent to a maximum 16 GW available for

propulsion after having passed through the Van Allen belt. This, then, is an upper limit used to determine technical feasibility.

In calculating the size of solar array, it was assumed that only those portions actually required in order to accomplish LEO-GEO transfer would be deployed; the exposed to unexposed area ratio was taken to be directly proportional to the ratio of available to potential power. (Note that this would not necessarily be true if the thickness or type of shield used to protect those solar cells were different from that used to protect the solar cells which are only deployed upon arriving on station in GEO.)

The model used to describe the way in which solar cells degrade as a function of time is based upon a Radiation Impact curve appearing in a Boeing Quarterly Report (Ref. 5-53) (Fig. 5-23). An exponential having a time constant of 300 days was found to provide excellent agreement with this curve. Subsequent analysis in Section 5.4, however, indicates that degradation rates in excess of that shown by the Boeing curve may be expected. Since the results of this analysis, which neglected both saturation and self-healing due to annealing effects, indicate an almost linear rate of degradation with total damage occurring on the order of 65 days, a somewhat more optimistic compromise module, exponential decay with a 120 day time constant, was used in anticipation of research breakthroughs in the protection of solar cells.

The time for which the SECS array will be exposed to Van Allen belt radiation has, for simplicity, been assumed equal to the duration of the transfer from 500 km (270 n.m.) to 35,878 km (19,358 n.m.). An estimate of this time is obtained initially using a constant thrust/mass (thrust/weight) ratio, continuous low thrust model (Appendix G-4). This estimate is then employed in a first pass to evaluate masses of the SPS, engines, propellant, and tanks. The time estimate is then refined by employing the constant low thrust equations with the thrust/mass ratio recalculated each orbit. In order to compensate for occultation effects which may add as much as 10 days to 54 day transfer (Ref. 5-54), the calculated time is increased by 10%. The effects of aerodynamic drag and solar pressure on trip time are relatively small in comparison and have been neglected.



\* ANNEALING AND SATURATION EFFECTS NOT INCLUDED

FIGURE 5-23 SOLAR CELL DEGRADATION

The minimum  $\Delta V$  required for continuous low thrust LEO to GEO transfer is 4,542 m/sec. (19,903 ft./sec.) at the equator (Appendices G-3 and G-4). If a Cape Kennedy due east launch is assumed, additional  $\Delta V$  would be needed in order to accomplish the plane change. If the plane change is done entirely at GEO altitude, 35,878 km (19,358 n.m.), the minimum  $\Delta V$  increment is 1,528 m/sec. (5,012 ft./sec.) determined from the equation:

$$\Delta V = V_{\text{GEO}} (\pi / 180)^i \quad (\text{Ref. 5-55})$$

where  $i$  is the angle of inclination,  $28.5^\circ$ . It should be stressed that this is a minimum value and does not include thrust vector losses associated with the nonimpulsive plane change. It is clear, however, that the plane change at GEO altitude will increase total trip time approximately 33 to 100%. (Total trip time and overall  $\Delta V$  may be reduced if the plane change is accomplished enroute from LEO to GEO (Ref. 5-56). This would probably increase the time that the solar cells are exposed to Van Allen belt radiation, resulting in a compensatory as insufficient information is available at this time.)

In order to arrive at a realistic evaluation of propellant loads required for the various mission profiles, the minimum  $\Delta V$ 's presented above must be increased.  $\Delta V$  estimates were raised a total of 12% above the minimums to account for gravity gradient losses and provide for reserves (Ref. 5-57). This results in a  $\Delta V$  requirement of 5,087 m/sec. (16,691 ft./sec.) for an equatorial launch and 6,829 m/sec. (22,405 ft./sec.) for a Kennedy launch. The Kennedy launch  $\Delta V$  figures also include an additional 2%  $\Delta V$  penalty for thrust vector losses associated with the nonimpulsive plane change.

An estimate of the mass fraction of liquid hydrogen (LH<sub>2</sub>) was obtained from a study written by J. C. Smithson in which the cryogenic tankage system of a LO<sub>2</sub>/LH<sub>2</sub> chemical OTV was designed (Ref. 5-58). While it is recognized that factors such as time spent in LEO and tank size will alter the results, a propellant mass fraction of 0.83 was utilized in the calculations for LH<sub>2</sub>. For the purpose of estimating total transportation costs it was necessary to ascertain what portion of the gross lift-off weight (GLOW) represented hydrogen. Based on data presented in the Smithson report, a value of 0.89 was used.

Since detailed mass fraction calculations for large volume argon and ammonia tankage requirements are not available, estimates based on the oxygen data in the Smithson study have been used in the analysis. The pertinent parameters are listed in Table 5-13.

In addition to the SPS itself a certain amount of cargo will be transported to GEO. The additional load, 120 tonnes (264,555 lbm) for GEO base repair supplies and 40 tonnes (88,185 lbm) for provisions represents only a relatively small portion of the total mass. A more significant fraction of the total mass is represented by the engine cluster rotators and support structures, discussed in a later section. At the time of writing, however, a detailed analysis of the engine supports has not been performed. As it is not clear how the mass of such structures would vary as a function of other SPS design parameters, it has been neglected in this analysis.

Determination of the actual power demand of the various thruster candidates requires an accounting of the losses associated with the power conditioning equipment. It is estimated that the relatively complex ion engine power conditioning equipment would operate at a conversion efficiency of approximately 90%

(Ref. 5-59). As significantly fewer control voltages are required for the other engines, conversion efficiencies of 95% have been assumed.

### 5.5.1.2 COMPARATIVE ANALYSIS OF ELECTRICAL THRUSTER PERFORMANCE

An examination of the relative performance of electrical thruster candidates has been performed by identifying key factors which affect the cost and/or chances of success of the SPS orbit transfer. Chief among the factors considered are:

- a. Area of Solar Energy Collection System Deployment (collisions, drag).
- b. Number of engines (cost, complexity).
- c. Total Solar Energy Collection System size (cost).
- d. Mass in LEO at start of orbital transfer (cost).

These factors have been calculated for each of the candidate thrusters employing the assumptions and data presented in Sections 5.5.1.1 and 5.1. The results are tabulated for an initial thrust to mass ratio equal to  $g_0 \times 10^{-4}$  ( $T/w = 10^{-4}$ ) in Table 5-14a, b, c, and d, corresponding to a Kennedy launch/300 day degradation time constant, a Kennedy launch/120 day degradation time constant, an Equatorial launch/300 day degradation time constant, and an Equatorial launch/120 day degradation time constant, respectively.

A cursory examination of the table will reveal that the 30 cm ion engine requires an extraordinarily large number of engines--far more than for any of the other thruster candidates listed. This large number of thrusters is attributable to the relatively low thrust and small thrust to mass ratio (including associated power conditioning equipment) of the 30 cm ion engine. Engines in such numbers would present difficulties in deployment and servicing and would be prohibitively expensive when compared to other alternatives. It is for these reasons that the 30 cm ion engine is dismissed as a candidate for SPS propulsion and will not be considered further.

The entries in Tables 5-14a, b, c, and d, are arranged in order of increasing specific impulse. It is interesting to note that the amount of SECS area deployed or equivalently, the power required by each engine type to accomplish the orbital transfer, also increases in this order. In fact, the power requirements of the 100 cm ion engines are so great that it is not possible to use

Table 5-13 MASS FRACTION ESTIMATES

	Mass Fraction	Fraction of GLOW
Liquid Argon	.95	.98
Liquid Hydrogen	.83	.89
Liquid Ammonia	.97	.98

this engine for the particular mission profiles for which the table was generated. Even if lower initial thrust to mass ratios (longer trip times) were considered, the 100 cm engine would still require more engines and a greater area of solar array deployment than any of the other electrical thruster candidates remaining under active consideration. Thus, in addition to the problems and penalties associated with a high engine count, a relatively large SECS deployment would lead to higher collision probabilities, larger aerodynamic drag effects, and greater compensatory SECS growth, making the 100 cm ion engine a rather unattractive candidate. As such, it too will not be considered further in this report as a viable means of OTV propulsive power.

It is also noted in Tables 5-14a, b, c, and d, that, quite as expected, a higher LEO start mass is required when the relatively low specific impulse resistojet is considered for primary propulsion than for any of the other cases tabulated. As this corresponds (fairly) directly to the number of HLLV launches required, it is an indication of the relatively high costs involved in transporting the SPS from LEO to GEO using resistojets. When it is considered that, for this case, most of the start mass corresponds to LH<sub>2</sub> and its associated tankage, the resistojet looks even more unsatisfactory from an economic standpoint (Chapter 8).

The total LEO start mass data presented in Tables 5-14a, b, c, and d, is pictorially presented in combined form in Figure 5-24. The mass data is broken down into three subgroups, (1) MTPS and cargo, (2) SECS, and (3) engines, propellants, and tanks to better assess the impact of latitude of launch and solar cell degradation rate variations. A reference line indicating the nominal SPS plus cargo mass is also provided.

As is expected, the latitude of the launch site has a significant bearing on the mass of propellant required. While this is most noticeable in case of the relatively low specific impulse resistojet, where large changes in total LEO mass are indicated, savings in propellant mass and hence propellant and tankage costs on the order of 26% may be realized for the relatively high specific impulse argon-MPD. The variation in propellant mass, has, in turn, a bearing on the amount of power required for the orbit transfer maneuver. However, this change is insignificant when compared to compensatory variations in SECS mass associated with changes in the rate of radiation degradation or, when viewed from another perspective, the length of time required to travel through the Van Allen radiation belt.

A comparative study was performed to evaluate the effect of variations in orbital transfer time on the major factors employed in assessing electrical thruster candidate tradeoffs. The thrust to mass ratio was varied over a range of  $3.0 \times 10^{-5} g_0$  to  $3.6 \times 10^{-4} g_0$  with the data being plotted in terms of time to go from LEO to GEO equivalent altitude, exclusive of plane change. The mission was assumed to originate in a LEO orbit having an inclination of 28.5° (Kennedy launch). An exponential radiation degradation model with a 120 day time constant was also assumed for the solar array.

Variations in the area of the Solar Energy Collection System that must be deployed to accomplish a mission are plotted in Figure 5-25 as a function of time. It is noted that extremely large areas must be exposed if relatively short travel times are considered. This follows from the fact that more engines would be re-

Table 5-14a ELECTRICAL THRUSTER PERFORMANCE DATA

THRUSTER	PROP	Isp Secs	NUMBER OF SECS AREA EXPOSED SECS GROWTH			MASS IN LEO 10 <sup>3</sup> tonnes (10 <sup>6</sup> lbs)	TRIP TIME DAYS
			ENGINES	KM <sup>2</sup> (MILES <sup>2</sup> )	%		
Resistojet	LH <sub>2</sub>	1K	423	16.5 (42.7)	1.7	192.1 (423.5)	46
Arc-Jet	NH <sub>3</sub>	1.5K	6327	18.5 (73.8)	3.1	143.5 (316.4)	51
Arc-Jet	LH <sub>2</sub>	3K	5175	38.4 (99.5)	4.5	117.4 (258.5)	56
30 cm ION	Ar	5K	1,430,860	60.7 (157.2)	7.3	129.8 (286.2)	58
MPD	Ar	10K	4414	76.2 (197.4)	9.3	100.1 (220.7)	58
100 cm ION	Ar	20K	----	-----	---	-----	--

Table 5-14b ELECTRICAL THRUSTER PERFORMANCE DATA

THRUSTER	PROP	Isp Secs	NUMBER OF ENGINES	SECS AREA EXPOSED KM <sup>2</sup> (MILES <sup>2</sup> )	SECS GROWTH %	MASS IN LEO 10 <sup>3</sup> tonnes (10 <sup>6</sup> lbs)	TRIP TIME DAYS
Resistojet	LH <sub>2</sub>	1K	433	21.4 (55.4)	4.9	196.7 (433.8)	48
Arc-Jet	NH <sub>3</sub>	1.5K	6616	38.5 (99.7)	9.3	150.0 (330.8)	51
Arc-Jet	LH <sub>2</sub>	3K	5533	54.3 (140.6)	14.0	125.6 (276.7)	56
30 cm ION	Ar	5K	1,601,637	90.6 (234.7)	23.9	145.2 (320.3)	58
MPD	Ar	10K	5101	117.1 (304.8)	31.2	115.7 (255.1)	58
100 cm ION	Ar	20K	----	-----	---	-----	--

Table 5-14c ELECTRICAL THRUSTER PERFORMANCE DATA

THRUSTER	PROP	Isp Secs	NUMBER OF ENGINES	SECS AREA EXPOSED KM <sup>2</sup> (MILES <sup>2</sup> )	SECS GROWTH %	MASS IN LEO 10 <sup>3</sup> tonnes (10 <sup>6</sup> lbs)	TRIP TIME DAYS
Resistojet	LH <sub>2</sub>	1K	347	13.5 (35.0)	1.4	157.6 (347.5)	49
Arc-Jet	NH <sub>3</sub>	1.5K	5582	25.1 (15.0)	1.7	126.6 (279.1)	51
Arc-Jet	LH <sub>2</sub>	3K	4818	35.8 (92.7)	4.2	109.3 (240.9)	56
30 cm ION	Ar	5K	1,363,401	57.8 (149.7)	7.0	123.7 (272.7)	58
MPD	Ar	10K	4325	74.6 (193.2)	9.1	98.1 (216.3)	58
100 cm ION	Ar	20K	----	-----	---	-----	--

Table 5-14d ELECTRICAL THRUSTER PERFORMANCE DATA

THRUSTER	PROP	Isp Secs	NUMBER OF ENGINES	SECS AREA EXPOSED KM <sup>2</sup> (MILES <sup>2</sup> )	SECS GROWTH %	MASS IN LEO 10 <sup>3</sup> tonnes (10 <sup>6</sup> lbs)	TRIP TIME DAYS
Resistojet	LH <sub>2</sub>	1K	354	17.6 (45.6)	4.1	160.8 (354.5)	49
Arc-Jet	NH <sub>3</sub>	1.5K	5806	33.6 (87.5)	8.1	131.7 (290.3)	51
Arc-Jet	LH <sub>2</sub>	3K	5128	50.4 (130.5)	12.9	116.3 (256.5)	56
30 cm ION	Ar	5K	1,517,666	85.9 (222.4)	22.7	137.7 (303.5)	58
MPD	Ar	10K	5011	116.7 (302.3)	31.4	113.7 (250.6)	59
100 cm ION	Ar	20K	----	-----	---	-----	--

06

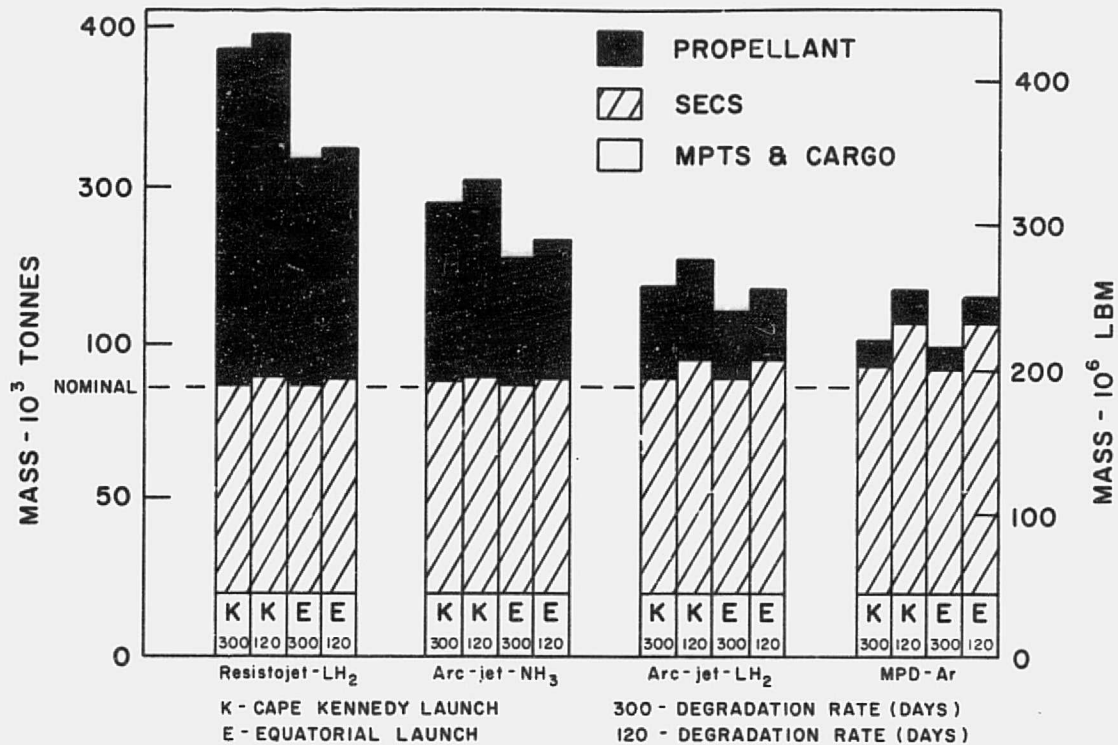


FIGURE 5-24 MASS ANALYSIS

quired to provide the faster acceleration rates. As the thrust to mass ratio is decreased, a trip time may be found for which the amount of exposed solar cell area is a minimum. Beyond this point, lower engine power demands are more than offset by increases in solar cell deployment necessary to compensate for radiation degradation. The location and magnitude of this minimum will, of course, shift in time if a different degradation time constant is considered.

As it is desirable to expose as little solar cell area as possible to Van Allen belt radiation, one would like to operate near the minimum point. However, economic considerations, as well as collision probability estimates, would probably warrant a somewhat shorter trip time. The data points corresponding to a thrust to mass ratio of  $10^{-4}g_0$  seem to be reasonably well situated when viewed from this standpoint.

It is noted that the amount of solar cell area deployed if the argon-MPD were used for primary propulsion is greater than that required for the other engine types and twice that required for its nearest competitor, the

hydrogen-arcjet. As a result, the compensatory solar array growth of an MPD propelled SPS would be much larger than that required if any of the other remaining electrical thruster candidates were employed.

The growth of the total SECS area of the SPS is depicted in Figure 5-26 as a function of trip time. As the Solar Energy Collectin System accounts for the majority of SPS mass, compensatory SECS increases would increase HLLV costs. Furthermore, since the cost of increasing the total area of the solar array would not have to be borne if chemical propulsion were employed in going to GEO, the costs of SECS growth must be included as a cost of transportation when using electrical propulsion (Chapter 8). It is clear, then, that relatively long trip times would tend to increase total SPS transportation costs.

An assessment of relative HLLV costs may be made by considering the total LEO start mass for the SPS and its associated transportation system. Examining Figure 5-27 it is observed that it may be possible to select an operating point for which the mass of the SPS, includ-

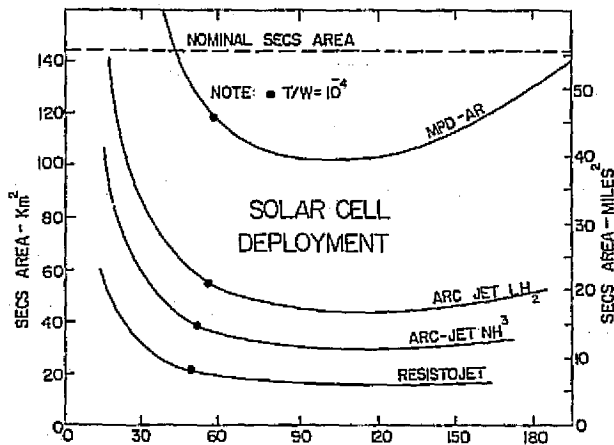


FIGURE 5-25 TRIP TIME DAYS (NOT INCLUDING PLANE CHANGE)

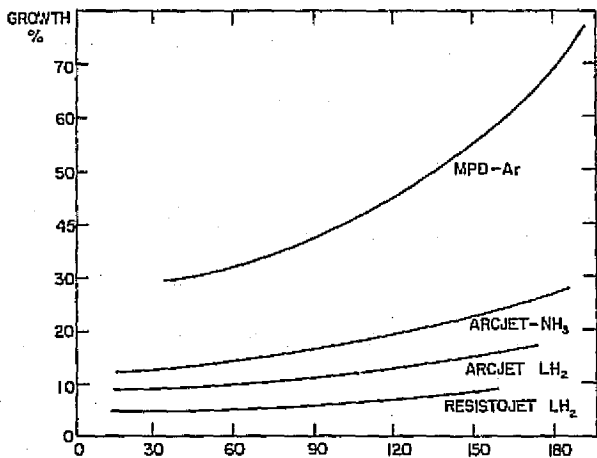


FIGURE 5-26 TRIP TIME, DAYS NOT INCLUDING PLANE CHANGE  
SEC GROWTH

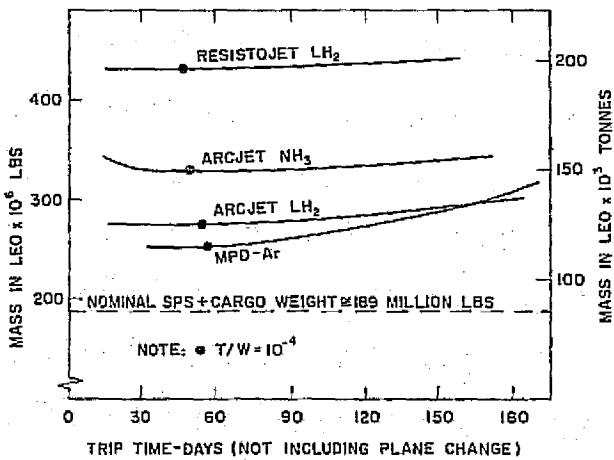


FIGURE 5-27 LEO START MASS SENSITIVITY

ing SECS growth, cargo, engines, propellant, and tankage is a minimum. The minimum is attributable to increases in the number and hence, mass of engines required for very rapid accelerations on the one hand, and increases in the mass of the Solar Energy Collection System to account for long exposures to Van Allen belt radiation on the other. Thus, the location, magnitude, and broadness of this minimum will vary with mission and engine parameters.

In terms of LEO start mass it would appear that the most attractive candidates considered for SPS propulsion are the argon-MPD and the hydrogen arcjet. The ammonia arcjet, which proves to be competitive costwise when SECS growth and propellant costs are considered, does not compare favorably when viewed in terms of the additional dangers posed by large HLLV cargos of its toxic propellant. A launch aborted in the early stages of flight, presents a potentially hazardous situation, not only in the vicinity of the launch site, but downwind as well.

It is observed that when relatively rapid trip times are considered, the argon-MPD propelled SPS has a lower LEO start mass than its hydrogen-arcjet propelled counterpart. This situation is seen to reverse, when longer trip times are considered, due to the larger SECS increases required by an MPD vehicle to counter radiation degradation. It must be noted, however, that this result depends strongly on the rate at which solar cells degrade when exposed to Van Allen belt radiation.

Summing up the case for the various electrical thruster candidates, it would seem that the hydrogen-arcjet is, at the present time, the most likely choice for SPS orbital transfer propulsion. When compared to the argon-MPD, its lower power consumption per unit thrust results in a decreased deployment of the Solar Energy Collection System during LEO to GEO transfer. Thus, an LH<sub>2</sub>-arcjet propelled SPS would be subjected to smaller aerodynamic drag effects and would have a lower space debris collision probability than its argon-MPD counterpart. In addition, the smaller area of solar cell deployment during its long transit through the Van Allen belt results in less total solar cell degradation, an effect which can be estimated at best and needs further study. Since the Solar Energy Collection System is one of the most massive and expensive parts of the SPS, radiation degradation would in all probability rule out the argon-MPD unless significant ad-

vances could be made in protective solar cell covers and the reduction of solar cell weights.

The hydrogen-arcjet seems to be more favorable than the argon-MPD from another point of view as well. It has a more simple design and is further along in its development (Ref. Section 5-1). Thus, it is more likely to be available for primary SPS propulsion in 1995.

### 5.5.2 Transorbital Configurations

Alternative configurations in which the SPS may be transferred from LEO to GEO have been considered. Basically, these may be separated into two fundamental categories--transorbital shipment of the SPS (a) in one piece, or (b) in the form of modular sections. In either case, some construction would be required in GEO as well as LEO, although it is apparent that construction requirements in GEO would be more extensive for case (b).

#### 5.5.2.1 CONFIGURATION COMPARISONS

A number of advantages accrue if the SPS is constructed almost entirely in LEO before being transferred to GEO. Since low earth orbit is at a much lower gravitational energy level than geosynchronous orbit, transportation costs for the construction crew, their housing and supplies, as well as the manufacturing equipment required would be lower as shown in Chapter 8. Radiation levels, which preclude all but emergency EVA in GEO, are relatively lower at LEO (Section 5.4.3), thus permitting a limited number of extravehicular tasks to be performed as necessary. A third advantage is that the SPS would have to rendezvous with a point above the surface of the earth as a single unit, a sharp contrast to the multiple rendezvous and complex docking procedures required for modular sections.

Orbital transfer of the SPS is not without disadvantages, however. As the structure is fabricated, it would suffer altitude losses due to the effects of aerodynamic drag (Section 5.4.1). This would become more pronounced as the solar array is deployed resulting in a reduction of the orbital lifetime of the structure. Furthermore, as large surface areas of the structure are covered, the probability of undergoing a collision with space debris would also increase as shown in Section 5.4.2; an SPS, severely damaged in a collision during construction or orbital transfer, represents a potentially

more serious collision problem and poses the possibility of having to make extensive repairs prior to leaving LEO or upon reaching GEO. On the other hand, small modular sections transferred to GEO as soon as they are completed, would, individually and as a whole, have a much higher probability of surviving the combined construction and orbit transfer phases undamaged due to their smaller area and shorter stay in LEO.

The technique of transporting the SPS in small sections would not only reduce overall collision probabilities and aerodynamic altitude losses, it would also permit a certain amount of GEO testing and construction to proceed, even as the remaining portion of the SPS were in transit or under construction in LEO. Economies in propellant consumption may also be realized if the modular technique is employed. As gravity gradient torques are proportional to the square of the length, smaller modules would be easier to control than the larger one-piece satellite. In addition, each section would, to a first approximation, require proportionally less propellant than the entire SPS as a single unit. This would tend to reduce average on-orbit boil-off resulting in an increase in the propellant mass fraction.

#### 5.5.2.2 MODULE DESIGN

It is proposed that the baseline SPS module design for low thrust orbital transfer be square in shape. The selected transfer module configuration is illustrated in Figure 5-28. Primary propulsion is provided by two banks of electrical thrusters located at opposite corners of the square. They are free to rotate about the roll axis and, therefore, provide attitude control in pitch and yaw. Control about the roll axis is achieved by relatively small banks of fixed, oppositely directed thruster pairs located at the other two corners. As these thrusters are not required for main propulsion, they need only be large enough to counter disturbing torques such as those produced by the primary thruster rotators, gravity gradients and aerodynamic drag.

In operation, the module would be positioned so that its SECS array would be perpendicular to the solar line of sight to a high degree of accuracy (Appendix M). The yaw angle would then be adjusted to align the main thruster banks with the orbital plane. This inertially fixed position permits the primary thruster banks to provide maximum horizontal thrust over all sunlit

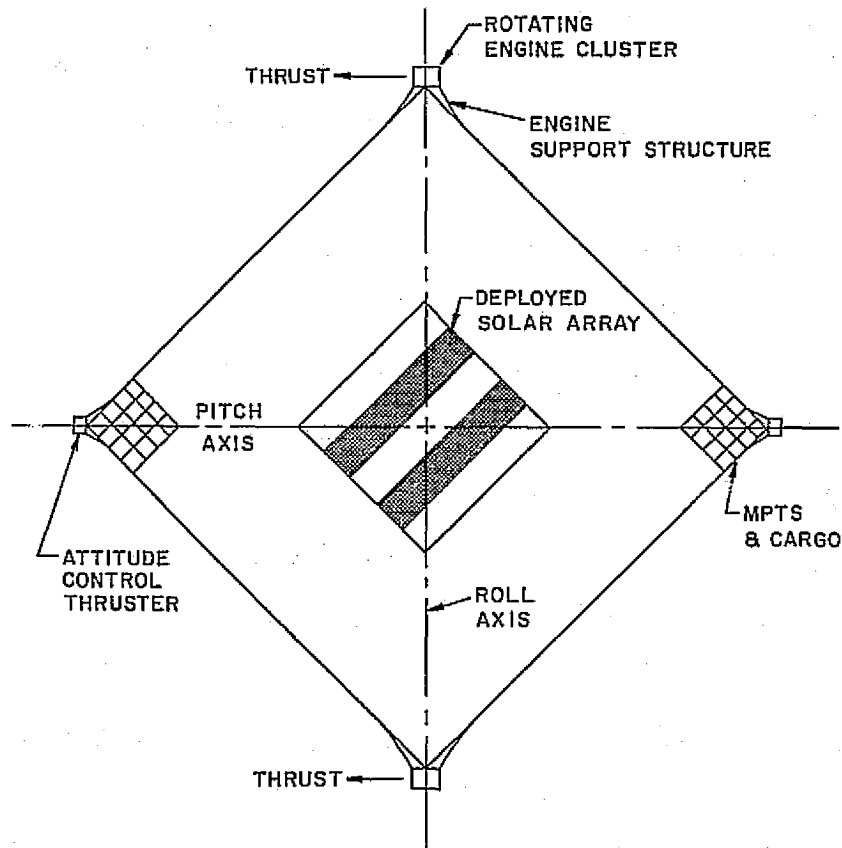


FIGURE 5-28 ORBITAL TRANSFER MODULE

portions of the orbit. It should be noted that this would not have been the case had main engines been placed at all four corners or along the sides. It does, however, require that the thruster banks make one complete revolution about the roll axis each orbit. Electrical power and propellant would be supplied to the engines through the shaft, a problem of considerably less complexity than that associated with the MPTS rotating joint. A design simplification might be obtained if redundant thrusters oriented in several fixed directions were employed instead of the rotating thruster banks. Although such an arrangement would simplify electrical mechanical connections, it would, of necessity, be associated with thrust vector losses and would result in higher engine, fuel, tankage, and HLLV costs.

A preliminary approximate analysis in Section 3.7 indicates that engine-mounting appears attainable, although in some cases, additional structure must be added. Such supplementary structures with engines would necessarily have to be removed wherever they interfered with modular assembly in geosynchronous orbit. Once removed, the extra structure and engine assemblies could either be fastened to the SPS undercarriage, or, if chemical return OTV capability were provided, ferried back to the assembly region in LEO.

Considering Figure 5-28 again, it is observed that the solar array is deployed only near the center of the satellite. This arrangement was chosen to lessen the possibility of damaging the solar array with the  $2\pi$  steradian, high velocity exhaust plume of the electric

thrusters. Further protection may be afforded the array by providing temporary shielding about the perimeter of the deployed section.

Beneath the array, and shielded from the sun, are the propellant tanks. This location not only decreases propellant boil-off (which would be sent through the thrusters in any event) it reduces the module moment of inertia as well. On the other side of the ledger, however, the propellant would have to be piped to the engines over distances of approximately 1.8 km (1.1 miles) which is clearly undesirable. As an alternative, tanks could be placed close to the thrusters served by them. Additional shielding might have to be provided to prevent propellant boil-off at mass rates in excess of that required by the thrusters. This would, however, lead to a situation where the moments about the roll and pitch axes vary with time and with respect to each other.

At the present time we are unable to assess all of the tradeoffs involved with propellant tank placement and leave it as an open question.

As each module is prepared for orbital transfer it is loaded with cargo destined for GEO. This cargo consists of consumables and supplies for the GEO operation as well as MPTS subassemblies which have been manufactured in LEO or, as in the case of the rotary joints, preassembled on earth. The cargo would be equally apportioned among the 22 modular sections so that a standard design may be affected. A portion of the cargo would be attached on opposite sides of the module, near the roll axis attitude control thrusters, as shown in Figure 5-28; this material would serve as counterweights to balance the moments of inertia about the pitch and roll axes. The remaining cargo would be stowed underneath the solar array as close to the centroid as possible to minimize control moments. This would be where each of the rotary joints would be affixed during their separate electrically powered flights to GEO.

## **5.6 SUMMARY AND CONCLUSIONS**

### **5.6.1 Conclusions**

5.6.1.1. The SPS should be assembled in modular sections in LEO. As each section is completed it should be immediately started on its way to GEO, carrying a

cargo of subassemblies as well as provisions and supplies destined for GEO. The antenna rotors would be included as a part of this cargo.

5.6.1.2. The shape of the module should be square with primary propulsion provided by two rotating clusters of engines located at opposite corners. Only that part of the solar array necessary for propulsion will be deployed and the deployed section of the array should be in the center portion of the square.

5.6.1.3. The antenna rotator attachment and antenna construction and array subassembly attachment should be done in GEO.

5.6.1.4. The hydrogen, electric arcjet is the most likely choice for thrusting the modules to GEO.

5.6.1.5. Manned operation in LEO can last up to 4 months with a shield thickness of 2 g/cm within the present standards for radiation dose limits, if the orbit does not include the South Atlantic Anomaly.

5.6.1.6. Operation in geosynchronous orbit is possible for a similar length of time with the same shield thickness in the absence of solar flare events. It should be possible to park space "junk" (spent engines, tanks, etc.) around the manned craft in order to reduce the otherwise extreme shielding requirements of the manned craft proper against solar flare events.

5.6.1.7. Shield thickness for geosynchronous orbit is considerably greater than that of existing space suits. Development of improved suits is indicated; the layer effect could be used to reduce Bremsstrahlung and there should be strategically placed extra thickness.

5.6.1.8. Legal aspects of radiation standards presently used for space must be reviewed in terms of application to future crews. These may come under the much more stringent standards used for industrial radiation on workers.

5.6.1.9. Geomagnetically trapped radiation constitutes a severe restriction on the use of solar cells for propulsion in orbital transfer.

5.6.1.10. The solar cell degradation is calculated to be 81% for an orbital transfer of 54 days, based on an assumed  $9.6 \times 10^{-3}\%$  degr./rad., (g/cm<sup>2</sup> shield).

5.6.1.11. The solar cell degradation is approximately 35% for 30 years in GEO with a Si crystal and a 1 mil. quartz case.

5.6.1.12. The solar array and the central sections should be protected from the thrusters exhaust plume, either by placement or by the addition of shields.

5.6.1.13. Manufacturing capacity will have to be increased to provide the necessary amount of the chosen propellant.

### **5.6.2 Recommendations:**

5.6.2.1. Apply considerable resources to the development of electrical thrusters.

5.6.2.2. Study the effects of the exhausted propellant on man's environment.

5.6.2.3. Study the possible shielding requirements for portions of the satellite.

5.6.2.4. Study the effect of long term exposure of solar cells to Van Allen Belt radiation.

5.6.2.5. Develop lightweight solar cells and protective covers.

5.6.2.6. Study problems involved with controlling large, non-rigid structures.

5.6.2.7. Study methods for assembling modular sections.

5.6.2.8. Determine if electrical thrusters may be returned to LEO for reuse.

5.6.2.9. Study methods for optimizing orbital transfer through simultaneous plane and altitude changes.

5.6.2.10. Study the long-term, chronic exposure to "low" radiation dose rates.

5.6.2.11. Perform ground tests to simulate hypervelocity impacts on complex structures.

5.6.2.12. Design and fly a shuttle payload to monitor the buildup of objects in earth orbit.

5.6.2.13. Design a collision avoiding system for spacecraft.

5.6.2.14. Impose restraints on payloads to minimize the amount of debris in space.

5.6.2.15. Institute a program to return objects from space which no longer serve a useful function.

## **REFERENCES**

**5-1** Mickelson, W. R., Auxiliary and Primary Electric Propulsion, Present and Future, Journal of Spacecraft and Rockets, November 1967, pp. 1409-1423.

**5-2** NASA; A Forecast of Space Technology 1980-2000, January 1976, pp. 4-20-4-48.

**5-3** Lausten, Merle, Potential OTV Thruster Characteristics, NASA, 1976.

**5-4** Boeing, Future Space Transportation Systems

**5-5** NASA, A Forecast of Space Technology, 1980-2000.

**5-6** Lausten, Merle, and Hooper, John, Compilation of Electrical Thrusters Data, 1976.

**5-7** Lyon, W. C., Propellant Condensation on Surfaces Near an Electric Rocket Exhaust, J. Spacecraft, Vol. VII, No. 12, December 1970, pp. 1494-1496.

**5-8** Hall, David F., and others, Electrostatic Rocket Exhaust Effects on Solar-Electric Spacecraft Subsystems, J. Spacecraft, Vol. VII, No. 3, March 1970, pp. 305-311.

**5-9** Advance Copy, Initial Technical, Environment, and Economic Evaluation of Space Solar Power Concepts, Volume I-Summary, July 15, 1976.

**5-10** Discussions with Gus R. Babb, Advanced Mission Design Branch, Mission Planning and Analysis Division, JSC.

**5-11** Wolverton, Raymond W., editor, "Flight Performance Handbook for Orbital Operations," John Wiley and Sons, 1963.

**5-12** Glasstone, Samuel, "Sourcebook on the Space Sciences," D. Van Nostrand Company, 1965.

**5-13** Brooks, D. R., Gibson, G. G., and Bess, T. D., Predicting the Probability That Earth-Orbiting Spacecraft will collide With Man-Made Objects in Space, International Astronautical Federation, XXVth Congress, Paris, France, 1974.

**5-14** Donahoo, M. E., Collision Probability of Future Manned Missions with Objects in Earth Orbit, JSC IN 70-FM-168, NASA, Houston, TX, 1970.

**5-15** Simpson, E. M., Independence of the

Classical Orbital Parameters, TASK A-106, TRW Interoffice Correspondence, TRW Systems, Florida Operations, 1967.

**5-16** Simpson, E. M., Stationarity of the Classical Orbital Parameters, TASK A-106, TRW Interoffice Correspondence, TRW Systems, Florida Operations, 1967.

**5-17** Simpson, E. M., Pseudo Collision Probabilities, TASK A-106, TRW Interoffice Correspondence, TRW Systems, Florida Operations, 1967; Collision Probability of the Apollo Spacecraft with Objects in Earth Orbit, JSC IN 67-FM-44, NASA, Houston, TX, 1967.

**5-18** Simpson, E. M., Approximate Collision Probabilities, TASK A-106, TRW Interoffice Correspondence, TRW Systems, Florida Operations, 1967.

**5-19** Kessler, D. J., A Guide to Using Meteoroid-Environment Models for Experiment and Spacecraft Design Applications, JSC TN D-6596, NASA, Houston, TX, 1967.

**5-20** Kessler, D. J., Space Debris-Environmental Assessment Needed, Unpublished manuscript, NASA, Houston, TX, 1974.

**5-21** Freeman, J. W., Jr., Second Symposium on Protection Against Radiation in Space, Gatlinburg, TN, October 12-14, 1964, NASA SP-71.

**5-22** Hess, W. N., and Mead, G. D., The Boundary of the Magnetosphere, in Introduction to Space Science, W. N. Hess, editor, Gordon and Breach Science Publishing Company, NY, 1965.

**5-23** Frank, L. A., van Allen, S. A., and Hills, H. K., A Study of Charged Particles in the Earth's Outer Radiation Zone with Explorer XIV, J. Geoph. Res. 69, 2971 (1964).

**5-24** Russak, S., and Richardson, K., Proton Flux, Dosage, and Damage Estimates in the Van Allen Belt, NASA SP-71, op. cit.

**5-25** Bailey, J. Vernon, Dosimetry During Space Missions, Personal written communication, JSC, Houston, TX, July 1976.

**5-26** McDonald, F. B., Review of Galactic and Solar Cosmic Rays, NASA SP-71, op. cit.

**5-27** Weddington, C. J., J. Phys. Soc., Japan, Vol. 17, Suppl. A-III 63, 1962.

**5-28** Badkwar, G. D., Daniel, R. R., and Vyayalakshmi, B., Prag. Theoret. Phys., Vol. 28, 1969.

**5-29** Radiation Protection Guides and Constraints for Space Mission and Vehicle Design Studies Involving Nuclear Systems, Space Science Board, Na-

tional Academy of Sciences, Washington, D.C., 1970.

**5-30** Bailey, J. Vernon, Hoffman, R. A., and English, R. A., Radiological Protection and Medical Dosimetry for the Skylab Crewmen, Proceedings on the Skylab Life Sciences Symposium, Vol. 1, NASA, JSC, Houston, TX, 1975.

**5-31** Keller, F. L., and Pruett, R. G., The Effect of Charged Particle Environments on Manned Military Space Systems, NASA SP-71, op. cit.

**5-32** Wright, J. J., and Fishman, G. J., Radiation Environment and Hazards for a Geosynchronous Space Station, NASA Technical Memorandum, NASA TMX-64983, February 1976.

**5-33** International Commission on Radiological Protection: Recommendations, Pergamon Press, 1959.

**5-34** National Bureau of Standards (U.S.) Handbook No. 59, Permissible Dose From External Sources of Ionizing Radiation, 1954.

**5-35** Federal Radiation Council, Staff Report No. 1, Background Material for the Development of Radiation Protection Standards, May 13, 1960.

**5-36** Orbital Construction Demonstration Study, Grumman Aerospace Corp., Contract NAS 9-14916, January 1976.

**5-37** Future Space Transportation Systems Analysis Study, Boeing Aerospace Corp., Contract NAS 9-14323, December 1975.

**5-38** Wolf, M., Historical Development of Solar Cells, Proceedings, 25th Annual Power Source Conference, U.S. Army Electronics Research and Development Laboratory, Fort Monmouth, NJ, 1972.

**5-39** Laferski, Joseph J., Principles of Photovoltaic Energy Conversion, Proceedings, *ibid.*

**5-40** Vook F. L., Radiation Effects in Semiconductors, James Worbett and George D. Watkins, eds., Gordon and Breach Science Publishers, Ltd., 1971.

**5-41** Fan, H. V., Radiation Effects on Semiconducting Materials, NASA SP-71, op. cit.

**5-42** Space-Based Solar Power Conversion and Delivery Systems Study, Futurism Summary Report, ECON Incorporated, Contract NASA 8-31308, March 1976.

**5-43** Sarles, F. W., Jr., The LES-G Solar Cell Experiment After Six Years, Eleventh EEE Photovoltaic Specialists Conference, Scottsdale, AZ, May 1975.

**5-44** Spicer, W. E., Radiation Effects in Optical Material, NASA SP-71, op. cit.

**5-45** Wise, Joseph F., Solar Energy Conversion Development Relative to Department of Defense

Space Power Requirements, Proceedings, 25th Annual Power Source Conference, op. cit.

**5-46** Goldsmith, J. V., Large Area Silicon Solar Array Development, Ibid.

**5-47** Hall, David F., and others, Electrostatic Rocket Exhaust Effects on Solar-Electric Spacecraft Subsystems, J. Spacecraft, Vol. VII, No. 3, March 1970, pp. 305-311.

**5-48** Lausten, Merle, and Hooper, John, Discussion, June 1976.

**5-49** Boeing, Future Space Transportation Systems.

**5-50** Exec. Summary, July 15, 1976.

**5-51** Ibid.

**5-52** Ibid.

**5-53** Future Space Transportation Systems, Phase II, Quarterly Report, March 15, 1976.

**5-54** Conversation, Gus Babb, JSC, Advanced Mission Design Branch.

**5-55** Ibid.

**5-56** Future Space Transportation System Analysis Study, Phase I Extension, Transportation Systems Reference Data, Contract NAS 9-143.

**5-57** Ibid.

**5-58** Cryogenic Propulsion Stage for the Solar Power Satellite, EP53/JC Smithson:lg:4/12/76:4027.

**CHAPTER 6**  
**ORBITAL TRANSFER BY CHEMICAL PROPULSION**

## CHAPTER 6

# ORBITAL TRANSFER BY CHEMICAL PROPULSION

### 6.1 INTRODUCTION AND GROUND RULES

For chemical propulsion, the interorbit region is characterized by negligible gravitational, solar, and fluid environment forces. The satellite assembly will be done at the geosynchronous end of the interorbit region, hence the cargo will have a high strength to weight ratio. GEO assembly also includes a considerable amount of personnel transportation. These requirements call for a special vehicle--the chemical orbit transfer vehicle (OTV).

In this chapter chemical propulsion is utilized. Specific considerations have been made only for a system with a specific impulse of about 460 sec. (i.e., LOX and LH<sub>2</sub>). Implicitly, the assumption is extended to accelerations greater than  $10^{-2}$  and interorbit flight times in the range from 1/2 to 5 days. Furthermore, certain vehicle features are assigned that will require technology and DDT&E durations prorated to 1990. As an example, fuel to payload ratios have been taken at what would currently constitute a high stage fraction vehicle.

Ultimately, it is expected that a number of vehicles will be pressed into service. However, what is proposed is that a single stage type vehicle will be employed and that mission diversity will be gained by coupling units together for multiple stage use. The payloads will be modularized into corresponding integral units and personnel will be transported in "personnel carrier modules," PCM's, which are described in some detail later. It is also assumed that an emergency return capability from GEO directly to earth will be supplied that employs the same type of stage.

The stage that has been chosen for this unified approach is the JSC "nominal" (Ref. 6-1 and 6-2). Virtually all the background data used are from the JSC "nominal" vehicle for GEO construction ("COTV<sub>G</sub>"). However, the stage size is not restricted and can easily be scaled up or down with the modeling equation presented in the discussion of "Cargo Transportation,"

### 6.3. Modeling equations for gross features of the OTV

are developed which are slightly less optimistic than the JSC "nominal" but which are in substantial accord. They enable a quick calculation of flight cost and mass relationships and are adequate for early stages of design. One exception to the single vehicle approach is the small OTV mentioned in the Column-Cable section of the Structures chapter (3.4.3) as a means of transporting specialty cargo. There is no incongruity involved, however, since the modeling is considered applicable for both.

The consideration of OTV fleet size and the increase and decrease with the satellite construction rate has been described in Appendix H. One specific interrelation is the lifetime expectation in round trips, L, Table 6-2.

There will be a staging base at the low earth orbit (LEO) interface between the heavy lift launch vehicle transport and the OTV transport. The operations and facilities are described in the next section along with an emphasis on the importance of this link in the satellite construction sequence.

### 6.2 LOW EARTH ORBIT STAGING BASE

The simplest version of a scenario for satellite construction to GEO would not include a LEO staging base. Materials and men would flow from earth to the GEO construction site in an uninterrupted flight. However, as the introduction has indicated, a LEO staging base has been included in the chemical transport scenario. This is because the earth-LEO and the LEO-GEO regions have different sets of transport requirements. There are several reasons why the HLLV and OTV cannot be considered as simply successive stages of the same vehicle. The differentiation calls for a staging base at the interface.

One of the main reasons for the base is that the HLLV is not man-rated. The shuttle must, therefore, be used and the personnel carrier that it deploys must be coupled immediately to a refurbished OTV that is ready to proceed to GEO. The most crucial reason for a

Table 6-1 OTV MASS MODELING TABLE

RATIO	1990 EXPECTATION VALUE	RANGE
$\frac{m_{\text{VEHICLE}}}{m_{\text{PAYLOAD}}}$	9.4	6% - 32%
$\frac{m_{\text{TANKAGE}}}{m_{\text{PAYLOAD}}}$	6.8 (expendable portion 3 - 6%)	4% - 9%
$\frac{m_{\text{PROPELLANT}}}{m_{\text{PAYLOAD}}}$	217%	180% - 300%
$\frac{m_{\text{LAUNCH}}}{m_{\text{PAYLOAD}}}$	333%	290% - 440%

Table 6-2 OTV FLIGHT COST MODELING

COEFFICIENT	1990 EXPECTATION VALUE	RANGE
L	30	10 - 100
$f_1$	0.36	0.10 - 1.00
$f_2$	0.05	0.01 - 0.25
K	0.020	0.0034 - 0.227
$K_1$	0.0022	0.018 - 0.030
$C_{\text{FLIGHT}} = m_{\text{PL}} (K c_V + K_1)$ <p style="text-align: center;">(\$M) (MT) (\$M/MT)</p>		

LEO staging base is, however, propellant economy. To reach the 2:1 order of magnitude in the ratio of propellant to payload, the OTV must either be a single-stage vehicle that is completely discarded after its trip to GEO, or multiple staging must be employed. Since the latter has the advantage and economy of hardware reuse, it has been chosen; with it are the requirements for refurbishment and loading of propellant which will in turn require LEO facilities.

The weakest aspect of any chemical propulsion scenario is the large propellant mass that must be delivered from earth to LEO. The delivery by HLLV is the dominant item in the transportation cost equation (8.3.4). The weakness is minimized by gaining the lowest average propellant to payload ratio. That corresponds with minimizing the mass that must be returned from GEO (e.g., people). Down payload is a severe encumbrance to the average because the ratio required is four or five times greater (see 6.3.2.2). Therefore, the mass of propellant that must be lifted from earth increases.

The existence of a substantial LEO staging base is one way to minimize the down payload requirement. The conclusion is, while assembly is necessarily at GEO, the personnel or equipment that will need to be returned must be minimized. This is a reinforcement of the argument for automated GEO assembly. One example of this has been discussed in Section 3.4.3.

The goal in this chapter has been to provide an overall description of the 1990 expectations for chemical orbital transfer and for the required vehicles. The vehicle is not described as an assemblage of hardware, but is specified by the various missions that it will perform.

## 6.3 CARGO TRANSPORTATION

### 6.3.1 Vehicle Types and Scaling

#### 6.3.1.1 REDUCTION TO THREE INDEPENDENT VARIABLES

Under the restrictions imposed in the introduction there will be a single type of OTV. It will resemble Figures 6-1, 6-2, and 6-3, but the mundane items like valves, nozzles, fasteners, and structural shapes must be left unspecified at this phase of the design. Distinctions will be made between types within the specie. The typing will be done by establishing values for a set of pertinent ratios. For example, vehicles are considered to be different types if there is a launch to

payload ratio of 3.0 and another has a ratio of 3.5, even though they both employ the same chemical propulsion system. The full range of "types" is illustrated by the last column in Table 6-1.

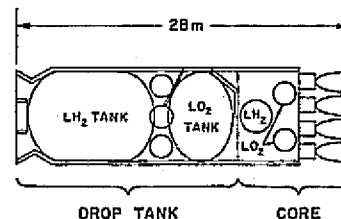


FIGURE 6-1 UNISTAGE

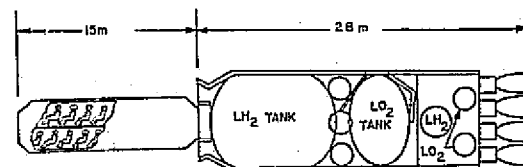


FIGURE 6-2 PERSONNEL CARRIER MODULE ON UNISTAGE

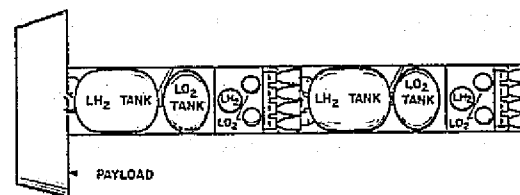


FIGURE 6-3 2 1/2 STAGE WITH HLLV COMPATIBLE PAYLOAD BASED ON UNISTAGE

In lieu of an exact set of OTV specifications, the independent variables must be ordered and reduced before a final design can be considered. The number of degrees of freedom allowed the design is reduced by assigning values to ratios of some of the variables. This procedure is equivalent to establishing a "type." For the modeling in Sections 6.3.2, 6.3.3, and 6.3.4, the number of independent variables was three. They are payload mass,  $mp_1$ , vehicle cost per unit mass,  $C_v$ , and staging. The first and second variables were chosen because they seemed to be identifiable as mission-oriented. The third was chosen because (not being a magnitude) it was difficult to formulate into any ratio.

### 6.3.1.2 THE ABSOLUTE SIMPLEST MASS MODEL

In this forerunner to Mass Modeling, a set of ratios is posed to represent a single-stage fully expended vehicle in a from LEO to GEO with current technology. First, assume that it is a "10% device;" that the ratio of inert mass to propellant is 0.1. Second, assume a performance that achieves a propellant to payload ratio of 2.0. The simple model is now posed with a set of two ratios and payload mass as the independent variable.

$$\frac{m_{\text{INERT}}}{m_{\text{PAYLOAD}}} = 0.2 \quad \frac{m_{\text{PROPELLANT}}}{m_{\text{PAYLOAD}}} = 2.0$$

$$m_{\text{LAUNCH}} = m_{\text{PAYLOAD}} (1.0 + 2.0 + 0.2) \\ = 3.2 m_{\text{PAYLOAD}}$$

### 6.3.1.3 THE ABSOLUTE SIMPLEST FLIGHT COST MODEL

In this simplified representation, the cost flight is determined directly from the vehicle cost per mass and the payload mass. The vehicle is a single-staged version, but fully reusable with no payload return (for the distinction between this staging and the one in 6.3.1.2 see Appendix G-5). Furthermore, the vehicle makes a large number of roundtrips. The total cost per flight is given by:

$$C_{\text{FLIGHT}} = 1/50 (c_V) (m_{\text{PAYLOAD}}) \\ \text{\$/M} \quad (\text{\$/MT}) \quad (\text{MT})$$

### 6.3.1.4 MODELING LIMITS

For all the modeling sections a statement of limitation is in order. Rather than repeat the statement in each section it is presented here and intended to be in-

clusive. The contribution of the modeling approach is one of grouping and simplification rather than any action from basic principles. The linear scalings proposed to model gross aspects of the OTV are inherently suspect outside ranges of existing experience. However, all the vehicle types to be considered for chemical transport of the SSPS lie beyond experiential ranges. The extensions are not only in size but performance level and the more obscure issue of repeated reuse. The discussion in the following sections investigates some observed ranges and relative degree of optimism.

## 6.3.2 MASS MODELING

### 6.3.2.1 THE MODEL

The orbital transfer vehicle is to be fully described in terms of the payload mass and the staging scheme. All other information is entered as ratios which are considered fixed during modeling. The model is strictly linear; however, nonlinear behavior could be introduced at a later date by inserting functions in place of the constant ratios.

The mass elements to be considered as tankage (retained and expended), vehicle, propellant, and payload. The sum of all these will be termed "launch mass." The sum of the vehicle and all of the tank masses will be termed "inert mass."

$$m_{\text{LAUNCH}} = m_{\text{PAYLOAD}} + m_{\text{PROPELLANT}} \\ + m_{\text{INERT}}$$

$$m_{\text{LAUNCH}} = m_{\text{PAYLOAD}} \left( 1 + \frac{m_P}{m_{\text{PL}}} + \frac{m_V}{m_{\text{PL}}} \right. \\ \left. + \frac{m_T}{m_{\text{PL}}} \right)$$

The succeeding sections culminate in determinations of the three pertinent ratios along with ranges of uncertainty for each and are charted in Table 6-1. The 1990 expectation vehicle is then described as:

$$m_{\text{LAUNCH}} = m_{\text{PAYLOAD}} (1.000 + 2.170 + 0.094 + 0.068) \\ m_{\text{LAUNCH}} = 3.33 m_{\text{PAYLOAD}}$$

The JSC "nominal" lies within the range established in Table 6-1. It uses a launch to payload mass ratio of 3.04. The primary difference is in the more optimistic propellant to payload ratio used by JSC. However, the JSC value is for a single, no down payload mission, while the number used here is intended to represent an average mission as described in 6.3.2.2

### 6.3.2.2 MASS MODELING

The 2:1 rule of thumb is used to indicate the mass of propellant required per unit mass of payload. It has meaning only for a particular value of the ratio  $\Delta V / I_{sp}$ . For LEO-GEO transportation with chemical propulsion, the value will be taken as 31 (e.g.,  $\Delta V = 14260$  fps (4346 m/s) and  $I_{sp} = 460$ s). The rule also depends on the stage mass fraction,  $f_s$ , which will be taken as less than 0.97, which corresponds to an empty weight of about 3% of the propellant weight.

The fuel to payload ratio should be minimized for maximum fuel economy. In that respect nothing can compare with a single-stage vehicle that is deserted after the flight. Vehicles can easily be designed to meet the 2:1 rule and might even be scaled down to 1.7:1 ( $f_s = 0.97$ ).

The ratio is denoted, P, in Appendix G-5 and is related to  $f_s$ . Appendix G-5 treats the P to  $f_s$  relationship analytically for the two limiting cases of staging. It is notable that no preflight or during-flight propellant boil-off has been included. Some maneuvering might be allowed by the V which is slightly greater than the Hohmann minimum with 28.5 degree plane change in the second firing. The absolute limit for P is shown to be  $\exp(\Delta V / I_{spg_0}) - 1$ . This limit is not physically realizable since it represents a zero mass empty vehicle returning to LEO on zero propellant.

Any attempt to return equipment to the original orbit severely increases the propellant to payload ratio. In fact, a fully reusable single-stage vehicle cannot reach a ratio as low as 2:1 and 3:1 would be a more realistic guideline. "Tug era" design seemed to prefer a 6:1 level. Multiple staging lowers the ratio. A two stage reusable vehicle with a very low inert weight can perform at 2:1 but a more representative value would be 2.25 and a "10% device" would get about 2.5:1.

The 2:1 rule of thumb is very optimistic for the type of scenarios under consideration. Payload return vehicles

would operate at only 6:1 to 10:1 and would play some pertinent part in a GEO construction scheme. For example, if 8:1 operations were required for as much as 5% of the transport the average value would be raised to 2.3:1. The long-range average, however, for predominantly one-way mass transport might be as low as 2.16:1, therefore, that number will be used in this model. The latter is 8% more pessimistic than the 2:1 rule of thumb.

### 6.3.2.3 VEHICLE TO PAYLOAD RATIOS

The 10% rule of thumb is used to indicate the ratio of the inert vehicle weight to the propellant weight. The design range is represented by values from 5% to 20%. The JSC nominal (Ref. 6-1 and 6-2) is about 7.5% and seems reasonable for 1990 technology. In retrospect the "tug era" design was directed at 10% vehicles, and was intended to have been operational with current technology. It is notable that the ratio of inert vehicle weight to propellant weight is directly related to the staging fraction,  $f_s$ , (see Fig. G-5) by the equation (if,  $M_{INERT} = M_e$ )

$$\frac{m_{INERT}}{m_{PROPELLANT}} = \frac{1-f_s}{f_s}$$

Any reduction in fractional inert weight (from 10% toward 4%) is important. The fraction represents the mass that must fly a roundtrip and therefore has a higher propellant requirement per unit mass than a unit of payload or a unit of propellant. However, the return inert mass is only 12% (9% vehicle + 3% tank) as large as the payload, and is a 1% further reduction in the rule of thumb (i.e., 7.5% to 6.5%) would provide a 2% increase in the payload. That increase would require a 13% reduction in the vehicle mass which, at this level, would cause a severe increase in DDT&E and a decrease in vehicle reliability.

The 7.5% value would have to be raised to permit man-rating for use with the PCM described below in 6.4.

### 6.3.2.4 TANK TO PAYLOAD RATIO

The 3% rule of thumb has been used to represent the mass of tankage per mass of contained propellant. In this context, this ratio is used to represent both LOX and LH<sub>2</sub> in their respective tanks. It, therefore, does not represent either, but the average. When converted to

this basis, different design projections (Ref. 6-3 and 6-4) use ratios from 1.8% to 4%. In this case the conceptual is much smaller--perhaps 1/10 as large if a nonrigid type of containment were used. The scenarios under consideration for transportation require high density for earth launch, which necessitates either filled rigid tanks or collapsed nonrigid tanks. Further, while the actual LEO-GEO flight loads would be small, staging and refueling operations (see 6.3.4 and 6.3.5) will induce handling loads which must be considered dominant. The handling implications are high local stress and sloshing which tend to rule out nonrigid containment. In any case it seems that attainments below the 2% level would incur such a severe penalty in development and reliability that any gains would be marginal.

The staging aspect of tankage consideration is basically established in the ratio of expended tankage to total tankage (see 6.3.3.2). The ground rules spelled out in the first section of this chapter make the ratio 1:2 for a 2-1/2 stage vehicle, and 1:3, 1:4, etc., for other schemes.

The ratio used in these modelings is based on payload and not propellant. The conversion is done with a simple product of tankage to propellant ratio with the propellant to payload ratio.

### 6.3.3 Flight Cost Modeling

#### 6.3.3.1 THE MODEL

The model used includes four elements. They were, (1) the amortized vehicle cost, (2) the cost for an expendable tank, (3) the cost of propellant actually used, and (4) the cost for turnaround. Using  $L$  for the amortization life in number of trips:

$C_{FLT} = 1/LC_V + C_{ET} + C_P + C_{TA}$  Relating the cost explicitly to the mass of payload and using small "c" for costs per mass:

$$C_{FLT} = M_{PL} c_V \left(\frac{M_V}{M_{PL}}\right) \frac{1}{L} + c_{ET} \left(\frac{M_{ET}}{M_V}\right) \left(\frac{M_V}{M_{PL}}\right) + c_P \left(\frac{M_P}{M_{PL}}\right) + C_{TA}$$

The mass ratios have all been itemized in Table 6-1. The intention now is to reduce the remainder of the equation so that it has only two explicit variables; payload mass,  $M_{PL}$ , and cost per mass for the vehicle,  $c_V$ . The tank cost per mass is taken to be a fraction of the vehicle cost, per mass  $c_{ET}/c_V = f_1$ . The expectations for the value of "F<sub>1</sub>" are discussed below in Section 6.3.3.2 and Table 6-3. The turnaround is taken as proportional to the total vehicle cost,

$$C_{TA} = f_2 c_V \frac{M_V}{M_{PL}} M_{PL}$$

the expected values for  $f_2$  are discussed in Section B and Table 6-2. The cost of propellant per mass,  $c_P$ , is spelled out in Section D and summarized in Table 6-2.

The flight cost is then reduced to:

$$C_{FLT} = M_{PL} c_V \left[ \left(f_2 + \frac{1}{L}\right) + f_1 \left(\frac{M_{ET}}{M_V}\right) \left(\frac{M_V}{M_{PL}}\right) \right] + c_P M_{PL} \left(\frac{M_P}{M_{PL}}\right)$$

which is written more simply as:

$$C_{FLT} = M_{PL} (K, c_V + K_1) \quad 6-2$$

The sections below evaluate the two constants,  $K$ , which are given in Table 6-2 with expected ranges.

Example: For a vehicle that transports a 500 MT payload and can be built for \$1,000 a kilogram, the flight cost will be 11.1 million dollars.

#### 6.3.3.2 TANKAGE COST

Within the parenthesis in equation 6-1 is the product of coefficient  $f_1$  with the mass ratio  $M_{ET}/M_V$ . The modeling conclusion has been to choose the nominal value of each of these as 0.36; hence, the 36% double rule. The product is 0.13.

The mass ratio  $M_{ET}/M_V$  is much more well-defined than  $f_1$ , which represents costs of several types of hardware lumped. This is based on a 2-1/2 stage vehicle with a single tank expended per flight. If refueling considerations make it necessary to replace both

Table 6-3 NUMBER OF HLLV LAUNCHES REQUIRED PER SPS FOR EACH AREA INDICATED

	Payload for GEO	LH <sub>2</sub> to LEO	LO <sub>2</sub> to LEO
Number of HLLV Launches	122	38	208

- Assumptions:
1. Each payload for GEO is a unitized 250 tonnes (257.6 tons).
  2. 365 OTV missions required.
  3. 2 common stage OTV used.
  4. 800 tonnes (882 tons) payload assumed for HLLV.

tanks, this number would double. Then  $f_1$  can be estimated from the limits of its range. Since all the plumbing and precision machinery is associated with the vehicle, it is not expected that the tank cost per mass would exceed the vehicle cost per mass. Therefore, the maximum for  $f_1$  was assumed to be 1.00. The minimum value of the ratio found by inference for a variety of vehicles was 0.09. (This is only slightly less than the value obtained by setting the cost per flight equal for expended tanks and vehicles.)

The number derived by inference from the JSC nominal (Ref. 6-1) was  $f_1 = 0.36$ . This was midrange and seemed to be reasonable. Any further refinement would require a detailed look at the hardware involved. Any attempt to recycle the expended tanks would magnify both factors. That is, the tanks would weigh more and cost more per unit mass. For that case, the expected value of  $f_1$  would be 1.0.

### 6.3.3.3 PROPELLANT COST

The propellant cost is 1 \$/Kg. This figure is very important to the flight cost and it is seemingly difficult to establish the price for the tremendous quantities to be called for in the time frame of 1990 and beyond. Nevertheless, the figure of 1\$/Kg seems to be universally accepted.

This cost is derived from the loading ratio of LOX to LH<sub>2</sub> of 6:1 (adjusted from the 8:1 stoichiometric). Then the price of LOX is taken as 6.6 cents/Kg and that of LH<sub>2</sub> as 6.6\$/Kg. Combining the two gives an average of 1\$/Kg.

### 6.3.3.4 TURNAROUND FRACTIONALIZED

The turnaround costs for an OTV are the softest numbers involved in estimating flight cost. Certain portions of the craft might be replaced or refurbished on occasion but the every-flight tank replacement and refueling would be expected to dominate and is discussed in 6.3.5 in some detail.

For modeling purposes the best way to include turnaround cost is to set it as a fraction,  $f_2$ , of the vehicle cost. This fraction is intimately related to the choice of the amortization life,  $L$ . The interrelation is seen in equation 6-1, so that the latitude in  $F_2$  can be taken up  $1/L$  and vice versa.

For simplicity, the two factors could be lumped and considered as a single parameter. The only explicit estimate that was found for any OTV was 2.3 \$M on a 45\$M vehicle; thus,  $f_2$  has been set at 5% which corresponds to an effective replacement life of 20 trips.

### 6.3.4 Staging Rationale

#### 6.3.4.1 THE COST ASPECTS

The cost aspects of staging stem primarily from the technique of fuel saving by leaving parts of the equipment along the way. Either the destaged elements would return independently to be reused or would be discarded.

The "rules of thumb" discussed previously have the staging as an implicit consideration. If the equipment to be destaged at GEO were fully reusable in SPS construction, the choice would clearly be to use a one-

stage expendable vehicle. However, if design does not permit that possibility, one must include staging to get reuse and reasonable fuel economy. The ratio of fuel to payload decreases with increasing number of stages, but operations and recoverability considerations will only permit a small number of stages.

#### 6.3.4.2 RECOVERABILITY ASPECTS

Recoverability aspects of staging are stimulated by two factors above and beyond cost. First is the desire not to pollute space with debris, and secondly, to avoid creating obstacles to navigation. Perhaps the simplest approach would be to use as many of the destaged elements as possible and to lump the residual in a near-GEO orbit where it would be easily avoided and positioned.

The most obvious use for tanks is as habitation and storage modules. However, since those requirements are small relative to the number of tanks destaged at GEO, other possibilities need to be researched. A prime consideration is the use of supplying material for "hard spots" in the satellite structure. One concept is to design the tanks with elements about a thousand times smaller. These structure-sized elements will be assembled into a tank. Once the fuel is expended and it comes into equilibrium temperature at GEO, the elements will be easily removable.

#### 6.3.4.3 OPERATIONS ASPECTS

Operations aspects of staging preclude many of the conceptual designs that would appear very favorable from the cost or recycling points of view. There is first the operation of reconnoitering and maneuvering to the LEO staging base. The recovery will worsen with multiple staging and the intra-vehicle collision probability must be considered to have an exponential growth. But the factor most likely to dominate the multiplicity decision is the complexity of the refurbishment operation.

#### 6.3.5 Mode of Propellant Resupply

##### BACKGROUND

The mode of propellant resupply for the cargo orbital transfer vehicles has the potential for influencing operations and systems far beyond the primary location where resupply physically occurs. Options selected for propellant resupply can reduce the flex-

ibility of these related operations and systems. Consequently, it is important to examine the impact of these options on related systems prior to the selection process.

There are several reasons for the degree of influence which propellant resupply exerts on the balance of the transportation system. Two of these are presented below.

**a.** Propellants, tankage, and the orbital transfer vehicles make up approximately 60% of the average HLLV payload with propellant accounting for about 55% (see Figs. 4-11 and 4-12). The magnitude of this factor can be seen by considering the orbital transfer vehicle configuration illustrated in Figure 6-4. This is a 2-1/2 stage vehicle which has expendable propellant tanks and is one of two primary LO<sub>2</sub>/LH<sub>2</sub> orbital transfer vehicles discussed in Reference 6-1. It requires 475 tonnes (523.6 tons) of propellants per mission. Hence, over 173,000 tonnes (190,700 tons) will be required for the 365 OTV missions needed for each Column/Cable SPS.

**b.** The activity band of OTV operations extends from a low earth orbit altitude of 500 km (270 n.m.) up to a geosynchronous orbit altitude of 36,000 km (19,440 n.m.). These operations interface with the heavy lift launch vehicle payloads at LEO and with the solar power satellite construction site at GEO. Various maneuvers and events which occur in this activity band are given in Figure 6-5 which is an ascent/deboost profile for the 2-1/2 stage OTV referred to in reason a, above.

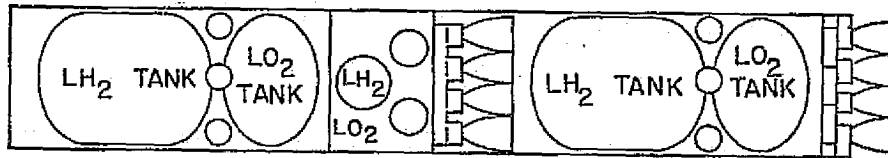
##### GROUND RULES:

**a.** Uncertainties in the physical characteristics of the materials required at the solar power satellite construction site prevented a detailed analysis of prospective payloads.

**b.** This study addresses the transportation system during the early years of the solar power satellite placement scenario "B."

**c.** No partitioning and reassembling of payloads which have been delivered to LEO but are required at GEO is performed at the LEO staging base. Only unitized cargo, which is ready for mating with OTV's would be received at the LEO base.

**d.** The two modes of propellant resupply considered are both feasible.



2-1/2 STAGE LO<sub>2</sub>/LH<sub>2</sub>

LENGTH: 48m

LIFE: 30 MISSIONS

DIAM: 8.4m

PAYLOAD: 250 tonnes

TOTAL WEIGHT: 510 tonnes

≈ 1/5 IOM/F/I.

PROPELLENT WEIGHT: 475 tonnes

FIGURE 6-4 ORBITAL TRANSFER VEHICLE CHARACTERISTICS  
(FIGURE VI-6 OF REF. 6-1)

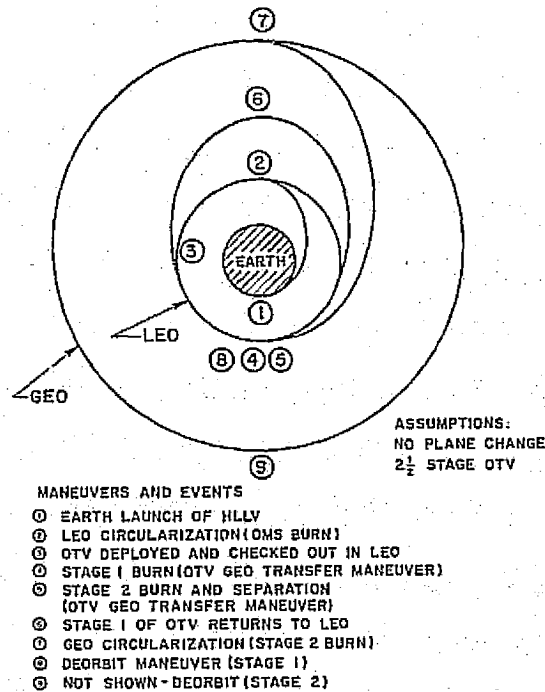


FIGURE 6-5 GEOSYNCHRONOUS ASCENT/DEBOOST  
PROFILE

e. The various payload configurations considered for the HLLV and the OTV are technically feasible in the sense that they meet density, safety, center of gravity, and other constraints imposed by the vehicle.

Two options of OTV propellant resupply are considered here; the first is transfer of propellant tanks and the second is transfer of propellants. Combinations were not examined. Several of the areas which are influenced by alterations in the mode of propellant resupply are listed in Figure 6-6. The impact of the two resupply options on each of the four categories given in Figure 6-6 will now be explored.

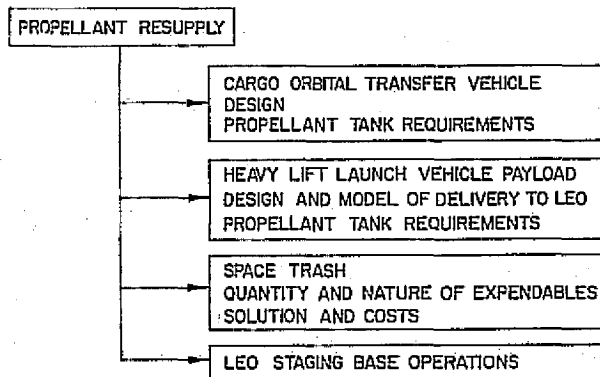


FIGURE 6-6 INFLUENCES OF MODE OF PROPELLANT RESUPPLY

### 6.3.5.1 IMPACT ON THE ORBITAL TRANSFER VEHICLE

#### TRANSFER OF TANKS OPTION

DESIGN--The baseline 2-1/2 stage OTV would have a modular design. The expendable components consisting of stage 1 and stage 2 drop tanks would incorporate into their structure most of the tankage system required for LO<sub>2</sub>/LH<sub>2</sub> propellants, auxiliary propulsion system propellants and fuel cell reactants (if required). The propellant feed system would be designed to facilitate component interchange. The reusable component or core of stage 1 would consist of engines, avionics, and additional reusable systems. The core of stage 2 would be similar except it would have sufficient propellant for return to LEO after deploying payload and the stage 2 expendable tank at GEO.

PROPELLANT TANK REQUIREMENTS--A primary driver of propellant tank design is its expendability. An opposing but equally significant driver is loss of cryogenics (due to seepage, boil-off, etc.) which is dependent in part upon the duration of the mission and the degree of insulation in the tank design. Mission duration refers to the time elapsed between initial earth launch of the propellant tanks as part of an HLLV payload and return of the OTV stages to the LEO staging area. Maximum loss of propellants will occur between earth launch and the initial OTV burn at LEO. Propellant losses are controllable in several ways. A tankage systems consisting of a pressure vessel, polyurethane foam and honeycomb was considered as Reference 6-4. This particular system was capable of propellant losses of less than 2% for a seven day period. Another requirement for tanks might result from the need to dock the expended tanks for temporary storage or to dispose of the tanks. It would be beneficial to provide the necessary physical configuration for that capability in the initial design. Finally, since OTV propellant tanks and propellants make up 60% of the HLLV payload, packing, stacking, and loading constraints imposed by the HLLV payload configuration may influence tank design. For example, payload diameters of 15 meters for the heavy lift launch vehicles are being considered. This would suggest that the OTV profiles given in Figure 6-7 might be more accurate dimension wise than those in Figure 6-4.

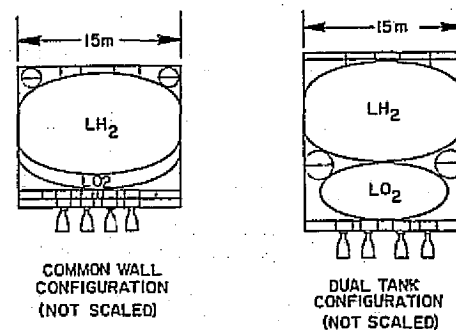


FIGURE 6-7 ORBITAL TRANSFER VEHICLE PROFILES

## TRANSFER OF PROPELLANT OPTION

**DESIGN**--The OTV stages should be compatible with the propellant transfer system. The baseline OTV design for the transfer of propellant option would be a two common stage vehicle with both stages having the configuration of stage 1 in Figure 6-4. Propellant tanks are not assumed detachable. With regard to this two stage OTV, systems which on a per mission basis require maintenance (for example, flushing of the tankage systems) or which may require replacement (for example, the auxiliary propulsion system propellant tanks and fuel cell reactants) should be accessible. It should be noted that each stage of this two stage OTV returns to LEO intact.

**PROPELLANT TANK REQUIREMENTS**--The tankage system would have a lifetime consistent with the balance of the OTV systems. The design should minimize boil-off, seepage, and losses which result from propellant transfer. The propellant feed and fill system should be appropriate for the LEO propellant transfer station environment and degree of man involvement.

### 6.3.5.2 IMPACT ON THE HEAVY LIFT LAUNCH VEHICLE PAYLOAD

#### TRANSFER OF TANKS OPTION

**DESIGN AND MODE OF DELIVERY TO LEO**--This is independent of other factors if a chemical OTV is used with the characteristics and configurations considered in this section. Then it will be necessary to transport 2 Kg (lb) of propellants to LEO for each Kg (lb) of payload to GEO. Most of the HLLV missions will transport significant quantities of propellant. If it is assumed that mixed HLLV payloads of propellants and GEO bound payloads are acceptable then potential HLLV payloads can be specified. The frame of reference is the 2-1/2 stage OTV with a 250 tonnes (275.5 tons) payload to GEO. Figure 6-8 gives several potential HLLV payload compositions. Reference lines at the 450 to 900 tonne levels are indicated since they represent baseline payload capabilities of some of the heavy lift launch vehicles considered in Reference 6-2. Assuming the three configurations in Figure 6-8 are compatible with HLLV loading constraints, it would seem that future sizing of HLLV payloads should be closer to the 800 metric ton (882 tons) range. Another alternative would be to scale up the OTV characteristics including payload capability.

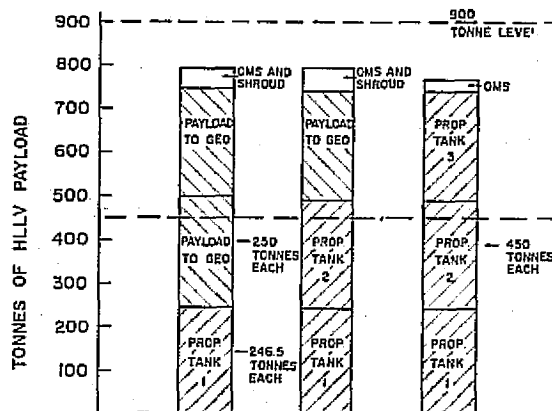


FIGURE 6-8 POTENTIAL HLLV PAYLOAD COMPOSITIONS

## TRANSPORTATION SCENARIO I

The second configuration considered in Figure 6-8 will be used as a baseline operation. It will be referred to as Transportation Scenario I. This scenario was selected due to its operational simplicity. The sequence of events for Scenario I from earth launch to GEO deployment of cargo follows:

### SEQUENCE OF EVENTS FOR SCENARIO I

#### EVENT:

- a. Shroud contained GEO bound payload of 250 tonnes (275.6 tons) mated with two OTV expendable propellant tanks and propellants.
- b. HLLV delivers its 800 tonnes (882 tons) payload to elliptical orbit. The OMS burn places the payload into LEO.
- c. (1) The lower OTV expendable tank is mated with an OTV core propulsion unit to form stage 1.  
(2) The upper OTV expendable tank (still docked with the GEO bound payload) is mated with another OTV core to form the second stage of the OTV.  
(3) Stage 1 is docked with stage 2 and the OTV is deployed and checked out.
- d. Stage 1 burn occurs
- e. Stage 2 burn and stage 1 separation occur.
- f. Stage 1 returns to LEO.
- g. (1) Stage 2 circularization burn puts stage 2 and payload into GEO.  
(2) Payload and expendable tank undocked from stage 2 core.
- h. Stage 1 deorbit maneuver occurs.
- i. Stage 2 deorbit maneuver occurs.

Figure 6-9 gives a schematic of the sequence of events for Scenario I.

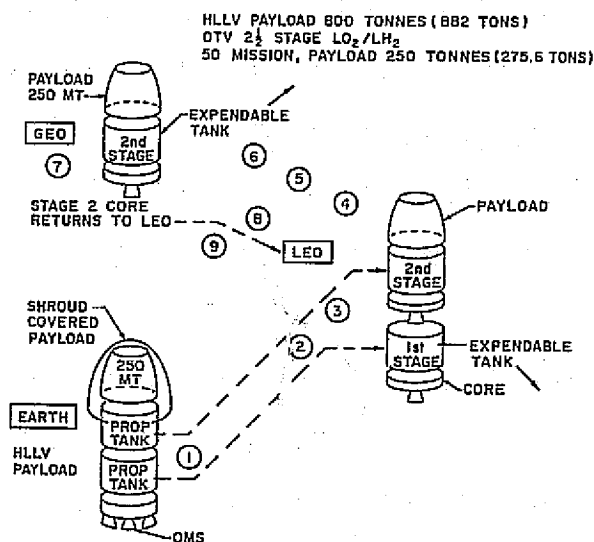


FIGURE 6-9 EARTH TO GEO DELIVERY TRANSPORTATION SCENARIO I

Propellant tank requirements for the transfer of tanks option has already been discussed.

### TRANSFER OF PROPELLANT OPTION

**DESIGN AND MODE OF DELIVERY TO LEO**--This option assumes the existence of a method of refueling orbital transfer vehicles in LEO from large propellant tanks brought to LEO from earth. The refuel method might employ an artificial gravity idea. It is assumed that unitized payloads for GEO of 250 tonnes (275.6 tons) are delivered to LEO. In addition, large propellant tanks suitable for mating with the refueling station arrive periodically.

**PROPELLANT TANK REQUIREMENTS**--The significance of the role that the cryogenic tankage systems play in the SPS transportation scenarios suggested that a brief study of a potential system would be of value. Two basic designs for a LO<sub>2</sub>/LH<sub>2</sub> tankage system for a chemical propulsion stage have been considered by J. C. Smithson of the Power Generation Branch in Reference 6-4. Ground rules and mission requirements are provided in that study. The data below have been modified to reflect performance for a seven day mission.

### LH<sub>2</sub> TANK CHARACTERISTICS

The LH<sub>2</sub> tank is assumed to be cylindrical with ellipsoidal heads of major diameter D and a minor diameter of  $D/\sqrt{2}$  where  $D = 15.24$  meters (50 ft.). The total length is 36.24 meters (119 ft.). A pressure vessel forms the inner wall which is in turn surrounded by 7.62 cm (3 inches) of polyurethane foam. The outer wall is high phenolic resin honeycomb.

Gross Weight 453.6 tonnes (500 tons)  
 Volume 5,849.6 m<sup>3</sup> (206,577 ft<sup>3</sup>)  
 Liquid Residual 7,620 kg (16,799 lbs.)  
 Pressurant Gas 1,448 kg (3,192 lbs.)  
 Boil-off (7 day mission) 5,909 kg (13,027 lbs.)  
 Structure (inert wt.) 50,486 kg (111,303 lbs.)

Available Impulse Propellant equals:

$$453.6 - 65.5 = 388.1 \text{ tonnes (428 tons)}$$

### LO<sub>2</sub> TANK CHARACTERISTICS

The LO<sub>2</sub> tank is assumed to be spherical with diameter 9.13 meters (30 ft.). The insulation system is identical to that of the LH<sub>2</sub> tank except the foam has a thickness of 15.24 cm (6 inches).

Gross Weight 453.6 tonnes (500 tons)  
 Volume 397.7 m<sup>3</sup> (14,045 ft<sup>3</sup>)  
 Liquid Residual 4,309 kg (9,500 lbs.)  
 Pressurant Gas 1,148 kg (2,531 lbs.)  
 Boil-off 706 kg (1,556 lbs.)  
 Structure (inert wt.) 9,947 kg (21,929 lbs.)

Available Impulse Propellant equals

$$453.6 - 16.1 = 437.5 \text{ tonnes (482 tons)}$$

Each of the above tanks are assumed compatible with payload requirements of an HLLV with a 450 tonnes (500 tons) payload capacity. The LH<sub>2</sub> tank would provide sufficient propellant for 11 OTV stages while the LO<sub>2</sub> tank would refuel only two OTV stages. This assumes minimal propellant loss during transfer.

### TRANSPORTATION SCENARIO II

In order to be consistent with Scenario I, we assume an HLLV payload capacity of 800 tonnes. An LO<sub>2</sub> tank sized for 800 tonnes (882 tons) HLLV payload can deliver 710 tonnes (783 tons) of propellant to LEO. This provides propellant for 3.5 OTV stages, including OMS and shroud penalty. An LH<sub>2</sub> tank sized for the 800 tonnes (882 tons) payload capability should be able to deliver 650 metric tons (716.5 tons) of LH<sub>2</sub> to LEO. This

will refuel 19 single OTV stages, and due to boil-off losses, its delivery would occur after delivery of some GEO payload and LO<sub>2</sub> refueling. It is assumed that 3 unitized 250 tonne (275.6 tons) GEO payloads can be delivered in an HLLV. The number of HLLV launches required for each of three areas discussed above is given in Table 6-3. Figure 6-10 provides a visual interpretation of Scenario II.

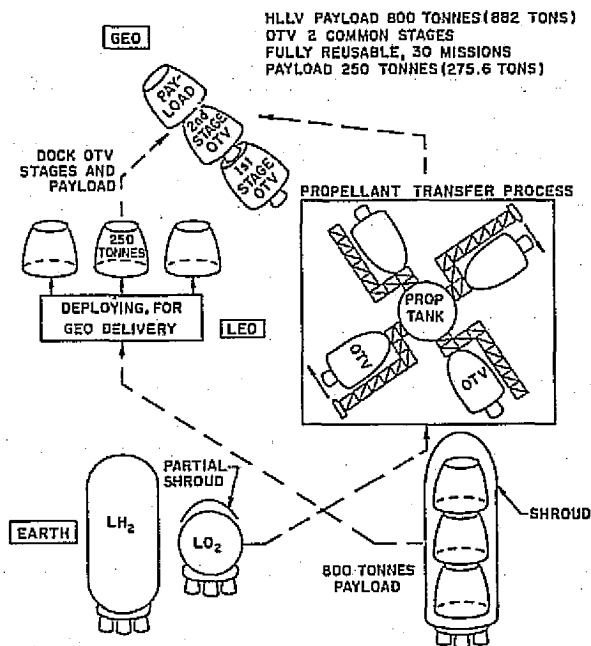


FIGURE 6-10 HLLV PAYLOADS TRANSPORTATION SCENARIO II

### 6.3.5.3 IMPACT ON THE SPACE TRASH PROBLEM

Delivery, construction, and assembly of a solar power satellite of the magnitude studied will result in substantial quantities of discarded items. These items will range in mass from a few grams up to several tons and in volume up to 450 cubic meters (15,892 ft<sup>3</sup>). Experience has indicated that space missions can be limited in duration by waste accumulation due to the number of personnel, amount of construction, and time duration of the project; provisions will need to be made for the systematic elimination of expended items. Potential sources of expendable items are indicated in Figure 6-11. The primary concern, in keeping with the

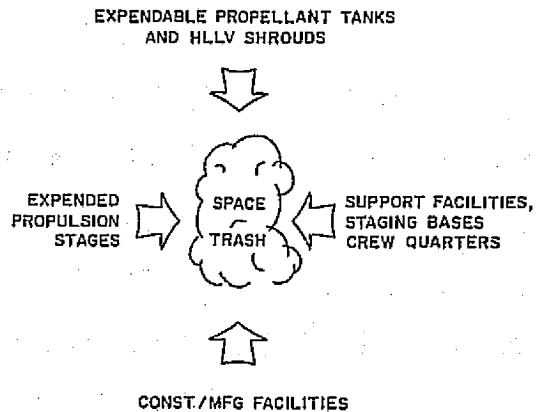


FIGURE 6-11 SOME SOURCES OF EXPENDABLE ITEMS

mode of propellant resupply, shall be with expendable propellant tanks. Since the propellant tanks of Scenarios I and II are of concern in this section, it was necessary to establish some of the characteristics of the tankage systems for the two OTV configurations. Linear extrapolation of the tankage data in Section 6.3.5.2 was assumed valid for the range considered. The ratio of LO<sub>2</sub> to LH<sub>2</sub> was taken as 6 to 1.

### LH<sub>2</sub> TANK CHARACTERISTICS

Inert weight per stage 3.7 tonnes (4.08 tons)  
Volume 433 m<sup>3</sup> (15,290 ft<sup>3</sup>)  
LH<sub>2</sub> weight 34 tonnes (37.5 tons)

### LO<sub>2</sub> TANK CHARACTERISTICS

Inert weight per stage 4.5 tonnes (4.96 tons)  
Volume 178 m<sup>3</sup> (6,286 ft<sup>3</sup>)  
LO<sub>2</sub> weight 204 tonnes (225 tons)

### 6.3.5.4 IMPACT ON THE STAGING BASE OPERATION

**TRANSFER OF TANKS OPTION**--This option would need a docking area for mating expendable tanks with OTV core units and the personnel required for this function. It is considered to impose the least requirements on the LEO staging base and to require the least technological advances.

**TRANSFER OF PROPELLANT OPTION**--This option would require development of a scheme of propellant transfer in space and the machinery necessary to accomplish the actual transfer. Transfer of large propellant tanks to the machinery and connect/disconnect operations would be required. Propellant losses would

need to be minimized. OTV units would require movement to and from the propellant transfer site. These reasons suggest that this option would be the most complex of the two and require technological advances.

## 6.4 PERSONNEL TRANSPORTATION

The following study of transportation of personnel for the solar satellite power system was undertaken in order to determine how a systematic movement of personnel between earth and GEO could be achieved, and, in addition, to provide cost data for this phase of the transportation system. The study will address the personnel carrier module (PCM) and to a lesser extent the use of the personnel orbital transfer vehicle. The first part involving the PCM is an effort to establish a system having uncomplicated logistics and utilizing the hypothesized OTV fleet as opposed to the creation of a separate POTV fleet.

### 6.4.1

#### Personnel Carrier Module

##### 6.4.1.1 BACKGROUND AND RELATED FACTORS

One alternative to the use of the personnel orbital transfer vehicle which is required for electrical propulsion systems is a personnel carrier module. The PCM would be carried from earth to LEO internally in the payload of an orbiter, modified orbiter, or SSTO. Transition of the module from LEO to GEO would be achieved by docking the PCM with a cargo orbital transfer vehicle. Several factors suggest that a PCM capable of transporting in excess of 50 passengers would represent an optimal method of personnel transportation from the dual viewpoint of cost and logistics. These factors are:

- a. No development of a POTV would be required.
- b. Frequency of OTV missions to GEO would certainly meet rotational requirements of construction and support personnel required at the SPS site. Baseline data indicated that approximately 365 missions per SPS per year would be required of the OTV fleet with a vehicle payload capability of 250 metric tons (275.6 tons). Estimated average man trips for the COL-UMN/CABLE SPS configuration is 780 and 940 for the

Truss configuration (Ref. 6-2).

- c. Total mission time from the deployment of the OTV and payload including the PCM at the LEO staging base until deployment of the payload and PCM at the SPS construction site at GEO would be less than one day.

d. Rescue capability would not require additional standby units as in the case of the POTV due to the size of the OTV fleet and OTV mission frequency.

e. Refurbishment and maintenance of the PCM fleet should be more cost effective than in the case of a POTV fleet.

f. In the event of an OTV malfunction, the transfer of the PCM from the vicinity of the failure to another rescue OTV would be similar to the operations required for personnel transfer from one POTV to another rescue POTV.

##### 6.4.1.2 REQUIREMENTS

The personnel carrier module shall be capable of providing life support to a TBD number of personnel which are to be transported from earth to a GEO construction site. Module transportation from earth to LEO will be by orbiter or modified orbiter. The module will be part of the payload of an OTV from LEO to GEO. The extent of man rated capability needed by the OTV will be determined by mission requirements. The exact capacity of the PCM will be determined by constraints imposed by the SPS construction scenario and by the physical constraints of weight and dimension imposed on the PCM by compatibility with the orbiter or modified orbiter. Figure 6-13 gives the mission events sequence for the PCM.

##### MISSION REQUIREMENTS

a. DOCKING SITE--The primary PCM docking site for launch and recovery shall be the same location as that for the Shuttle or modified shuttle. Secondary docking sites are at LEO and GEO staging bases.

b. ABORT CAPABILITY--The extent of abort capability and rescue are to be determined.

c. EMERGENCY STAY TIME--Life support shall be provided for emergency passenger stay time in the PCM of at least 48 hours.

d. PASSIVE DOCKING--The PCM shall be capable of passive docking in LEO or GEO for an indefinite

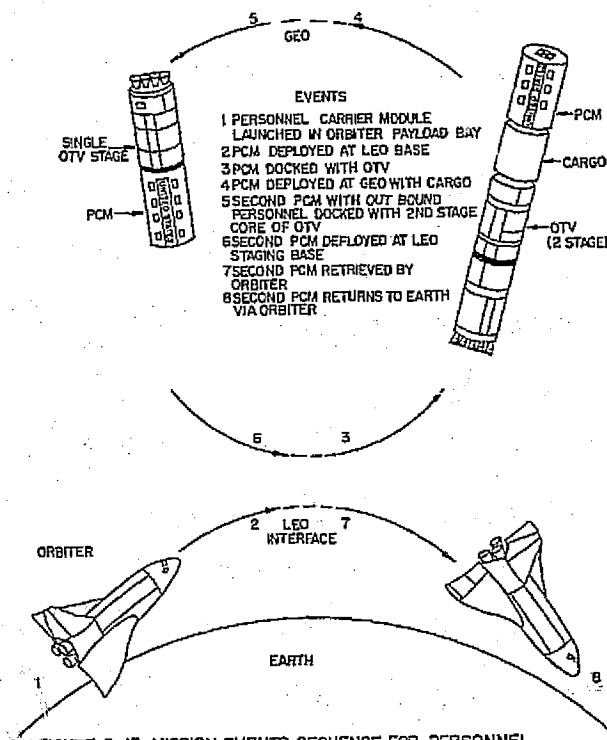


FIGURE 6-13 MISSION EVENTS SEQUENCE FOR PERSONNEL CARRIER MODULE

period.

#### PERFORMANCE REQUIREMENTS

**e. PASSENGER CAPACITY**--The PCM shall be capable of transporting at least 50 passengers to either the LEO or GEO staging bases.

**f. ENERGY REQUIREMENTS**--The PCM shall be capable of meeting all mission related energy requirements including those resulting from an aborted OTV mission where rescue is required.

**g. LIFE SUPPORT REQUIREMENTS**--The PCM shall be capable of meeting all life support requirements for all passengers for a five day time period.

**h. STRUCTURAL REQUIREMENTS**--The PCM structure shall be compatible with the launch loads, dimension requirements, and mating requirements associated with the appropriate Earth Launch Vehicle.

**i. DOCKING REQUIREMENTS**--The PCM will meet docking requirements as imposed by the Earth Launch Vehicle, the OTV, LEO/GEO staging bases, and rescue mission requirements.

**j. ENVIRONMENT REQUIREMENTS**--The PCM shall meet the conditions of the natural and induced environments of the combined, PCM, Earth Launch Vehicles, and OTV systems during all phases of operation, ground and flight. This includes Van Allen Belt transition.

**k. REUSABILITY REQUIREMENTS**--The PCM should be capable of a significant number of missions. Refurbishment should be operationally simple consisting of the reconstitution of most systems by removal and replacement.

**l. OPERATIONAL INTERFACE REQUIREMENTS**--Interfaces will exist between the PCM and operation centers including the earth launch system to support the necessary coordination, information transfer, etc. Interface candidates would include voice communications, computer to computer data transfer, and transmission of facsimile and video. The PCM shall be capable of monitoring critical functions of the OTV with override capability.

**m. SAFETY REQUIREMENTS**--The PCM should be equipped with a fail-safe locator beacon and have limited self-deploy ability in the event of an aborted OTV mission.

#### 6.4.1.3 CONCERNS

One concern is the manner of docking and the location of the PCM relative to the OTV and cargo which may constitute the balance of the OTV payload. Related to the above problem is the need to determine what type of event could occur which would result in an OTV mission abort where the OTV has a PCM as payload and hence a rescue mission would be required. Consequently, it is required to find the type of interfaces which should exist between the OTV and PCM and to what extent the PCM should be able to self-deploy in the event of an OTV accident.

#### 6.4.1.4 PHYSICAL CHARACTERISTICS

The problem of establishing personnel transportation costs required assumptions concerning baseline configurations. This section includes the necessary baseline data and illustrative figures. Figure 6-14 indicates that deployment of the PCM from the orbiter has occurred at LEO and that docking of the PCM for transfer to GEO by OTV is to occur shortly. A view of a personnel carrier module and physical data are given in Figure 6-15. Data and Figure 6-15 are from Reference 6-2.

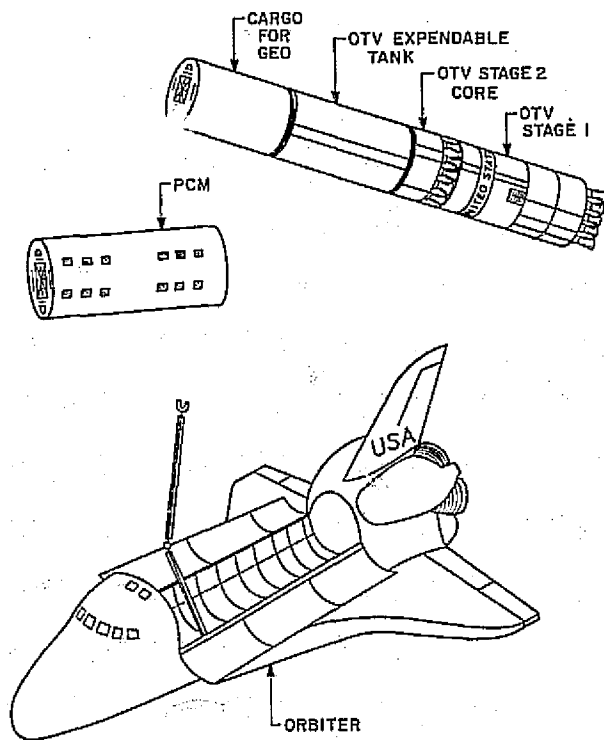


FIGURE 6-14 TRANSFER AT LEO OF GEO BOUND PASSENGER MODULE FROM ORBITER TO OTV

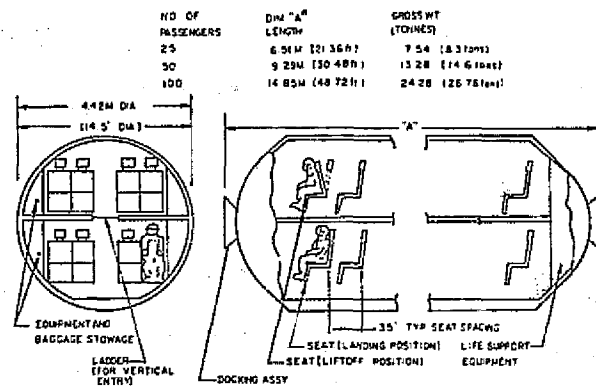


FIGURE 6-15 PERSONNEL CARRIER MODULE (FIGURE VI-E-2 OF REF 6-2)

It was necessary to determine the magnitude of the penalty that a PCM would impose on a normal 250 tonnes (275.6 tons) OTV payload. That is, it was required to calculate the amount of offloading of the cargo payload needed at LEO in order to deploy and retrieve a PCM at GEO. Gus Babb of the Advanced Mission Design Branch has provided technical assistance for this section. The range of OTV having the 2-1\* stage configuration given in Figure 6-4 are described as follows:

	Min.	Nom.	Max.
Payload (in metric tons)	250	250	250
Stages	2-1/2	2-1/2	2-1/2
Isp, sec.	470	460	455
Mass Fraction	.94	.93	.92
Total Inert Weight (metric tons)	29	35	43
Prop. Weight (metric tons)	453	475	494
Expended Tank Inert Weight (metric tons)	7	9	11
Flight Cost \$M/Flt.	5	10	20
Flight Turnaround, days	5	7	10
Mission Life	50	30	20

The PCM is assumed to have a capacity of 100 passengers and have a gross weight of 30 tonnes (33 tons) (included 20% contingency). It was necessary to assign a weight decomposition for the stages of the OTV to obtain a first approximation to the offloading re-

quired. This is summarized below:

Expendable Tank Stage 2 9 tonnes (9.92 tons)  
 Stage 2 Core 10 tonnes (11.02 tons)  
 Stage 1 16 tonnes (17.6 tons)

The conclusions in metric tons are as follows:

	OFF LOADING (PENALTY)	PAYLOAD TO GEO	RETURN PAYLOAD TO GEO
Equatorial Launch (0°)	130	90 tonnes cargo + PCM	PCM
KSC Launch (28.5°)	150	70 tonnes cargo + PCM	PCM

An alternative to offloading is that one stage of the OTV is capable of deploying and retrieving a PCM at GEO, but no additional payload capability exists.

#### COST SUMMARY

Costs for DDT&E and TFU for the personnel carrier module have been estimated at \$150M and \$7M respectively. Lifetime should be in excess of 1000 missions. The following conclusions are based on an equatorial launch site. The division of the \$10M per flight cost of the OTV is determined by assigning normal cost of \$40/kg to the 90,000 kgs. (198,416 lbs.) of cargo and the balance to personnel. Thus, we have:

Cargo Transportation \$3.6M  
 Personnel Transportation \$6.4M

This results in a round trip transportation cost of \$64,000 per man.

#### SUMMARY

If the following assumptions are valid, namely:

- a.** The solar power satellite is to be constructed or assembled in GEO;
- b.** A dedicated chemical propulsion system such as the OTV system will be used as the transportation mode from LEO to GEO;
- c.** The concerns of 6.4.1.3 regarding safety can be resolved without imposing significant cost penalties upon the OTV and PCM systems;

**d.** Projected personnel requirements at the GEO site are not altered significantly;

then, preliminary considerations of the personnel carrier module as parasitic payload of the Shuttle and OTV seem to suggest this mode of passenger transportation as being the optimal method as regards costs, operational simplicity, and flexibility. The PCM will be the baseline mode of passenger travel for the chemical propulsion system.

### 6.4.2 Personnel Orbital Transfer Vehicle

#### 6.4.2.1 BACKGROUND

In the event electrical propulsion is the mode of transportation from LEO to GEO for the solar power satellite program, then a number of factors suggest the need for a special purpose chemical delivery system. These factors include:

- a.** Electrical propulsion of modules (if required) of the SPS from LEO to GEO will involve a trip time of approximately 54 days.
- b.** Environmental hazards to personnel being moved on board the SPS in support bases would be significant. These hazards include radiation dangers from passage through the Van Allen Belt and the probability of a collision of the SPS with space debris.

c. There may be a need of additional high priority equipment and cargo at GEO.

d. Transportation will be required to return construction/support personnel from GEO and to meet requirements of maintenance crews.

Hence, for partial construction at LEO of the SPS, a dedicated personnel orbital transfer vehicle (POTV) will be needed. This study did not address the POTV concept; however, in the interest of completeness, certain aspects of this type of vehicle will be provided. The source of this data is section VI-E of Initial Technical, Environmental, and Economic Evaluation of Space Solar Power Concepts (JSC 11443).

#### 6.4.2.2 DISCUSSION

The normal POTV mission is initiated at LEO operational altitudes and after deploying and/or retrieving a module at GEO, the vehicle returns to LEO for subsequent docking at the staging base. The POTV is able to reenter the above cycle after refurbishment, servicing, refueling, and testing.

Potential payloads for the POTV include passenger carrier modules, station resupply modules, and crew modules for a GEO sortie. The PCM which was first considered in 6.4.1 would again be transferred by the orbiter from earth to LEO. However, the POTV would provide the propulsion system for transfer of the PCM from LEO to GEO. The resupply module would provide replenishment of the GEO station consumables, supplies, and equipment necessary for 180 days. All components of the POTV concept including the stages of the POTV and the modules are assumed compatible with the Orbiter payload bay. The range of POTV is given as follows:

	Min.	Nom.	Max.
Passengers	75	75	75
Isp, sec.	470	462	455
Mass Fraction ( $\lambda$ )	.89	.89	.88
Inert Weight, MT	17	19	23
Prop up, MT	93	106	126
Prop down, MT	47	53	63
Flight Cost, \$M/Flt.	7	12	22
Mission Life	50	30	20

This results in a nominal \$/passenger cost of \$160,000. Figure 6-16 illustrates the configuration and some characteristics of a POTV.

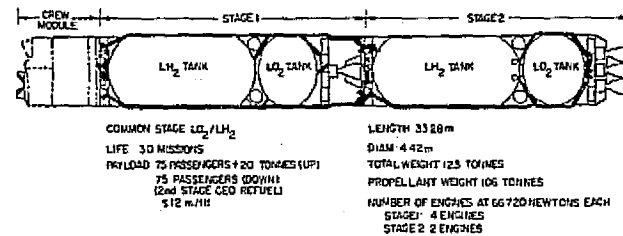


FIGURE 6-16 PERSONNEL ORBITAL TRANSFER VEHICLE (POTV) CHARACTERISTICS (FIGURE VI-10 OF REF 6-1)

#### 6.5 SUMMARY AND CONCLUSION

For minimum DDT&E and operational simplicity, the orbital transfer vehicle (OTV) fleet should be composed of vehicles which employ a single stage type--the "unistage." The unistage will be baselined by the second stage of the JSC nominal vehicle. All OTV's will be made from integral combinations of unistages.

Models have been posed to generate gross mass and flight cost features of the "unistage." The models use a reduction of independent variables to enable a linear scaling in terms of payload mass, vehicle cost per mass, and the staging.

A description is given of a "personnel carrier module," PCM, to be used for interorbit personnel transport. The module is shuttle (modified) compatible and with 100 passengers it can be flown round trip by a single unistage with no other payload. If a 2-1/2 stage vehicle is used, the PCM will cause an "offloading" of payload proportional to the number of personnel transported.

For cargo transport, two unistages will be used together with a 250 m.t. payload. The mission will be flown as 2-1/2 stage, however, and the second drop tank will also be left upon return to LEO. That is, two tanks will be disposed for each round trip--one at GEO and one at LEO.

Transportation must be provided for disposal of unusable items, predominately expended tanks at LEO and GEO. The GEO tanks will be clustered in groups of 13 and taken to escape by a retired stage. The LEO tanks will be attached in pairs to an OMS core and forced to reenter the atmosphere and return to earth. These

schemes for disposal will require additional propellant to be brought up from earth.

The extreme propellant penalty that must be paid for return payload strongly reinforces the idea that personnel in GEO must be minimized; hence, automation should be maximized.

Multiple staging is necessary for propellant economy (i.e.,  $M_p/M_{pL} = 2$ ) and a LEO staging base is necessary for repeated reuse of unistage cores (life of 30 trips). The propellant resupply and core refurbishment operations will need a support station.

#### RESEARCH AND DEVELOPMENT SUGGESTIONS

**a.** DDT&E is needed on repetitive firing-refurbishment-docking-propellant-resupply operations sequence for large numbers of cycles on modeled versions of the chemical OTV.

**b.** A Mission/Traffic model should be developed for outflights of cargo, round trip flights of the Personnel Module, and flights for disposal.

**c.** A compatibility study should be made for the interfacing of the OTV and HLLV. One of the main aspects is envisioned to be partitioning and reassembly of cargo. The impacts on the LEO staging base will also be included.

**d.** DDT&E is needed for tanks that can be recycled spontaneously (i.e., without returning the material to bulk form). The categories to be considered should include structure, habitation, electrical grid "hard spots," and counter weights. This is a transportation cost driver.

**e.** Design should be made for tanks that minimize boil-off of LH<sub>2</sub> and minimize basis cost for those not recyclable.

**f.** Power schemes need to be developed for the equipment at the LEO staging base for refurbishment and structure fabrication that will be operational before the array is deployed. The propellant resupply scheme would be employed to run small turbo generators or fuel cells.

## 6.6 CONCLUSIONS

The two common stage OTV can have an LH<sub>2</sub>/LO<sub>2</sub> tankage system capable of boil-off losses of less than 2% for a seven day mission if an inert tankage weight per stage of 9 tonnes (9.92 tons) is acceptable.

The 2-1/2 stage OTV can have an expendable tankage system capable of similar performance if an expendable tank weight of approximately 11 tonnes (12.12 tons) per stage is acceptable.

## TRANSFER OF TANKS OPTION

**QUANTITY AND NATURE OF EXPENDABLES**--Scenario 1 will be considered. It used the 2-1/2 stage OTV with both stages having expendable tanks. The expendable tanks weigh between 9 and 11 metric tons. Each OTV mission results in one expendable tank deposited in GEO and in LEO. Thus per SPS, 365 tanks are left in each orbit with a total mass between 3,285 (3,621 tons) and 4,015 tonnes (4,426 tons). For reference, the total mass in both orbits is equal to approximately 9% of the SPS mass.

**SOLUTION AND COSTS**--Preliminary estimates of the number of expended tanks which could be incorporated into the GEO support base or used for disposal of waste generated by all operations at the GEO construction bases are in the range of 10 to 20% Henry Wolbers of McDonnell-Douglas Astronautics Company has indicated that each person in a space station requires approximately 5.66 m<sup>3</sup> (200 ft<sup>3</sup>) of living space. If it is assumed that living space constitutes about 20% of the volume necessary for working space then 28.3 m<sup>3</sup> (1000 ft<sup>3</sup>) will be required per person. Assuming a usable space of 400 m<sup>3</sup> (14,126 ft<sup>3</sup>) per LH<sub>2</sub> tank and a personnel loading of 500 it is concluded that 36 tanks are required for the GEO support bases. Due to uncertainty about potential uses of tanks, a procedure was created which would allow for disposal of all excess expended tanks at a modest cost.

The method assumes that tanks given an escape velocity do not constitute a future menace. Expended tanks at GEO are grouped until 26 tanks are available. An OTV second stage which has completed 27 missions would be mated with another stage in LEO. Offloading of 35 tonnes (38.5 tons) of the 250 tonnes of cargo would be done prior to launch. The second stage of the OTV would arrive at GEO with 215 tonnes (237 tons) of payload and approximately 45 tonnes (49.6 tons) of excess propellant. This second stage would not return to LEO but would be mated with six expended tanks in parallel. An additional seven tanks would be reversed and docked in series to the initial cluster. This dual cluster of 14 expended tanks having a mass of approximately 136 tonnes (150 tons) would

then use the excess propellant in the second stage to achieve escape velocity. A first stage which has completed its mission quota would be mounted as a second stage for another OTV at LEO. Offloading of cargo would occur and in this way the above sequence could be repeated with a first stage. Orbits higher than GEO but not assuming escape trajectories could be obtained at less cost. The costs of disposing of 14 tanks excluding operations required in GEO would be \$1.4 million or \$100,000 per tank. If tank construction is costed at \$60/kg, then construction and disposal of expendable tanks costs about \$.75 million each unit.

Disposal of the 365 tanks at LEO would be achieved by using the OMS units. The OMS units which perform the circularization for the LEO orbit would be augmented by about .5 tonne of propellants prior to earth launch. The expended tanks would be reverse docked and mated with the OMS unit. This configuration would be retrofired for reentry into the Indian Ocean. It would be necessary to assume restart capability for the OMS. Recovery of the OMS was not considered. The cost of this operation was not addressed but should be minimal. Environmental impact on the Indian Ocean was not considered. Figure 6-12 illustrates these operations.

#### TRANSFER OF PROPELLANT OPTION

**QUANTITY AND NATURE OF EXPENDABLES**--Scenario II will be considered as representative of the propellant transfer mode. Table 6-3 provides part of the required data. Since an LH<sub>2</sub> tank of the size considered may not meet HLLV payload density and dimension constraints, it may be necessary to have more frequent but smaller deliveries of hydrogen. However, for computational purposes, we assume the scenario is feasible. Scenario II will result in 38 LH<sub>2</sub> tanks with an inert weight of 85.5 tonnes (94.2 tons) and 208 LO<sub>2</sub> tanks with an inert weight of 16.2 tonnes (17.9 tons) left in LEO. In addition, 26 OTV stages will be expended.

**SOLUTION AND COSTS**--It is assumed that the tanks will serve as waste receptors prior to disposal. Disposal will be done according to the methods of the previous scenario. Since each tank is delivered by an OMS unit, it will be assumed that an additional three metric tons of propellant is provided for each OMS prior to earth launch for each LH<sub>2</sub> tank to be returned. The increment for the LO<sub>2</sub> tank is .5 metric tons. Subsequent to the propellant transfer, the tanks would be remated with the OMS units and retrofired into the Indian Ocean. The tanks would not be recovered. Expendable LH<sub>2</sub> tanks would cost \$5.1 million and LO<sub>2</sub> tanks \$1 million each. Tank elimination including penalties and operational cost should not exceed \$.1 million each. OTV's would be expended as in Scenario I after completing their mission quota.

Table 6-4 lists the alternatives as regards disposal of expendable items. The modes of elimination discussed in this section were more characteristic of the early period of the SPS program. A mature program with completion of several satellites a year would introduce the potential of utilizing the recycle alternatives in Table 6-4 more fully.

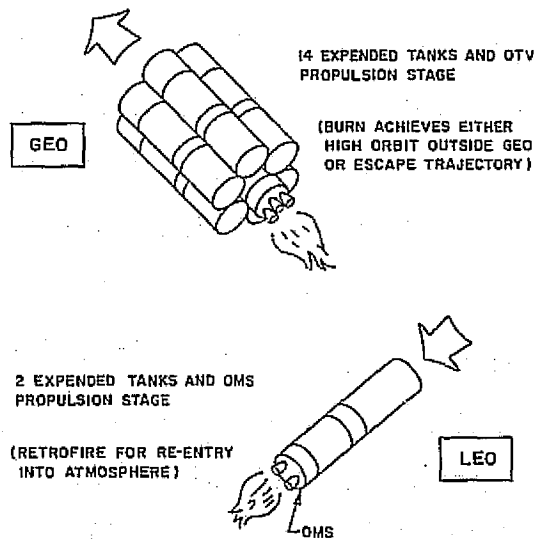


FIGURE 6-12 TANK DISPOSAL FOR SCENARIO I

Table 6-4 EXPENDABLE ITEMS -  
THE ALTERNATIVES

- |   |
|---|
| <ol style="list-style-type: none"><li>1. LEAVE IN ORBIT<ul style="list-style-type: none"><li>• TAKE NO ACTION</li><li>• CREATE JUNKYARD</li></ul></li><li>2. DISPOSE OF ITEMS<ul style="list-style-type: none"><li>• INSERT--ESCAPE TRAJECTORY</li><li>• REINSERT--EARTH'S ATMOSPHERE</li></ul></li><li>3. RECYCLE<ul style="list-style-type: none"><li>• USE IN UNMODIFIED FORM</li><li>• USE IN COMPATIBLE STRUCTURES</li><li>• PROCESS FOR REFABRICATION</li></ul></li></ol> |
|---|

## CHAPTER 6

### REFERENCES

**6-1** Initial Technical, Environmental, and Economic Evaluation of the Space Solar Power Concepts, Volume I, Summary, NASA, Houston, July 1976.

**6-2** Ibid., Volume II.

**6-3** Babb, G. R., Advanced Mission Design Branch, Johnson Space Center; numerous personal conversations and supplied information on state-of-the-art and calculations.

**6-4** Smithson, J. S., JSC Memorandum, "Cryogenic Propulsion Stage for the Solar Power Satellite," lq 4/12/76:4027.

**CHAPTER 7**  
**CONSTRUCTION OF SOLAR POWER SATELLITE:**  
**FABRICATION AND ASSEMBLY**

# CHAPTER 7

## CONSTRUCTION OF SOLAR POWER SATELLITE: FABRICATION AND ASSEMBLY

### 7.1 INTRODUCTION

The successful construction of a solar power satellite (SPS) depends on the availability of efficient structural fabrication and assembly techniques. The very large size and low operational density of the SPS structure dictate the necessity of having space fabrication of the structural elements and a high degree of automation for assembly. The fabrication and assembly methods will have profound impacts on the transportation requirements and cost.

This chapter will discuss the construction and deployment of the solar blanket, the construction of the power distribution system, and the construction of the microwave transmitting antenna. The control system, which is essential to successful SPS construction and operation will also be discussed. At the present time, the technology for space fabrication and assembly has not been developed, so emphasis will be more on the identification of key technology issues rather than on specific methodologies of fabrication and assembly. The influence of fabrication and assembly methods on the transportation cost is stressed.

### 7.2 TECHNOLOGY ISSUES

#### 7.2.1 Solar Blanket and Structures

##### 7.2.1.1 STRUCTURES

In concept, the technological issues involved with the structure are simple. A machine must be developed having the capabilities of high speed and high accuracy for the fabrication of the array structure. High accuracy machines on earth tend to be massive; the mass required for a machine of this type in space is unknown. The actual material to be used in the fabrication of the structure is also unknown at this time.

The two most likely material candidates are a hollow aluminum alloy tubing and a graphite epoxy compound (Ref. 7-1). From a mass production point of view, the aluminum is attractive. Rolls of aluminum foil could be

shipped into orbit and fabricated into hollow cylinders. One could envision a machine patterned after a cigarette machine, producing millions of rolled cigarettes per day. The rolled aluminum should be produced with the ends accurately contoured to allow for electron beam welding of the individual pieces without any crimping or bending of the aluminum cylinder. Crimping of the aluminum will drastically alter its resistance to buckling. Electron beam welding would be desirable since it would not add mass to the structure. Small sections, typically one meter in length, are used to form a triangle, then these are used to form bigger triangles, etc., until one has a completed truss structure of rolled aluminum as illustrated in Figures 3-6 to 3-12.

Another concept of construction envisions a graphite epoxy unit coming from a mold. Units 20 m x 30 m could be molded in a work station and then assembled outside into the truss structure. Again there are severe problems. Assuming that a curing time of about twenty minutes per unit is needed before the unit can be handled, and assuming there are  $10^5$  of these units needed for the truss, then almost  $10^9$  days would be needed for one machine to produce all the required truss material. Based on this estimate, six of these machines would be needed to complete the truss structure in six months.

##### 7.2.1.2 SOLAR BLANKET

The technological issues involved in fabricating the solar blanket are much more complex than those of the structure. Ideally, a solar blanket is to be developed which can yield a ten percent efficiency at an operating temperature of  $100^\circ\text{C}$ , be radiation resistant enough to have a thirty year lifetime, be low enough in mass so that transportation costs are not prohibitive, and be low enough in cost so as to allow the project to be cost competitive. Too often, an improvement in one of these areas is made at the expense of at least one of the others. Each of these areas will be considered separately.

A typical bulk p-n junction solar cell is shown in Figure 7-1. A minimum amount of energy,  $E_g$ , is needed to excite a charge carrier into the conduction band; the gap energy depends upon the structure of the energy bands. Because of contact potentials associated with the n and p type materials there is an equilibrium distribution of positive and negative charge carriers at the p-n junction even in the absence of light. This equilibrium distribution arises from a basic law of thermodynamics that the Fermi level, or chemical potential, of two systems in contact must be equal. In a simplistic view, this distribution may be considered as a parallel plate capacitor at a voltage  $\phi$  the contact potential difference. When photons of energy greater than  $E_g$  are absorbed in the bulk material, electron-hole pairs are formed. Consider one of these electron-hole pairs in the p-type material. The electron would be termed a minority carrier. If it exists in this free state long enough to drift to the charge distribution, it will go across the junction and thereby lower the equilibrium contact potential difference by an amount  $V$ . It is this difference,  $V$ , which appears as a measurable voltage across the device. The fractional change occurring in the number of charge carriers on either side of the junction is given by  $\exp(eV/kT)$ . When  $V$  is zero, there is no change occurring or no output voltage. As the temperature increases, the device efficiency therefore decreases because the fractional change in charge carriers has decreased. A hole (+) in the n-type material is the minority carrier, and the above analysis can be repeated for holes. The p-n junction then, serves as an effective charge separator for electron-hole pairs created by radiation.

The electrical current available from the device will depend upon the band gap of the material and the lifetime of the minority carriers. The minority carrier can recombine directly in the bulk material, be induced by several mechanisms to recombine at the surface, and be induced to recombine in the bulk due to radiative impurities. Since holes have a lower relative mobility the junction in Figure 7-1 (b) is shown formed very close to the surface.

For a given carrier lifetime, the device current is given by (Ref. 7-2)

$$I = q \int_{E_g}^{\infty} Q(h\nu) N_{pH}(h\nu) d(h\nu) \quad (7.2.1)$$

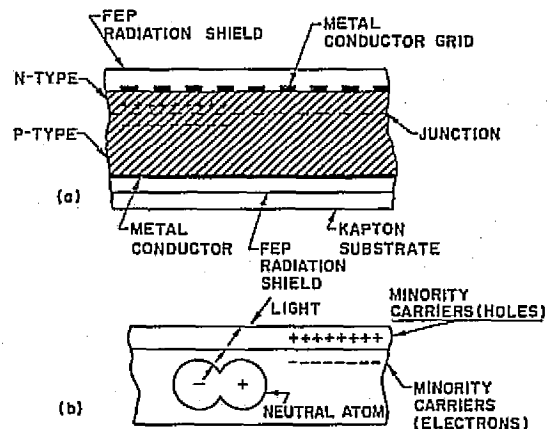


FIGURE 7-1 TYPICAL P-N JUNCTION SOLAR CELL

where  $\nu$  is the photon frequency,  $Q$ , the collection efficiency, and  $N_{pH}$  the photon density. Since there is no output at photon energies less than  $E_g$ , the lower limit of integration must start at the gap energy. Using the spectral density function of sunlight, one finds that the output current must decrease as the gap energy increases. The dependence of current on  $E_g$  is easy to see; the situation is more difficult when considering the device voltage. In a simple representation, the output voltage is due to the rate  $\alpha^+$  which electron-hole pairs combine; if they have a long lifetime, a large charge imbalance will build up across the junction before equilibrium is achieved. The difference in energy between the electron and hole in the free state is  $E_g$ . The probability of their combination decreases as the gap energy increases, and the output power therefore goes through a maximum as a function of gap energy, see Figure 7-2.

The theoretical efficiency is also a function of temperature; the thermal vibrations of the crystal reduce the effective lifetime of the carriers and decrease the fractional percentage of charge carriers. The temperature dependence of the theoretical efficiency is given in Figure 7-2. From these curves, the maximum efficiency of silicon at room temperature is about 20 percent; at 100°C it is down to about 13 percent. Silicon does not have the best theoretical characteristics among the elements shown in Figure 7-2, still it is the most widely used, mainly because of worker familiarity.

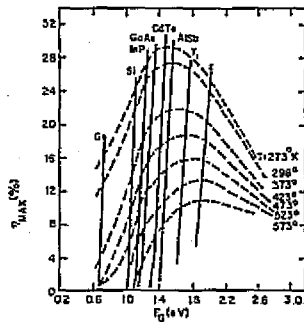


FIGURE 7-2 EFFICIENCY VERSUS GAP ENERGY AT DIFFERENT TEMPERATURES (REF 7-2)

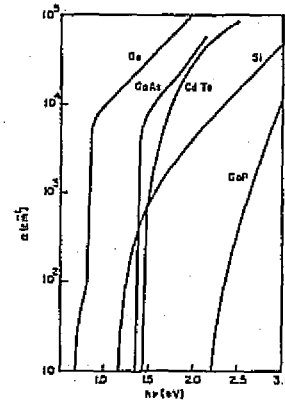


FIGURE 7-3 ABSORPTION CONSTANT  $\alpha$  VERSUS ENERGY (REF 7-2)

GaAs is very near the peak in Figures 7-2 and 7-3. Its theoretical efficiency does not decrease as rapidly as that of silicon because of its larger band gap. In actual devices, though, silicon outperforms GaAs and is cheaper. If better performing materials are to be developed by 1985, there must be more fundamental work done in understanding the basic physics of the device. GaAs shows high promise as a thin film device because of its high absorption coefficient,  $\alpha$ . As indicated in Figure 7-3, the major portion of incoming radiation is absorbed within a distance  $\alpha^{-1}$  of the surface. This implies that solar cells of GaAs could be about  $1 \mu$  thick. Possibly, the reason one does not obtain good devices with these thin films is that too little is known about the behavior of junctions close to the surface. If an empirical understanding is emphasized toward the goal of obtaining efficient devices then the tendency would probably be toward improving the quality of silicon devices. A breakthrough in obtaining better efficiencies with materials like GaAs would have the added benefit that the radiation resistance qualities would be improved also.

### 7.2.1.3 RADIATION RESISTANCE

The radiation resistance of the solar cells is a strong function of the thickness of the glass shield covering the cell. An experimental satellite containing various types of solar cells has been studied by Lincoln Laboratory over a six and one-half year period (Ref. 7-3).

Radiation cover thicknesses of one and six mils were studied. The best performance was by silicon cells having a six mil thick glass cover and ion implanted impurities. Sharp drops of about two percent occurred during a period of high solar flare activity, from which the cells never recovered. The time needed for efficiency to decay to one-half of its original value varied from 30 to 100 years, based on an extrapolation of data.

At this point in time, the allowable amount of decay in efficiency is not known. If the solar array is considered dead when  $\eta$  decreases by 20%, then the allowable range is 300-2000 days. These numbers illustrate the need for a continuous regulation of the voltage building components of the array.

The monitored power output of the cells studied by Lincoln Laboratory exhibited two distinct decay slopes, attributed to slow and fast proton bombardment. There are other possibilities for this degradation; this suggests the need for explicit studies in space of radiation damage to cells. It is quite conceivable that there are high speed dust particles in space that could in effect sand blast the anti-reflective coating off the outside of the protective glass cover. When that is done, the overall efficiency will decrease more rapidly for the same radiation flux because the light intensity into the cell will be decreased. It is not known at this time if the power loss is due to radiation effects alone. The radiation could also be damaging the glass cover plate faster than it is damaging the cell. Another possibility is that the radiation affects the minority carriers in the

two sides of the junction at two different times. There must be an improvement in the fundamental understanding of radiation effects before the directions for technological advances can be charted.

Previous mention was made of the inherent radiation resistance of thin film devices employing GaAs. A simplified explanation of this behavior is the following. The carrier lifetime and mean free path in GaAs is small. There must be a very large concentration of radiation defects in the semiconductor crystal before the minority carrier, on the average, can live long enough to encounter one. When the carrier approaches a radiation defect (a radioactive particle which penetrated the crystal and displaced a lattice atom) it is induced to recombine. Typical solar cells do not become seriously affected by radiation until the total particle flux has reached about  $10^{14}/\text{cm}^2$ . For a solar cell 0.2 mm thick with these radiation defects evenly spread throughout the crystal, there will be about  $1 \mu$  distance between defects. If the order of magnitude of the carrier mean free path is smaller than this, the carrier is scattered by intrinsic impurities, phonons (lattice vibrations), and donor or acceptor atoms. Thus, radiation effects can be expected to become very serious when the radiation defect distance is comparable to the carrier mean free path.

Very little is known at the present time about the self-annealing properties of solar cells under the operating conditions of the SPS. Most radiation studies have been made utilizing monoenergetic beams of electrons or protons, and annealing studies have usually been done at room temperature. One radiation study (Ref. 7-4) found that after irradiating two sets of cells with an integrated flux of  $10^{15}/\text{cm}^2$  of 1 MEV electrons, the set at  $90^\circ\text{C}$  had an efficiency about 3% higher than the set at  $28^\circ\text{C}$ . This is significant; from the theoretical curves of efficiency versus temperature for silicon in Figure 7-2, a 50% drop in cell efficiency could be expected going from  $28^\circ\text{C}$  to  $90^\circ\text{C}$ .

### 7.2.2 Power Distribution System

The power distribution system is a dc network which consists of two parts. One is on the solar energy collector side for combined electric current from every solar cell; the other is on the microwave antenna side for delivering required power to each dc-rf converter (amplifron or klystron). A rotary joint is used to bridge these two parts.

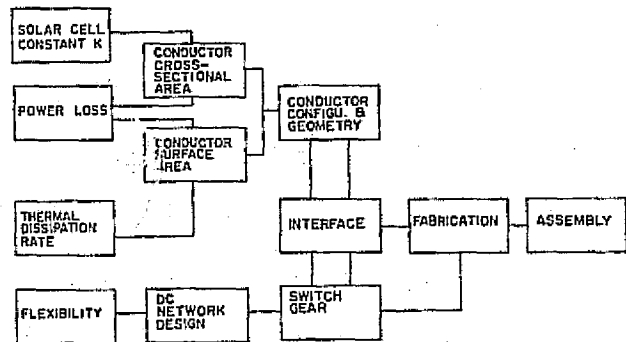


FIGURE 7-4 FUNCTIONAL DIAGRAM FOR POWER DISTRIBUTION SYSTEM

Low loss and high flexibility are the primary considerations for the power distribution system. The power distribution logic is given in Figure 7-4. Low loss means less heat generated within the distribution conductors; resistance is lower and deployment of fewer additional solar cells is required. The minimum power loss will be determined among three factors: (1) conductor total weight; (2) additional solar blanket deployment; and (3) heat dissipation rate. The relationship between (1) and (2) has been studied (Ref. 7-5) and an optimum current density is determined by the equation:

$$J = \frac{I}{A} = \sqrt{\frac{\rho}{K\rho_e}} \quad (7.2.2)$$

where:

- J = current density in the conductor,
- I = electric current,
- A = cross-section area of the conductor,
- $\rho$  = specific weight of the conductor,
- $\rho_e$  = resistivity of the conductor,
- K = solar blanket constant.

The configuration geometry of the conductor is a very important factor in power distribution, and can be determined by A in Equation 7.2.2. The conductor surface area, S, given by Equation 7.2.4, is derived as follows: let the per unit length power loss and thermal dissipation rate be p and q respectively, then:

$$p = RI^2 = \rho_e (I/A)^2 = \rho_{e0} [1 + \alpha (T - T_0)] I^2/A \quad (7.2.3)$$

$$q = \sigma \epsilon S (T^4 - T_\infty^4) \quad (7.2.4)$$

where:

- R = Resistance per unit length,
  - $\rho_{e0}$  = resistivity of the conductor at room temperature,
  - $\alpha$  = thermal coefficient of the conductor,
  - T = conductor temperature,
  - $T_0$  = room temperature,
  - $\sigma$  = Stefan-Boltzmann constant,
  - $\epsilon$  = thermal emissivity of the conductor,
  - S = surface area per unit length of the conductor,
  - $T_{\infty}$  = environmental equilibrium temperature.
- Since  $\rho_{e0}$ ,  $\alpha$ ,  $\sigma$ , and  $\epsilon$  are constants, for a given I and a maximum temperature T, Equations 7.2.3 and 7.2.4 yield the following relationship.

$$S = K_1/A \quad (7.4.4)$$

where  $K_1$  is a constant.

As an example, if aluminum is the conductor and  $I = 8,000$  AMP,  $T = 150^\circ\text{C}$ , and  $K = 2.13 \times 10^{-3}$  kg/w, then:

$$K_1 = 3.08 \times 10^{-3} \text{ m}^4$$

$$A = 1.15 \times 10^{-3} \text{ m}^2$$

$$S = 2.68 \text{ m}^2$$

The simplest geometrical configuration satisfying these data would be a flat sheet with a width of 1.34 m and a thickness of 0.86 mm. Next simplest might be a thin tubular conductor with a diameter of 0.85 m and thickness of 0.43 mm.

High flexibility requires a thorough design of the dc distribution network to minimize the transient effects as the system state changes. The design should also provide for quick isolation from the troubled area in case any short-circuit occurs so that the rest of the system would function properly without any interruption.

### 7.2.3 Microwave Transmitting Antenna

For transmitting large amounts of power from space to earth, a microwave power transmission system (MPTS) (Ref. 7-6 and 7-7) was selected because a microwave beam can transverse the atmosphere with small attenuation under all known disturbances. The technical

requirements of the necessary microwave system will have been met in all likelihood should the SPS be deployed in the 1995 timeframe.

Figure 7-5 illustrates the concept of space to earth microwave power transmission system and the corresponding functional blocks are shown in Figure 7-6. In this section only the construction of the subsystems in space will be considered.

Efficiency is a prime consideration in any transmission system; it appears that the SPS elements must average over 90% if the overall efficiency is to be around 60%. For efficiency reasons, the antenna was chosen to be of the order of 1 km in diameter and the frequency was selected to be 2.45 GHz. At this frequency there is minimum attenuation due to atmospheric disturbance.

Having introduced scale and frequency considerations, attention will now be given to the technical aspects of the major building blocks. The areas of critical technology requiring priority attention will be summarized.

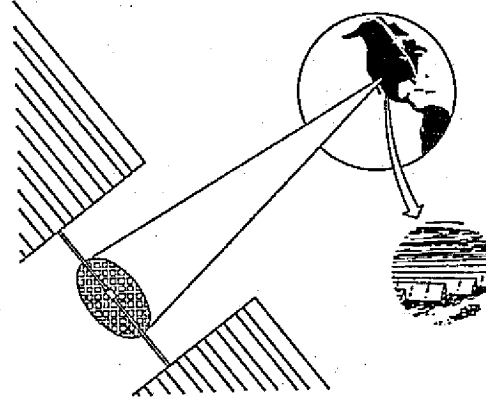


FIGURE 7-5 MPTS CONCEPT [REF. 7-6]

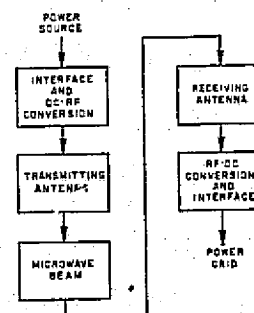


FIGURE 7-6 MPTS FUNCTIONAL DIAGRAM [REF. 7-6]

### 7.2.3.1 DC TO RF CONVERSION

In this study two generic types of devices were examined for converting dc power to rf power at microwave frequencies: the amplitron or crossed field amplifier, and the klystron which is a linear beam device. In current usage the amplitron is characterized by high efficiency and low gain; the klystron is known for moderately high efficiency, high gain, and low noise.

The cross-sectional view of an amplitron and a klystron designed at 2.45 GHz are shown in Figures 7-7 and 7-8 respectively. A summary of specific weight, specific cost, and power budget for the amplitron and klystron is given in Table 7-1.

A first glance at Table 7-1 may indicate that the amplitron is a better choice than the klystron since the efficiency is several percent higher, the specific weight is only one-third, and the specific cost is less. However, the klystron may have two potential advantages over the amplitron: (1) fewer higher power tubes may simplify the assembly task, and (2) low noise and narrow band-width reduce radio frequency interference, offsetting the need for heavy and troublesome filters.

### 7.2.3.2 TRANSMITTING ANTENNA AND PHASE FRONT CONTROL

Goubau and Schwering (Ref. 7-8) showed theoretically that microwave power can be transferred at high efficiency when the transmitting antenna is illuminated with an amplitude distribution that is near Gaussian, as illustrated for the MPTS in Figure 7-9, and when the phase front of the beam is focused on the receiving antenna. For the extreme transmission distance from GEO, the curvature of the phase front is very slight, but nevertheless the front must be controlled with high precision to maintain high efficiency.

One approach to control of the phase front to the required precision requires that the antenna be sectored into numerous subarrays. A typical quadrant for an antenna on the order of 1 Km in diameter is shown in Figure 7-10. The figure also gives an example of how the array could be organized to provide the necessary center to edge amplitude taper. Selection of 10 m x 10 m size subarrays tends to minimize the power loss due to thermal distortion and mechanical offset from attitude control limit cycling. Phase control electronics must be present in each subarray so that there will be a trade-off of power loss versus controls cost.

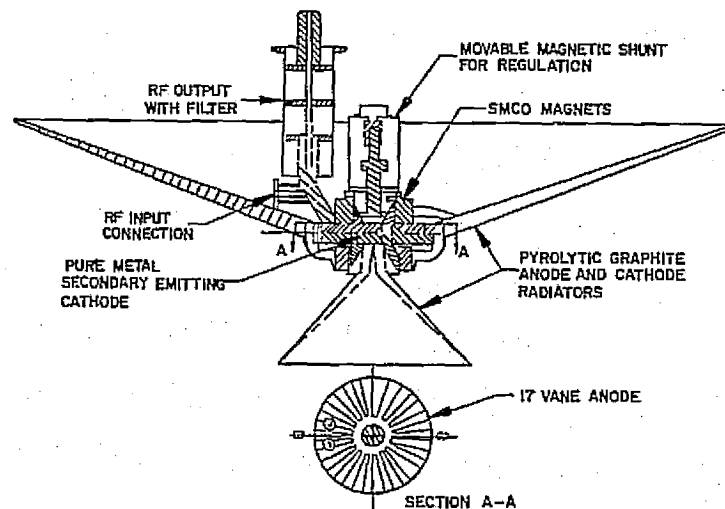


FIGURE 7-7 AMPLITRON ASSEMBLY (REF 7-6)

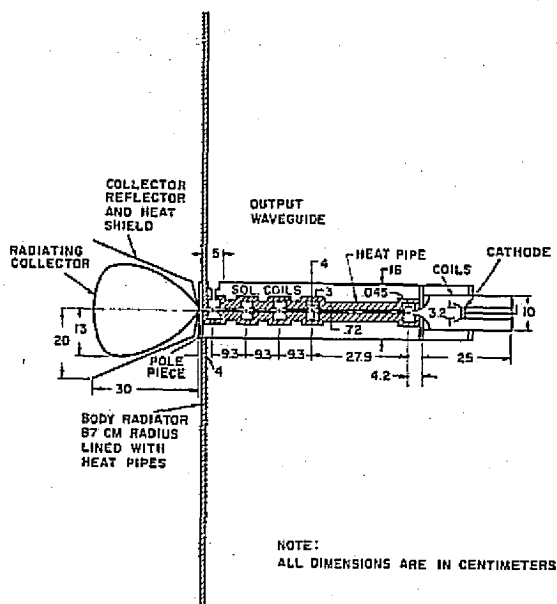


FIGURE 7-8 OUTLINE OF THE 48 KW SOLENOID KLYSTRON [Ref. 7-6]

Efficiency and safety needs dictate that a closed loop form of control should be implemented for phase front or beam formation. Two approaches, adaptive and command, have been formulated and are illustrated in Figure 7-11. The slotted waveguide approach to subarray design is selected because it has very high antenna efficiency while also serving as an efficient means to distribute the microwave power from the dc-rf converters to the radiating elements.

### 7.2.3.3 POINTING CONTROL

Fine pointing by electronic phase control can direct the power beam to an accuracy of about 0.04 arc sec (about 7M at earth), but there will be reduced efficiency if mechanical pointing is not reasonably accurate. An error of 1 arc sec, corresponding to a power loss under 1%, was selected for the design goal and is accomplished with control in elevation and azimuth as shown in Figure 7-12. The azimuth rotary joint is located at the mast interface with a solar oriented power source for which relative rotation is 360° per day. Additional antenna motion in azimuth and elevation is required to compensate for spacecraft (power source) limit cycling which would nominally be on the order of 1 degree (Ref. 7-9). Details of the rotary joint are given in Figure 7-13. Power is carried across the azimuth interface by silver alloy brushes and slip rings, and across the elevation drive by flexible cable where motion is limited to ±8 degrees.

Table 7-1 DC-RF CONVERTER PARAMETERS

	5 Kw Amplitron	48 Kw Klystron
Specific Weight	0.33 g/w	1.01 g/w
Specific Cost	0.018 \$/w	0.039 \$/w
Power Budget		
RF Output Power	5000 w	48362 w
Total Power Loss	747 w	12698 w
DC Input Power	5747 w	61060 w
Gross Efficiency	87%	79.2%

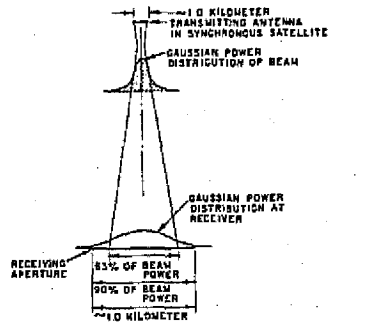


FIGURE 7-9 MICROWAVE POWER BEAM—IDEALIZED [REF. 7-6]

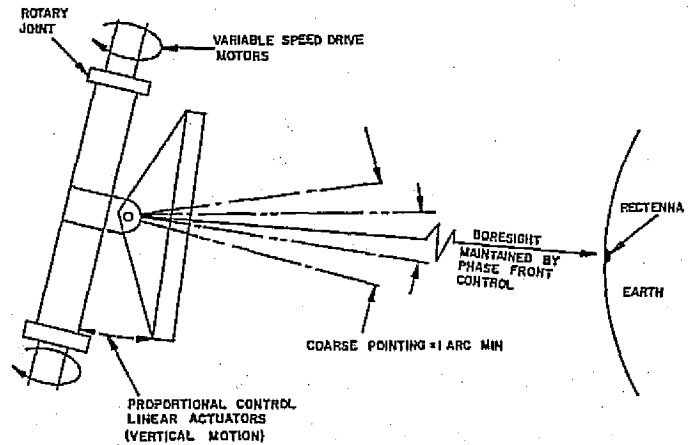


FIGURE 7-12 MICROWAVE ANTENNA MECHANICAL POINTING SYSTEM [REF. 7-6]

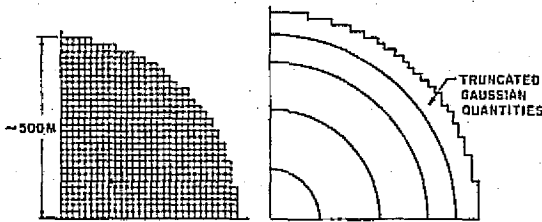


FIGURE 7-10. ARRAY SUBARRAY ORGANIZATION [REF. 7-6]

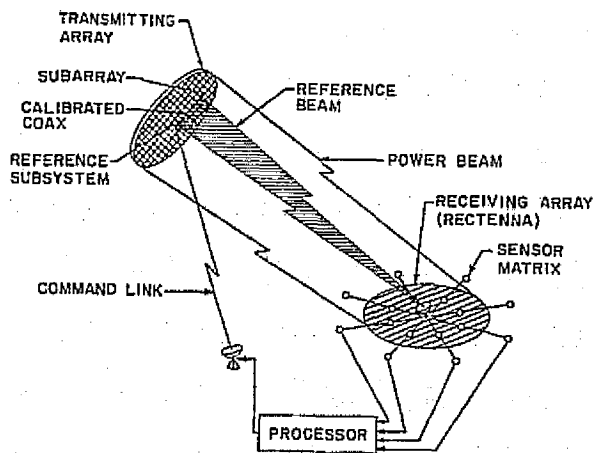


FIGURE 7-11 COMMAND AND ADAPTIVE PHASE FRONT CONTROL CONCEPTS [REF. 7-6]

Thermal analysis of the overall system will be a key aspect of further study since distortion and bending affect the error budget for beam phase control and the determination of maximum heat flux density that can be tolerated at the center of the antenna and still stay within the structural material temperature limit.

## 7.3 FABRICATION AND ASSEMBLY

### 7.3.1 Solar Blanket and Structure

The fabrication and assembly of the solar blanket and structure will be discussed assuming both automated and manual type of construction. There are two reasons for this. First, only by comparison of the labor costs, transportation costs, and completion times can one decide whether it is really worthwhile to develop a space manufacturing industry. If it is more feasible for man to perform many of the work functions, and if man can complete the work before being exposed to a potentially dangerous radiation dosage, then it may not be worth the risk of developing and deploying sophisticated machinery in GEO. The second reason is that these hypothetical machines simply may not exist at the time they are needed.

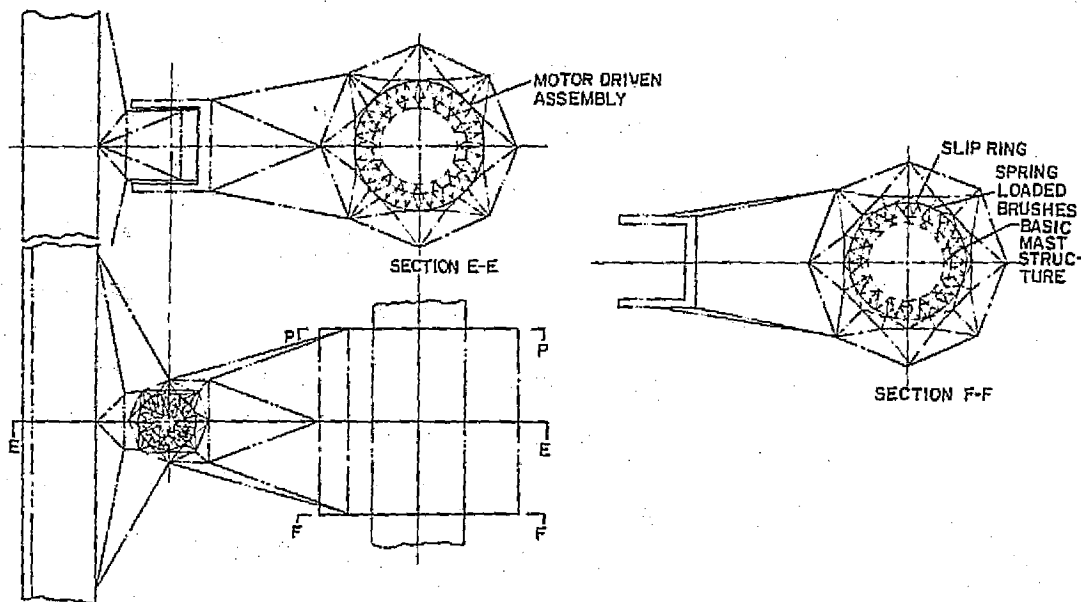


FIGURE 7-13 SCHEMATIC ROTARY JOINT  
[REF 7-6]

### 7.3.1.1 THE MANUAL MODE

For simplicity in visualization of modular construction, assume that the support for the solar blanket will be the truss type (Ref. 7-1). The manual dexterity required in the handling of hollow tube aluminum for the structure, the welding, etc., is prohibitive. In the manual mode, a basic unit must be molded in a work station and conveniently attached to others. One convenient basic unit could be a 30 m x 20 m braced section, molded so that one piece would have a circular cross-section while its counterpart on the other side of the unit would be an open cup-like structure into which the cylindrical piece would snap, as shown in Figure 7-14. The 30 m length units could then be made into larger beams. The triangular cross-section of the truss beam could be constructed with the same pieces. By overlapping the three triangular cross-section pieces, the structure would be self-aligning and would not require cementing of the cup-cylinder joints.

Approximately  $3 \times 10^4$  of the basic units would be needed for the structure. The limiting factor in an idealized construction situation envisioned here would be the curing time needed for the composite mold. An estimate of twenty minutes per unit is used for molding

and curing time. It is assumed that during the curing time material for the next unit will be loaded and prepared in a hopper and work crews will have taken out and placed the previous unit so that everything is ready for the next unit. Assuming construction of 72 units per day, about 2 days of structural work will be required before a corresponding section of solar cells can be attached to form a basic truss module. Overall construction would proceed with four work crews, each working out from the center on their own rectangular section. Assuming an automated molding press, the support personnel for each work crew would include an engineer to supervise structure alignment, two workers to load material into the machine, a machine operator, two workers to unload finished material, and a four man construction crew outside. Counting workers to supervise docking and resupplying, there are a total of 104 for two work shifts for the entire structure. The work crews should be able to complete the structure well within the estimated six months maximum radiation exposure time (Ref. 7-1). At a hypothetical yearly cost of \$80,000 per man, the labor cost, spread over one year to include training, etc., would be about eight million dollars.

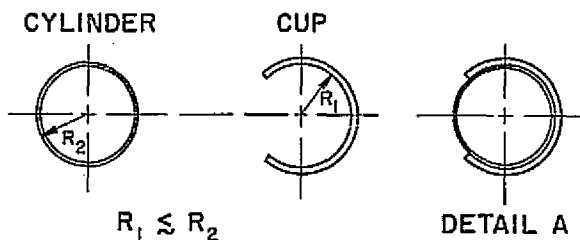
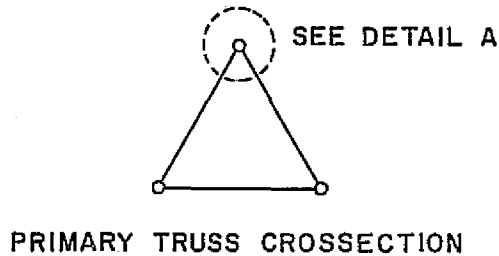


FIGURE 7-14 SNAP JOINT METHOD

The cost of the work stations is estimated to range from 1 to 6.4 million dollars per man-year, including transportation costs. This results in an estimated life support-work station cost ranging from 52 to 332 million dollars. The life support work station then is the driving cost factor in the fabrication and construction of the array structure. In the manual mode that factor will probably override the material costs also.

The solar blanket must cover an area of  $58 \times 10^6 \text{ m}^2$  when using reflectors at 2:1 concentration ratio. This assumes a 10% solar cell efficiency at  $100^\circ\text{C}$  and energy conversion systems such that 15GW of dc power from the cells yields 10GW on the ground. Based on present cells, each 5 cm x 8 cm solar cell would produce about 0.5 volt and 2.5 amp of current, or about  $312 \text{ W/m}^2$ , taking into account ineffective areas. The solar blanket mass would have to be about  $23 \times 10^6 \text{ Kg}$  based on a  $50 \mu \text{ m}$  thick solar cell and a  $75 \mu \text{ m}$  radiation shield. The blanket density is then  $0.339 \text{ Kg/m}^2$ .

The blanket strips would be folded much like a road-map, with  $1 \text{ m}^2$  pieces as the basic unit and sent to GEO. Within each  $1 \text{ m}^2$  unit the cells could be used in series so that each represents 125 V and 2.5 amp. The hinged folds between the blanket units would also be the electrical connectors. After the first basic module of the structure is assembled, that area would be available for solar cells. At the halfway point a conducting cable can be strung across the open area. All the cells up to the cable could be run in series to build the voltage to about 40 Kv at 2.5 amp. The strip next to this one can be fastened to it by rigid male-female connectors, wired so that the two strips are in parallel. A segment can then be producing about 40 KV at 533 amp. The next half of this rectangle can be wired in parallel with it so that the basic rectangle bounded by the structure is producing 1066 amp at 40 KV. The electrical cable across this basic rectangle could connect to the two aluminum reflectors on either side of the cell array. This is illustrated in Figure 7-15.

Once a central module of the structure is completed, workers can start assembling the blanket, spreading out in four directions as the structural workers move out. In each newly constructed structural module two groups of workers can be working, starting from two opposite corners and working toward the central cable. The speed at which the blanket strip can be deployed is going to be limited by the rigidity of the blanket itself. It is estimated that 128 workers would be needed to deploy the blanket in about 130 days. This amounts

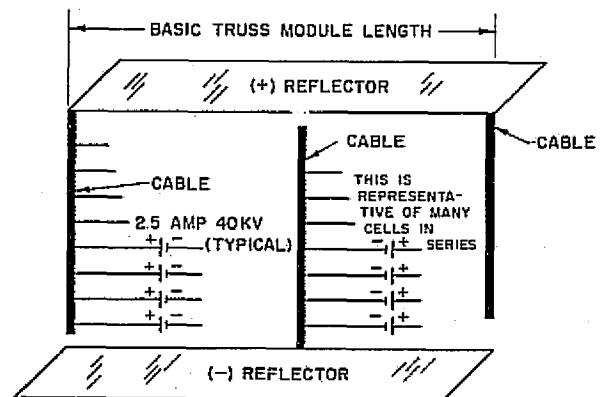


FIGURE 7-15 BASIC SOLAR CELL MODULE POWER DISTRIBUTION

to labor and life support costs slightly larger than that for building the structure. Aluminum costs for the reflector amount to about \$10 million based on current aluminum foil costs.

The more significant cost factor will probably be the material cost for the solar blanket. The present cost for a single solar cell is about \$2/KWH. Based on projected research and development funding, ERDA estimates that the 1985 cost of large scale terrestrial solar cells will be \$0.5/watt, or \$7.5 billion for 15 GW in space. At present, because of the much higher quality control requirements for space usage, solar cell costs tend to be about ten times higher for space applications. Thus, the ERDA estimate of \$7.5 billion for the solar blanket may well be a lower limit. This limit can be approached only by a better understanding of the cell behavior and response to radiation. Quality control, radiation cover encapsulation and cell fabrication will all have to be done on a mass production basis. Many of the separate steps involved in the present manufacture of cells must be eliminated or combined. These steps will help on the overall cost of the system but will not solve all of the problems. On the other hand, if they are not accomplished, the cost of the solar blanket will be prohibitive.

In summary, there should be a balanced approach to the research and development of solar cells. Work on mass production at the expense of efficiency and lifetime probably would not accomplish much. On the other hand, any small increase in the average cell efficiency would result in a smaller array area and decreased transportation costs. Also, radiation resistance improvements in the cell would lead to a longer lifetime and lower overall cost of the total energy produced.

### 7.3.1.2 THE AUTOMATED MODE

The assembly of the primary structure, the deployment of the solar blanket, the connection of the power distribution system and the installation of the solar cell concentrators must be executed in terms of modules in this order. Some preliminary concepts for the construction of the Column-Cable configuration, and the Truss configuration, including the deployment of solar cell concentrators, are shown in Figures 7-16 to 7-18 respectively (Ref. 7-5). Since the assembly of the primary structure consists of a sequence of repetitive operations of putting basic building elements in a

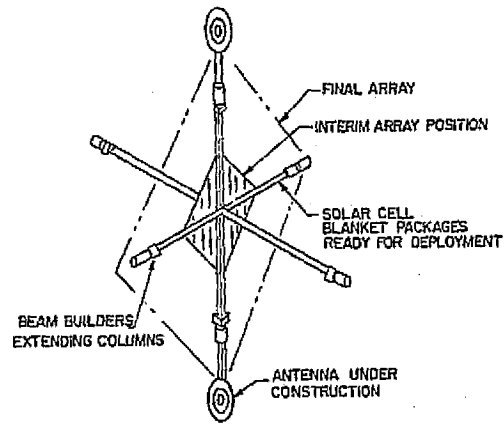


FIGURE 7-16 PARTIAL CONSTRUCTION OF COLUMN/CABLE CONFIGURATION

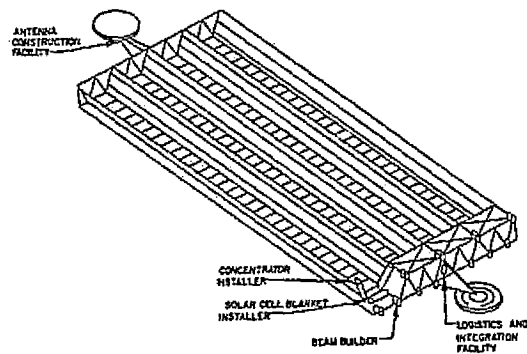


FIGURE 7-17 CONSTRUCTION BASE CONCEPT FOR TRUSS CONFIGURATION (REF 7-5)

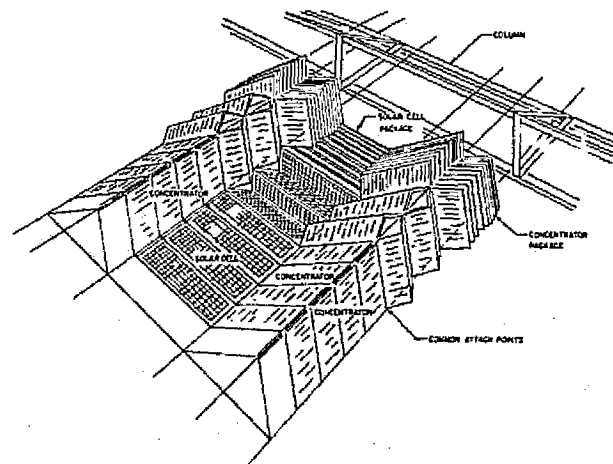


FIGURE 7-18 CONCEPT FOR SOLAR CELL CONCENTRATOR DEPLOYMENT (REF 7-5)

specified configuration, a computer-controlled automatic assembly scheme is proposed. As is shown in Figure 7-19, the system consists of the fabrication unit, the buffer storage and dispensing unit, and the assembly unit. The fabrication unit generates the basic building elements from prefabricated stock. The fabrication rate (estimated as high as 190 Kg/hr.) may not be the same as the assembly rate ( $5 \times 10^3$  Kg/hr.); thus some buffer storage unit will be needed. The buffer storage and dispensing unit will serve to interface between the fabrication unit and the assembly unit. The mobil assemblers will perform four basic functions: fetching, positioning, aligning, and joining the basic elements to the structure. The construction will start with the deployment of the fundamental core unit (reference unit) and the working platform that supports the fabrication and assembly units. All subsequent assembly tasks will be executed by the intelligent mobil assemblers (with onboard computers, imaging devices, laser beam alignment sensors, and sophisticated control systems and actuators). The assembly sequences will be controlled by an optimal assembly algorithm tele-operated by the central computer on the ground. The ground control computer will also control functions of the fabrication unit. According to the present forecast (Ref. 7-10), by the year 2000 the computer memory density can be increased to  $10^{15}$  bits/m<sup>3</sup>. The imaging information can be transmitted at  $10^{15}$  bits/day. The required high level computer language will become available. The advanced microprocessors will have very high computing capability and small volume. The adaptive control systems and precision position sensors available at that time are expected to have the required precision. Assuming these optimistic forecasts the development of an intelligent mobil assembler is feasible. In order to achieve a high assembly rate, an optimal assembly algorithm needs to be developed. Considering the primary structure as a network of nodes (joints) and branches (truss beams), then the entire structural configuration can be completely defined by the spatial coordinate of each node and hence each branch. Thus, each beam position is completely specified. The optimal assembly algorithm will require of the mobil assemblers the least amount of travel and will maintain as much symmetry as possible for the entire structure during the construction phase. In Figures 7-20 and 7-21 are shown the computer generated graphics of the primary and the antenna structures

respectively (Ref. 7-11). The use of computer graphics with graph theory should make possible the development of an optimal assembly algorithm. The development of such an assembly will accomplish the following objectives:

- a. Provide high machine assembly rate.
- b. Require minimum human involvement in assembly.
- c. Require a less sophisticated space station.
- d. Facilitate the construction in GEO.

### 7.3.2 Power Distribution System

Fabrication of the power distribution system will occur on the ground because the system will be extremely complex and yet will require high reliability. The components constructed on earth will cause little or no packing problems, as they will be heavy enough to satisfy the payload density and sturdy enough for sustaining the launch load effects.

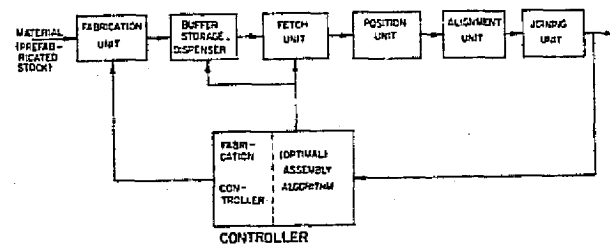


FIGURE 7-19 COMPUTER CONTROLLED AUTOMATIC FABRICATION AND ASSEMBLY CONCEPT

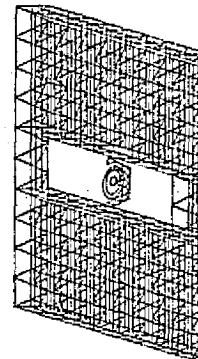


FIGURE 7-20 COMPUTER GRAPHICS OF SOLAR ARRAY STRUCTURE (REF 7-11)

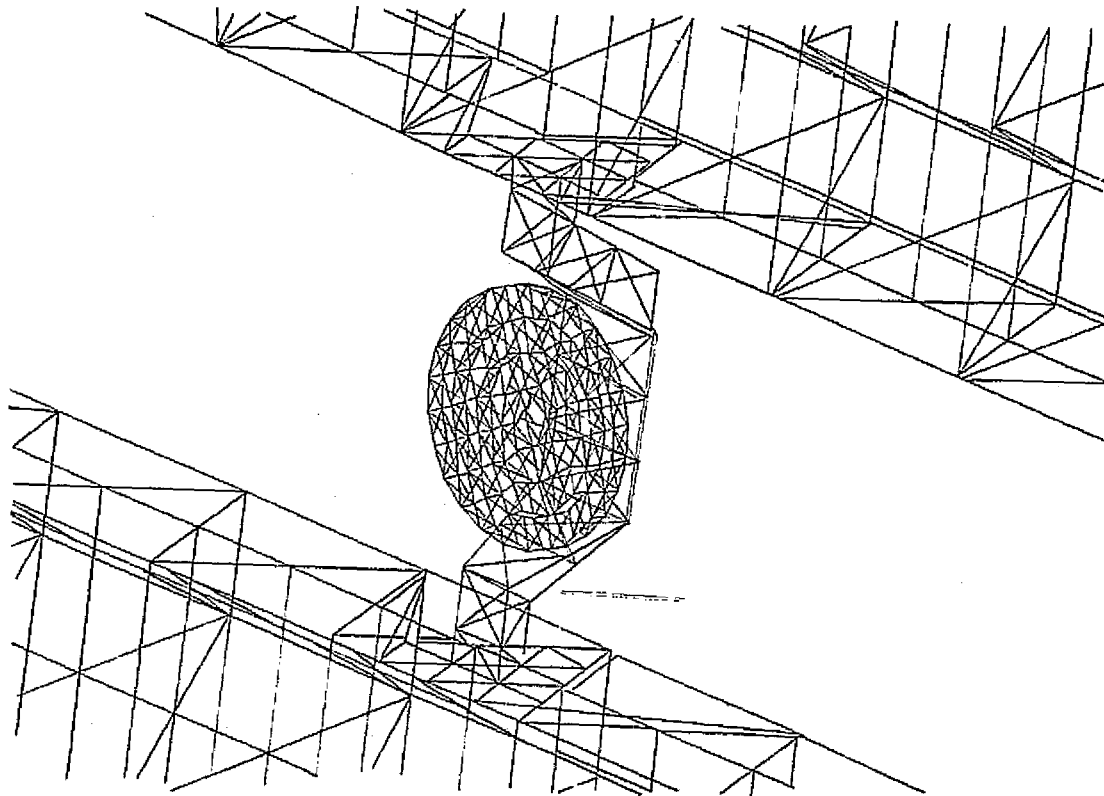


FIGURE 7-21 COMPUTER GRAPHICS OF MICROWAVE ANTENNA STRUCTURE  
[REF. 7-11]

Portions of the power distribution system, shown in Figure 7-22, will be preassembled on the ground with portions of the microwave antenna so that tedious in-orbit assembly work will be minimized (Ref. 7-8). The tertiary, the secondary, and the primary feeds will be assembled manually in parallel during the time that the subarrays are constructed. For making simple and rapid electrical connections, a form of mechanical connector should be developed. This will reduce the EVA durations. The power distribution switchgear is divided into two categories: one category consists of centralized apparatus to control the system operations and the other category is incorporated with each subarray. The switchgear arrangements must be highly reliable and flexible, yet amenable to simple assembly operations.

### 7.3.3 Microwave Antenna

The fabrication of the microwave power transmission system will involve the use of highly accurate manufacturing methods. Next to the exacting work required to manufacture solar cells, the construction of the transmitting antenna will require the closest tolerances in the entire project. Although the microwave power transmission system actually involves the entire SPS, this discussion will address only the most important part of that system, namely, the microwave transmitting antenna.

The microwave transmitting antenna is made of the following components:

- Klystrons or amplitrons
- Waveguides

- Slotted array panels
- Suntele gear
- Power distribution cable system
- Receiving antenna
- Central phase and reference control systems electronics
- Subarray phase conjugation system
- Fiber optics transmission system
- Heat shield reflector
- Antenna primary structure
- Adjustable screw jacks

Of the components listed, two seem to be prime candidates for fabrication in space. These are the antenna primary structure and the wave guides. The slotted array panels and the receiving antennas are also possible candidates for fabrication in space, especially if they can be fabricated out of composite materials.

### 7.3.3.1 TRANSMITTING ANTENNA PRIMARY STRUCTURE

The transmitting antenna primary structure construction can be done in parallel with that of the primary structure used for the solar array. Both of these structures may be made from the same material, and the sequence of structural assembly from basic elements to primary and secondary trusses can be done in similar fashion.

As indicated in Chapter 3, one of the prime candidate materials for the structure (including the antenna structure) is a composite material. Advantages that can be obtained with the use of composites include the following:

- minimum subarray deflection due to thermal stresses caused by heat given off in dc to rf conversion.

- minimum power loss
- maximum waste heat power density (up to 8,100 W/m<sup>2</sup> according to Ref. 7-2)

- desirable 5:1 db taper for the microwave Gaussian distribution (Ref. 7-2)

- high probability that this type of structure can be fabricated in space from composite materials which allow high density payloads.

- lighter overall structure due to lower density material: graphite epoxy has a density between 1.12-2.40 g/cm<sup>3</sup> while aluminum has a density between 2.62-2.82 g/cm<sup>3</sup>.

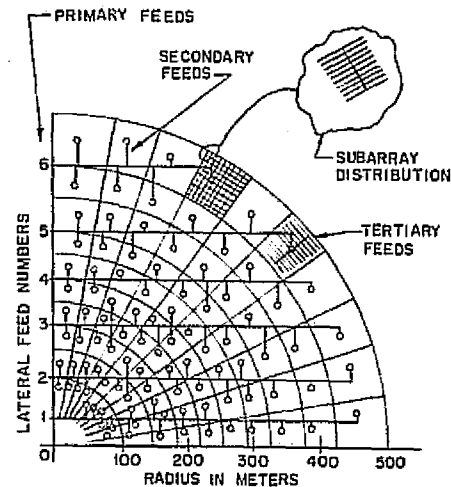


FIGURE 7-22 POWER DISTRIBUTION LATERAL POWER FLOW [REF. 7-6]

### 7.3.3.2 SLOTTED WAVEGUIDE SUBARRAY PANELS

The slotted waveguide subarray panels are the basic modular units making up the microwave transmitting antenna. At this point in the design of the SPS there are various configurations for the basic structure of these panels. One configuration uses dimensions which are 10 m x 10 m while another uses 19 m x 18 m. A Martin Marietta Report (Ref. 7-12) estimates that the packing density of composite materials for waveguides will be about 6.1 lb/ft<sup>3</sup>. Recommendations made by ECON (Ref. 7-1) included building the primary structure for the waveguide subarrays from triangular girders.

## 7.4 CONTROL SYSTEM

Because of the very large size (144 Km<sup>2</sup>) and low density (0.16 Kg/m<sup>3</sup>) of the solar power satellite (SPS) structure (Ref. 7-5), the attitude control of the SPS cannot be adequately treated by rigid body dynamics. A more realistic approach is to treat the SPS as a flexible vehicle (Ref. 7-13). Therefore, it is necessary to include structural bending mode considerations in the design of the SPS attitude control system. A functional block diagram of the SPS attitude control system is shown in Figure 7-23. It can be seen that the control forces not only generate a control torque but also excite the system's elastic bending modes. The elastic

feedback loop may cause the system to become unstable if the system is not properly designed. In order to ensure the proper design of the control system, an analytical analysis based on multi-mode flexible body dynamics (Ref. 7-13) should be performed. Various parameters for such an analysis will have to be determined as soon as the SPS structural configuration and material choice are defined. Since the operational load on the SPS structure will be very small, the fundamental frequency of the SPS will be  $2.3 \times 10^{-5}$  Hz due to the gravity gradient torque. Thus, a fundamental bending frequency of  $2.3 \times 10^{-4}$  Hz (5.6 cycles a day) will be practical. The gravity gradient torque can be countered by a reaction control system, but this can only be done at a substantial propellant cost.

One alternative that can be used to reduce gravity gradient torque is to increase the length-to-width ratio (i.e., to increase the SPS north-to-south length). However, the power distribution losses or increased weight of the power buses may also limit the structural length. Another way of countering the gravity gradient torque would be to use counterweights of about  $10^6$  Kg in the Column-Cable configuration. The trade-off between the control propellant and the weight of the counterbalance is not clear at the present time. Since the control system will be the major maintenance cost driver, the selection of the control system configuration for balancing the gravity gradient torque will require very careful examination.

The key issues regarding the control system that will require further studies are:

a. The dynamic responses of the large, flexible structure in space to disturbances such as gravity gradient control torques, orbital station-keeping control torques, and the low frequency oscillations induced by thermal gradients resulting from the earth's eclipse of the SPS.

b. Modeling of the multi-mode flexible body dynamics.

c. Development of low cost electric propulsion units for SPS attitude control.

d. Dynamic analysis of the SPS structural transient responses to impulsive disturbances. This may be very critical during the construction phase of the SPS.

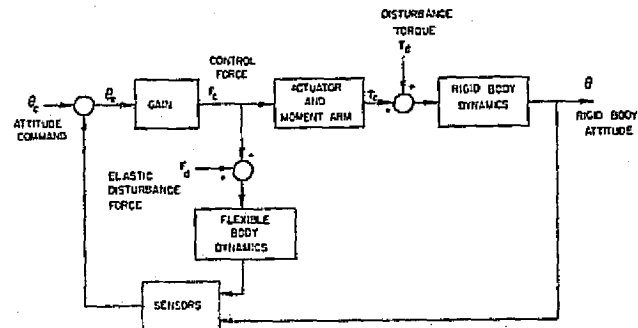


FIGURE 7-23 FUNCTIONAL BLOCK DESIGN DIAGRAM OF THE SPS FLEXIBLE BODY ATTITUDE CONTROL SYSTEM  
REF 7-13

## 7.5 CONSTRUCTION ALTITUDE CONSIDERATIONS

Several altitudes could be considered for partial or full construction and assembly of the primary structures. In this investigation two construction altitudes were considered, namely, Low Earth Orbit (LEO): below 460 Km (250 n.m.) and Geosynchronous Orbit (GEO): at 35,800 Km (19,300 n.m.).

The presence of the Van Allen Radiation Belt (from 500 Km (270 n.m.) to 13,000 Km (7,000 n.m.)) is the main reason for considering the higher assembly altitude. The LEO assembly altitude was chosen because it is high enough to have minimal air drag effect and is low enough to be below the Van Allen Belt.

The high thrust of orbital transfer chemical propulsion engines rules out the full satellite assembly at LEO. The cost saving of partial assembly in LEO over that of full assembly in GEO is found to be no more than 4% (see Chapter 8). Thus, if a chemical propulsion system is used to go from LEO to GEO, full assembly in GEO seems to be a better choice.

If the electric propulsion system is used to go from LEO to GEO, factors that are unfavorable to LEO assembly are the following:

- a. Appreciable air drag effect.
- b. High probability of collisions with space debris.
- c. Degradation of solar cells in passing through the Van Allen Belt.

d. Long transit time to go from LEO to GEO. and:

e. Extra power installations for lighting due to the day-night cycles and for the construction machinery. payload capacity utilization efficiency

$$= \frac{22}{23} = 0.95.$$

The only justification for LEO assembly will then be the possible substantial savings in transportation cost of using the electric propulsion system to go from LEO to GEO. Earlier reports (Ref. 7-1 and 7-12) indicated that 2 to 3-fold savings in transportation cost would result if full assembly were done in LEO and if the electric propulsion system were used to go from LEO to GEO. However, by including penalties of replacing damaged solar cells and using long transit times, this investigation indicates that only small savings over that of chemical propulsion and full assembly in GEO can be achieved.

Therefore, as far as assembly altitude is concerned, full assembly in GEO appears to be the best choice.

## 7.6 CONSTRUCTION IMPACT ON THE TRANSPORTATION COST

It was mentioned earlier that the very low densities of the solar array structure ( $0.16 \text{ Kg/m}^3$ ) and the microwave antenna structure ( $25.1 \text{ Kg/m}^3$ ) dictate the necessity of fabrication in space of those structural elements in order to have reasonable transportation cost and a cost effective SPS program. Some simple computations based on data presently available are given to illustrate why space fabrication of structural elements is absolutely necessary for a cost effective SPS program.

According to Ref. 7-12, as many as 3,582 additional Fly-back DOL (payload capacity 88.5 m.t.) flights per SPS (normally 23) would be required for delivery of the volume represented by  $1.95 \times 10^6 \text{ Kg}$  mass of solar array and antenna structures if they were prefabricated on the ground.

Using these data, the following were derived:

$$\frac{(\text{density of prefabricated stock})}{(\text{density of ground-fabricated beams})}$$

$$= \frac{3605}{23} = 156.7$$

The above data will now be used to evaluate the impact of space fabrication of structural elements in the transportation cost of the SPS program using the present configuration (Ref. 7-4). Assume that the heavy lift launch vehicles, HLLV, (900 metric tons payload capacity and \$20 million cost per flight) are used for delivery of the volume represented by  $6.65 \times 10^6 \text{ Kg}$  (of which the solar array structure is  $5.74 \times 10^6 \text{ Kg}$  and the microwave antenna structure is  $1.21 \times 10^6 \text{ Kg}$ ). With the truss-type SPS 1,246 additional HLLV flights would be required if the beams are ground-fabricated. This will result in an increase of \$24.9 billion per SPS and 2.8 trillion for the 112 unit SPS program just in the cost of transportation alone of going from ground to LEO. Thus, space fabrication of structural elements is absolutely necessary if a cost effective SPS program is to be achieved.

The man/machine productivity, environmental considerations for crew's safety, and logistic support required in space are the main factors involved in selecting the appropriate assembly modes. GEO appears to be the better choice for the assembly altitude. The radiation effect in GEO plus the fact that manual assembly with extensive EVA results in a low assembly rate (8 to 11 Kg/m-hr.) both lead to the conclusion that EVA assembly should be ruled out in GEO except for very limited contingency purposes. The semi-automated assembly done by remote manipulators supervised and assisted by men inside the space station may be acceptable for near-term programs of limited scale but certainly would not be desirable for large scale construction required for the SPS program. For the semi-automated assembly method, the number of personnel required in the space station at the peak of construction is estimated to be about 500 (Ref. 7-5).

Logistic support for the 500 man space station will be a big problem as the space station will have to be a closed system. The construction of such a space station may be as difficult and costly as the first SPS. At present, the cost estimate for the space station ranges

from \$1 to \$6.4 million per man-year. If a fully automated assembly system (with computer-controlled intelligent assemblers tele-operated by the optimal assembly algorithm supervised by the central computer on the ground) is developed, there can be a high assembly rate and minimal man involvement. The total cost reduction in the space station requirement alone will range from \$67.2 billion to \$430 billion for the 112 SPS Program. The saving is roughly 20% of the current estimated cost of the SPS program.

The automated assembly method will have great impact on the total SPS cost, but its impact on the transportation cost is believed to be not very significant. However, the impact of space fabrication on the transportation cost is very significant and should not be overlooked.

## **7.7 CONCLUSIONS AND RECOMMENDATIONS**

### **7.7.1 Technological Issues**

- a.** Dc-rf converters need further development for higher efficiency, longer life, more phase stability.
- b.** Phase front control technology requires testing programs before installation.
- c.** Pointing control poses no problem on the ground; it may need modifications when used in space.
- d.** High voltage dc distribution technology is not available today. A development program should be started.
- e.** Aluminum conductors for high current capacities often give connection deficiencies; a thorough test program should be carried out before deployment.
- f.** Thermal behavior of the structures, waveguides, and insulator materials must be studied.
- g.** EM interference may be a potential problem with many SPS units in orbit, each having a tremendous energy level.
- h.** A detailed study of the volume and weight characteristics of each ground fabricated component will be necessary before a HLLV payload density can be defined.
- i.** Transient dynamic behavior of structures subjected to impulsive perturbations during construction need more attention.

**j.** Control system requirements for SPS construction may be more critical than those for SPS operations.

**k.** The cost of fabrication and assembly may constitute a fairly significant portion of the total SPS cost, perhaps more than 25 percent of the total cost.

**l.** A better understanding of the nature of radiation damage must be obtained.

**m.** Mass production of the solar array alone may not be the essential driving factor in the blanket cost.

**n.** There must be a balanced approach to the R&D associated with the solar blanket. R&D associated with the manufacturing process should not overshadow the R&D associated with cell efficiency and lifetime.

### **7.7.2 Construction of SPS**

**a.** Full assembly in GEO is more desirable than partial or full assembly in LEO.

**b.** SPS structural configurations should have as much modularization as possible.

**c.** Onsite space fabrication of basic building blocks is more desirable than receiving the prefabricated items from the ground.

**d.** The degree of man involvement in the EVA assembly should be minimized.

**e.** High degree of automation is desirable and needed in machine assembly to achieve a high assembly rate.

**f.** It seems feasible to have the assembly tasks done automatically by computer-controlled mobile assemblers which are remotely tele-operated from the ground.

**g.** In comparison, assembly is more complicated than fabrication and is believed to be the most critical area in the construction of the SPS.

**h.** The possibility of having a high rate of machine malfunction in automatic assembly operations should be recognized.

**i.** The potential impacts of fabrication and assembly on the transportation cost need more careful assessment.

**j.** Complicated components, e.g., dc-rf converters, waveguides, control electronics, and switchgear are thought to be more economical if fabricated and assembled in modular form on the ground and then transported into orbit for final assembly.

## **CHAPTER 7**

### **REFERENCES**

**7-1** 'Space-Based Solar Power Conversion and Delivery Systems Study,' Interim Summary Report, Contract NAS 8-31308, ECON Incorporated, March 31, 1976.

**7-2** Loferski, J. J., Proceedings of the 24th Annual Power Sources Conference, 1972, page 124.

**7-3** Sarles, F. W. Jr., 11th IEEE Photovoltaic Specialists Conference, 1975, p. 190.

**7-4** Proceedings of 17th Annual Power Sources Conference, 1963, p. 15.

**7-5** "Initial Technical Environmental and Economic Evaluation of Space Solar Power Concepts," Volume I, Summary, JSC 11443, NASA, July 15, 1976.

**7-6** "Microwave Power Transmission System Studies," Contract Report NAS 3-17835, Raytheon Company, December 1975.

**7-7** Brown, W. C., "Experiments in the Transportation of Energy by Microwave Beam," 1964 IEEE Int. Conv. Rec., Volume 12, pp. 8-17.

**7-8** Goubau, G. and Schwering, F., "On the Guided Propagation of Electromagnetic Wave Beams," IRE Trans. Antenna Propagation, Volume AP-9, pp. 248-263, May 1961.

**7-9** Glaser, P. E.; Maynard, O. E.; Mackovciak, J. Jr.; and Ralph, L. E.; "Feasibility Study of a Satellite Solar Power Station," NASA Contractor Report CR-2357, NASA, Washington, D.C., February 1974.

**7-10** "A Forecast of Space Technology, 1980-2000," NASA SP-387, January 1976.

**7-11** Stebbins, F. J., "ADAGE Computer Graphics--SPS Simulation," NASA/JSC, June 1976.

**7-12** "Orbital Assembly and Maintenance Study," NAS 9-14319, Final Report, Martin Marietta Corporation, August 1975.

**7-13** Quinn, R., "Selection of the Baseline Altitude Control for the SSPS and a Stability and Performance Analysis of the Elastic Coupling Between the Control System and the Spacecraft's Structural Modes," ASP-611-m-1009, Grumman Aerospace Corporation, September 1972.

**7-14** Kline, R. and Nathan, C. A., "Overcoming Two Significant Hurdles to Space Power Generation: Transportation and Assembly," AIAA Paper No. 75-641, AIAA/AAS Solar Energy for Earth Conference, Los Angeles, CA, April 21-24, 1975.

**CHAPTER 8**  
**ECONOMIC CONSIDERATIONS**

## CHAPTER 8

### ECONOMIC CONSIDERATIONS

#### 8.1 INTRODUCTION

The analytical techniques applied in this project provided a limited cost analysis. The approach was two-fold in nature. The first stage was to develop a generalized cost model that illustrated the interrelationships of the various components of the transportation problem. The second stage involved estimating the cost of the inputs into the model.

The project required a comparison of the total cost of achieving a completed satellite in geosynchronous orbit using two distinct sequences of production. The generalized model had to be adjusted to accommodate both the chemical propulsion and the electrical propulsion procedures. The overall model illustrated in Section 8.2.1 relates directly to the chemical propulsion alternative. A second model or sub-model was developed to estimate the cost of electrical propulsion from low earth orbit to geosynchronous orbit. The results of the second model were then combined into the first, replacing components that were not relevant to electrical propulsion. Thus, in the overall comparison, similar cost components in the two scenarios were estimated in a common fashion and dissimilar components were estimated through techniques appropriate for each sequence.

The two analytical approaches, the input cost estimating techniques and a comparison of the resultant cost structures of the chemical and electrical sequences are provided in Sections 8.2 through 8.6.

#### 8.2 COST APPROACHES

##### 8.2.1 Transportation Cost Model

One of the most important criteria used in comparing the various transportation scenarios is the cost. A method was developed for computing the cost of transportation of cargo and personnel which would be applicable to all types of vehicles and any scheme for construction and fabrication. This method is referred to as the cost model. The expression for total transportation cost in simplified form is:

$$C_T = a_H m_L + (a_C f_C + (1 - f_C) a_T) m_G + (b_G f_{P,G} + b_L) N_P + C_O \quad (8.1)$$

where:

- $C_T$  = total cost of transportation per satellite (\$)
- $a_H$  = unit transportation cost for the HLLV (\$/Kg)
- $m_L$  = mass of cargo transported from earth to LEO (Kg)
- $a_C$  = unit transportation cost for the COTV (\$/Kg)
- $f_C$  = fraction of orbital transfer by the COTV
- $a_T$  = unit transportation cost for the tug (\$/Kg)
- $m_G$  = mass of cargo transported from LEO to GEO
- $b_G$  = POTV flight cost (\$/man trip)
- $f_{P,G}$  = fraction of construction and support personnel in GEO
- $b_L$  = PLV flight cost (\$/man trip)
- $N_P$  = total number of man trips per satellite
- $C_O$  = other costs (\$)

The first two terms represent the cost of transporting the cargo (satellite and construction, fabrication, and support equipment) from earth to LEO and from LEO to GEO respectively, the third term gives the cost of transporting personnel, and the last term includes any other transportation costs not accounted for elsewhere.

Note that the transfer of cargo from LEO to GEO may be done by two different types of vehicles. This flexibility is incorporated in the model so that the option of partial assembly of the satellite in LEO can be considered. The transport of a partially assembled structure may require a vehicle (tug) having different characteristics than the vehicle (COTV) which transports cargo in a higher density configuration due to limitations on acceleration the structure can withstand safely.

The unit transportation costs for the HLLV, COTV, and tug may be computed from:

$$a = (C_V/L + f_{P,G} C_{PMP} + C_{TA} + C_{ET})/m_{PL} + C_{DEV} \quad (8.2)$$

where:

$C_V$  = cost of one vehicle (\$)
   
 $L$  = vehicle lifetime (trips)
   
 $f_{PL}$  = propellant loss factor
   
 $c_p$  = propellant unit cost (\$/Kg)
   
 $m_p$  = mass of propellant per flight (Kg)
   
 $C_{TA}$  = turnaround cost (\$)
   
 $C_{ET}$  = cost of expendable tanks (\$)
   
 $m_{PL}$  = payload of vehicle (Kg)
   
 $C_{DEV}$  = development cost allocated to one flight

(\$)

The masses of cargo which must be transported by the launch and orbital transfer vehicles are computed from:

$$m_G = m_S + m_{B,G} \quad (8.3)$$

and

$$m_L \text{ scf} 2R m_G + m_{B,L} + N_C m_{V,C} + N_T m_{V,T} + T_C (f_{PL,C} m_{p,C} + m_{ET,C}) + T_T (f_{PL,T} m_{p,T} + m_{ET,T}) \quad (8.4)$$

where:

$m_S$  = mass of satellite (Kg)
   
 $m_{B,G}$  = mass of support and construction equipment in GEO (Kg)
   
 $m_{B,L}$  = mass of support and construction equipment in LEO (Kg)
   
 $m_{V,C}$  = inert vehicle weight (not including expendable tanks) of the COTV (Kg)
   
 $m_{V,T}$  = inert vehicle weight (not including expendable tanks) of the tug (Kg)
   
 $f_{PL,C}$  = propellant loss factor of the COTV
   
 $m_{p,C}$  = mass of propellant per flight of the COTV (Kg)
   
 $m_{ET,C}$  = mass of expendable tanks of the COTV (Kg)
   
 $f_{PL,T}$  = propellant loss factor of the tug
   
 $m_{p,T}$  = mass of propellant per flight of the tug (Kg)
   
 $m_{ET,T}$  = mass of expendable tanks of the tug (Kg)

The number of trips and number of vehicles required for orbital transfer are computed from:

$$T_C = (f_{T,C} m_S + m_{B,G}) / m_{PL,C} \quad (8.5)$$

$$N_C = T_C / L_C \quad (8.6)$$

$$T_T = (1 - f_{T,C}) m_S / m_{PL,T} \quad (8.7)$$

and

$$N_T = T_T / L_T \quad (8.8)$$

where:

$T_C$  = number of trips per satellite for the COTV
   
 $f_{T,C}$  = fraction of orbital transfer by the COTV
   
 $m_{PL,C}$  = payload of the COTV (Kg)
   
 $N_C$  = number of COTV's required per satellite
   
 $L_C$  = lifetime of a COTV (trips)
   
 $T_T$  = number of trips per satellite for the tug
   
 $m_{PL,T}$  = payload of the tug (Kg)
   
 $N_T$  = number of tugs required per satellite
   
 $L_T$  = lifetime of a tug (trips)

An examination of the equations listed above indicates that there are nineteen parameters which must be specified before the total transportation cost can be computed. They are  $a_H, a_C, m_{PL,C}, m_{V,C}, (f_{PL,C} m_{p,C} + m_{ET,C}), L_C, a_T, m_{PL,T}, m_{V,T}, (f_{PL,T} m_{p,T} + m_{ET,T}), L_T, b_L, b_G, m_{B,G}, m_{B,L}, f_{T,C}, f_{p,G}, N_p,$  and  $C_D$ . In addition, the mass of the satellite must be specified. The calculations are then carried out in the following order. Equations (8.5) and (8.7) are used to determine the number of trips for the COTV and tug. The number of orbital transfer vehicles required may then be calculated from equations (8.6) and (8.8). The masses of cargo to be transported are calculated from equations (8.3) and (8.4). The total transportation cost is then calculated from equation (8.1).

The computation of total cost is relatively simple and may be done by hand calculation. If a large number of cases are to be analysed, the use of a digital computer is preferable. A statement listing and output of the cost model is given in Appendix H.

### 8.2.2 Cost Estimating Methodology for Electrical Propulsion

Data, either technical or financial, are not readily available for estimating the cost of large scale electrical propulsion. The current state-of-the-art provides little basis for costing a transport system accurately using electrical thrusters. The technical requirements for such a system generally are known, however, and do provide a basis for modeling the component requirements of a LEO to GEO movement of the SPS.

The physical model developed for electrical propulsion was illustrated in Section 5.5.1.1. The model required cost inputs for engines, tanks, propellant, and solar cells. The procedures for estimating the cost inputs varied, depending on the nature of the component involved. Several estimating techniques were utilized in

all cases, except for the solar cells, and what appeared to be the best estimate was selected for inclusion in the model.

The cost estimates for engines and tankage were made with the use of a series of Cost Estimating Relationships (CER's) developed for NASA (Ref. 8-3 and 8-4). The process of estimating cost parameters with use of CER's is a standard procedure when the item to be costed is not commercial production or when future technology is in the estimate. The CER is essentially a least squares regression technique using historical data defined in terms of technologically related components. The estimate derived from the application of appropriate CER's was adjusted for complexity through the use of a complexity factor developed in the cited references. All estimates were adjusted to a base of

The cost for fuels were derived from NASA-JSC estimates where such data were available. The cost per pound of ammonia was obtained from commercial producers of the product. The cost for argon was based on the price paid for the item by organizations using this material in currently ongoing research efforts. The costs assigned to both ammonia and argon may be high compared to a future price which would be predicated on large volume production.

The NASA-JSC estimate of \$500/KW for solar cells was applied in the model. No explicit learning curve was applied to adjust any of the estimates. In the use of CER's, some implicit learning curve is present, but unspecified, because of the use of historical data. The NASA-JSC estimate for solar cells currently is based on a 70% learning curve.

The cost parameters estimated for use in the model are as follows:

**Engines:**

Resistojet.....\$50,000 TFU  
 Arc-Jet.....\$41,000 TFU  
 MPD-Argon.....\$41,000 TFU

**Tanks:**

LH<sub>2</sub> 10<sup>6</sup> lbs of fuel....\$30 million TFU  
 NH<sub>3</sub> 10<sup>6</sup> lbs of fuel....\$12 million TFU  
 Argon 10<sup>6</sup> lbs of fuel....\$12 million TFU

**Fuel:**

LH<sub>2</sub> .....\$3/lb  
 NH<sub>3</sub> .....\$.10/lb  
 Argon .....\$2.84/lb

**Solar Cells:**

Solar Cells:.....\$500/KW

Only theoretical first unit costs were utilized in the model. Design, Development, Testing & Evaluation (DDT&E) costs were not estimated and, hence, are not allocated in the model. DDT&E cost could be estimated with appropriate CER's.

**8.3 APPLICATIONS OF THE TRANSPORTATION COST MODEL.**

The cost model discussed in Section 8.2.1 was developed for the purpose of estimating the total cost of transportation, determining the effect of various parameters on the cost, and comparing the costs of various transportation scenarios. It must be stressed at the outset that all cost data used in the following calculations are approximate. The data for the HLLV are extrapolations of the characteristics of current launch vehicles and are expected to be reasonably accurate. Cost data for the COTV's (particularly if electric propulsion is used) and for fabrication techniques and equipment are much less reliable (since there is little or no experience on which to base these data). They may prove to be off by a factor of two or more. Nevertheless, it may be argued that performing calculations based on questionable data is justified if the accuracy of the input data can be estimated and the risks associated with drawing conclusions based on the calculations are recognized. As better data become available, the calculations may be updated.

### 8.3.1 Baseline Data and Total Transportation Cost

A "baseline" estimate of the total cost of transportation was computed based on the following assumptions.

- a. The Column/Cable type of SSPS having a mass of 81813 m.t. is used.
- b. Chemical propulsion is used for all transportation.
- c. All assembly is performed in geosynchronous orbit.
- d. Personnel are transferred from LEO to GEO in capsules carried by the COTV.

The baseline data, taken from the JSC Executive Summary (Ref. 8-1), are given in Table 8-1. Note that only 13 parameters are listed since complete assembly in GEO eliminates the need for the tug and its characteristics are not used in the calculations. The results of the baseline calculations are given in Table 8-2. It is apparent that the cost of transportation of cargo is much larger than that of personnel transport and that the operation of the heavy lift launch vehicles is the largest single item.

As discussed earlier, it is important to have some estimate of the accuracy of  $C_T$ . This depends on the accuracy of each of the parameters used to calculate  $C_T$ . The method (Table 8-2) used here may be summarized as follows. Let:

$$y = f(X_1, X_2, \dots, X_N)$$

be a function of  $N$  independent variables. Then:

$$\Delta y = \left( \sum_{i=1}^n \left[ \left( \frac{\partial y}{\partial X_i} \right) \Delta X_i \right]^2 \right)^{1/2} \quad (8.9)$$

gives the probable error in  $y$  caused by errors,  $\Delta X_i$ , in the parameters used to calculate  $y$ . In our case  $C_T$  corresponds to  $y$  and the thirteen parameters in Table 8-1 correspond to the  $X_i$ 's.

The difficulty which remains is estimating the maximum errors which might be expected in each parameter. The masses of propellant, expendable tanks, and the orbital transport vehicle may be calculated from orbital mechanics relations and design equations and should be accurate to  $\pm 10\%$ . The COTV lifetime is much less predictable and may be in error by 50%. The unit cost for the HLLV is based on more

advanced existing technology than that for the COTV, POTV, and PLV. An accuracy estimate of 25% was assigned to  $a_H$  and  $a_C$ ,  $b_L$ , and  $b_G$  may be assumed to be in error by 50%. The mass of support and construction equipment and the number of personnel trips required may be off by a factor of 2. Based on these assumed errors in the input parameters, equation 8-9 is used with equations 8.1 and 8.3-8.8 to calculate  $\Delta C_T$ . The result is  $\Delta C_T = 3.03$  or the probable error in  $C_T$  is 24%.

The accuracy analysis is certainly not precise since the accuracies of the input parameters are estimates. It does strongly indicate, however, that even though some of the input parameters may be off by a factor of 2, the accuracy of  $C_T$  will be much better than this. This results from the fact that the dominant terms in the cost analysis are those which are known with greatest accuracy.

### 8.3.2 Sensitivity Analysis

An analysis was performed to determine which parameters have the greatest effect on the total transportation cost. This was done by using the baseline cost as a reference and calculating the sensitivity which is defined as the percent change in  $C_T$  caused by a 1% change in an individual parameter. The results are given in Table 8-3 for those parameters which may be considered independent.<sup>1</sup> This again points out the dominance of cargo transport and shows that the transport of personnel and the number of personnel required are much less important in their effect on  $C_T$ .

### 8.3.3 The Effect of Various Changes on Transportation Costs

Several areas were investigated to determine whether significant savings in transportation costs might be realized. In each case the economic effect of some change in the transportation scheme was calculated relative to the baseline cost. Each of these areas is discussed separately. It should be emphasized that all discussion in this section is restricted to chemical propulsion.

<sup>1</sup>Parameters such as  $m_{V,C}$ ,  $m_{PL,C}$ , and  $(f_{PL,C} m_{PC} + m_{ET,C})$  are not independently variable and are analyzed separately.

Table 3-1 BASELINE DATA

Parameter	Value
$a_H$	32. \$/Kg
$a_C$	40. \$/Kg
$m_{PL,C}$	250 m.t.
$m_{V,C}$	26 m.t.
$(f_{PL,C} m_{P,C} + m_{ET,C})$	484 m.t.
$L_C$	30 trips
$b_L$	\$200,000/man trip
$b_G$	\$65,000/man trip
$m_{B,G}$	9422 m.t.
$m_{B,L}$	352 m.t.
$f_{P,G}$	.73
$N_P$	777.
$C_0$	0

Table 8-2 BASELINE TRANSPORTATION COST ESTIMATE

	\$B	% of Total
Cargo		
Earth to LEO	8.60	69.1
LEO to GEO	3.65	29.4
Personnel		
Earth to LEO	.15	1.2
LEO to GEO	.04	.3
Other Cost	Neg	---
<b>TOTAL</b>	<b>12.44</b>	<b>100.0</b>

Table 8-3 SENSITIVITY OF INDEPENDENT PARAMETERS

Parameter	Sensitivity
$a_H$	.69
$a_C$	.29
$L_C$	.0008
$b_L$	.0124
$b_G$	.003
$N_P$	.015

### 8.3.3.1 PARTIAL ASSEMBLY IN LEO.

Partial assembly in LEO has the effect of lowering the total weight which must be transported to GEO. The effect of this change on total transportation cost is estimated based on the following assumptions.

a. The fractional distribution of personnel and construction and support equipment between LEO and GEO varies linearly with the percent of assembly done in LEO.

b. The orbital transfer vehicle used to move the partially assembled structure has the same characteristics as the COTV used in the baseline study.

Total transportation cost is calculated using the transportation cost model. The results are given in Table 8-4. The maximum estimated potential saving is quite significant. From a practical point of view it does not appear that a large percentage of the fabrication can be done in LEO if chemical propulsion is used for orbital transfer so the potential saving is probably less than 1.0% of the total transportation cost. It is not clear whether any saving can be achieved since a partially assembled structure will not be able to withstand large accelerations and a special vehicle will have to be designed for transporting these structures. The cost per Kg for these vehicles may be higher than that of the COTV used to transport high density cargo.

A definite conclusion cannot be drawn at this point since further detailed study of the fabrication techniques and the characteristics of orbital transfer vehicles may alter the results presented here. One may tentatively conclude, however, that partial assembly in LEO will not offer major economic benefits and may in fact prove to be more costly than complete assembly in GEO.

### 8.3.3.2 EQUATORIAL LAUNCH

The baseline cost estimate assumes a Cape Kennedy launch. An equatorial launch would eliminate the need for a plane change in geosynchronous orbit and the COTV would require significantly less propellant with a resulting saving in transportation costs. The amount of propellant required is given in Section 4.2 for the range of launch latitudes between 0 and 28.5°.

There may, however, be added costs associated with the launch from a site distant from the continental

United States. These costs have not been estimated. The transportation cost model is used to calculate  $C_T$  for various launch latitudes taking into account the effects of latitude on the mass of propellant but does not include these marginal ground costs. Results are shown in Figure 8-1. It appears that a significant cost saving will result from a launch site near the equator and this option should be seriously considered.

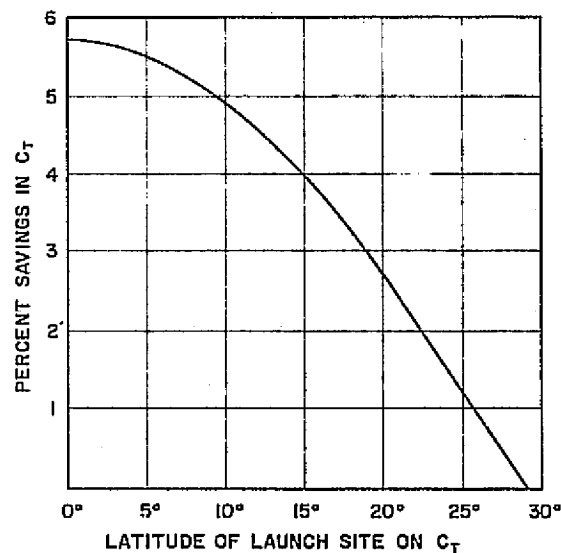


FIGURE 8-1 EFFECT OF LAUNCH SITE LATITUDE ON  $C_T$  (MARGINAL GROUND COSTS NOT ACCOUNTED FOR)

### 8.3.3.3 TRANSFER OF PERSONNEL BY COTV

The possibility of transporting personnel using the cargo orbital transfer vehicle has been discussed in Section 6.4. The cost was found to be approximately \$65,000 per man flight. This cost is identical to that using the POTV recommended in Ref. 8-1. The decision of which method to use should, therefore, be based on other considerations.

### 8.3.3.4 REUSABILITY OF THE HLLV PAYLOAD SHROUD

Estimates of the cost of the HLLV payload shroud for both a reusable and expendable case were made in Section 4.3.4. Use of these numbers in the transportation cost model indicates that  $C_T$  could be as much as

Table 8-4 EFFECT OF PARTIAL ASSEMBLY IN LEO ON TOTAL TRANSPORTATION COST

% of Construction in LEO	$f_{p,G}$	$m_{B,L}$ m.t.	$m_{B,G}$ m.t.	$C_T$ \$B	% Saving
0	.73	352	9422	12.44	0
10	.66	1294	8480	12.39	.4
25	.56	2708	7066	12.11	2.6
50	.36	5063	4711	11.79	5.2
100	0	9744	0	11.14	10.4

8% higher if the shroud is not reusable. It appears that the shroud should either be dedicated to some use in LEO (e.g., parts of the support system) or should be returned and reused. There are costs associated with retrieval and reuse which have not been accounted for in the comparison discussed here so the actual saving will be less than 8%. It is likely, however, that the saving will be significant and this area should receive further study.

### 8.3.4 Synthesis

An analysis of the cost of transportation shows clearly that the driver is the HLLV cost. A substantial effort should be dedicated to economically optimizing this phase of the transportation. Consideration of an equatorial versus a Cape Kennedy launch is only one area deserving further study. An application of equation 8.2 to the HLLV indicates two other important areas. Reusability of the shroud should be strongly considered as discussed in Section 8.3.3.4. The area which will have the greatest impact, however, is the turnaround cost. This is the dominant term in equation 8.2 and has not yet been carefully studied. A detailed investigation of the entire scenario of launch, retrieval, refurbishment, etc., will be required to determine the relative costs of the different types of HLLV's proposed in Ref. 8-3. No candidate should be eliminated from further consideration until such a study has been completed.

## 8.4 ELECTRIC PROPULSION

The total cost analysis of the electrical propulsion system was accomplished within the following framework.

a. Four engines were analyzed as candidates for the LEO to GEO orbit. The characteristics of the engines were provided in Chapter 5.

b. Two launch sites were compared, the one from Cape Kennedy and the other from an unspecified equatorial plane site.

c. Two decay rates for solar cells were included, one approximately e-T/300 and the other approximately e-T/120.

d. Two thrust conditions were applied, a constant thrust condition with variable orbit times and a variable thrust condition with a resultant determined orbit time.

e. Cost elements involved in the use of chemical propulsion for transfer of cargo and personnel were drawn from the estimates made in the chemical propulsion analysis. Per unit costs in this respect are identical in the two procedures so that total cost differentials are indicative of differences in weight requirements.

f. No consideration was given to such items as engine and tankage refurbishment and reusability, turnaround times for chemical propulsion vehicles, the allocation of DDT&E costs, and the probability of damage by collision with space junk.

The cost analysis using the 300 day decay rate was eliminated from consideration. The radiation effects on solar cells appeared to be extreme enough to make this particular decay rate unrealistic.

Tables 8-5 through 8-8 give the total transportation costs for the LEO to GEO movement of the satellite for each of the four candidate engines under constant thrust conditions and variable orbit times. The minimum costs periods range between 30 to 60 days orbit time. The Resistojet engine is associated with the highest transportation cost. The two Arc-jets and the MPD-Argon engines are all competitive in the lower orbit periods. The cost data are provided in comparative form in Figure 8-2.

The component cost structure for the variable T/W analysis is given in Figure 8-3. The relationships between solar cell requirements and the cost of transporting additional weight are evident in the comparative data. The engines remain in essentially the same competitive position as in the first analysis. However, the component cost relationships provide the basis for suggesting parameter changes that would affect the total cost for each engine.

The cost of solar cells constitutes a small proportion of total transport costs for the Resistojet engine. Reduction in tank and engine costs would make this particular engine a stronger candidate for use in the project. The MPD engine has the largest requirement in terms

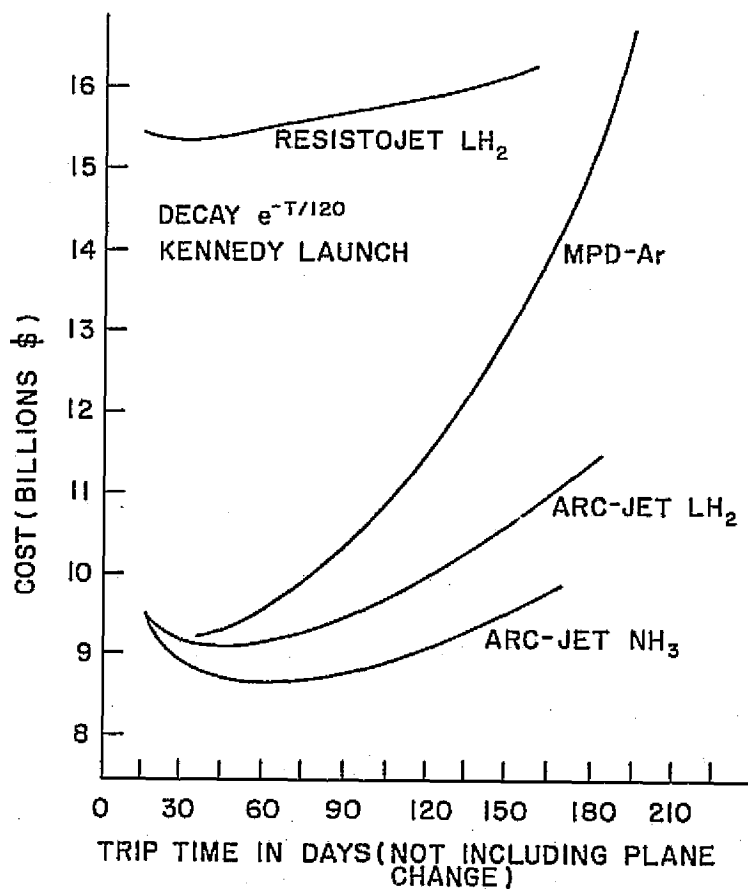


FIGURE 8-2 COST OF TRANSPORTATION

Table 8-5 TRANSPORTATION TIME-COST RELATIONSHIP FOR VARIABLE ORBIT TIMES  
RESISTOJET LH<sub>2</sub>

DAYS	COST (Billions \$)
14	15.544
27	15.476
40	15.535
53	15.583
66	15.653
80	15.754
93	15.831
106	15.910
119	16.028
133	16.148
146	16.272
159	16.424
Decay ~ e - T/120	
Kennedy Launch	
T/W = 10 <sup>-4</sup>	
Constant Thrust	

Table 8-6 TRANSPORTATION TIME-COST RELATIONSHIP FOR VARIABLE ORBIT  
TIMES ARC-JET LH<sub>2</sub>

DAYS	COST (Billions \$)
16	9.510
32	9.182
47	9.128
62	9.202
77	9.363
92	9.544
108	9.816
123	10.068
137	10.355
153	10.704
169	11.136
184	11.569
Decay ~ e - T/120	
Kennedy Launch	
T/W = 10 <sup>-4</sup>	
Constant Thrust	

Table 8-7 TRANSPORTATION TIME-COST RELATIONSHIP FOR VARIABLE ORBIT TIMES ARC-JET NH<sub>3</sub>

DAYS	COST (Billions \$)
15	9.560
30	8.916
44	8.737
57	8.708
71	8.748
86	8.861
100	8.963
114	9.090
128	9.241
142	9.412
156	9.666
171	9.902

Decay ~ e - T/120  
Kennedy Launch  
T/W = 10<sup>-4</sup>  
Constant Thrust

Table 8-8 TRANSPORTATION TIME-COST RELATIONSHIP FOR VARIABLE ORBIT TIMES NPD ARGON

DAYS	COST (Billions \$)
34	9.261
49	9.350
65	9.642
81	10.041
97	10.534
114	11.348
129	12.061
145	12.893
161	13.878
178	16.237
194	16.830
Decay $\sim e^{-T/120}$	
Kennedy Launch	
$T/W = 10^{-4}$	
Constant Thrust	

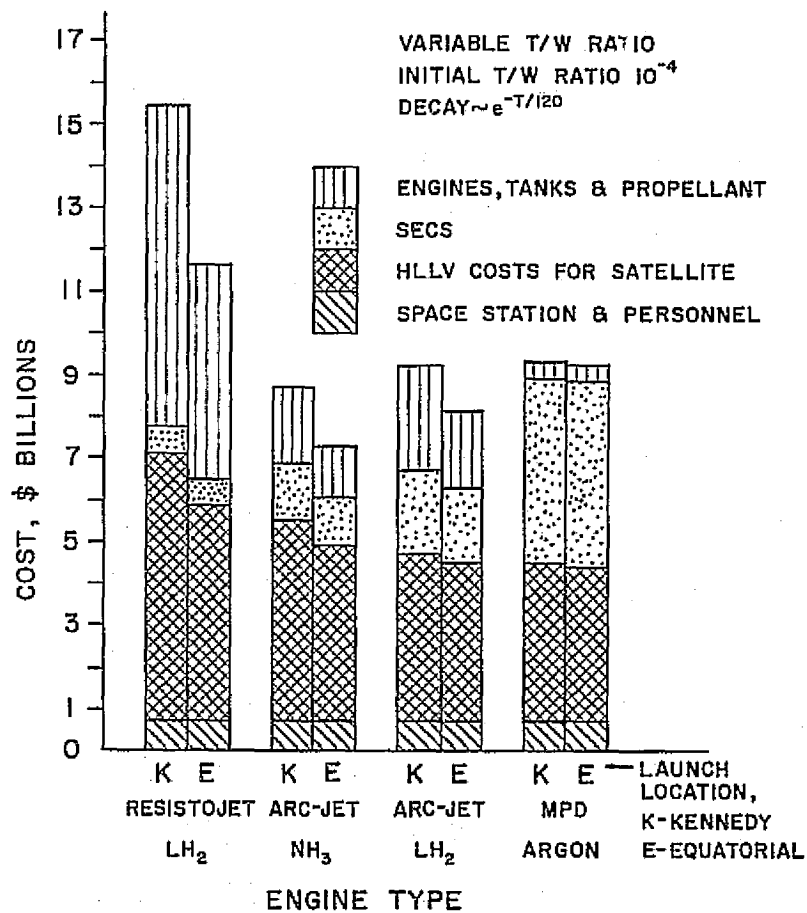


FIGURE 8-3 TRANSPORTATION COST COMPONENTS

of SECS cost. Improvements in the satellite that would reduce solar cell decay (in the case of the MPD) would reduce both the SECS cost and the cost of HLLV transport, since less weight would be required to provide a transport system.

The major cost drivers for the electrical propulsion systems are indicated by the elasticity measures given in Table 8-9. These measures are defined as the relative change in total transport cost related to a 1% change in the indicated variable. The measures are pure numbers that can be readily compared among diverse variables.

The principle drivers are those variables which determine the time required to transport the satellite and the requirement for solar cell usage during the trip.

In order to compare the electrical propulsion system with the chemical propulsion cost estimates, a single engine and its related transportation cost was selected. The Arc-jet engine, using LH<sub>2</sub> as a fuel, was chosen as a prime candidate. The total transportation cost with construction of the satellite in LEO is given in Table 8-10. The cost estimates for both the 28° launch and the equatorial launch are provided. A transport cost savings of approximately 11.5% could be ob-

Table 8-9 ELASTICITY MEASURES FOR ELECTRICAL PROPULSION

VARIABLE	ENGINES*			
	RESISTOJET LH <sub>2</sub>	ARC-JET LH <sub>2</sub>	ARC-JET NH <sub>3</sub>	MPD Argon
Engine Cost	.001	.03	.03	.02
Fuel Cost	.04	.02	.001	.005
Tank Cost	.46	.22	.17	.02
Specific Impulse	.98	.59	.15	.12
Thrust	.14	.03	.03	1.58
T/W	.00	.03	.01	.03
Kw/Lb of Thrust	.06	.29	.22	.73
Conversion Efficiency	.06	.33	.22	.65
Mass Fraction	.60	.44	.48	.07
Propellant Glow Fraction	.04	.02	.001	.005
Delta V	1.0	.45	.62	1.71
Degradation Time	.01	.40	.26	.86

\*Initial T/W of  $10^{-4}$ , decay  $\sim e^{-T/120}$

Table 8-10 TOTAL TRANSPORTATION COST-ELECTRICAL PROPULSION

COST COMPONENT	LAUNCH POSITION	
	KENNEDY	EQUATORIAL
Material-Earth to LEO	4.42	3.88
Material & Satellite LEO to GEO	4.54	4.01
Personnel-Earth to LEO	.21	.21
TOTAL	9.18	8.11

\*Using the Arc-Jet LH<sub>2</sub> engine, T/W of  $10^{-4}$  and decay  $\sim e^{-T/120}$

tained in equatorial launch plane since the procedure would require no time for plane changes.

The total cost estimates for the electrical propulsion scenario appear in Table 8-11. The cost savings between the two sites ranges from 6.5% to 8.4% depending upon the time assigned for the cost of capital under the Kennedy launch conditions. The cost of capital could be reduced, thus lowering the total cost of the Kennedy launch and reducing the Kennedy-equatorial differential, by making the plane and altitude changes at the same time during the orbiting out process. However, the procedure would require more time in the Van Allen Belt which may lead to increased degradation of solar cells. Since the SECS costs are drivers in this system, the savings obtained in reduced capital requirements could be offset by increased costs of solar cells. Some optimal relationships probably exist between the two conditions and should be pursued through further analysis.

## **8.5 ECONOMIC COMPARISONS OF SATELLITE DELIVERY SCHEMES**

### **8.5.1 The Effect of Delivery Delays on the Time Value of Money**

The cost estimates of the alternative delivery schemes given in sections 8.3 and 8.4 include the value of all the resources necessary to deliver one SPS unit to an online mode in geosynchronous orbit. What has yet to be considered is the effect of the potential delivery delay implicit in the LEO/Electric construction approach. This potential delay has two adverse effects on the economic desirability of the SPS system. First, the delay creates incremental costs to construction in the form of interest charges on idle SPS units during their delivery phase. Interest charges must be added to the present value of construction costs whenever one mode of delivery results in delays not experienced by alternative delivery modes.

Table 8-12 gives the interest charges (as proportions) for various delays at alternative interest rates. These alternative interest rates are to be interpreted as the opportunity costs of funds committed to the SPS system. These values are the rates that funds used in the SPS system could have earned in ventures of equal

duration and similar risk had they not been used for the SPS system. The terms "Cost of Capital" and "Cost of Money" have been used to designate these charges. These charges may also be thought of as the minimum rate of return required to justify the commitment of funds to a particular program, or, simply, "The Required Rate of Return" (RRR). Thus, if the RRR is fifteen percent and a delivery delay of four months is anticipated, an additional 4.18 percent in interest charges should be added to the online costs of the delayed SPS delivery system--in this case the LEO/Electrical construction alternative. If the delay could be reduced to two months, the additional charges would amount to 2.12 percent of the otherwise completed cost of an SPS unit.

The second effect a delayed installation has on the economic desirability of the project is the equal time lag in realizing the revenue the SPS could be generating. In other words, a delayed installation not only adds interest charges to the cost of the satellite, but reduces in an equivalent manner (assuming the RRR and internal rate of return (IRR) are identical) the present value of the net cash flow (net of operating, maintenance, and other similar expenses--but not depreciation) that the SPS would generate over its assumed economic life of 30 years. Returning to the previous examples, a four (4) month delay at 15 percent interest would reduce the present value of the net cash flow of an SPS another 4.18 percent. Assuming the cost of a completed, online SPS via chemical propulsion of \$30 billion, the delays mentioned above would create a differential between the two approaches of \$2.5 billion and \$1.3 billion respectively.

For purposes of this study it is assumed that the only difference between the SPS units is the cost of transportation (including any ancillary considerations necessitated by the different transportation modes). The LEO/Electric alternative would have to be, depending upon the delay, \$1.3-\$2.5 billion cheaper than the GEO/Chemical approach just to breakeven with it. From section 8.3 and 8.4 the cost differential is found to be approximately \$3.25 billion, for a Kennedy launch and \$3.59 billion for an equatorial launch. As explained in earlier sections, the time delay using the electrical transportation mode and a Kennedy launch ranges from a low of 90 days to a high of 120 days. Using a 15 percent rate of discount, these delays translate into \$1.6 and \$2.1 billion respectively.

Table 8-11 TOTAL COSTS - ELECTRICAL PROPULSION

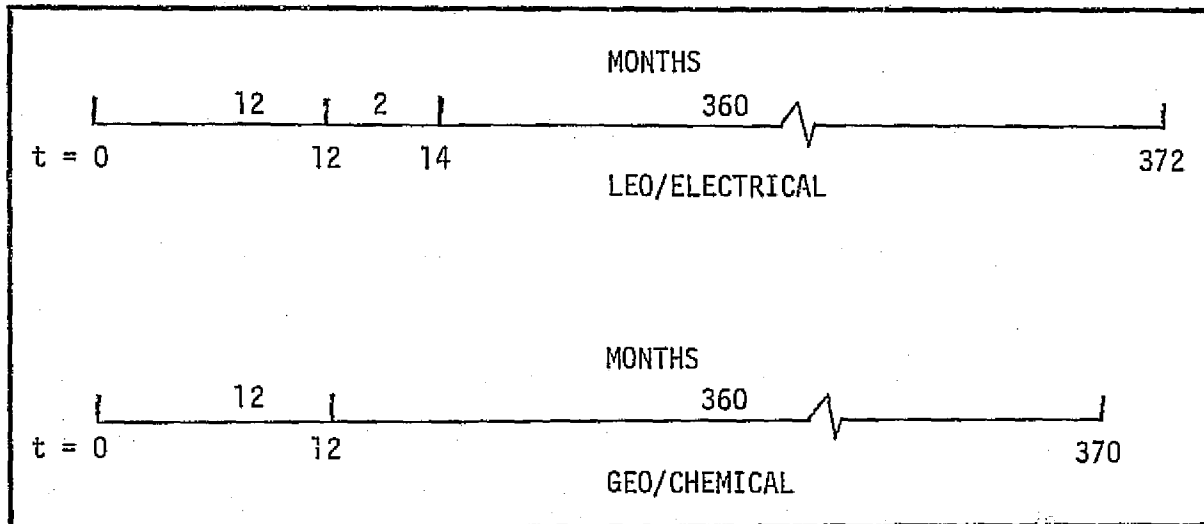
ITEM	LAUNCH POSITION	
	KENNEDY	EQUATORIAL
Satellite	10.58	10.58
Rectenna	4.23	4.23
Transportation	<u>9.18</u>	<u>8.11</u>
Subtotal	23.99	22.92
Interest Interest Adjustment <sup>2</sup>		
60 days		.98
90 days	1.58	
120 days	<u>2.10</u>	
TOTAL COST	25.57    26.09	23.90

<sup>1</sup>Using the Arc-Jet LH<sub>2</sub> engine, T/W of 10<sup>-4</sup> and Decay

<sup>2</sup>Appropriate interest adjustment depends on time estimate of plane change in orbit from LEO to GEO.

Table 8-12 INTEREST ADJUSTMENT FACTORS FOR DELIVERY DELAYS OF SPS UNITS

MONTHS DELAY (t)	INTEREST RATES					
	.075	.100	.120	.150	.180	.200
1	.0058	.0075	.0088	.0109	.0124	.0133
2	.0115	.0149	.0175	.0212	.0245	.0265
3	.0172	.0222	.0262	.0315	.0365	.0394
4	.0228	.0295	.0247	.0410	.0484	.0521
5	.0285	.0368	.0431	.0519	.0600	.0646
6	.0341	.0440	.0515	.0619	.0715	.0769



NOTE: All PV's are discounted back to time "0". Costs, other than interest charges, and revenues of alternatives are assumed equal.

## FIGURE 8-4 TWO COMPARATIVE APPROACHES

Assuming the cost differential between the "Truss" (Electrical) and "Columnal" (Chemical) satellites to be \$.53 billion (JSC:11443) the range of cost difference between the transportation modes reduces to \$1.12 billion to \$.60 billion. Assuming only a 60 day delay using an equatorial launch and a \$.53 billion satellite cost difference, the net savings of the electrical approach is reduced by \$1.04 billion to \$.202 billion after taking into consideration the time value of money factor. It is conceivable that after allowing for repair costs due to collision damage and other immeasurables associated with the electrical approach, the costs of chemical transportation could be considerably below that of electrical. Table 8-13 summarizes the cost differentials. It must be recalled that these cost estimates reflect the baseline approach of the JSC study. Using alternative approaches suggested in previous chapters herein, the cost estimates could change significantly in at least their absolute magnitudes, if not their relative position as well. It should be further noted that as the online costs of the SPS are reduced by technological advances or other reasons the "advantage" of faster delivery erodes. Likewise, the more profitable the SPS (higher IRR and RRR) the greater the advantage of a rapid delivery system. This conclusion leads to the not-so-startling

implication that unprofitable (costly) programs should be delayed and profitable programs accelerated. For further discussion on this point see Section 8.6.

### 8.5.2 The Effect of the Time Value of Money on the Cost of Generated Electricity

If a system, such as the SPS, is to be self-supporting, it must be able to generate sufficient revenues net of all operating expenses to cover its full in-place cost including a return to invested capital sufficient to justify the use of the funds designated for this purpose. More simply put, the net cash flow must be sufficient to return both principle and interest to the suppliers of these funds. The RRR is the rate of interest that must be earned since any lesser rate would imply that the funds could have been employed more beneficially elsewhere.

Table 8-14 shows how alternative required rates of return affect the annual capital charges for a 10 GW SPS with an economic life of 30 years. For comparison purposes these charges are also converted into mills per kilowatt hour. These factors are given on a per billion dollar cost of one SPS unit. Thus, if the cost of

Table 8-13 BASELINE COST COMPARISONS OF ALTERNATIVE TRANSPORTATION MODES

ITEM	CHEMICAL		ELECTRICAL	
	KENNEDY	EQUATORIAL	KENNEDY	EQUATORIAL
Satellite	\$10.05 B	\$10.05 B	\$10.58 B	\$10.58 B
Rectenna	4.23	4.23	4.23	4.23
Transportation	<u>12.43</u>	<u>11.70</u>	<u>9.18</u>	<u>8.11</u>
Subtotal	\$26.71	\$25.98	\$23.99	\$22.92
Interest Adj. (60)				1.04
(90)			1.60	
(120)			<u>2.10</u>	
TOTAL COST	\$26.71 B	\$25.98 B	\$25.59	\$26.11 B
			\$26.11 B	\$23.96

Table 8-14 INTEREST FACTORS FOR CAPITAL CHARGES IN ANNUAL PAYMENTS AND MILLS PER KILOWATT HOUR PER BILLION DOLLAR COST OF COMPLETED SPS

REQUIRED RETURN	ANNUAL PAYMENT	MILLS PER KILOWATT HOUR <sup>1</sup>
.075	.0847	1.0510
.100	.1061	1.3165
.120	.1241	1.5399
.150	.1523	1.8898
.180	.1813	2.2497
.200	.2008	2.4916

<sup>1</sup>Assumes .92 Utilization Factor

one unit was \$30 billion, the annual capital charges would be (at 15 percent) \$4.569 billion or 56.69 mills per kilowatt hour. If the RRR were 12 or 18 percent, the capital charges per kilowatt hour would be 46.2 and 67.49 mills respectively. It should be noticed that if the cost of the satellite could be reduced to \$20 billion, as some estimates indicate, the savings could be wiped out by a change in the RRR from 12 to 18 percent. The mills per kwh would, at 12 percent, fall to 30.8 but would increase to 45.0 as a result of the increase in the RRR to 18 percent, or approximately the amount of the original charge (46.2). A cost saving of one-third could be negated by an increase of six percentage points in the RRR. This hypothetical illustration was given solely to indicate the magnitude of the effect of interest charges on a multiyear lifetime project. This illustration does not mean to imply that cost reductions are necessarily accompanied by increases in the discount rate. It should also be noted that the factors given in Table 8-14 will not change appreciably as a result of extending the economic lifetime of an SPS. For example, a 50 year lifetime would, at 15 percent, only change the payment factor from .1523 to .1501. An infinite life would only further reduce this factor to .1500.

### **8.5.3 Comparison of Capital Charge Requirements and Estimates of Future Electrical Charges**

#### **8.5.3.1 EFFECTS OF INTEREST RATES ON ESTIMATES OF FUTURE ELECTRICAL CHARGES**

According to JSC Memo EZ6-76-144, the relative cost of electricity is expected to rise 36 percent from 1976 to 2025. Assuming a cost of 30 mills/kwh in 1976, the equivalent 2025 cost would be 40.8 mills/kwh in 1976 dollars. Abstracting temporarily from operating costs, these figures, together with those given in Table 8-14, indicate that an SPS unit costing \$30 billion could earn an internal rate of return over 30 years of approximately 10 percent. Therefore, if the required rate were 15 percent, the SPS could not be economically justified at an assumed cost of 40.8 mills per kwh for electricity. However, if the cost of an SPS could be reduced to \$20 billion the mills/kwh would be within the assumed 40+ mills/kwh range, again using a 15 percent RRR. (Note: all costs are given in 1975-1976 dollars.)

The appropriate rate of interest that should be charged against the earnings of an SPS is not easily determined. Conceptually it should at least be that rate charged against earth bound power systems in the relevant time frame. Currently this rate is around 12 percent. Additionally, there is strong argument that the SPS RRR should be higher since there are additional elements of risk associated with the SPS not applicable to conventional terrestrial power systems. With regard to these additional elements or risk it should be mentioned that the LEO/Electric and GEO/Chemical approach have different risk characteristics. From Chapters 5 and 6 it should be evident that the former approach is subject to, at least at the present time, greater uncertainty than the latter approach. If this additional risk does exist, then the discount rate should be made correspondingly greater for the LEO/Electric approach. All of the above analysis has assumed identical discount rates for each approach. For purposes of illustration, it can be assumed that if 15 percent is an appropriate RRR for the GEO/Chemical alternative, then perhaps 18 percent could be used as the appropriate RRR for the LEO/Electrical alternative. If these rates did apply, the present value of \$1 per year for 30 years at 15 percent is \$6.57, while at 18 percent it is \$5.52, or a 16 percent difference. This result means that the present value (PV) of the net cash flow (NCF) for the LEO/Electrical approach is 16 percent less than the PV of the NCF associated with the GEO/Chemical approach. This difference is in addition to the interest-cost differential due to the delay in delivery of the SPS unit. Indeed, that differential would now be greater since the interest adjustment applies to the period of delay as well as the net cash flow. Continuing with the illustration involving the 15 and 18 percent rate, there is an approximate 5 percent saving in cost of carrying charges due to the fact the SPS is generating revenue two months earlier. The total saving, therefore, would amount to approximately 26 percent. The illustrations, at this point, are mainly conjectural, since determining the cost of capital of a new venture 20 years in advance is highly tenuous at the very least. They do serve, however, to point up the significant impact that factors such as cost of capital, time delays, and risk have on the economic feasibility of a long term project. Any ultimate decision as to delivery systems must be made with careful attention given to the factors discussed above.

### 8.5.3.2 REGIONAL ELECTRICAL MARKETS AND THE ECONOMIC RATIONALIZATION OF THE SPS UNIT

A current price of 30 mills/kwh was assumed for electricity in the previous section in a preliminary discussion of the economic justification of an SPS unit. The resultant price after allowing for an increase in relative cost of electricity of 36 percent was 40.6 mills/kwh. Whereas this price may be appropriate in some geographic markets it is undoubtedly inappropriate in other such markets. Table 8-15 gives a cross-section comparison of various electrical markets in the USA. From the diversity of charges as evidenced by this table, it would appear that the SPS generated electricity would be marketable in some areas and not in other areas (if the increase in the relative cost of electricity is assumed to be uniform across regional markets). It would make little sense to market SPS electricity in eastern Tennessee or western North Carolina, whereas, New York would represent a more viable market. It would appear that at the present time, the most reasonable cost estimates of an SPS would lie in the \$20-\$30 billion price range with interest rates ranging from 12-18 percent. These ranges would produce a subsequent range of 30.8 to 67.5 mills/kwh that would be required to cover the capital charges of the SPS unit. This range would, according to Table 8-15, clearly be within the price range of such markets as Connecticut, New York, Delaware, and perhaps Georgia. A word of caution is in order with regard to these estimates. The prices are for generation and delivery of electricity to the final customer. Production costs amount to only about 70 percent of the final cost to the customer and it is this latter figure which should be compared with the prices determined above for an SPS unit since surface handling and distribution charges have not been herein considered. This omission is offset by the fact that the figures given for each area are for the lowest rate step for residential service. The average charge would be somewhat higher depending upon the rate schedule and average household use. Ignoring both of these effects implicitly assumes they are completely offsetting. This assumption probably results in a small understatement of the average residential kwh costs of electricity. Residential rates have been used here since they usually are the lowest rates for electrical service. The impact of these assumptions is to conservatively estimate the kwh cost of electricity by the year 2000.

### 8.5.4 Summary

From the preceding analysis it is evident that if SPS unit cost is confined to the \$20-\$30 billion range and the cost of capital lies in the 12-15 percent range, SPS generated electricity could be competitive in the 1995-2025 time frame in at least some major domestic markets (37.8-56.7 mills/kwh). At the existing (1976) cost of capital for electrical utilities (12 percent) the SPS is already competitive with some regional electrical services (30.8-46.2 mills/kwh). These statements presume, of course, the validity of estimates of not only SPS costs but 1995+ cost estimates of alternative sources of electricity. The estimated 36 percent increase in the relative cost of electricity over the next 30 years may be conservative, particularly in light of recent history. Recall also that only the lowest step of residential rates have been used to estimate the year 2000 electrical rates. One conclusion that this analysis produces is that (at least at this time) SPS generated electricity has not been shown to be economically unjustified. Indeed, there exists strong reason to believe that, technology permitting, SPS costs could decline and surface generated electricity could rise to a greater extent than assumed in this analysis.

## 8.6 SATELLITE SCHEDULING

### 8.6.1 The Effects of Scheduling on Payoff and Initial Funding

It will be assumed in the following discussion that (1) the SPS system will generate equivalent cash flows in each of the various scheduling schemes; (2) that the internal rate of return is equal to the required rate of return; (3) that the life of an SPS is 30 years; (4) that the cash flows are net of operating expenses and taxes but not depreciation; and (5) that each scheme allows two years for construction of the first SPS. The only variable will be the rate at which the satellites are brought online. Figure 8-5 identifies the four assumed satellite scheduling schemes. Schedule A is the JSC schedule identified in Reference 8-1. It should be noted that all scheduling schemes identified herein assume "Scenario B"--that of providing 50 percent of the estimated new electrical demand in the 1995-2025 time frame. Schedule B is an accelerated Schedule A. Schedule C is a steady flow schedule of four SPS's per year and Schedule D is the extreme of building all of the 112 SPS's in the first year. The latter

Table 8-15 1975 ELECTRIC RATES AND 2000 PROJECTIONS FOR SELECTED AREAS, USA

AREA	BASIC m/kwh <sup>1</sup>	FUEL ADJ. <sup>1</sup>	TOTAL	2000 EST. m/kwh
1. Alabama	20/11 <sup>2</sup>	6.4	26.4/17.4	35.9/23.7
2. Tennessee	9	10.7	19.7	26.7
3. Georgia	21.6/10	7.8	29.4/17.8	40.0/23.9
4. Texas	16.5/11.5	4.3	20.8/15.8	28.3/21.5
5. Conn.	35.6	3.2	28.8	52.8
6. New York	35.3	17.9	53.2	72.4
7. Ohio	19	8.3	27.3	37.1
8. Delaware	29.1/16.3	13.2	42.3/29.5	57.5/40.1
9. Louisiana	16.7	8.0	24.7	33.6
1973 USA Residential Average 28.3 m/kwh.				

<sup>1</sup>Source: Federal Power Commission, 1975 Electrical Rates, Annual Report.

<sup>2</sup>Figures separated by slash refer to seasonal rates.

schedule is used for illustrative purposes only and should not be considered as a viable alternative.

Table 8-16 summarizes for each schedule at various alternative interest rates the number of years necessary to accomplish two goals. The first goal is to generate sufficient cash flow to fund present and future SPS units. The second goal is to pay back those SPS units already in existence. Two potential objectives of the SPS program might be to reduce either the absolute amount of initial capital (whatever its source) or to minimize the amount of time required to accomplish the above two goals. These goals involve a tradeoff, for reducing one involves an increase in the other. For instance, from Tables 8-16 and 8-17, it can be seen that at 15 percent interest the scheduling scheme that

minimizes the time to pay off is Schedule D, which is also the schedule that maximizes the number of SPS units outstanding at any one time. The tables show that, as a general rule, faster scheduling minimizes the payoff period while maximizing the number of units which must be financed by initial capital.

### 8.6.2 The Effects of Scheduling on Present Value

Table 8-18 indicates that the present values of both cash inflow and cash outflow are greater the faster the units in question are brought online. The net present value (the difference between the PV of cash flows) while always negative, since only the first 1 years are discounted, improves as scheduling is accelerated.

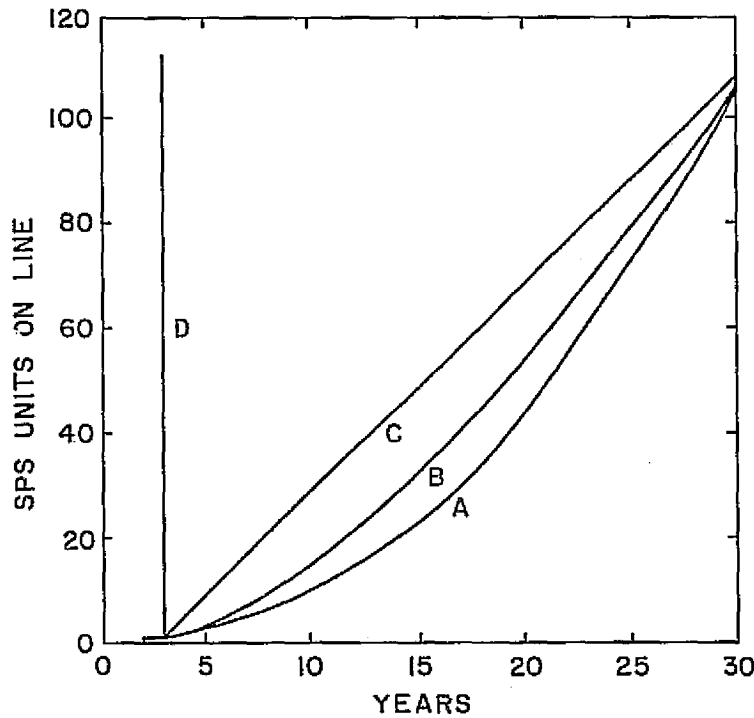


FIGURE 8-5 SCHEDULING SCHEMES FOR SPS SYSTEM

Table 8-16

NUMBER OF YEARS REQUIRED FOR SPS SYSTEM TO COVER ALL CAPITAL CHARGES  
AND BECOME SELF SUPPORTING AT VARIOUS SCHEDULING SCHEMES AND  
INTEREST RATES

SCHEDULE SCHEME	INTEREST RATES					
	.075	.100	.120	.150	.180	.200
A	32	28	24+	-	15+	14
B	30+	25	21+	17+	15+	14
C	25+	20+	18+	15+	13	12
D	14+	13+	11+	9+	8+	8+

<sup>1</sup>For Scheduling Schemes see Figure 8-5.

Table 8-17

MAXIMUM NUMBER OF SPS UNITS OUTSTANDING (UNPAID) FOR  
VARIOUS SCHEDULING SCHEMES AT VARIOUS RATES OF INTEREST

SCHEDULE SCHEME	INTEREST RATES					
	.075	.100	.120	.150	.180	.200
A	23	13	8	5	3	3
B	20	14	11	7	5	5
C	22	17	14	12	9	8
D	103	100	98	95	92	90

Table 8-18

PRESENT VALUES OF CASE INFLOWS AND CASH OUTFLOWS (NET OF OPERATING AND  
MAINTENANCE EXPENSES) OF SPS SYSTEM FOR VARIOUS SCHEDULING SCHEMES  
AND INTEREST RATES EXPRESSED IN REVENUE YEARS

SCHEDULE SCHEME	INTEREST RATES					
	.075	.100	.120	.150	.180	.200
A	231.1 <sup>3</sup> (346.9)	145.0 (192.7)	102.6 (126.8)	63.7 (72.9)	41.6 (45.3)	32.3 (34.3)
B	279.0 (389.3)	178.5 (224.2)	128.1 (151.4)	81.1 (90.1)	53.7 (57.4)	41.8 (43.9)
C	376.3 (479.1)	250.1 (293.2)	185.1 (207.2)	122.6 (131.2)	84.7 (88.3)	67.6 (60.7)
D	1042.2 (1066.4)	783.9 (795.0)	634.1 (144.0)	481.6 (484.9)	375.2 (377.0)	322.2 (323.7)

<sup>1</sup>First 31 Years Only

<sup>2</sup>Assumes Required Rate of Return Equals Internal Rate of Return, i.e.  
no Economic Profit (Loss).

<sup>3</sup>Inflow (Outflow)

These results are not unexpected since the only difference between the alternatives is the time-spacing of the SPS units; hence, those values closer to the present will be of greater magnitude. The relative advantage of the faster schemes is not very significant in any of the cases in terms of the effect on net present value. Figures 8-6 and 8-7 are given to show the relative cash flows of scheduling schemes A and C. The dashed lines represent the annual net cash flow associated with each scheme. The vertical axes are designated both in revenue years and number of SPS units.

### 8.6.3 Satellite Scheduling Summarized

Table 8-19 summarizes those factors of importance which affect scheduling decisions. These considerations assume that the scheduling will not be pursued to such an extent that the market cannot absorb the increase in facilities without resulting in excess capacity. With this constraint in mind, an accelerated scheduling rate will result in: (1) a shorter period in which the system on a cash flow basis becomes self-supporting; (2) higher initial funding requirements (which means more external financing required); (3) higher present values of both cash inflows and outflows; and (4) a greater net present value. Factors VI and VII have not been previously discussed but bear an important part in the scheduling decision. These two factors, as will be seen, are not totally unrelated. Where significant relative price increases of relevant resources pose a potential threat to any program, such as right-of-way for future roads or recreational areas, it might pay to accelerate the program. Accelerated scheduling is economically justified where the sector inflation rate exceeds the alternative cost of the funds required to pursue the program. That is, the savings of faster purchasing exceeds the revenue that could be earned in other endeavors. This phenomenon has characterized the residential construction industry for the past 15 years. Those who have waited to build have actually "lost" money as the cost of housing has risen at a rate almost twice the overall inflation rate.

Whereas anticipated inflation of certain products may suggest speeding up their purchase, anticipated advances in technology suggest a "go slow" process. Technological advancements not only make projects more feasible, they concomitantly reduce the costs of the projects which lead to price reductions where

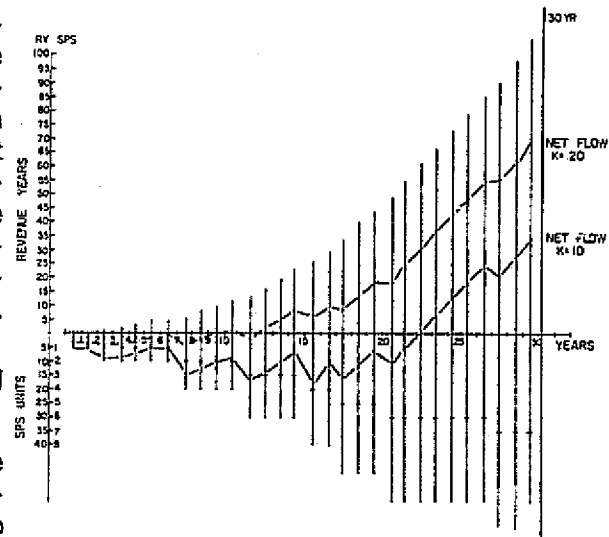


FIGURE 8-6 SCHEDULE A CASH FLOW@20 AND 10 PERCENT INTEREST

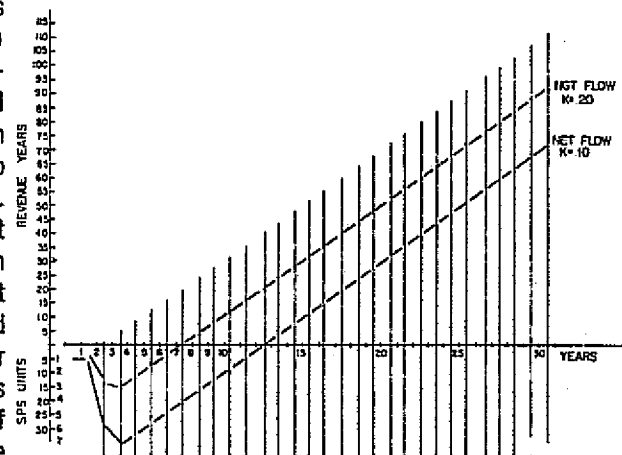


FIGURE 8-7 SCHEDULE C CASH FLOWS@ 20 AND 10 PERCENT INTEREST

the advances in technology exceed the increase in demand. In recent years, the pocket calculator market has experienced this phenomenon. The longer a decision to purchase can be postponed the lower the ultimate purchase price. This strategy is economically justified as long as the rate of decrease in the purchase price exceeds the yield that could be earned

Table 8-19 CONSIDERATIONS FOR ACCELERATED SPS SCHEDULING

- I. Shorter payoff period (to become self-supporting)
- II. Larger number of units outstanding at any one time (lump sum capital requirements higher)
- III. Higher Present Value for annual capital charges
- IV. Higher Present Value for annual net cash inflow
- V. Net Present Value (IV-III) greater
- VI. Hedge against inflation
- VII. Detrimental technology effect

on the asset if purchased immediately. For example, if the price of a SPS would fall an average of 20 percent per annum while the return, if purchased now, would be 15 percent, it would pay to wait until the former rate fell to match the latter. Technology and price are reciprocals of each other. It is possible, however, that changes in demand could offset this relationship. For most practical purposes, however, changes in supply (technologically based) and demand can be assumed independent of each other. Thus, increases in supply can be expected to result in lower prices than what would otherwise be anticipated. For SPS units, this phenomenon might be especially appropriate with regard to solar cell development.

In sum, those consideration which bear an important influence on scheduling decisions are: (1) forecasted market demand; (2) anticipated relative price increases of relevant resources; (3) anticipated technological advances; (4) expected internal rate of return; and (5) the alternative cost of funds (cost of capital). Increases in factors (1), (2), and (4), would generally favor faster scheduling while increases in (3) and (5) would favor slower scheduling. The determination of the economic desirability of any scheduling scheme must include a careful study of all these factors and their potential influence on the project and each other.

## CHAPTER 8

### REFERENCES

- 8-1** "Initial Technical, Environmental, and Economic Evaluation of Space Solar Power Concepts," Volume I, Summary, JSC 11443, Advance Copy, July 15, 1976.
- 8-2** Doebelin, E. O., "Measurement Systems-Application and Design," McGraw-Hill, New York, NY, 1966.
- 8-3** Op cit., JSC, "Initial Technical, Environmental, and Economic Evaluation."
- 8-4** McDonnell Douglas, Optimized Cost Performance Design Methodology, Volume II, "Data Review and Analysis," Book 3, "Detail Cost Analysis." Report G975, Contract NAS 2-5022.
- 8-5** Planning Research Corporation, Analysis and Derivation of Cost Estimating Relationships and Trends for Airframe Structural Elements of Advanced Space Transportation Systems, NASA CR-132736, Contract No. NAS 1-13869.
- 8-6** Ramos, A.; Costigan, M.; Banch, G. T.; and Chisholm, G. Jr.; "A Technique for Using Cost as Design Parameter," JSC Internal Note, May 10, 1973.

**CHAPTER 9**  
**FINDINGS AND RECOMMENDATIONS**

## **CHAPTER 9**

### **FINDINGS AND RECOMMENDATIONS**

#### **9.1 SUMMARY OF MISSION ALTERNATIVES**

Initially it was the intent of the design team to consider four alternatives as regards transportation and construction of the solar power satellite. These included: (1) partial assembly in LEO, and (2) complete assembly in GEO where chemical propulsion would be used for interorbital transfer; (3) partial, and (4) full assembly in LEO where transportation to GEO would be by an electrical propulsion system. Technical and economical reasons, and to a lesser extent time limitations resulted in a concentration on two of the four alternatives. The scenarios which received maximum consideration (Fig. 2-2, Chapter 2) were construction and assembly at GEO using chemical orbital transfer vehicles for LEO to GEO transportation, and preliminary construction of modules at LEO and subsequent propulsion to GEO using electrical thrusters attached to the modules. Final assembly of the modules would then occur at GEO.

The remaining sections of this chapter report the findings and recommendations for future research and development.

#### **9.2 FINDINGS**

This section presents condensed versions of the findings which are developed in the body of the report. In addition to these findings, the study concluded that a number of technical areas required additional research and development. Section 9.3 lists these research and development topics.

The scope and complexity of the solar power satellite and of the various transportation systems together with the time limitation imposed on this systems design study prevent the deduction of absolute conclusions. All of the findings herein should be read with cognizance of how they were developed in the earlier chapters where ground rules and working hypotheses were stated. The findings can be categorized as belonging to one of three classes. In the order presented, these classes are transportation, space environment, and the solar power satellite.

#### **9.2.1 Transportation**

##### **9.2.1.1 EARTH LAUNCH**

**1.** Preliminary analysis indicates that regardless of the mode of interorbital transfer (chemical or electrical), an equatorial launch site presents several well-defined technical advantages over alternative sites such as Kennedy Space Center.

**2.** Investigation of characteristics and mission cost projections of various heavy lift launch vehicle candidates indicated no obvious choice as the optimal vehicle. A major reason for this uncertainty is that recovery and refurbishment costs of these vehicles may exceed 50 percent of the total mission costs and at present almost no reliable costing information exists for this area.

##### **9.2.1.2 CHEMICAL PROPULSION**

**3.** For chemical propulsion, complete assembly at GEO of the solar power satellite is recommended.

**4.** In order to reduce costs and provide operational simplicity all stages of the chemical orbital transfer vehicle should use common components and, whenever possible, should be identical units.

**5.** Models of the orbital transfer vehicles are proposed in order to generate gross mass numbers and flight cost features. The models encompass a reduction of independent variables to enable linear scaling in terms of payload mass, vehicle cost per mass, and the staging.

**6.** Initial analysis of the two modes of OTV propellant resupply, namely, transfer of propellant tank and transfer of propellant (refuel), resulted in the conclusion that propellant tank transfer is the more promising mode.

**7.** Potential opportunities for secondary uses of expended items (for example, propellant tanks and shrouds), exist in such areas as radiation shields, primary structures for support base and habitability modules, storage and debris receptors, and in the solar power satellite itself, in either an unmodified or

modified form.

**8.** A simple, systematic technique of surplus tank disposal was developed and is reported in Chapter 6.

### 9.2.1.3 ELECTRICAL PROPULSION

**9.** For the electrical propulsion mode, partial assembly of the solar power satellite in square modules at LEO is recommended.

**10.** It is planned for each module to propel itself and certain items of cargo consisting of supplies and components for final assembly to GEO immediately upon completion of construction in LEO.

**11.** Propulsion of the modules to GEO will be provided by two rotating clusters (one degree of freedom) of engines located at opposite vertices of the square module.

**12.** The hydrogen electric arcjet engine appears to be the most likely choice for thrusting the modules to GEO.

**13.** Modular construction at LEO and immediate launch to GEO reduces the probability of collision with space debris (compared to that of a completed SPS) by a factor of  $1/n$  where  $n$  equals the number of modules.

**14.** Energy for propulsion and control of the modules during transit will be provided by deploying a portion of the solar array in the center of the module.

**15.** Solar arrays and control sections are expected to require protection from the exhaust plume of the thrusters. Protection will be provided through location of the arrays or by use of deflection shields.

**16.** Deployment of presently available silicon solar cells would result in a degradation of approximately 81 percent for a 54 day transit time calculated on a base of  $9.6 \times 10^{-3}$  percent degradation/rad and  $1 \text{ g/cm}^2$  of shielding.

**17.** The antenna rotator attachment, antenna construction, and quick assembly of array modules will be accomplished at GEO.

### 9.2.1.4 PERSONNEL TRANSPORTATION

**18.** For both chemical and electrical propulsion modes the crew transportation system will utilize some forms of personnel carrier module (PCM).

**19.** Passenger transit between earth and LEO will be achieved by docking the personnel carrier module into the payload bay of the orbiter portion of a

modified shuttle or shuttle derived vehicle.

**20.** For GEO construction, and with a chemical propulsion system, the interorbital (LEO-GEO) transfer of personnel in the PCM will use a dedicated chemical OTV fleet.

**21.** For LEO construction of modules, and with an electrical thruster system, movement of the PCM will require the use of a new chemical personnel orbital transfer vehicle (POTV).

### 9.2.1.5 TRANSPORTATION ECONOMICS

**22.** The cost comparison between chemical propulsion and electrical propulsion, using the best available information for both systems, yielded inconclusive results as to which would provide the lower cost system. The degree of possible error in the data will need to be reduced in order to warrant further consideration.

**23.** An equatorial launch site presents the possibility of considerable cost savings provided the costs of building the site and ground transportation to the site are not significantly greater than similar costs at Cape Kennedy.

### 9.2.2 Space Environment

**24.** Geomagnetically trapped radiation constitutes a severe restriction on the use of currently available silicon solar cells for electrical propulsion in orbital transfer.

**25.** Manned operation in LEO or GEO is possible for four months with a  $2 \text{ g/cm}^2$  shield under present radiation standards.

**26.** Solar flare events make heavy shielding necessary in GEO. Expedient items of equipment may possibly provide low cost shielding if refurbishing measures are kept simple.

**27.** Legal aspects of present Space Radiation Standards need to be reconsidered prior to application to future crews. Future crews may come under more stringent industrial standards.

### 9.2.3 Solar Power Satellite

#### 9.2.3.1 STRUCTURE

**28.** The truss configuration follows established structural design methods, whereas the column-cable configuration requires solutions to a number of unresolved questions.

**29.** Final assembly at GEO will be by simple,

quick connect procedures.

**30.** Use of conventional thin wall tube structure with rigid joints is preferable to less stable forms of structure.

**31.** Use of a column slenderness ratio greater than 150 eliminates the need to use high-strength alloys or composites.

**32.** Nodes or "hard spots" must be provided for attachment of thrusters, antenna, switchgear, etc., where portions of the structure are to be transported from LEO to GEO in segments or modules.

#### 9.2.3.2 FABRICATION AND ASSEMBLY

**33.** Control system requirements during the GEO construction phase, or for final assembly in GEO of the square modules transferred from LEO, may be more difficult than control requirements after project completion.

**34.** Onsite space fabrication of certain simple, basic units is more desirable than receiving prefabricated pieces from the ground.

**35.** A high degree of automation is essential if the high assembly rates indicated are to be achieved.

### 9.3 RECOMMENDED AREAS OF RESEARCH AND DEVELOPMENT

#### 9.3.1 General

**1.** The technical and economical advantages of an equatorial launch are judged sufficient to recommend an indepth analysis of alternative sites and their implications for the SPS program.

**2.** An investigation of the risks and costs of recovery and refurbishment of HLLV's is considered necessary. Especially important is a comparison between horizontal ground landing candidates (2 stage winged) and vertical water landing candidates (2 stage ballistic). The rationale for this is that projected space programs of the immediate future (next quarter century) will almost certainly benefit from vehicles with a high reusability factor, and, in fact, support for future programs can be partially based upon the fact that economical earth to LEO transportation is available.

**3.** Further mission and cost analysis is recommended for expendable OTV propellant tanks, OMS units and shrouds versus the use of an HLLV with a second or third stage capable of LEO retrieval of tanks which could be refueled on earth and reused.

#### 9.3.2 Chemical Propulsion

**4.** Development of a simple, efficient technique of cryogenic transfer in space is needed.

**5.** More consideration should be given to the compatibility of the physical characteristics (dimension, mass, etc.) of the OTV stages with the HLLV payload configurations and capabilities.

**6.** Additional investigation is recommended into secondary uses in space of potentially expendable items such as propellant tanks and shrouds.

#### 9.3.3 Electrical Propulsion

**7.** In order to seriously consider electrical propulsion as a form of transportation during the early years of the proposed SPS program, it is necessary to initiate a dedicated research and development program now.

**8.** Further analysis of the reusability potential of electrical thrusters is needed.

**9.** A study of the effects of exhausted propellants from electrical thrusters on man's environment and on the SPS modules is recommended.

**10.** Study methods for optimizing orbital transfer through simultaneous plane change and altitude change should be devised.

#### 9.3.4 Economics

**11.** There should be additional economic analysis undertaken of the SPS project to determine the volume of resource usage involved and the effect such usage will have on the national economy.

**12.** Electrical market analysis for the sales of SPS output, particularly in terms of regional markets, should be greatly expanded.

#### 9.3.5 Space Environment

**13.** Concerns for the potential effects of radiation resulted in the following recommended areas for additional study:

a. Long term exposure of solar cell candidates to Van Allen Belt radiation.

b. Long term chronic exposure of personnel to "low level" radiation.

c. Potential consequences of solar flare activity upon the SPS and construction personnel in GEO.

d. Revision of the legal aspects of Space Radiation Standards.

**14.** Another area of concern centered upon the quantity of space debris and the potential hazard it presents to the proposed Solar Power Satellite program. The following recommendations are suggested:

a. Design and fly an orbiter payload whose purpose it is to monitor the buildup of objects in earth orbit.

b. Plan and institute a program to return or dispose of objects from space which no longer serve a useful function.

### **9.3.6 Solar Power Satellite**

#### **9.3.6.1 STRUCTURE**

Further study and research are recommended on the following aspects of design and construction of structures in space:

**15.** Development of new materials, such as metal-matrix composites, etc.

**16.** Development of radiation-resistant materials such as plastics and plastic composites.

**17.** Development of suitable adhesives for proper (long life) bonding in the deep space environment.

**18.** Fusion welding techniques for thin-walled members to be used in space.

**19.** Quick joining methods for modular construction in space.

**20.** Automated manufacturing and fabrication methods in space.

**21.** Development of an appropriate "Structural Index" for large space structures.

**22.** Identification of thruster characteristics (size, shape, mass, power, etc.) for orbital transfer of structural segments or subassemblies.

#### **9.3.6.2 FABRICATION AND ASSEMBLY**

**23.** Study problems of controlling the SPS structure during and after construction regardless of whether construction is done entirely in GEO or is merely the assembly of modules transported from LEO.

#### **9.3.6.3 SPACE BASED MANUFACTURING SITE**

**24.** An indepth study of the potential benefits of creating a space based manufacturing site (in support of the solar power satellite program) is recommended. Areas of interest include the following:

a. Analyze baseline SPS configurations in order to determine "basic building blocks" of the various portions of the satellite.

b. Determine potential functions to be performed at the space base; candidates might include processing, rolling of stock, fabrication, growing of crystals, and assembly.

c. Find materials most amenable to limitations and benefits of space processing and manufacturing.

d. Examine all potential sources of raw materials needed at the site including earth, lunar, and expended items from the transportation system.

e. Attempt to evaluate the extent of human resources, material resources, energy, and support equipment necessary to carry out the various functions required.

f. Examine logistics, orbital location, and economics of a space manufacturing site.

APPENDICES

APPENDIX A

STATEMENT OF WORK

3

NASA-ASEE SUMMER FACULTY  
FELLOWSHIP PROGRAM  
ENGINEERING SYSTEMS DESIGN PROJECT  
STATEMENT OF WORK

LARGE STRUCTURES IN GEOSYNCHRONOUS ORBIT  
(MISSIONS-TRANSPORTATION-CONSTRUCTION)

February 15, 1976

L. B. Johnson Space Center  
University of Houston  
Rice University

## I. INTRODUCTION

### Background

NASA has recently begun consideration of operating large systems in geosynchronous orbit. In particular, consideration is being given to satellite power systems (SPS) which may involve many square kilometers of area and millions of kilograms in weight. These are large, rigid, structures which must be assembled or manufactured in space from much smaller subassemblies, modules or materials. Among the most significant questions which such an assembly operation raises is how to transport and where to assemble the final system. For instance, is it best to assemble an entire satellite in a low earth orbit and then transfer it intact to geosynchronous orbit or is it best to assemble it directly in geosynchronous orbit?

### Objective

Accordingly, the objective of this study is to investigate and determine the relative merits of various approaches to transporting large quantities of material from earth to low earth orbit and subsequently to geosynchronous orbit. The investigation will integrate considerations including propulsion systems, orbital mechanics, structures, power systems, environmental (radiation) effects, operational suitability, manufacturing, and economics.

## II. TASKS

Very briefly, NASA will provide an objective, certain constraints on its execution, and available information on all reasonable propulsion systems and transfer profiles. The study team will then define, evaluate and compare various alternatives. Three scenarios for accomplishing the overall objective will then be developed, evaluated, and compared.

NASA will provide a "baseline" SPS design for a functioning satellite in geosynchronous orbit. It will include weights and various functional and structural characteristics. NASA will also provide information on a number of propulsion systems and their characteristics for (1) accomplishing a low earth orbit rendezvous and (2) a geosynchronous rendezvous. For the alternative of accomplishing assembly in low earth orbit, reasonable propulsion systems and their characteristics will be identified for (3) transporting the SPS intact to geosynchronous orbit and (4) transporting various degrees of partially assembled satellites to geosynchronous orbit for final assembly.

It will be assumed that the assembly operations will require man and manned transportation to and from low earth orbit and geosynchronous orbit will be considered in final comparisons. No in depth consideration will be given in this study to special assembly techniques, but only to the transfer of subassemblies to a stationkeeping point and the definition of the degree of assembly to be accomplished on the ground, low earth orbit, and geosynchronous orbit, respectively.

There are related NASA studies from which the latest information will be made available to the summer study team. They are the Space Power System, Orbital Assembly, and Structural Analysis studies being done by JSC and the Heavy Lift Launch Vehicle Study being done by MSFC.

## III. COMPARE ALTERNATIVES

For each of the four kinds of transportation tasks listed above, the study team will compare and evaluate the identified candidates. Suitable criteria will be developed which will include, but not be limited to the following kinds of interrelated considerations: cost (including any penalties in power generation due to transfer time), reliability,

design complexity and feasibility, operational difficulty and flexibility, subjection to radiation damage, satellite structural considerations, and so forth.

#### IV. DESIGN PARAMETRIC APPROACHES

Based on the comparative analysis, the study team will develop scenarios for accomplishing each of the following approaches to the transportation problem:

- o All assembly in low earth orbit and intact transfer to geosynchronous orbit.
- o A degree of partial assembly in low earth orbit and final assembly in geosynchronous orbit.
- o All assembly in geosynchronous orbit.

These scenarios will include such items as propulsion systems definitions, weights, maneuver sequences, and propellant requirements. They will consider disposable vs. reusable vehicles and define manufacturing requirements.

#### V. EVALUATE APPROACHES

The three scenarios will be evaluated and compared. Considerations will be made for manned participation in assembly (in accordance with information supplied by NASA) in the sense that manned participation in geosynchronous orbit is more costly than in low earth orbit. Evaluation criteria will be established and will include such items as costs (including R&D, manufacture and operations), reliability, operational suitability and complexity, safety, radiation degradation, and so forth.

APPENDIX B  
INSTITUTE PARTICIPANTS

1976  
NASA-ASEE ENGINEERING SYSTEMS DESIGN INSTITUTE  
University of Houston - JSC  
Participating Fellows

Harm Buning,  
Professor  
Aerospace Engineering Department  
University of Michigan  
Ann Arbor, Michigan 48109

BSE, University of Michigan (Aero)  
MSE, University of Michigan (Aero)

Reinaldo Cintron,  
Assistant Professor  
Department of Chemical Engineering  
University of Puerto Rico  
Mayaguez, Puerto Rico 00708

BSCLE, University of Puerto Rico at Mayaguez  
ME, Stevens Institute of Technology (Chem.)  
Ph.D, Stevens Institute of Technology

Dale Cloninger,  
Associate Professor  
Department of Finance  
University of Houston, Clear Lake City  
Houston, Texas 77058

BS, Georgia Institute of Technology  
MBA, Emory University  
DBA, Florida State University

Thomas L. De Fazio,  
Associate Professor  
Department of Mechanical Engineering  
Florida Institute of Technology  
Melbourne, Florida 32901

SB, Massachusetts Institute of Technology  
SM, Massachusetts Institute of Technology  
Sc.D, Massachusetts Institute of Technology

Kenneth W. French,  
Associate Professor  
Department of Mechanical Engineering  
John Brown University  
Siloam Springs, Arkansas 72761

BS, Purdue  
MS, University of Minnesota  
Ph.D, State University of New York

Salvador R. Garcia,  
Instructor  
General Academics  
Moody College of Marine Sciences and Maritime  
Resources  
Galveston, Texas 77550

BA, University of Texas at Austin  
M.Ed., Texas A & M University

Thomas J. Gerson,  
Assistant Professor  
Department of Electrical Technology  
Queensborough Community College  
Bayside, New York 11364

BE, City College of the City, University of New York  
(electrical)  
ME, City College of the City, University of New York  
(electrical)  
Ph.D, City University of New York (Engineering)

Euel W. Kennedy,  
Assistant Professor  
Department of Mathematics  
California Polytechnic State University  
San Louis Obispo, California 93407

BS, East Central State University (Math, Physics)  
MS, University of Utah  
Ph.D, University of Utah

Fred D. Lewallen,  
Assistant Professor  
School of Technology  
Oklahoma State University  
Stillwater, Oklahoma 74074

BSEE, Oklahoma State University  
MSEE, Oklahoma State University

Chung K. Liu,  
Associate Professor  
Engineering Technological Division  
University of Guam

BSE, National Cheng Kuang University  
MSEE, University of Minnesota  
Ph.D, Catholic University of America

Bernard McIntyre,  
Assistant Professor  
Physics Department  
North Texas State University  
Denton, Texas 76203

BS, Northeastern University  
MS, Rensselaer Polytechnic  
Ph.D, Brown University

Michael Mezzino,  
Associate Professor  
Department of Mathematics  
University of Houston, Clear Lake City  
Houston, Texas 77058

BA, Austin College  
MA, Kansas State University

Knud B. Pedersen,  
Professor  
Nuclear and Mechanical Engineering  
Puerto Rico Nuclear Center  
University of Puerto Rico  
Mayaguez, Puerto Rico 00708

BS, Iowa State College (Mech. E.)  
MS, Iowa State University (Nucl. E.)  
Ph.D, Iowa State University (Nucl. E.)

Shankaranarayana R.N. Rao,  
Professor  
Department of Civil Engineering  
Prairie View A & M University  
Prairie View, Texas 77445

BE, Mysore University (Civil)  
ME, Roorkee University (Water Resources Develop-  
ment)  
MS, University of Connecticut (Hydraulics)  
Ph.D, Rutgers (Thermal Soil Mechanics)

Norman M. Schnurr,  
Associate Professor  
Department of Mechanical Engineering  
Vanderbilt University  
Nashville, Tennessee 37205

B.Sc, University of Notre Dame (Mech. Eng.)  
M.Sc, Ohio State University (Mech. Eng.)  
Ph.D, Ohio State University (Mech. Eng.)

John W. Weatherly, III,  
Associate Professor  
Department of Mechanical Engineering  
Louisiana State University  
Baton Rouge, Louisiana 70803

BS, Georgia Institute of Technology (Chem. Eng.)  
MS, Vanderbilt University (Phys. Chem.)  
MS, Rutgers (Math. Stat.)  
Ph.D, Rutgers (Mech. Eng.)

Norman L. Weed,  
Associate Professor  
Department of Public Affairs and Economics  
University of Houston, Clear Lake City  
Houston, Texas 77058

BS, University of Nebraska  
Ph.D, Tulane

Min-Yen Wu,  
Associate Professor  
Electrical Engineering Department  
University of Colorado  
Boulder, Colorado 80309

BS, National Taiwan University  
M.Sc, University of Ottawa  
Ph.D, University of California

Study Manager

Charles H. Story,  
Professor  
Department of Industrial Education  
East Tennessee State University  
Johnson City, Tennessee 37601

BS, Murray State University  
MS, Southern Illinois University  
Ed.D, Texas A & M University

Associate Director

William J. Graff  
Professor  
Department of Civil Engineering  
University of Houston, Main Campus  
Houston, Texas

BSME, Texas A & M University  
MSME, Texas A & M University  
Ph.D, Purdue University

APPENDIX C

LIST OF PROJECT SEMINARS

RECORD OF SEMINARS

NASA-JSC PERSONNEL

DATE	NAME	LOCATION		Topic
		Bldg.	Room	
June 9 9:00 am	Clarke Covington	32	220	Satellite Configuration
June 9 1:00	Lyle Jenkins	32	220	Construction
June 10 9:30	C. R. Hicks	32	220	Operations
June 10 1:00 pm	Harold Benson	32	220	Economics
June 10 2:00 pm	Edward Hays	32	220	Background, Energy Resources
June 28 1:00 pm	Victor Bond Earl Crum	T-500 Lecture Room		Orbital Mechanics
July 7 2:00 pm	Fred Stebbins Bernard Stuckey	13	267	Adage Computer Graphics "SPS Simulation"
July 8 3:00 pm	Astronaut Jack Lousma	T-500 Lecture Room		Skylab and EVA
July 26 3:30 pm	Michael Z. Lowenstein	13	108	Energy and the Environment

RECORD of SEMINARS

JSC Contractors

DATE	NAME	LOCATION		TOPIC
		Bldg.	Room	
June 8 1:00 pm	Eldon Davis Gordon Woodcock Boeing Company	32	200	Future Space Transportation System
June 23 9:00 am	Al Nathan Ray Pratt Gumman Company	32	150	Orbital Construction Demonstration Study
July 7 11:30 am	Peter Glazer Arthur D. Little, Co.	T-500 Lecture Room		The Satellite Solar Power Station
Aug. 6 8:30 am	Henry Wolbers McDonnell-Douglas Astronautics Co.	32	200	Space Stations

DESIGN TEAM

RECORD OF SEMINARS

In-House Seminars

DATE	NAME	LOCATION	TOPIC
June 8 9:00 a.m.	C. H. Story	T-500 Complex	Orientation and Introduction to Systems
June 18 1:00 p.m.	Harm Buning	T-500 Complex	Orbital Mechanics
June 23 9:30 a.m.	Mike Mezzino	T-500 Complex	Computer Graphics

1976 SEMINAR SCHEDULE

NASA-ASEE Systems Design and Research Faculty Fellows

1:00 - 3:00 PM

Auditorium of Building 30, JSC unless otherwise noted

- June 24  
(Thursday) "Food Production in Arid Regions"  
Mr. Dewey P. Compton  
Agri-Business Director  
KTRH Radio  
Houston, Texas
- June 29  
(Tuesday) "NASA Space Shuttle Program Planning"  
Mr. R. Wayne Young, Manager  
Shuttle Research and Scheduling Office  
NASA Johnson Space Center  
Houston, Texas
- July 2  
(Friday) "Geothermal Energy Resources in the U.S."  
Dr. Glenn E. Coury  
Consultant: Geothermal Energy; Water Desalting, Reuse and Disposal; Environmental  
Studies  
Denver, Colorado
- July 9  
(Friday) "Gasification and Liquefaction of Coal as Alternate Energy Source to Petroleum"  
Professor Dale Briggs  
Chemical Engineering Department  
University of Michigan  
Ann Arbor, Michigan
- July 16  
(Friday) "U.S. Energy: Today and Tomorrow"  
Dr. John J. McKetta  
Chemical Engineering Department  
University of Texas  
Austin, Texas
- July 23  
(Friday) "Transitions of International Terrorism Related to Changes in Technology"  
Major John D. Elliot  
U.S. Army; Concepts Analysis Agency  
Aberdeen, Maryland
- July 30  
(Friday) "The Technology of Custom Quality Handmade Paper"  
Mr. Howard Clark  
Twinrocker Handmade Paper Company  
Brookston, Indiana

APPENDIX D

CONSULTANTS AND ADVISORS

## NASA TECHNICAL ADVISORS

NAME	SPECIALTY
Arndt, Dickey	Microwave System
Babb, Gus	Orbital Mechanics
Bailey, Vernon	Manned Environment (Radiation)
Benson, Harold	Economics
Bond, Victor	Orbital Mechanics - Mission Planning
Bristow, Robert B.	HLLV
Covington, Clarke	Satellite Design
Crum, Earle	OTV
Hicks, Clay	Operations
Hooper, John	Thrusters
Jenkins, Lyle	Construction and Assembly
Jones, Mac	Model Development
Kessler, Don	Objects in Space
Livingston, Louis	Satellite Design
Ried, Bob	Thermal Considerations

## OTHER NASA CONSULTANTS

Baiamonte, Frank	Micro-Electronics
Davis, Hugh	Transportation
Harron, Ron	Costing
Kosinski, Robert E.	Microwave System
Smithson, Jerry	Propulsion Tanks
Webb, Debbie	Economics

APPENDIX E  
SYSTEMS ANALYSIS

## APPENDIX E—SYSTEMS ANALYSIS

### Group Organization

To investigate the problem described in the statement of work (Appendix A), the design fellows were organized into two teams of nine members. The teams, designated Red and Blue, investigated the two primary types of propulsion, electrical and chemical (Figure E-1 and Table E-1). Each team selected a captain to serve until the seventh week of the project. Recorders were also selected to keep records of all team proceedings. After midterm, the two teams were consolidated to synthesize the research data for the technical report. Six groups were formed in the transition (shown in Figure E-2) after midterm. Editors were appointed in each group; membership varied from three to six persons. The main body of the technical report resulted from this group organization—one major chapter from each group. Table E-2 lists the contributors to these chapters.

The administrative organization for the institute is shown in Figure E-3. In addition to the two primary technical advisors from the Urban Systems Office, fourteen technical advisors were assigned for program support. This enabled the design fellows to work frequently with Johnson Space Center personnel on a one to one basis.

### Program Control

During the first week of the program, a GANTT (progress and status) chart was developed for the five phases of the systems design process. The first task in developing this chart was to determine the controlled and intermediate milestone dates. Secondly, a design process was identified and articulated with the nature of the subject being investigated. The chart was used primarily as a communication tool—for the management reviews and the design fellows, Figure E-4.

A second technique was utilized to explore relationships among the various activities and tasks. This technique, called PERT (Program Evaluation and Review Technique) revealed interrelationships and priorities better than the GANTT method. Since the project was in existence during a fixed time period of eleven weeks, no attempt was made in determining a critical path through the network. Figure E-5 shows the final PERT Network for the entire project. The events, represented by numbers and circles, are simply points in time. The various activities are represented by letters of the alphabet; each activity is assumed to consume both time and resources. Dummy activities are represented by a dotted line and arrowhead; their purpose is merely to show relationship between two events.

### Systems Analysis Flow Chart

Figure E-6 shows the systems analysis flow chart used in preparation of the final report. A systematic plan for execution of the technical report was formulated first, then represented graphically on the chart. Preliminary milestones are represented in the first column of elliptical shapes. The five main parts of the report are represented (with the various milestones) in the second column.



PURPOSE: TO RESEARCH AND DEVELOP  
PROJECT SCENARIOS AS PRESCRIBED;  
DESIGN PARAMETRIC APPROACHES TO  
THE PROBLEM.

FIGURE E-1  
TEAM ORGANIZATION

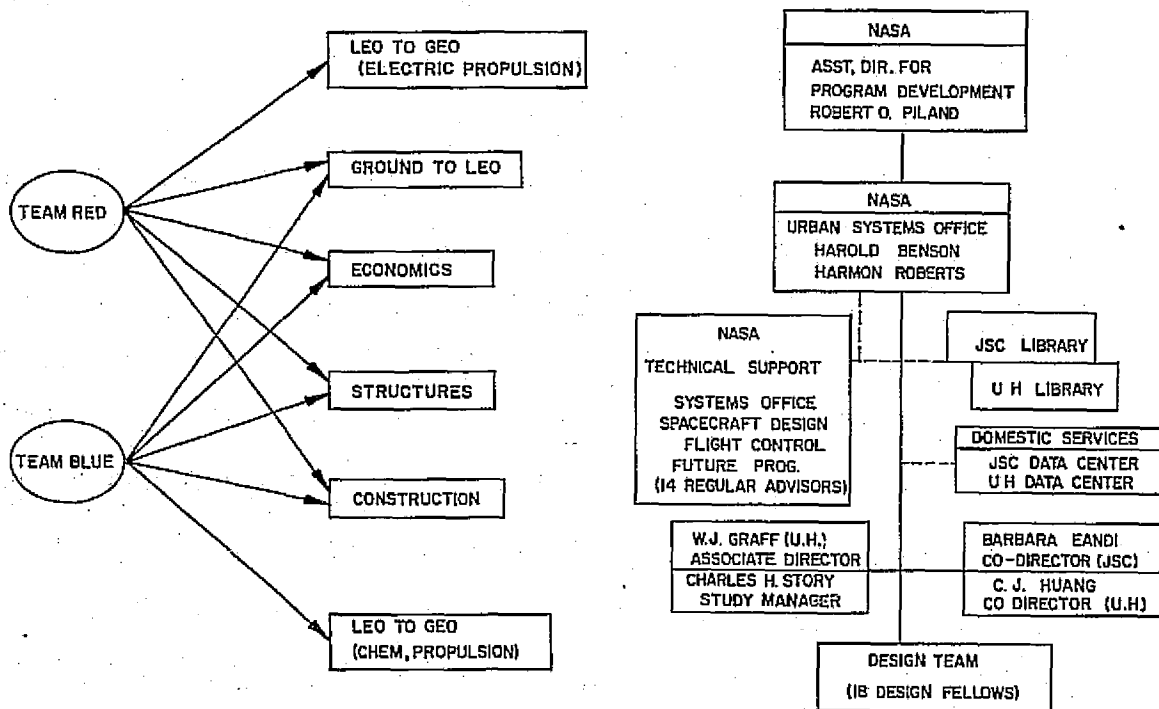
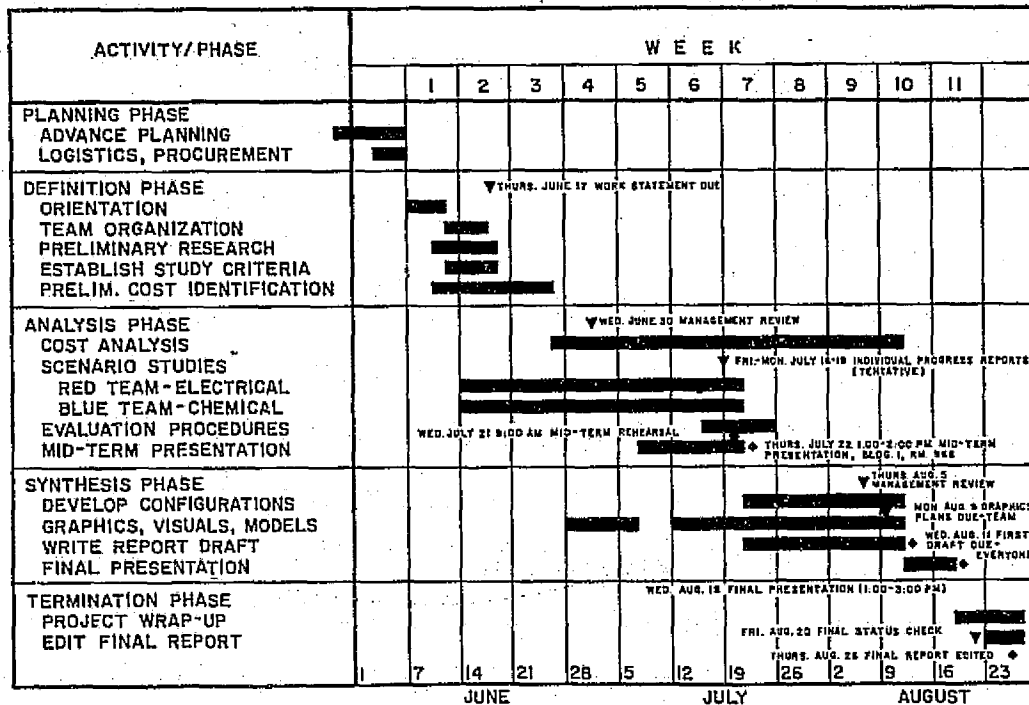


FIGURE E-2 GROUP ORGANIZATION (MID-TERM TRANSITION)

ADMINISTRATIVE ORGANIZATION 1976 INSTITUTE  
FIGURE E-3

SOLAR POWER SATELLITE STUDY



JUNE 7 TO AUGUST 20, 1976

NASA/ASEE ENGINEERING SYSTEMS DESIGN GROUP  
FIGURE E-4 GANTT CHART

◆ CRITICAL DATES (CONTROLLED MILESTONES)

▼ INTERMEDIATE MILESTONES

ORIGINAL PAGE IS  
OF POOR QUALITY

### P.E.R.T. NETWORK

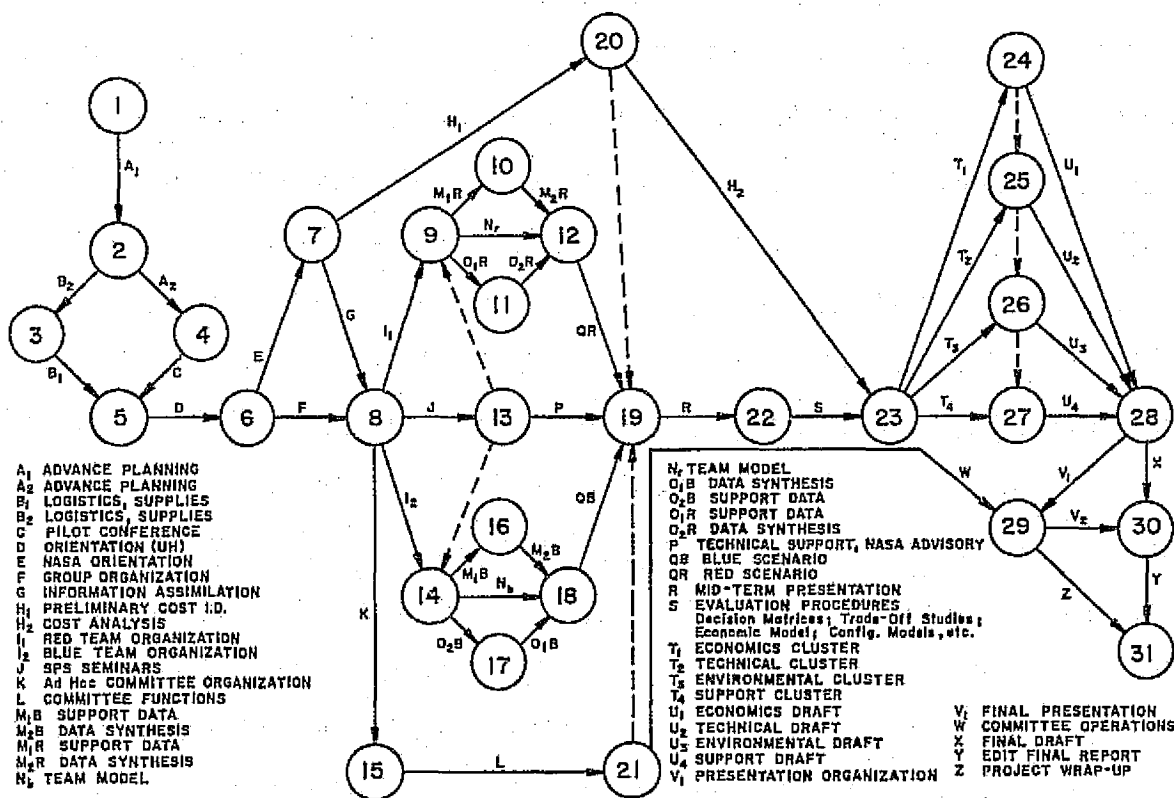


FIGURE E-5

ORIGINAL PAGE IS  
OF POOR QUALITY

**SYSTEMS ANALYSIS FLOW CHART  
FINAL REPORT**

1976 NASA-ASEE FACULTY  
INSTITUTE  
JSC HOUSTON, TEXAS

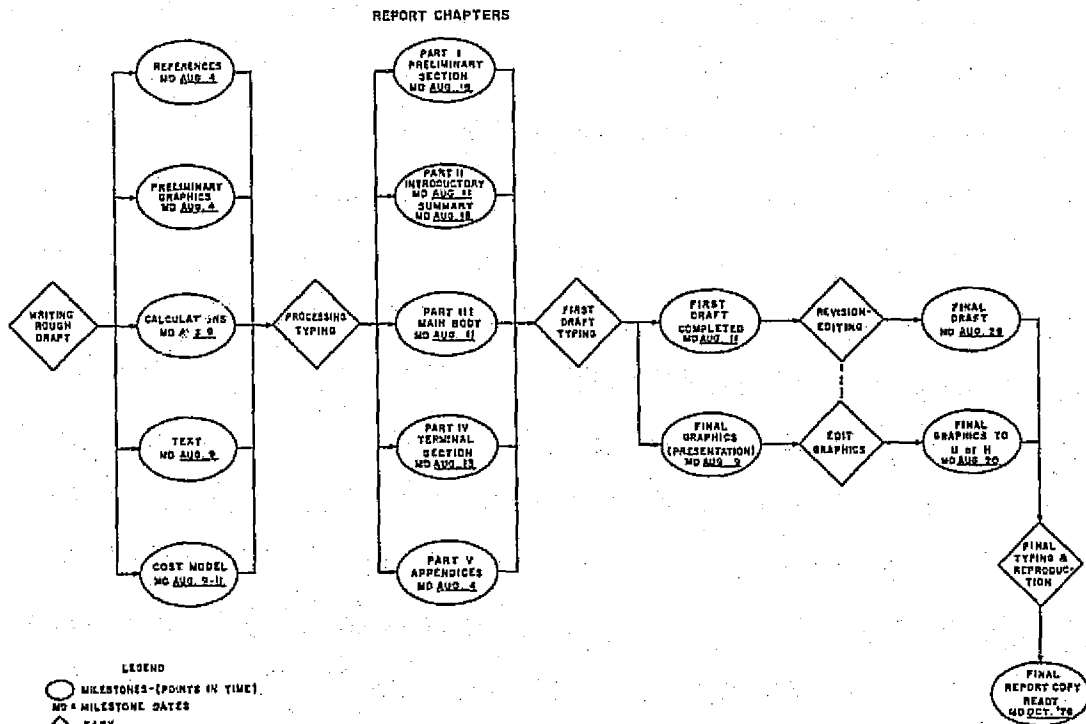


FIGURE E-6

ORIGINAL PAGE IS  
OF POOR QUALITY

TABLE E-1  
STUDY TEAMS

RED TEAM  
(Electrical Propulsion)

NAME	PRIMARY INTEREST
Fred Lewallen	Power System; Propulsion
Tom Gerson	Power System; Propulsion
Knud Pedersen	Environmental
R. N. Rao	Structures
Tom De Fazio	Structures; Dynamics; Stability; Controls
Salvador Garcia	Manufacturing; Fabrication
Norman Weed	Economics
Mike Mezzino	Operations and Planning
Harm Buning (Captain)	Orbital Mechanics

BLUE TEAM  
(Chemical Propulsion)

NAME	PRIMARY INTEREST
Reinaldo Cintron	Chemical Propulsion
Min-Yen Wu	Satellite Power Generation
Bernard McIntyre	Satellite Power Transmission
John Weatherly	Orbital Mechanics
Kenneth French	Structures
Chung Liu	Manufacturing
Euel Kennedy	Operations and Planning
Norman Schnurr	Environmental
Dale Cloninger (Captain)	Economics

TABLE E-2  
REPORT ORGANIZATION

Chapter No.	Title	Contributors
CHAPTER 1	Summary	Editors
CHAPTER 2	Introduction	Editors
CHAPTER 3	Structures	De Fazio (Editor) Rao French
CHAPTER 4	Transportation to Low Earth Orbit	Weatherly (Editor) Cintron Kennedy
CHAPTER 5	Orbital Transfer by Electric Propulsion	Lewallen (Editor) Pedersen Gerson Buning
CHAPTER 6	Orbital Transfer by Chemical Propulsion	French (Editor) Kennedy
CHAPTER 7	Construction of SPS: Fabrication and Assembly	Liu (Editor) Wu McIntyre Garcia
CHAPTER 8	Economics	Weed (Editor) Mezzino Schnurr Cloninger
CHAPTER 9	Findings, Conclusions, Recommendations	Editors

APPENDIX F

GLOSSARY - ACRONYMS - NOMENCLATURE

## GLOSSARY OF ACRONYMS

ACS	Attitude Control System
ADL	Arthur D. Little, Inc.
ASTP	Apollo Soyuz Test Project
BLOW	Booster Lift-Off Weight
BP	Boilerplate
CEQ	Council on Environmental Quality
CLV	Cargo Launch Vehicle
CMG	Control Moment Gyro
COTV	Cargo Orbital Transfer Vehicle
CPS	Chemical Propulsion Stage
CY	Calendar Year
DDT& E	Design Development Testing & Engineering
DOL	Deploy Only Launcher
DT	Drop Tank
EDF	Edge-defined, Film-fed growth (Silicon)
EIA	Environmental Impact Assessment
EMU	Extravehicular Mobility Unit
EOS	Earth-to-Orbit-to-Synchronous
ERDA	Energy Research and Development Administration
ET	External Tank
EVA	Extra-Vehicular Activity
FPC	Federal Power Commission
FY	Fiscal Year
GEO	Geosynchronous Orbit
GLOW	Gross Lift-Off Orbit
GW	Gigawatts ( $10^9$ watts)
HLLV	Heavy Lift Launch Vehicle
IPS	Ion Propulsion Stage
Isp	Specific Impulse
JSC	Johnson Space Center
JURG	Joint User Requirements Group
KSC	Kennedy Space Center
L/D	Lift to Drag Ratio
L/D	Length to Diameter Ratio
LEO	Low Earth Orbit

LH <sub>2</sub>	Liquid Hydrogen
LO <sub>2</sub>	Liquid Oxygen
LOX	Liquid Oxygen
LRB	Liquid Replacement (or Rocket) Booster
mill	<sup>1</sup> / <sub>10</sub> of a cent
MMU	Manned Maneuvering Unit
MPD	Magneto-Plasma Dynamics
MPTS	Microwave Power Transmission System
MRCs	Microwave Reception and Conversion System
MSC	Marshall Spacecraft Center
MSFC	Marshall Space Flight Center
MS/MS	Materials Science/Manufacturing in Space
MT	Metric Tons
NASA	National Aeronautics and Space Administration
NEPA	National Environmental Policy Act
OBF	Orbital Burden Factor-Ratio of weight placed in Orbit to on-station weight
OLow	Orbiter Lift-Off Weight
OMES	Orbital Maneuvering Engine System
OMS	Orbital Maneuvering System
OMSF	Office of Manned Spaceflight
OPS	Oxygen Purge System
OTV	Orbital Transfer Vehicle
P/L	Payload
PLV	Personnel (and Priority Cargo) Launch Vehicle
POP	Perpendicular to Orbit Plane
POTV	Personnel Orbital Transfer Vehicle
PPLV	Personnel and Priority Cargo Launch Vehicle
PPU	Power Processing Unit
PRS	Power Relay Satellite
RCS	Reaction Control System
REM	Roentgen Equivalent Man
RF	Radio Frequency
RIV	Refueled Interorbit Vehicle
RMS	Remote Manipulation System (Shuttle)
RP	Rocket Propellant (Similar to kerosene-typed numerically; e.g. RP-1)
SECS	Solar Energy Collection System
SEP(s)	Solar Electric Power (System)

SEPS	Solar Electric Propulsion System
SH <sub>2</sub>	Hydrogen SLOsh
SOW	Statement of Work
SPS	Solar Power Satellite
SRB	Solid Rocket Booster
SRT	Supporting Research and Technology
SSLO	Second Stage Lift-Off Weight
SSME	Second Stage Main Engine
SSME	Space Shuttle Main Engine
SSPD	Space Shuttle Payload Data
SSTO	Single Stage To Orbit
ST	Space Tug
STS	Space Transportation System
TBD	To Be Determined
TBS	To Be Supplied
TFU	Theoretical First Unit
TLM	Telemetry
T/W	Thrust to Weight Ratio (lbs force/lbs mass)
VAFB	Vandenberg Air Force Base
Wp/WPL	Propellant Weight To Payload Weight Ratio

## NOMENCLATURE

a	unit transportation cost (\$/Kg) acceleration ( $m/s^2$ ) semi-major axis (m)
$a_c$	unit transportation cost, COTV (\$/Kg)
$a_H$	unit transportation cost, HLLV(\$/Kg)
$a_T$	unit transportation cost, tug (\$/Kg)
A	area
b	width
$b_G$	POTV flight cost (\$/man trip)
$b_L$	PLV flight cost (\$/man trip)
c	propagation velocity
$c_p$	propellant unit cost (\$/Kg)
$c_T$	cost of tanks per unit mass (\$/Kg)
$c_v$	cost of vehicle per unit mass (\$/Kg)
$C_D$	coefficient of drag
$C_{DEV}$	development cost allocated to one flight (\$)
$C_{ET}$	cost of expendable tanks
$C_O$	other costs (\$)
$C_p$	propellant cost (\$)
$C_T$	total cost of transportation per satellite (\$)
$C_{TA}$	turnaround cost (\$)
$C_v$	cost of one vehicle (\$)
COL	cut-on-line

D	diameter
e	unit charge ( $1.602 \times 10^{-19}$ coulomb)
E	Young's modulus
$E_g$	energy band gap (ev)
$f_c$	fraction of orbital transfer by the COTV
$f_{P,G}$	fraction of construction and support personnel in GEO
$f_{PL}$	propellant loss factor
$f_{PL,C}$	propellant loss factor, COTV
$f_{PL,T}$	propellant loss factor, tug
$f_s$	stage mass fraction
F	force
$F_c$	propellant loss factor of COTV
$F_T$	propellant loss factor of tug
g	acceleration of gravity ( $m/s^2$ )
$g_0$	standard gravitational acceleration on earth ( $9.807 m/s^2$ )
G	shear modulus universal constant of gravitation
h	altitude (Km)
i	orbit inclination interest rate
I	moment of inertia electric current
$I_{sp}$	specific impulse (s)
IRR	internal rate of return
J	electric current density

k	Boltzmann's constant ( $1.3806 \times 10^{-23}$ J/K) discount rate
K	a solar blanket constant
$K_1$	a constant relating the conductor geometric configuration
L	vehicle lifetime (trips) length
$L_c$	vehicle lifetime for the COTV (trips)
$L_T$	vehicle lifetime for the tug (trips)
m	mass
$m_{B,G}$	mass of support and construction equipment in GEO
$m_{B,L}$	mass of support and construction equipment in LEO
$m_{ET}$	mass of expendable tanks
$m_{ET,C}$	mass of expendable tanks of the COTV
$m_{ET,T}$	mass of expendable tanks of the tug
$m_G$	mass of cargo transported from LEO to GEO
$m_L$	mass of cargo transported from earth to LEO
$m_p$	mass of propellant per flight
$m_{p,c}$	mass of propellant per flight of COTV
$m_{p,T}$	mass of propellant per flight of the tug
$m_{PL}$	payload mass
$m_{PL,C}$	payload mass of COTV
$m_{PL,T}$	payload mass of tug
$m_s$	satellite mass
$m_T$	tankage mass
$m_v$	inert vehicle weight (not including expendable tanks)

$m_{v,c}$	inert vehicle weight (not including expendable tanks) of the COTV
$m_{v,t}$	inert vehicle weight (not including expendable tanks) of tug
$M$	moment
$n$	an integer
$N_c$	number of COTV's required per satellite
$N_p$	total number of man trips
$N_T$	number of tugs required per satellite
$NCF$	net cash flow
$NPV$	net present value
$NRV$	net revenue years
$p$	electric power
$P$	propellant to payload mass ratio
$P_c$	total probability of collision
$P_{c_j}$	the probability of a collision between the $j$ th object in earth orbit and the target spacecraft
$PV$	present value
$q$	dynamic pressure, $N/m^2$ heat dissipation
$r$	distance from center of earth (Km) radius
$R$	radius of earth (6375.4 Km) resistance radius of curvature
$R_0$	radius of the earth
$RRR$	required rate of return

RY	revenue years
S	conductor thermal disipation surface area
t	time thickness
T	temperature thrust
$T_c$	number of trips per satellite for the COTV
$T_L$	orbital lifetime (days)
$T_o$	room temperature
$T_T$	number of trips per satellite for the tug
T	environmental equilibrium temperature
V	potential difference (volts) velocity (m/s) volume
$V_c$	characteristic speed (local circular speed at R.) m/s
$V_{lc}$	local circular speed (m/s)
$W_o$	weight (on earth's surface)
x	cartesian coordinate
y	cartesian coordinate
z	cartesian coordinate
$\alpha$	radiation absorption coefficient ( $cm^{-1}$ ) angular acceleration angle
$\gamma$	shear strain
$\Delta V$	difference in velocity
$\epsilon$	strain

$\eta$	solar cell efficiency
$\theta$	angle
$\lambda$	a factor which varies from zero to one
$\mu$	gravitational parameter, ( $m^3/sec^2$ )
$\mu_x$	linear attenuation coefficient ( $cm^{-1}$ )
$\nu$	Poisson's ratio
$\nu$	radius of gyration
$e$	resistivity
$e_0$	resistivity at room temperature
$\sigma$	stress
$\tau$	period circular period
$\phi$	contact potential difference (volts) angle
$\omega$	angular velocity

SUBSCRIPTS

A	pertaining to apogee
p	propellant
p	perogee
pId	payload

APPENDIX G

ORBITAL MECHANICS DERIVATIONS AND EQUATIONS

## APPENDIX G

### ORBITAL MECHANICS DERIVATIONS AND EQUATIONS

- G.1 Numerical Constants
- G.2 Commonly Used Equations
- G.3 Impulsive  $\Delta V$  Orbit Transfer
  - G.3.1 Numerical Data for Low and Geosynchronous Earth Orbits
  - G.3.2 Coplanar Transfer from LEO to GEO
  - G.3.3 Transfer from LEO to GEO Including Plane Change
  - G.3.4 Duration of Impulsive Transfer
- G.4 Low Thrust Orbital Transfer
  - G.4.1 The Equations of Motion
  - G.4.2 Low Thrust Simplification of Equations
  - G.4.3 The Ideal Speed Increment
  - G.4.4 Duration of Transfer
  - G.4.5 Flight Path Angle
- G.5 Propellant Ratio Calculations

## G.1 Numerical Constants

The following numerical earth constants were used in the orbital mechanics calculations presented in this Appendix and in the text (Ref. G-1).

Gravitational Parameter:

$$\mu = 3.986032 \times 10^{14} \text{ m}^3/\text{sec}^2 \quad (1.4076539 \times 10^{16} \text{ ft}^3/\text{sec}^2) \quad \text{G.1-1}$$

Earth radius:

$$R_0 = 6375.4 \text{ km} \quad (20.917 \times 10^6 \text{ ft}). \quad \text{G.1-2}$$

Acceleration of gravity at  $R_0$ :

$$g_0 = 9.807 \text{ m/sec}^2 \quad (32.174 \text{ ft/sec}^2) \quad \text{G.1-3}$$

Characteristic velocity (local circular velocity at  $R_0$ ):

$$V_c = 7,907 \text{ m/sec} \quad (25,942 \text{ ft/sec}) \quad \text{G.1-4}$$

Orbital period of circular orbit at  $R_0$ :

$$\tau_0 = 84.40 \text{ min.} \quad \text{G.1-5}$$

## G.2 Commonly Used Equations

The following equations, presented without derivation are commonly used for preliminary design calculations in orbital mechanics. They apply to motion about a single central, inverse square force field.

Acceleration of gravity,  $g$ :

$$g = \frac{\mu}{r^2} = g_0 (R_0/r)^2 \quad \text{G.2-1}$$

Local circular velocity,  $V_{lc}$

$$V_{lc} = \sqrt{\mu/r} = V_c \sqrt{R_0/r} \quad \text{G.2-2}$$

Orbital period,

$$\tau = \left( \frac{2\pi}{\sqrt{\mu}} \right) a^{3/2} = \tau_0 \left( \frac{a}{R_0} \right)^{3/2} \quad \text{G.2-3}$$

Relation between speed and radial distances (from the center of the earth) is an orbit with a semi-major axis

$$a \quad \frac{V^2}{2} - \frac{\mu}{r} = -\frac{\mu}{2a} \quad \text{G.2-4}$$

or

$$\frac{V}{V_c} = \sqrt{2 \frac{R_0}{r} - \frac{R_0}{a}} \quad \text{G.2-4a}$$

For speeds at perigee and apogee radii ( $R_p$  and  $R_A$  respectively) we have

$$\frac{V_p}{V_c} = \sqrt{\frac{R_o}{R_p} \cdot \frac{R_A}{a}} \quad \text{G.2-4b}$$

and

$$\frac{V_a}{V_c} = \sqrt{\frac{R_o}{R_A} \cdot \frac{R_p}{a}} \quad \text{G.2-4c}$$

In the above equations,  $a$  is the average between  $R_A$  and  $R_p$ :

$$a = \frac{R_A + R_p}{2} \quad \text{G.2-5}$$

### G.3 Impulsive $\Delta V$ Orbit Transfer

We consider here the two-impulse transfer between a circular low earth orbit (LEO) and an altitude of 500 km (270 n.m.) to the equatorial geosynchronous orbit (GEO) both for the in-plane case as well as the case involving a plane change.

#### G.3.1 Numerical Data for Low and Geosynchronous Orbits

Numerical data for LEO and GEO are the following:

$$\frac{R_{LEO}}{R_o} = \frac{6375 + 500}{6375} = 1.0784 \quad \text{G.3.1}$$

From Eq. G.2-3, with  $\tau = 24$  hours:

$$\frac{R_{GEO}}{R_o} = 6.6275 \quad \text{G.3-2}$$

From Eq. G.2-2:

$$V_{1c_{LEO}} = V_c \sqrt{\frac{1}{1.0784}} = 7614 \text{ m/sec} \quad \text{G.3-3}$$

(24,980 ft/sec)

Similarly:

$$V_{1c_{LEO}} = 3071 \text{ m/sec} \quad (10,077 \text{ ft/sec}) \quad \text{G.3-4}$$

#### G.3.2 Coplanar Transfer from LEO to GEO

Along the elliptic transfer trajectory with perigee and apogee radii respectively equal to  $R_{LEO}$  and  $R_{GEO}$  (see Fig. G-1) we have, using Equations G.2-4b, 4c, and 5 (with  $a = 3.853 R_o$ ):

$$V_P = 9.986 \text{ m/sec (32,763 ft/sec)} \quad \text{G.3-5}$$

and

$$V_A = 1,625 \text{ m/Sec (5,330 ft/sec)} \quad \text{G.3-6}$$

To place the spacecraft, originally in LEO onto the transfer trajectory, a horizontal posigrade  $\Delta V_1$  is required of

$$\Delta V_1 = V_P - V_{1C_{LEO}} = 2,372 \text{ m/sec (7,783 ft/sec)} \quad \text{G.3-7}$$

To circularize at apogee, without a plane change, a posigrade  $\Delta V_2$  is needed:

$$\Delta V_2 = V_{1C_{GEO}} - V_A = 1,446 \text{ m/sec (4,747 ft/sec)} \quad \text{G.3-8}$$

The total  $\Delta V$  is then:

$$\Delta V = \Delta V_1 + \Delta V_2 = 3,818 \text{ m/sec (12,530 ft/sec)} \quad \text{G.3-8}$$

(no plane change)

### G.3.3 Transfer from LEO to GEO Including Plane Change

To circularize if the transfer trajectory has an inclination  $i$  relative to the equatorial plane, a dog-leg maneuver  $\Delta V_{DL}$  is required as shown in Fig. G-2.

$$\Delta V_{DL} = \sqrt{V_a^2 + V_{10_{GEO}}^2 - 2V_A V_{1C_{GEO}} \cos i} \quad \text{G.3-9}$$

For a due-East launch from Cape Canaveral  $i = 28.5^\circ$ . For this case

$$\Delta V_{DL} = 1817 \text{ m/sec (5963 ft/sec)} \quad \text{G.3-10}$$

The total  $\Delta V$ , including the  $28.5^\circ$  plane change is

$$V = \Delta V_1 + \Delta V_{DL} = 4190 \text{ m/sec (13,746 ft/sec)} \quad \text{G.3-11}$$

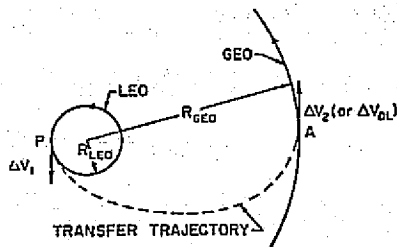


FIGURE G-1 ELLIPTIC TRANSFER TRAJECTORY FROM LEO TO GEO

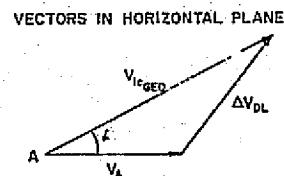


FIGURE G-2 GEOMETRY OF DOG-LEG MANEUVER COMBINING PLANE CHANGE WITH CIRCULARIZATION

Following a suggestion in Reg. G-4 it has been verified that a 25.6<sup>m</sup>/sec (84 ft/sec) saving in total  $\Delta V$  can be attained by making a 2.5° plane change during the perigee burn followed by a 26° plane change at apogee.

#### G.3.4 Duration of Impulsive Transfer from LEO to GEO

The duration of the transfer, exclusive of time required for phasing, is equal to half the period of the transfer orbit:

using Eq. G.2-3

$$t = \frac{\tau}{2} = \frac{\tau_0}{2} (3.853)^{3/2} = 5.32 \text{ hours} \quad \text{G.3-12}$$

#### G.4 Low Thrust Orbital Transfer

This section contains the derivation of some equations useful in the preliminary analysis of the low thrust transfer from one circular orbit to another coplanar circular orbit.

##### G.4.1 The Equations of Motion

Consider an axis system with its origin at the spacecraft location as shown in Fig. G-3. The positive x-axis is along the instantaneous velocity vector  $\vec{V}$ . The flight path angle,  $\gamma$ , is shown positive; its range is  $-90^\circ < \gamma < +90^\circ$ . The x-z plane is the vertical plane (containing  $\vec{V}$  and the center of the earth, O); the positive z-axis contains O if  $\gamma = 0$ . The y-axis completes the righthanded system.

The equations governing the in-plane motion (assuming no force in the y-direction) are:

$$\frac{\vec{F}}{m} = \vec{a}$$

or the x- and z- components

$$\frac{\vec{F}_x}{m} = \frac{dV}{dt}, \quad \frac{\vec{F}_z}{m} = (\dot{\theta} - \dot{\gamma}) V, \quad \text{G.4-1}$$

where  $\theta$  is the range angle measured from some inertial reference line as shown.

If the only forces are gravity and thrust, along  $\vec{V}$ , the equations become:

$$\frac{T}{m} - g \sin \gamma = \frac{dV}{dt}, \quad \text{G.4-2}$$

$$g \cos \gamma = (\dot{\theta} - \dot{\gamma}) V$$

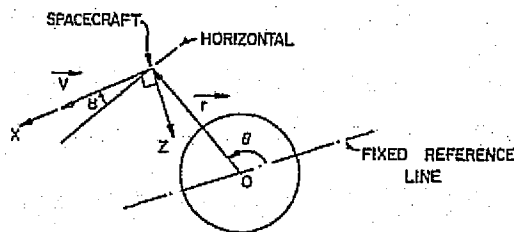


FIGURE G-3 AXIS SYSTEM FOR EQUATIONS OF MOTION

#### G.4.2 Low Thrust Simplification of Equations

With the initial orbit circular and with the thrust force sufficiently small compared to the (in-orbit) gravity force on the spacecraft, it may be assumed that the flight path angle, although no longer zero, remains small,

$$\cos \gamma \cong 1, \sin \gamma \cong \gamma$$

and that its rate of change is small compared to the orbital rate:

$$\dot{\gamma} \ll \dot{\theta}$$

Thus the equations of motion become

$$\frac{T}{m} - g\gamma = \frac{dV}{dt}, \quad \text{G.4-3}$$

$$g = \dot{\theta} V \quad \text{G.4-4}$$

Realizing the  $V \cong V \cos \gamma = r\dot{\theta}$ , Eq. G.4-4 can be solved for  $V$ . Using Eq. G.2-1:

$$V = \sqrt{gr} = \sqrt{\frac{g_0 R_0^2}{r}} = \sqrt{\frac{\mu}{r}} \quad \text{G.4-5}$$

which, according to Eq. G.2-2, is precisely the local circular speed. In this way we obtain a picture of the low-thrust trajectory: a shallow spiral with the speed always equal to the local circular value.

From Eq. G.4-5 the time derivative,  $\frac{dV}{dt}$ , can be developed:

$$\frac{dV}{dt} = \frac{d}{dt} \sqrt{\left(\frac{\mu}{r}\right)} = -\frac{1}{2} \left(\frac{1}{r}\right) \sqrt{\frac{\mu}{r}} \frac{dr}{dt}$$

Substituting the fact that  $\frac{dr}{dt}$  is the vertical component of  $V$ :

$$\frac{dr}{dt} = V \sin \gamma \cong V\gamma = \sqrt{\frac{\mu}{r}} \gamma,$$

we obtain

$$\frac{dV}{dt} = -\frac{1}{2} \left(\frac{\mu}{r^2}\right) \gamma = -\frac{1}{2} g\gamma \quad \text{G.4-6}$$

#### G.4.3 The Ideal Speed Increment

The ideal speed increment, defined by

$$\Delta V = \int_0^t \frac{T}{m} dt \quad \text{G.4-7}$$

is the increment in speed which the spacecraft would have acquired if the thrust had acted for a period of  $t$  seconds in the direction of the velocity vector at  $t = 0$  and in the absence of all other forces. It is the quantity to be used in the rocket performance equation (see Eq. G.5-1).

For the spiraling flight under consideration the ideal speed increment can be found by eliminating the quantity  $(g\gamma)$  from Equations G.4-3 and G.4-6 to give:

$$\frac{dV}{dt} = -\frac{T}{m} \quad \text{G.4-8}$$

Integration yields:

$$\Delta V = \int_0^t \frac{T}{m} dt = - \int_{V_{1c_{LEO}}^{V_{1c_{GEO}}} dV = V_{1c_{LEO}} - V_{1c} \quad \text{G.4-9}$$

Fig. G-4 shows the ideal  $\Delta V$  required to raise the orbit from  $h_{LEO}$  to  $h \leq h_{GEO}$ ; it is a plot of Eq. G.4-9 with the aid of Eq. G.4-5.

#### G.4.4 Duration of Transfer

For the case of constant thrust acceleration,  $\frac{T}{m}$ , Equation G.4-9 gives for the duration of the transfer from  $h_{LEO}$  to arbitrary altitude:

$$t = \frac{V_{1c_{LEO}} - V_{1c}}{T/m} = \frac{\Delta V}{T/m} \quad \text{G.4-10}$$

#### G.4.5 Flight Path Angle

A good approximation to the flight path angle,  $\gamma$  can be obtained by eliminating  $\frac{dV}{dt}$  from Equations G.4-3 and G.4-6:

$$\dot{\gamma} = 2 \frac{T}{W} \quad \text{G.4-11}$$

Note that the flight path angle increases with altitude as  $W$  decreases, even at constant mass.

#### G.5 Propellant Ratio Calculations

Commencing with a form of the classical rocket equation appropriate to inter-orbit transfer (Ref. G-3)

$$V = I_{sp} g_0 \ln \left[ \frac{m_{initial}}{m_{final}} \right] \quad \text{G.5-1}$$

and using the nomenclature:

$m_e$  = empty mass

$$K = \exp \frac{\Delta V}{I_{sp} g_0}$$

$m_p$  = total propellant mass

$f_s$  = stage mass fraction

$$m_p = m_{p1} + m_{p2}$$

$$f_s = \frac{m_p}{m_p + m_e}$$

$m_{pld}$  = payload mass

$P$  = propellant to payload mass ratio

$$P = \frac{m_p}{m_{pld}}$$

A relationship between  $P$  and  $f_s$  develops with  $K$  and staging as parameters. For a given mission a specific value can be assigned to  $K$ . If  $\Delta V$  is taken to be 4346 m/s (14,260 fps) and  $I_{sp}$  to be 460s, then  $K$  is 2.6209.

The two extreme cases of staging with no payload return are a single-stage vehicle expended (totally discarded) and a single-stage vehicle reused (completely recycled). These are treated as Case A and Case B below and are plotted on Fig. G-5.

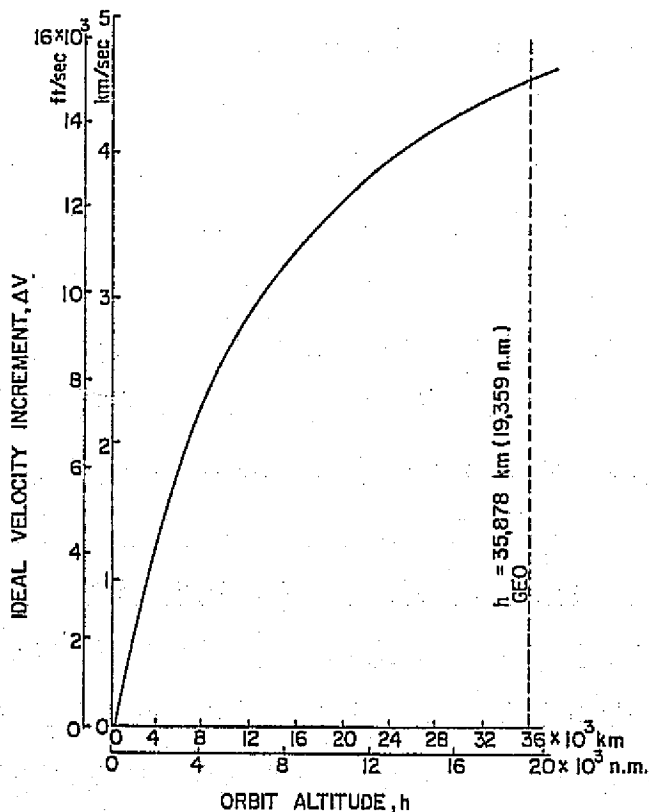


FIGURE G-4 IDEAL  $\Delta V$  FOR LOW THRUST CIRCULAR ORBIT TRANSFER

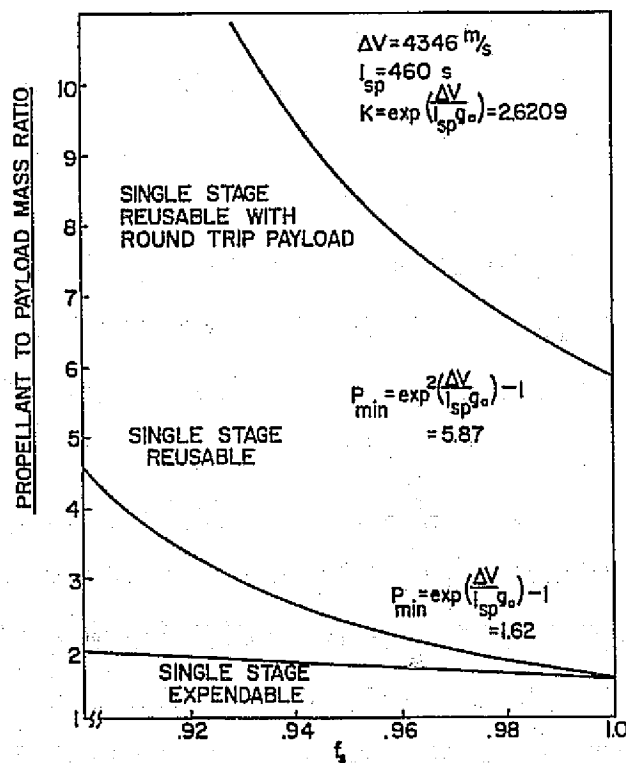


FIGURE G-5 STAGE MASS FRACTION

Case A: single-stage expended ( $m_{p2} = 0$ )

$$K = \frac{m_e + m_p + m_{p1d}}{m_e + m_{p1d}}$$

hence:

$$p = \frac{f_s (K - 1)}{K (f_s - 1) + 1}$$

G.5-2

$$P_{\min} = K - 1$$

Case B: single-stage reused

$$\text{out flight: } K = \frac{m_e + m_{p1} + m_{p2} + m_{p1d}}{m_e + m_{p2} + m_{p1d}}$$

$$\text{return flight } K = \frac{m_e + m_{p2}}{m_e}$$

$$\text{hence: } p = \frac{f_s (K - 1)}{K^2 (f_s - 1) + 1}$$

G.5-3

A third case is considered for a fully reusable single-stage vehicle that takes the payload (100%) roundtrip. This is given below as case C and is plotted Fig. G-5.

Case C: single-stage reused 100% payload return

$$\text{outflight } K = \frac{m_e + m_{p1} + m_{p2} + m_{p1d}}{m_e + m_{p2} + m_{p1d}}$$

$$\text{return flight } K = \frac{m_e + m_{p2} + m_{p1d}}{m_e + m_{p1d}}$$

$$\text{hence: } p = \frac{f_s (K^2 - 1)}{K^2 (f_s - 1) + 1}$$

G.5-4

$$P_{\min} = K^2 - 1$$

#### REFERENCES

- G-1 Apollo Navigation Working Group "Apollo Missions and Navigation Systems Characteristics." Technical Report No. AN-1.2, NASA, 1967.
- G-2 James B. Eades, Jr. "Elements of Orbital Transfer," Virginia Polytechnic Institute, Engineering Experiment Station Series No. 158, 1965.
- G-3 Arthur I. Berman, "Astronautics," John Wiley & Sons, Inc., 1961.
- G-4 Boeing Aerospace Company, "Future Space Transportation Systems Analysis Study," December 19, 1975.

APPENDIX H  
STATEMENT LISTING AND SAMPLE OUTPUT  
FOR THE TRANSPORTATION COST MODEL

This program is coded in the BASIC language. A loop begins at statement 40 and ends at 480 for  $J = 1$  to 20. When  $J=1$ , the baseline data are used to compute the baseline value of  $C_T$ . This value is retained under the label C9. For  $J=2$ , the sensitivity of  $C_T$  to the first of the nineteen input parameters is determined. The value of  $X(1)$  is increased by 1%,  $C_T$  is recalculated, and the percent change in  $C_T$  caused by the 1% change in  $X(1)$  is calculated. This is defined as the sensitivity for  $X(1)$ . As  $J$  is changed to 3,4, . . . , 20, this process is repeated and the sensitivity is determined for each of the other input parameters.

The output gives the baseline values for the 19 input parameters in order. The integer in the left column corresponds to  $(J-1)$ . It is followed in order by C1, C2, C3, C4, C, and 5. All computer symbols are defined at the end of this discussion. The first case is the baseline. The next nineteen cases give the sensitivity of each input parameter in order.

#### COMPUTER SYMBOLS

C	total transportation cost, $C_T$ (\$B)
C1	cost of transportation of cargo, earth to LEO (\$B)
C2	cost of transportation of cargo, LEO to GEO (\$B)
C3	cost of transporting personnel (\$B)
C4	other transportation costs (\$B)
C9	total transportation cost for the baseline case (\$B)
N	number of independent parameters
N1	number of COTV's required, $N_C$
N2	number of tug's required, $N_T$
S	sensitivity
T1	number of trips per satellite for the COTV, $T_c$
T2	number of trips per satellite for the tug, $T_T$
W	mass of the satellite (Kg)
W1	mass transported from LEO to GEO (Kg)
W2	mass transported from earth to GEO
X(1)	$a_h$
X(2)	$a_c$
X(3)	$m_{PL,C}$
X(4)	$m_{V,C}$
X(5)	$(F_{comp,C} + m_{ET,C})$
X(6)	$L_c$
X(7)	$a_T$
X(8)	$m_{PL,T}$
X(9)	$m_{V,T}$

X(10)	$(F_{T,p,T} + m_{ET,T})$
X(11)	$L_T$
X(12)	$b_L$
X(13)	$b_G$
X(14)	$m_{B,G}$
X(15)	$m_{B,L}$
X(16)	$f_{T,C}$
X(17)	$f_{P,G}$
X(18)	$N_p$
X(19)	$C_0$

ORIGINAL PAGE IS  
OF POOR QUALITY

LIS  
NORM

```
10 DIM XE50J
20 N=19
30 N3=N+1
40 FOR J=1 TO N3
50 L=J-1
60 XE1J=3.2E-08
70 XE2J=4.E-08
80 XE3J=250000.
90 XE4J=26000
100 XE5J=484000.
110 XE6J=30
120 XE7J=4.E-08
130 XE8J=250000.
140 XE9J=26000
150 XE10J=484000.
160 XE11J=30
170 XE12J=.0002
180 XE13J=.000065
190 XE14J=9.422E+06
200 XE15J=352000.
210 XE16J=1
220 XE17J=.73
230 XE18J=773.3
240 XE19J=0
250 W=8.1813E+07
260 IF J>1 THEN 310
270 FOR I=1 TO N
280 PRINT I,XEIJ
290 NEXT I
300 GOTO 320
310 XEIJ=1.01*XEIJ
320 W1=W+XE14J
330 T1=(XE16J*W+XE14J)/XE3J
340 N1=T1/XE6J
350 T2=(1-XE16J)*W/XE8J
360 N2=T2/XE11J
370 W2=W1+N1*XE4J+N2*XE9J+T1*XE5J+T2*XE10J+XE5J
380 C1=XE1J*W2
390 C2=(XE2J*XE16J+(1-XE16J)*XE7J)*W1
400 C3=(XE13J*XE17J+XE12J)*XE18J
410 C4=XE19J
420 C=C1+C2+C3+C4
430 IF J=1 THEN 450
440 GOTO 460
450 C9=C
460 S=ABS((C-C9)/C9)*100
470 PRINT L,C1,C2,C3,C4,C,S
480 NEXT J
490 STOP
500 END
```

ORIGINAL PAGE IS  
OF POOR QUALITY

RUN  
NORM

1	3.20000E-08			
2	4.00000E-08			
3	250000.			
4	26000			
5	484000.			
6	30			
7	4.00000E-08			
8	250000.			
9	26000			
10	484000.			
11	30			
12	.0002			
13	.000065			
14	9.42200E+06			
15	352000.			
16	1			
17	.73			
18	773.3			
19	0			
0	8.59732	3.6494	.191353	0
12.4381	0			
1	8.6833	3.6494	.191353	0
12.524	.691214			
2	8.59732	3.68589	.191353	0
12.4746	.2934			
3	8.54126	3.6494	.191353	0
12.382	.450734			
4	8.59742	3.6494	.191353	0
12.4382	8.12742E-04			
5	8.654	3.6494	.191353	0
12.4948	.455672			
6	8.59722	3.6494	.191353	0
12.438	8.12742E-04			
7	8.59732	3.6494	.191353	0
12.4381	0			
8	8.59732	3.6494	.191353	0
12.4381	0			
9	8.59732	3.6494	.191353	0
12.4381	0			
10	8.59732	3.6494	.191353	0
12.4381	0			
11	8.59732	3.6494	.191353	0
12.4381	0			
12	8.59732	3.6494	.1929	0
12.4396	1.24365E-02			
13	8.59732	3.6494	.19172	0
12.4384	2.95961E-03			

14	8.60619	3.65317	.191353	0
12.4507	.101562			
15	8.59732	3.6494	.191353	0
12.4381	0			
16	8.59732	3.6494	.191353	0
12.4381	1.53348E-05			
17	8.59732	3.6494	.19172	0
12.4384	2.95961E-03			
18	8.59732	3.6494	.193267	0
12.44	1.53808E-02			
19	8.59732	3.6494	.191353	0
12.4381	0			

DONE

ORIGINAL PAGE IS  
OF POOR QUALITY

APPENDIX I  
MODELS FOR DEVELOPING  
THE SPS DELIVERY FLEET

## APPENDIX - I MODELS FOR DEVELOPING THE SPS DELIVERY FLEET

### I-1 UTILITY OF THE MODEL

A MODEL for the optimum development rate of the SPS population is a crucial prerequisite to decision making for the delivery fleet. Once prepared, the model will provide development rates for vehicle fleets, and their propellant requirements. Several tabulated schemes have been generated for thirty year intervals, but apparently no attempt has been made to make functional models. These mathematical models would permit changes in the initial and final growth rates, time periods for development and the general scheme of time development.

The relationship between transportation elements, flight scheduling, and satellite construction rates have been established. Those relationships provide the necessary link between construction logistics and the material delivery rate. For example, the material delivery rate is directly dependent on the derivative of the function describing the SPS population.

### I-2 ECONOMIC CONSIDERATIONS

Desireable features of the population (SPS) development in time curve will eventually be indicated by economic considerations. The fraction project completion vs time proposed by Ron Harron in the Executive Summary of JSC 11443 as a tabulated quantity has been fitted with a parabola and plotted in Figure I-1. No rationale has been given for a parabolic shape, and it is most likely not optimal. In most industries the development has followed an "S-shaped curve". One function which may be used to generate such a curve is the hyperbolic tangent symmetric about the origin. This curve is also shown in Figure I-1 for comparison. The factors to be used in establishing optimal curve shape would be similar to those in section 8.6.3.

### I-3 THE "HYPERBOLIC TANGENT MODEL"

In the curve fit for Harron's data the parabola was used:

$$n = 0.117t^2 + 0.21 t$$

with t, the elapsed time: in years, and N the number of satellites completed. The total after 30 years was 112.

$$\int_0^{30} n dt = 112 = N$$

The parabola has an ever increasing slope, which in practice does not allow a tapering off of fleet sizes, work crews and assembly equipment. An alternate consideration may be based on the economic considerations above and then employing the hyperbolic tangent function. By adjusting the independent variable, the initial and final rates of change can be equal or different (symmetry about the origin) and can be varied from zero (effectively) to any constant by ranging over different portions of the curve, Figures I-2 and I-3. The integral is normalized so that N satellites are constructed in a period T.

$$\frac{n}{N} = 0.552 \tanh \left( \frac{t}{T} - 0.5 \right)$$

Is a version of the model that is plotted in Figure I-1. It has the constants set so that one satellite would be built the first year and one in the last year of the program. The construction rate is greatest half-way through the program. The integral of the right hand side over a period of t/T from 0 to 1 will give a value of one.

The model in its general form is

$$\frac{n}{N} = A \tanh \left( \frac{t}{T} - B \right) \text{ ----- I-1}$$

The slope is given by  $A (1 - \tanh^2(\frac{t}{T} - B))$  and is used to determine the fleet size necessary at any time,  $t$ .

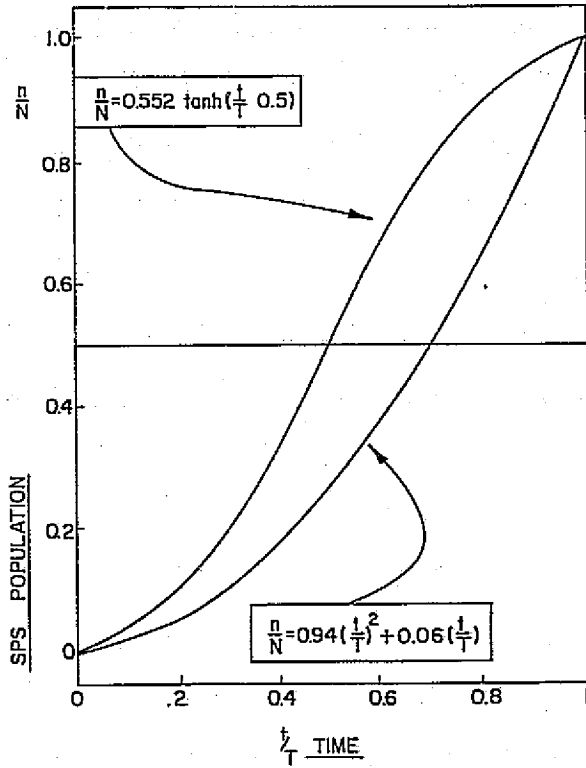


FIGURE I-1 SPS POPULATION

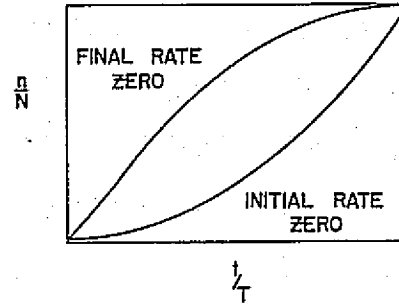


FIGURE I-2 ORIGIN SHIFT

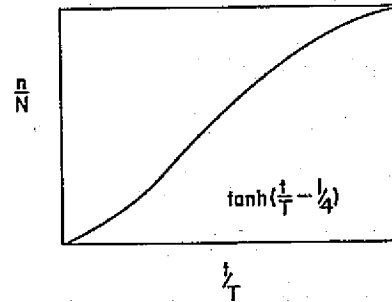


FIGURE I-3 UNSYMMETRICAL CASE

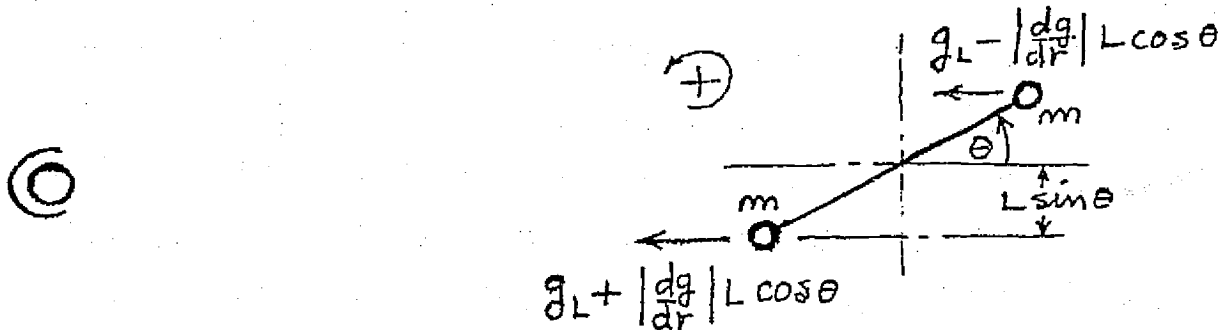
APPENDIX J

GRAVITY-GRADIENT TORQUES

APPENDIX J - GRAVITY-GRADIENT TORQUES

The question of calculation of gravity-gradient effects, including torques due to gravity gradient, arises early in the consideration of attitude-control of an orbiting body which has a non-spherical mass moment of inertia.

The effect may be seen by considering the following diagrams where  $\odot$  is the center of attraction,  $g_L$  is the gravitational acceleration at the center of gravity of an extensive body and  $2L$  is the length of the extensive body.



The effect of the specific forces shown are a force  $2g_L m$  (to first order) and a moment:

$$M = mL \sin \theta \left\{ g_L - \left| \frac{dg}{dr} \right| L \cos \theta - g_L - \left| \frac{dg}{dr} \right| L \cos \theta \right\}$$

or:

$$M = 2mL^2 \sin \theta \cos \theta \frac{dg}{dr} \quad (1)$$

Note that  $2mL^2$  represents the maximum moment of inertia of the extensive body about an axis in the plane of the diagram, and note too that other moments of inertia were zero. Were we to consider a body with non-zero maximum and minimum moments of inertia about axes in the orbit plane, as per the following diagram, (Fig. J-1).



FIGURE J-1 AXES IN THE ORBIT PLANE

equation 1 may be re-written as:

$$M = (I_{xx} - I_{yy}) \sin\theta \cos\theta \frac{dg}{dr} \quad (2)$$

But  $g = \mu r^{-2}$  so we may write:

$$\frac{dg}{dr} = -2\mu/r^3 \quad (3)$$

Noting that:

$$\frac{2\pi}{\tau} = (\mu/r^3)^{1/2} ,$$

Where  $\tau$  is the period of a circular orbit, we may also write:

$$\frac{dg}{dr} = -2 \left(\frac{2\pi}{\tau}\right)^2 \quad (4)$$

And in terms of period  $\tau$ , equation (2) may be re-written:

$$M = -2(I_{xx} - I_{yy}) \sin\theta \cos\theta \left(\frac{2\pi}{\tau}\right)^2 \quad (5)$$

Noting the  $dg/dr$  is negative, and noting the signs of the functions sine and  $\cos\theta$  and the sign convention for torque, we may conclude that the stable and the unstable orientations for a baton in orbit are as shown in Figure J-2.

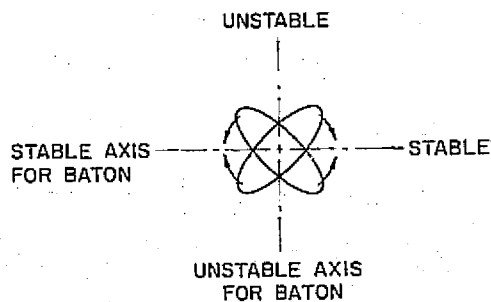


FIGURE J-2 ORIENTATION FOR BATON IN ORBIT

Note that if  $I_{xx} \gg I_{yy}$ , equation (5) yields the approximations:

$$\ddot{\theta}_{\max} \approx \left(\frac{2\pi}{\tau}\right)^2$$

$$M_{\max} \approx I_{xx} \left(\frac{2\pi}{\tau}\right)^2$$

$$\ddot{\theta} \approx 2\theta \left(\frac{2\pi}{\tau}\right)^2 \quad \text{For } \theta \ll 1$$

$$M \approx 2I_{xx} \theta \left(\frac{2\pi}{\tau}\right)^2 \quad \text{For } \theta \ll 1$$

For a body such as the 60km<sup>2</sup> truss in orbit, we have:

$$I_{xx} - I_{yy} \approx 2.7 \times 10^{14} \text{ (KGM}^2\text{)},$$

and in low-earth orbit,

$$M_{\max} \sim 4 \times 10^8 \text{ (KGM}^2\text{/SEC}^2\text{)}$$

$$\ddot{\theta}_{\max} \sim 1.4 \times 10^{-6} \text{ (SEC}^{-2}\text{)}$$

In geosynchronous orbit,

$$M_{\max} \sim 1.6 \times 10^6 \text{ (KGM}^2\text{/SEC}^2\text{)}$$

$$\ddot{\theta}_{\max} \sim 5.6 \times 10^{-9} \text{ (SEC}^{-2}\text{)}.$$

APPENDIX K  
ELECTRIC THRUSTER MASS AND  
TRANSPORTATION ANALYSIS PROGRAM

## Appendix K ELECTRIC THRUSTER MASS AND TRANSPORTATION ANALYSIS PROGRAM.

The digital computer program used for analysis and comparison of the electrical propulsion OTV candidates is written in BASIC. A listing of the program called COMBIN, appears as Figure K-1A-D. Definitions of the symbols used are provided in Table K-2.

COMBIN is an interactive program which is designed to accomplish the tasks listed below:

1. Evaluate SPS engine, propellant, tankage, and SECS growth requirements for various initial LEO thrust to mass ratios and mission profiles.
2. Determine the time of transfer from LEO to GEO equivalent altitude.
3. Provide a detailed breakdown of SPS transportation costs.
4. Permit an evaluation of the "elasticity" of transportation costs through a user called option which varies each of 12 parameters by  $\pm 1\%$ .

The operation of the program may be followed with the aid of a flow chart keyed to the program listing (Figure K-1). Steps 10 through 340 permit the user to define key engine parameters and assign costs to the various system components. Once this has been accomplished, the user is asked to select one of the three program options; he may either:

1. Run the program for a single thrust to mass ratio of  $10^{-4}g_0$  for each of the four cases corresponding to the combination of the two launch latitudes and two degradation rates.
2. Run the program for each of the four launch latitude/degradation rate cases stepping through a thrust to mass range of  $3.6 \times 10^{-4}g_0$  to  $3 \times 10^{-5}g_0$ .
3. Vary each of the 10 input parameters as well as the  $\Delta V$  and time constant by  $\pm 1\%$  for a nominal case.

Once the program parameters have been initialized, the computation begins at line 1600 with a calculation of the total mass of the SPS and a computation of the number of engines required. The expression for the number of engines is obtained by solving the following statement of Newton's third law:

Number of Engines x Thrust/Engine

$$= [\text{Satellite Mass} + (\text{Number of Engines}) \times \text{Mass/Engine} + \text{Mass of Propellant and Tankage}] \times \text{Acceleration}$$

$$= [\text{Satellite Mass} + (\text{Number of Engines}) \times \text{Mass/Engine}]$$

$$\times \left\{ \frac{\left[ \frac{\text{GEO Mass} + \text{Propellant Mass Required}}{\text{GEO Mass}} - 1 \right]}{\left[ \frac{\text{Useable Propellant Mass}}{\text{Total LEO Tank} + \text{Propellant Mass}} \right]} + 1 \right\} \times \text{Acceleration}$$

In terms of the program variables this becomes:

$$N*T = (M + N*TL) \{ [\exp(D/G*I) - 1] / M7 + 1 \} *A$$

where the usable propellant to total LEO tank and propellant mass ratio has been approximated by the propellant mass fraction.

Once the number of engines has been determined, this number is tested for feasibility. Should the result prove satisfactory, the engine power requirements are computed. As the power requirement corresponds to exposure of a certain amount of solar cell area for a specified length of time, SECS growth can be determined. A new total mass is then calculated, repeating the process. This technique is employed until the change in the number of engines from one iteration to the next is less than 1%.

Having converged on a solution for the number of engines and corresponding LEO start mass, the trip time is corrected to compensate for changes in the mass of the OTV enroute. The mass, which is recalculated once each orbit, depends on the propellant mass flow rate and varies with the accumulated orbital transfer time. The orbital transfer time is the sum of the time for each orbit as determined using the constant thrust to mass, low thrust equations (Appendix G-4).

Once GEO equivalent altitude has been attained, the accumulated time is increased by an additional 10% to account for occultation effects. (No compensation was made for thrust vector losses). The system masses are then recomputed using the updated trip time. This new result is then used to calculate the various transportation costs.

In closing, it should be noted that the technique employed in calculating the corrected trip time is unnecessarily time consuming. Considerable savings in CPU time may be achieved by using a more efficient iteration scheme.

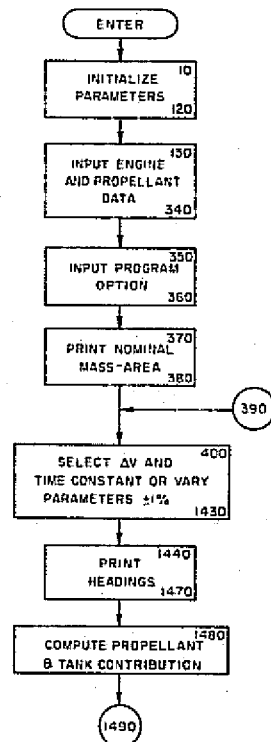


FIGURE K-1A  
COMBIN FLOW CHART

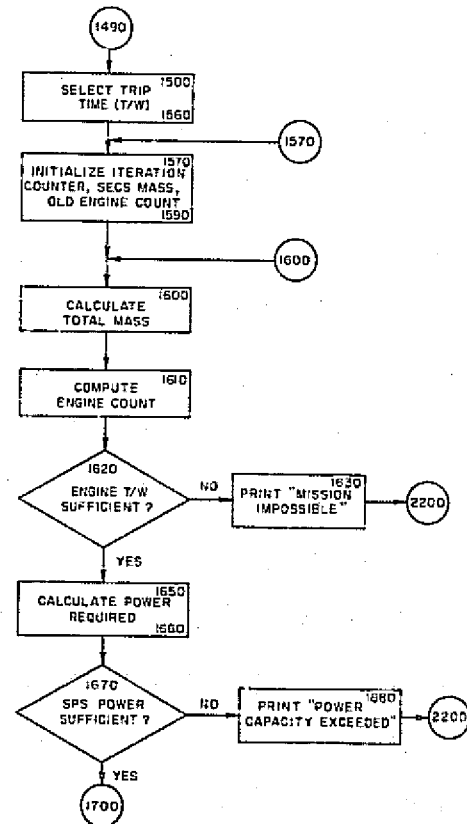


FIGURE K-1B FLOW CHART

ORIGINAL PAGE IS  
OF POOR QUALITY

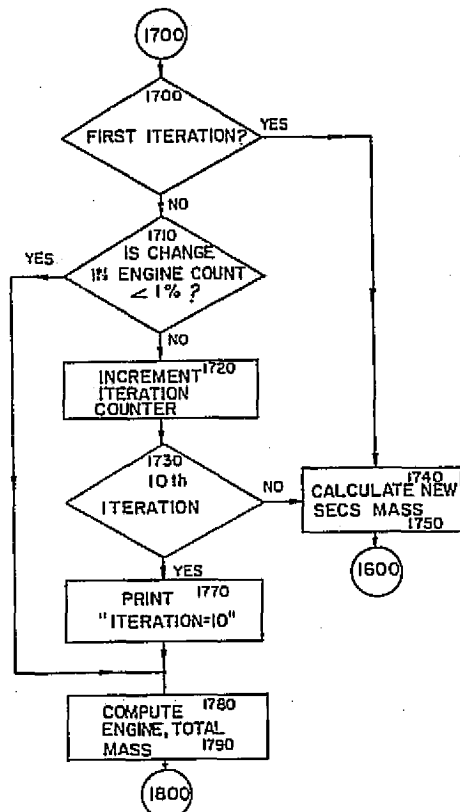


FIGURE K-1C FLOW CHART

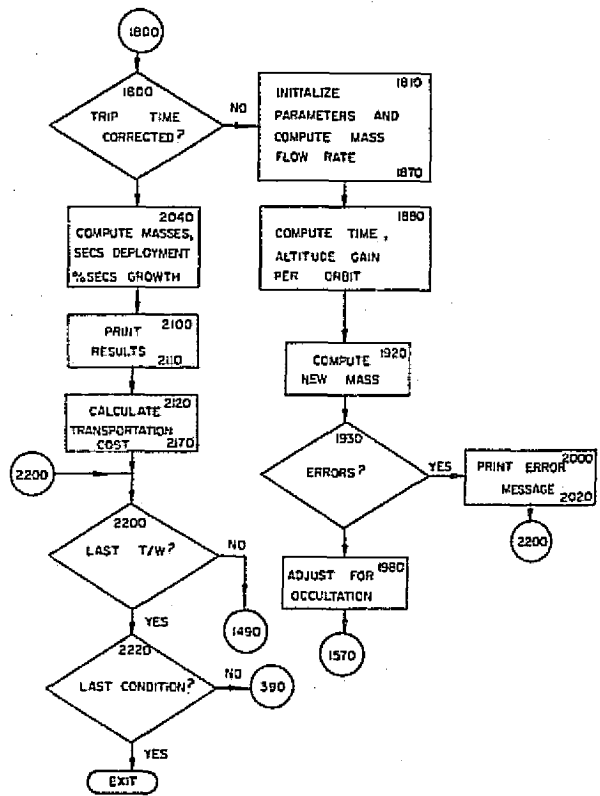


FIGURE K-1D FLOW CHART

ORIGINAL PAGE IS  
OF POOR QUALITY

TABLE K-1  
LISTING OF COMPUTER  
PROGRAM COMBIN

LIS  
COMBIN

```
10 DIM T$(30)
20 M1=20427+120+40
30 M2=65167.
40 C=4.536E-04
50 R0=3440
60 F4=12.5664
70 H8=270
80 T0=.058663
90 X=86400.
100 G=32.2
110 P1=1.6E+07
120 C1=1.E+06
130 PRINT "ENGINE TYPE"
140 INPUT T$
150 PRINT "ENGINE COST/UNIT"
160 INPUT F1
170 PRINT "FUEL COST/LB"
180 INPUT F2
190 PRINT "SPECIFIC IMPULSE"
200 INPUT I
210 PRINT "THRUST IN POUNDS"
220 INPUT T
230 PRINT "THRUST TO WEIGHT RATIO"
240 INPUT T1
250 PRINT "KW/LB THRUST"
260 INPUT F2
270 PRINT "CONVERSION EFFICIENCY"
280 INPUT X1
290 PRINT "MASS FRACTION"
300 INPUT M7
310 PRINT "PROPELLANT GLOW FRACTION"
320 INPUT F3
330 PRINT "TANK COST IN MILLIONS"
340 INPUT F4
350 PRINT "FULL SCAN=1, VARY PARAMETERS=2, ELSE=0"
360 INPUT X2
370 PRINT "NOMINAL MASS = 189E+6 LBM --- NOMINAL SECS AREA
= 144 SQ KM"
380 PRINT "NOMINAL SECS WEIGHT = 144E+6 LBS"
390 FOR X3=1 TO 36
400 IF X2#2 THEN 1350
```

```

410 IF X3#1 THEN 460
420 D=22405
430 T3=120
440 Z=1
450 Z1=1
460 GOTO Z1 OF 470,510,550,590,630,670,710,750,790,830,870,910
470 Z2=F1
480 PRINT USING 490
490 IMAGE #, "ENG'N COST "
500 GOTO 940
510 Z2=F2
520 PRINT USING 530
530 IMAGE #, "FUEL COST "
540 GOTO 940
550 Z2=I
560 PRINT USING 570
570 IMAGE #, "SPECIFIC IMPULSE "
580 GOTO 940
590 Z2=T
600 PRINT USING 610
610 IMAGE #, "THRUST "
620 GOTO 940
630 Z2=T1
640 PRINT USING 650
650 IMAGE #, "T/W "
660 GOTO 940
670 Z2=P2
680 PRINT USING 690
690 IMAGE #, "KW/LB OF THRUST "
700 GOTO 940
710 Z2=X1
720 PRINT USING 730
730 IMAGE #, "CONVERSION EFFICIENCY "
740 GOTO 940
750 Z2=M7
760 PRINT USING 770
770 IMAGE #, "MASS FRACTION "
780 GOTO 940
790 Z2=F3
800 PRINT USING 810
810 IMAGE #, "PROPELLANT GLOW FRACTION "
820 GOTO 940
830 Z2=F4
840 PRINT USING 850
850 IMAGE #, "TANK COST "
860 GOTO 940
870 Z2=D
880 PRINT USING 890
890 IMAGE #, "DELTA V "
900 GOTO 940

```

ORIGINAL PAGE IS  
OF POOR QUALITY

```

910 Z2=T3
920 PRINT USING 930
930 IMAGE #, "DEGRADATION TIME CONSTANT "
940 GOTO Z OF 950,990,1030
950 Z2=Z2*.99
960 PRINT USING 970
970 IMAGE "VARIED BY -1%"
980 GOTO 1040
990 Z2=Z2*1.01/.99
1000 PRINT USING 1010
1010 IMAGE "VARIED BY +1%"
1020 GOTO 1060
1030 Z2=Z2/1.01
1040 PRINT USING 1050
1050 IMAGE "EQUAL TO NOMINAL VALUE"
1060 GOTO Z1 OF 1070,1090,1110,1130,1150,1170,1190,1210,1230,1250,
1270,1290
1070 F1=Z2
1080 GOTO 1300
1090 F2=Z2
1100 GOTO 1300
1110 T=Z2
1120 GOTO 1300
1130 T=Z2
1140 GOTO 1300
1150 T1=Z2
1160 GOTO 1300
1170 P2=Z2
1180 GOTO 1300
1190 X1=Z2
1200 GOTO 1300
1210 M7=Z2
1220 GOTO 1300
1230 F3=Z2
1240 GOTO 1300
1250 F4=Z2
1260 GOTO 1300
1270 D=Z2
1280 GOTO 1300
1290 T3=Z2
1300 Z=Z+1
1310 IF Z#4 THEN 1440
1320 Z=1
1330 Z1=Z1+1
1340 GOTO 1440
1350 IF X3>4 THEN 2220
1360 GOTO X3 OF 1370,1370,1390,1390
1370 D=22405
1380 GOTO 1400
1390 D=16691

```

```

1400 GOTO X3 OF 1410,1430,1410,1430
1410 T3=300
1420 GOTO 1440
1430 T3=120
1440 PRINT USING 1450:D,T3
1450 IMAGE "DELTA V = ",5D,"FPS ---- TIME CONSTANT = ",3D,"DAYS"
1460 PRINT "DAYS      T/W      NUMBER ENGN  PROP      TANKS      SECS
TOTAL      DEPL-50 KM"
1470 PRINT "          LBS/LBM      ENG/RV MLBS/% MLBS/%  MLBS/%      %/%
MLBS/%  TRANS-M%"
1480 M3=(EXP(D/(G*I))-1)/M7+1
1490 FOR J1=15 TO 195 STEP 15
1500 IF J1=195 THEN 1540
1510 IF X2#1 THEN 2200
1520 J=J1
1530 GOTO 1550
1540 J=54
1550 I2=0
1560 A=.0054/J
1570 I1=0
1580 M4=M2
1590 N1=0
1600 M=(M1+M4)/C
1610 N=(A*M*M3)/((1-(A*M3)/T1)*T)
1620 IF N>0 THEN 1650
1630 PRINT "MISSION IMPOSSIBLE"
1640 GOTO 2200
1650 N=INT(N)
1660 F=N*T*P2/X1
1670 IF P <= P1 THEN 1700
1680 PRINT "POWER CAPACITY EXCEEDED"
1690 GOTO 2200
1700 IF N1=0 THEN 1740
1710 IF (N-N1)/N1<.01 THEN 1780
1720 I1=I1+1
1730 IF I1=10 THEN 1770
1740 N1=N
1750 M4=M2*(1+(F/P1)*(EXP(J/T3)-1))
1760 GOTO 1600
1770 PRINT "ITERATION=10"
1780 M8=N*T/(T1*C1)
1790 M6=(M/C1+M8)*M3
1800 IF I2#0 THEN 2040
1810 J=0
1820 I2=1
1830 N9=0
1840 M6=M6*C1
1850 M5=N*T/I
1860 T2=A

```

ORIGINAL PAGE IS  
OF POOR QUALITY

```

1870 H=H8
1880 F=1+H/R0
1890 N9=N9+1
1900 J=J+T0*(F ** 1.5)
1910 H=H+R0*T2*F4*(F ** 3)
1920 T7=M6-M5*J*X
1930 IF T7<0 THEN 2000
1940 T2=N*T/T7
1950 IF J>180 THEN 2020
1960 IF H >= 19358 THEN 1980
1970 GOTO 1880
1980 J=J*1.1
1990 GOTO 1570
2000 PRINT "ERROR -- WEIGHT"
2010 GOTO 2200
2020 PRINT "ERROR -- TIME"
2030 GOTO 2200
2040 M9=M6-M/C1-M8
2050 T4=M9*F3
2060 T5=M9-T4
2070 S2=(M4/M2-1)*100
2080 M4=M4/(C*C1)
2090 S1=P*EXP(J/T3)*144/P1
2100 PRINT USING 2110;J,A,N,M8,T4,T5,S2,M6,S1
2110 IMAGE 4D,2X,D,DDE,1X,7D,2X,3D,D,2X,3D,D,3X,3D,D,3X,3D,D,
3X,4D,D,6X,3D,D
2120 C3=N*F1/C1
2130 C5=T4*F2
2140 C4=M9*F4
2150 C6=S2*M2*2.19045E-03
2160 C8=M6*C*32000
2170 C9=C3+C4+C5+C6+C8+400+160+210+10
2180 PRINT USING 2190;T2,N9,C3,C5,C4,C6,C8,C9
2190 IMAGE "MEGA# ",D,DDE,4X,4D,1X,4D,D,1X,4D,D,1X,5D,D,1X,5D,D,
1X,6D,D,2X,7D,D
2200 NEXT J1
2210 PRINT " "
2220 NEXT X3
2230 END

```

TABLE K-2  
ELECTRIC THRUSTER MASS AND  
TRANSPORTATION COST ANALYSIS PROGRAM

SYMBOL TABLE

A	Initial Acceleration - g's (T/W)
C	Conversion Factor - tonnes to $10^6$ lbm
C1	Conversion Factor - $10^6$
C3	Total Engine Cost - $10^6$ s
C4	Total Tank Cost - $10^6$ s
C5	Total Propellant Cost - $10^6$ s
C6	Cost of SECS Increase - $10^6$ s
C8	HLLV Cost - $10^6$ s
C9	Overall Transportation Cost - $10^6$ s
D	Delta V - ft/sec
F	Normalized Radius of Orbit
F1	Engine Cost - \$/unit
F2	Propellant Cost - \$/lb
F3	Propellant Glow Fraction - fraction of propellant/total tank weight at lift-off
F4	Tank Cost - $10^6$ s/unit
G	Acceleration of Gravity - ft/sec <sup>2</sup>
H	Altitude - nautical miles
H8	LEO Altitude - nautical miles
I	Specific Impulse - seconds
I1	Iteration Counter - mass determination, max. = 10
I2	Pass Counter - Trip time calculated when I2 = 0
J	Days
J1	Day Counter
M	Satellite and Cargo Mass - lbm
M1	MPTS and Cargo Mass - tonnes
M2	Initial SECS Mass - tonnes
M3	$1 + [(Propellant + Tanks) Fraction]$
M4	Variable SECS Mass - tonnes
M5	Mass Flow Rate - lbm/sec
M6	Total LEO start Mass - $10^6$ lbm
M7	Propellant Mass Fraction - usable propellant/total tank weight at lift-off
M8	Engine Mass - $10^6$ lbm

ORIGINAL FILED  
DEPT. OF DEFENSE

M9	Mass of Propellant and Tanks - $10^6$ lbm
N	Number of Engines
N1	Engines from Previous Iteration
N9	Number of Orbits
P	Power Required - Kw
P1	Nominal Power in GEO - $16 \times 10^6$ kw
P2	Power/Thrust - kw/lb
P4	Constant - $4\pi$
R0	Radius of Earth - nautical miles
S1	SECS area Deployed - Sq. km
S2	% SECS Growth
T	Thrust - lbs
T0	Orbit Reference Time - Days
T1	Thrust/Mass Ratio - g's (T/W)
T2	Variable Thrust/Mass Ratio - g's (T/W)
T3	Degradation Time Constant - Days
T4	Mass of Propellant at Lift-off - $10^6$ lbm
T5	Mass of Tanks - $10^6$ lbm
T7	Total Mass Variable - $10^6$ lbm
Ts	Engine Name
X	Conversion Factor - days to seconds
X1	Power Conditioning Equipment Conversion Efficiency
X2	Decision Variable
X3	Iteration Counter - sets conditions
Z	Condition Counter - $\pm 1\%$ or $0\%$
Z1	Parameter Counter
Z2	Temporary Storage

APPENDIX I  
EFFECT OF ATTITUDINAL VARIATIONS  
RELATIVE TO THE SUN

## APPENDIX L - EFFECT OF ATTITUDINAL VARIATIONS RELATIVE TO THE SUN

The output power available from the Solar Energy Collection System is highly dependent on the amount of solar power incident upon it. As the SPS varies from perfect alignment with respect to the solar line of sight, the incident power and hence the output power of the satellite also vary. The effect of the solar concentrators on this variation is considered in detail in this appendix.

The configuration of the Solar Energy Collection System is trough-like with a cross-section as shown in Figure L-1. The slanted walls are reflectors, while the solar cells are deployed along the bottom of the trough. It is designed to have a concentration of two, i.e.,

$$\text{Concentration Ratio} = \frac{W_1}{W_2} = 2$$

Note that this geometry implies that  $\phi$  must equal  $60^\circ$  and that the area of each concentrator must equal that of the solar cell blanket, Figure L-2. If perfectly reflecting concentrators and precise alignment with respect to the sun is assumed, the effective cross-sectional area of the solar cells is doubled. The ratio of the effective cross-sectional area to the actual area of the solar cell blanket is referred to herein as the effective concentration ratio, K.

If the SPS is oriented such that the solar line of sight is  $n$  longer normal to the plane of the solar blanket, the effective concentration ratio is reduced. For simplicity, the problem is separated into two cases:

1. Angular variation in a plane perpendicular to the floor of the trough and parallel to the intersections of the trough walls and floor; a departure from perfect alignment of the solar line of sight with the solar cell blanket's normal in this plane is labeled  $\alpha$ .
2. Angular variation in a plane perpendicular to the walls and floor of the trough; a departure from perfect alignment of the solar line of sight with the solar blanket's normal in this plane is labeled  $\beta$ .

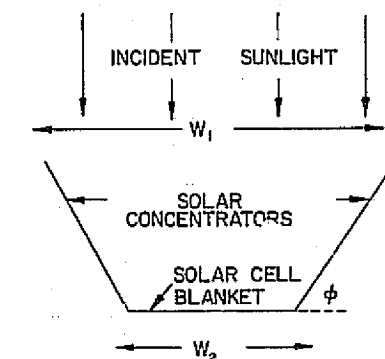
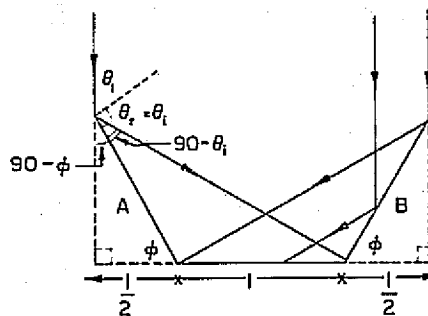


FIGURE L-1 SECS CONFIGURATION  
REF. 5-50



$$\frac{1}{2} = \sin(90 - \phi) = \sin(90 - \theta_1)$$

$$\phi = 60^\circ$$

$$A = B = \frac{1}{2} \div \cos \phi = 1$$

FIGURE L-2 GEOMETRY OF SOLAR CONCENTRATOR

### 1 Variations in $\alpha$ .

The case where  $\beta = 0$  and  $\alpha$  is permitted to vary is quite straight forward. Rotation in this direction merely causes a decrease in the projection of the array onto a plane perpendicular to the solar line of sight. The area of this projection, referred to as the perpendicular area, varies as  $\cos \alpha$ .

### 2 Variations in $\beta$ .

The case where  $\alpha = 0$  and  $\beta$  varies is considerably more complex. In order to tackle the problem, it must be divided into three major angular ranges.

1.  $0 \leq \beta \leq 30$  - Pre-occultation
2.  $30 \leq \beta \leq 60$  - Partial occultation

and 3.  $60 \leq \beta \leq 90$  -Total occultation

The third range, of course, is trivial and does not require further discussion.

### 2.1 Pre-occultation.

With this range, there are three contributions to the solar power incident on the blanket; referring to Figure L-3 these are direct light, light reflected from panel A and light reflected from panel B. Of these, the contribution of direct light is most easily determined being proportional only to the blanket's perpendicular area. Its contribution to the effective concentration ratio is therefore:

$$\text{Direct} = 1 \cos \beta .$$

Considering panel A, it is observed that as  $\beta$  increases, the panel's perpendicular area also increases, thus increasing the amount of power reflected by the panel. However, as  $\beta$  increases, the angle of incidence,  $\theta_i = \gamma_i = 60^\circ - \beta$ , decreases. As a result, not all of the reflected light reaches the solar panel. Only a fraction X, where

$$X = \frac{\sin (30^\circ - \beta)}{\sin (30^\circ + \beta)} ,$$

actually impinges on the solar cells, the remaining light being reflected away by panel B. Thus, the contribution of panel A to the effective concentration ratio is,

$$\text{Panel A} = \sin (30^\circ + \beta) \left[ \frac{\sin (30^\circ - \beta)}{\sin (30^\circ + \beta)} \right] = \sin (30^\circ - \beta)$$

Turning to panel B, it is found that all of the light reflected by this panel impinges on a fraction Y of the solar cell blanket. Using the law of sines, Y is determined to be

$$Y = \frac{\sin (30^\circ - \beta)}{\sin (30^\circ + \beta)}$$

Since the perpendicular area of panel B decreases with  $\beta$  as  $\sin (30^\circ - \beta)$ , the contribution of panel B to the overall effective concentration ratio is

$$\text{Panel B} = 0$$

$$0 \leq Y \leq 1 - Y$$

$$\text{Panel B} = \sin (30^\circ - \beta)$$

$$1 - Y \leq Y \leq 1$$

where y is the fractional distance across the bottom of the trough.

### 2.2 Partial Occultation.

When  $\beta$  is greater than  $30^\circ$ , panel B no longer makes a contribution to the effective solar concentration ratio. Rather, it reduces the effective concentration by blocking part of the incident light from reaching a fraction

$$Z = \frac{\sin (\beta - 30^\circ)}{\sin (90^\circ - \beta)}$$

of the solar blanket, Figure L-4. Thus, the contribution of direct light to the overall effective concentration ratio is

$$\text{Direct} = \cos$$

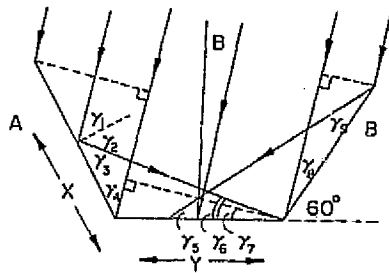
$$0 \leq Y \leq 1 - Z$$

$$\text{Direct} = 0$$

$$1 - Z \leq Y \leq 1$$

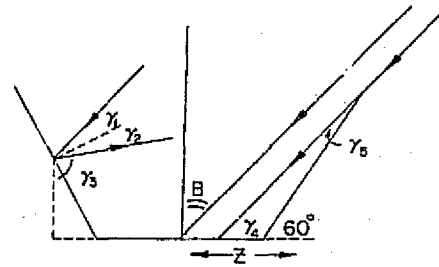
Note that the solar cell blanket is shielded from direct sunlight ( $Z = 1$ ) when  $\beta$  reaches  $60^\circ$ .

Turning now to panel B, it is found that it no longer contributes to the overall effective concentration ratio as its light is reflected away from the solar cells.



$$\begin{aligned} \gamma_2 = \gamma_1 &= 60^\circ - B \\ \gamma_3 = \gamma_4 = \gamma_5 &= 30^\circ - B \\ \gamma_6 = \gamma_6 = \gamma_6 &= 30^\circ - B \\ \gamma_7 &= B \\ 0 &= B < 30^\circ \end{aligned}$$

FIGURE L-3 GEOMETRY FOR REFLECTOR



$$\begin{aligned} \gamma_1 = \gamma_2 &= 60^\circ - B \\ \gamma_3 &= 60^\circ + B \\ \gamma_4 &= 90^\circ - B \\ \gamma_5 &= B - 30^\circ \\ 30^\circ &\leq B < 60^\circ \end{aligned}$$

FIGURE L-4 GEOMETRY FOR REFLECTOR  
NOTE: WALLS OF TROUGH AND FLOOR = 1 UNIT

### 2.3 Summary of Variations of K with $\beta$ .

The results for angular variations in  $\beta$  with  $\alpha = 0$  have been combined and are summarized below:

If  $0 \leq \beta \leq 30^\circ$  then

$$K = \cos \beta + \sin (30^\circ - \beta) \text{ for } 0 \leq y \leq 1 - Y$$

$$K = \cos \beta + 2\sin (30^\circ - \beta) \text{ for } 1 - Y \leq y \leq 1$$

$$\text{where } Y = \frac{\sin (30^\circ - \beta)}{\sin (30^\circ + \beta)}$$

If  $30^\circ < \beta < 60^\circ$  then

$$K = \cos \beta \text{ for } 0 \leq y \leq 1 - z$$

$$K = 0 \text{ for } 1 - z \leq y \leq 1$$

$$\text{where } z = \frac{\sin (\beta - 30^\circ)}{\sin (90^\circ - \beta)}$$

If  $60^\circ \leq \beta < 90^\circ$  then

$$K = 0$$

A plot of the resultant function is shown in Figure L-5.

### 3 Comparison of Results.

Figure 5 points out the need for precise attitude control of the SPS. While an angular variation of  $30^\circ$  in  $\alpha$  results in a 13.4% reduction of power incident on the solar cell blanket, a similar variation in  $\beta$  will result in a 56.7% reduction. While large angles of  $\alpha$  and  $\beta$  might be of interest when the SPS is first oriented towards the sun during the

initial phases of the flight, small variations in alignment and the resultant power dips they cause are of importance during orbital transfer and on station operations. Taking the derivative of  $K$  first with respect to  $\alpha$  and then with respect to  $\beta$ , it is easy to demonstrate that for small angles ( $\alpha$  and  $\beta$  both approximately zero) the rate of change in  $K$  with  $\alpha$  is approximately zero, while the rate of change of the effective solar cell concentration ratio with  $\beta$  is approximately 1.5%/degree. This result indicates that a high degree of pointing accuracy is required for the SPS

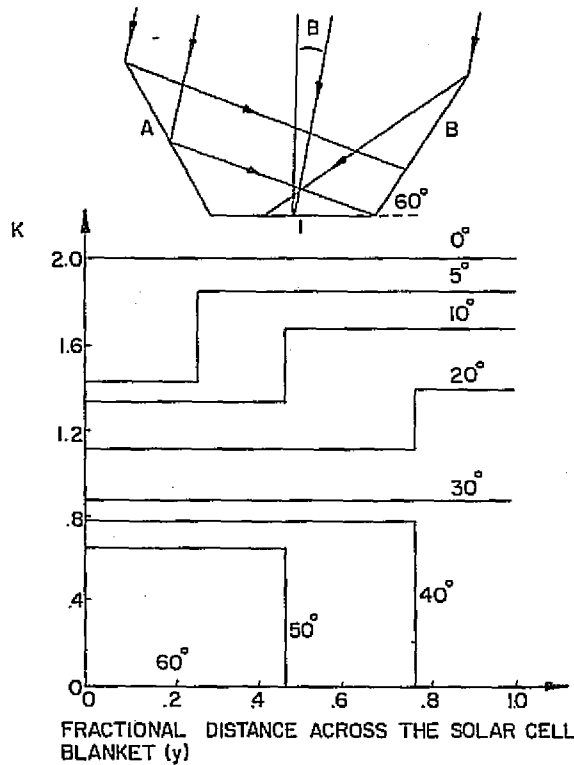


FIGURE L-5 EFFECTIVE SOLAR CONCENTRATION RATIO